THE UNIVERSITY *of* EDINBURGH

The function of M4 protein *in vitro* and *in vivo*

Xuan Wang

2013

Doctor of Philosophy

University of Edinburgh

Abstract

Herpesviruses are ubiquitous in both humans and animals and can cause life-threatening disease. The discovery of murine gammaherpesvirus 68 (MHV-68), which has many similarities in genome and pathogenesis as the human pathogens Epstein-Barr virus and Kaposi's sarcoma-associated herpesvirus, provides a model for further investigation of the pathogenesis of gammaherpesviruses. The M4 gene was found to be at the left end region of MHV-68 genome. The presence of the M4 protein is required during the early establishment of MHV-68 latency. However, the function of M4 protein remains unclear. The aim of this project was to investigate the function of the M4 protein *in vitro* and during infection.

By using an ELISA, the recombinant M4 protein was shown to bind several Cxc-chemokines and stop the interaction between Cxcl4 and GAGs. The role of M4 protein during MHV-68 lytic infection and in the early establishment of latency was studied by comparing the pathogenesis of virus which does not express M4 (M4stop) and wild type virus (WT). Compared to WT infection, this study found that M4stop was decreased in the lungs at day 8 post infection (p.i.). At the same time point, the viral loads were higher in M4stop infected spleens, which was accompanied by increased expression of the $CD4^+$ T cell activation marker PD-1 and the macrophage activation marker CD69. However, at day 14 p.i., the M4stop infected spleens had lower viral loads, and the expression of CD69 was decreased on $CD4^+$, $CD8^+$ T cells, B cells and macrophages. Furthermore, gene expression PCR arrays were used to investigate how cellular activation and inflammation were transcriptionally regulated. It has been found that the transcription of several genes, which are involved in germinal centre development, was lower in the spleens of WT infected mice at day 12 and 14 p.i. compared to day 10 p.i. of WT infection, as well as day 12 and 14 p.i.

of M4stop infection. In addition, the percentage of germinal centre B cells was found to be higher in spleens infected with M4stop at day 10 p.i.. However, there was no difference in percentages of T_{FH} and plasma cells in the spleens. Finally, in order to understand the role of IFN-γ in control of infection in M4stop infected mice, IFN-γR$^{-/-}$ mice were infected with M4stop and WT. Although there were differences in pathogenesis between WT and M4Stop virus infected IFN-γR$^{-/-}$ mice, there was no clear evidence that M4 function is involved in inhibiting IFN-γ pathways.

In this study, we found M4 can disturb the interaction of chemokine and GAGs and might delay virus trafficking to the spleen, which could lead to a reduction of cellular activation. M4 may also impair the development of germinal centres at the beginning of latent infection in the spleens.

Contents

Declaration

I declare that all work included in this thesis is my own except where otherwise stated. No part of this work has been, or will be, submitted for any other degree of professional qualification.

Xuan Wang

2013

Acknowledgement

I would like to thank my supervisors Dr Bernadette Dutia and Professor Tony Nash for their advice and technical assistance throughout this project. I would particularly like to thank Bernadette who has given me a lot of support and advice. More importantly she has shown tons of patience to me. Thanks to member of the ICHAIR group, especially Yvonne Ligerterwood, Marlynne Quigg-nicol, Karen Bryson and Ian Bennet who taught me techniques and helped me to manipulate the animal work. Moreover, I also appreciated the support and friendship from other PhD students. A big thank to Shonna Johnston, Suan Graigmiller, Martin Waterfall and Bob Fleming for their assistance with FACS and confocal. Lastly, I would like to thank Darren Shaw for statistics assistant.

I would like to thank my family, friends and my boyfriend for providing both moral and financial support. Finally, I would like to thank China Scholarship Council for offering me this chance to study in Edinburgh University.

List of Figures

List of Tables

Abbreviations

2-ME	2-mercaptoethanol
AP	ammonium persulphate
BAC	bacterial artificial chromosome
BARF	BamHI A rightward frame
Bcl-2	B-cell lymphoma 2
Bcl-6	B-cell lymphoma 6
BEVS	baculovirus expression vector system
BHK-21 cells	baby hamster kidney fibroblast cells
BHRF	BamHI H rightward frame
BL	Burkitt's lymphoma
Blimp-1	B lymphocyte-induced maturation protein-1
BSA	bovine serum albumin
CSR	class switch recombination
DMSO	dimethylsulphoxide
EBER	Epstein-Barr virus-encoded RNA
EBNA	EBV nuclear antigen
EBV	Epstein-Barr virus
EGFP	enhanced green fluorescent protein
EGs	early genes
EHV-1	equine herpesvirus type 1
ELISA	enzyme-linked immunosorbent assay
FCS	fluorescence activated cell sorting
FDC	follicular dendritic cells
GAGs	glycosaminoglycans
GAPDH	glyceraldehydes-3-phosphate dehydrogenase
GC	germinal centre
GMEM	Glasgow Modified Eagle's Medium
gp	glycoprotein
GPCR	G-protein coupled receptor
H&E	hematoxylin and eosin
HCMV	human cytomegalovirus
HEPES	N-2-hydroxyethylpiperazine-N-ethane-sulphonicacid

High-Five cells	*Trichoplusia ni* insect cells
His	histidine
HL	Hodgkin's lymphoma
HLA	human leukocyte antigen
HSV-1	herpes virus type-1
HVS	herpesvirus saimiri
ICP0	infected-cell polypeptide
IEGs	immediately-early genes
IFN-γ	interferon-gamma
Ig	immunoglobulin
IL	interleukin
IM	infectious mononucleosis
IRF4	interferon regulatory factor 4
kb	kilobase
kDa	kilodaltons
KS	Kaposi sarcoma
KSHV	Kaposi's sarcoma-associated herpesvirus
LAMP	latency-associated membrane protein
LANA	latency-associated nuclear antigen
LAT	latency-associated transcript
LB	Luria-Bertani
LGs	late genes
LMP	latent membrane protein
LP	EBNA-leader protein
M4sotp	M4 mutant virus M4in2
MACS	magnetic cell sorting
MCD	multicentric Castleman disease
MHV-68	murine gammaherpesvirus 68
mK3	MHV-68 K3
MLN	mediastinal lymph node
MOI	multiplicity of infection
MV	myxoma virus
NBF	neutral buffered formaldehyde
NFκB	nuclear factor kappa-B
NK	natural killer

NKT	natural killer T
NPC	nasopharyngeal carcinoma
ORF	open reading frame
PCR	polymerase chain reaction
PD-1	programmed cell death protein 1
PD-L	PD-ligand
PEL	primary effusion lymphoma
PFU	plaque forming units
PMA	phorbol 12-myristate 13-acetate
RCA	regulator of complement activation
RTA	transcription activation
SDS-PAGE	sodium dodecyl sulfate polyacrylamide gel electrophoresis
Sf9 cells	*Spodoptera frugiperda* insect cells
SPBS	sterile phosphate buffered saline
TAE	Tris-acetate-EDTA
TEMED	Tetramethylethylenediamine
TFH	T follicular helper
Th1, 2	T helper cell type 1, 2
TNF	tumour necrosis factor
TPB	tryptose phosphate broth
TR	terminal repeat
Treg	follicular regulatory T cells
vCCL1	viral CCL1
vCyclin	viral cyclin
vFLIP	viral FLICE inhibitory protein
vGPCR	viral G-protein coupled receptor
vIL-6	viral IL-6
VP16	virion protein 16
WT virus	wild-type BAC-derived virus PHA-4

Chapter 1

Introduction

1 Introduction

1.1 Herpesvirus

Herpesviruses are ubiquitous viruses that hosts carry for their life time. More than 130 herpesviruses have been identified so far. Herpesvirus infections are widely established in most vertebrates and in one invertebrate (Davison et al., 2009). The natural infection of herpesviruses has host specificity such that most herpesviruses infections are restricted to a single species. However, the host can be infected by one or more herpesviruses. The herpesvirus infection can induce an asymptomatic or mild symptomatic lytic infection. The lytic infection is followed by establishment of latent infection in which complete copies of the viral genetic information persist for extended periods without continuous production of infectious virus. During infection, latency is an ideal strategy used by the herpesvirus to evade the immune attack. There are two consequences of latent infection: the first is reactivation or reappearance of infectious virus under certain conditions, such as immunosuppression; the other aftermath of latent infection is the occasional neoplastic alteration of the latently infected cell and the formation of tumors. However, the latter only occurs in certain herpesvirus infections.

1.1.1 Structure

Herpesviruses are large double stranded DNA viruses, which have a 125-290 nm diameter. The virus consists of DNA-containing icosahedral (T=16) shaped

nucleocapsid, which is coated in a dense protein layer called the tegument. The tegument is surrounded by a lipid bilayer membrane, called the envelope, composed of viral proteins and glycoproteins (Flint et al., 2009).

1.1.2 Classification

Classification of herpesviridae was initially determined by their structure and biological properties, such as host ranges, reproductive cycles, and latency sites. Nowadays, molecular characteristics are also considered in classifying of herpesviruses. According to this, the herpesviridae are ordered in three subfamilies: the *Alphaherpesvirinae*, the *Betaherpesvirinae*, and the *Gammaherpesvirinae*, based on the report of the International Committee on Taxonomy of Viruses (ICTV, http://www.ictvonline.org). The classifications of common herpesviruses are listed in table 1.1. There are eight currently identified human herpesviruses: human herpes virus 1-8. The common names of these human herpesviruses are used in this thesis.

1.1.3 Life cycle

As mentioned before, herpesviruses have two distinct life cycles: lytic and latent replication. The cellular tropisms and mechanisms that support lytic and latent infection with different herpesviruses are various (reviewed in Penkert and Kalejta, 2011) (table 1.2). The life cycle of herpesvirus described below is based on the study of herpes simplex virus type 1 (HSV-1).

Table 1.1 Classification of common *Herpesviridae* and disease associations

	genus	**virus**	**common name**	**host**	**disease**
α	Simplexvirus	*Human herpesvirus 1,2*	Herpes simplex virus type 1,2	human	Recurrent herpetic stomatitis
	Varicellovirus	*Human herpesvirus 3*	Varicella-zoster virus (VZV)	human	Chickenpox, shingles
	Mardivirus	*Gallid herpesvirus 2, 3*	Marek's disease virus	chicken	T cell lymphoma
β	Cytomegalovirus	*Human herpes virus 5*	Human cytomegalovirus (HCMV)	human	Mononucleosis,
	Muromegalovirus	*Murid herpesvirus 1*	Mouse cytomegalovirus	mouse	hepatitis
	Roseolovirus	*Human herpesvirus 6, 7*	Human herpesvirus 6, 7	human	Roseola infantum, Encephalitis
γ	Lymphocryptovirus	*Human herpesvirus 4*	Epstein-Barr virus	human	Infectious mononucleosis, Burkitt's lymphoma
	Rhadinovirus	*Human herpesvirus 8*	Kaposi's sarcoma-associated herpesvirus	human	Kaposi's sarcoma, Castleman's disease
		Murid herpesvirus 4	Murine gammaherpesvirus 68	mouse	Lymphoma
		Saimiriine herpesvirus	Herpesvirus saimiri	monkey	Lymphoproliferative disease
	Macavirus	*Alcelaphine herpesvirus 1*	Malignant catarrhal fever virus	Cattle	Lymphoproliferative disease
	Percavirus	*Equine herpesvirus 2, 5*	Equine herpesvirus 2, 5	Horse	Respiratory disease

1.1.3.1 Lytic replication

Attachment and entry

Most herpesvirus virions bind to the cells by exploiting glycosaminoglycans (GAGs), usually heparin sulfate or chondroitin sulfate proteoglycans, on the cell surface (reviewed in Shukla and Spear, 2001). The reversible binding through HSV-1 glycoprotein B (gB) and gC manages to concentrate virus on the cell surface thus increasing the efficiency of viral entry (Herold et al., 1994; reviewed in Spear and Longnecker, 2003).

The initial entry of herpesvirus, however, interacts with entry receptor molecules on the cell surface. During entry, fusion between the viral envelope and the plasma membrane of cells requires four glycoproteins, gB, gD, gH and gL (Spear, 1993; reviewed in Spear and Longnecker, 2003). Other entry mechanisms have also been used to invade certain cellular types *in vitro* under special conditions. For instance, endocytosis is utilized by HSV to enter into Hela and Chinese hamster ovary cell lines at low pH conditions (Nicola, McEvoy, and Straus, 2003).

Gene expression

The virions are internalized and dismantled, releasing the tegument proteins and the nucleocapsids into the cytoplasm after viral entry. The viral nucleocapsids are transported along microtubules towards the cell nucleus where viral nucleocapsids dock at the nuclear pore, followed by the release of viral DNA into the nucleus

(reviewed in Campbell and Hope, 2003; Sodeik, Ebersold, and Helenius, 1997). Meanwhile, certain tegument proteins, such as virion protein (VP16), are transported to the nucleus as well.

Within the nucleus, transcription of viral genes takes place using the transcription machinery of the host. The transcription of viral genes was examined by Honess and Roizman who looked at the synthesis order and rate in infected cells based on the study of HSV-1 productive infection. Then these genes were classified into three major groups: immediately-early genes (IEGs), early genes (EGs) or late genes (LGs) (Honess and Roizman, 1974). IEGs are expressed transiently and rapidly before *de novo* protein synthesis during lytic infection. Unlike other DNA viruses, many herpesvirus IEGs are mediated by both viral transactivator proteins and virion tegument protein. In the case of HSV-1, VP16 is important in the initiation of the lytic programme. VP16 can bind with two host cell factors, DNA-binding transcriptional regulator Oct-1 and cell-proliferation regulator HCF-1, to activate HSV-1 IEG transcription (reviewed in Wysocka and Herr, 2003). The IEGs and their products are involved in viral DNA replication. During transcription, some IE mRNAs are spliced and transported to the cytoplasm, then translation of the IE mRNAs takes place in the cytoplasm. After that, the IE proteins are transported back to the nucleus, where they regulate transcription of IEGs and activate expression of the EGs. The early protein is involved in DNA metabolism and replication. The EG mRNAs are spliced and transported to the cytoplasm where they are translated. Some

Table 1.2 Cells that support the different types of herpesvirus infections. Adapted from a review of Penkert and Kalejta (2011).

Family	Virus	Lytic infection	Latency sites
α	HSV-1,2	Epithelial and keratinocyte	Neuron
	Varicella-zoster virus	Epithelial, keratinocyte, T cell, sebocyte, monocyte, endothelial, Langerhans and peripheral blood mononuclear cell	Neuron
β	Cytomegalovirus	Macrophage, dendritic, endothelial, smooth muscle, epithelial and fibroblast	$CD34^+$ hematopietic stem cell, monocyte
	Human herpesvirus 6	T cell	Bone marrow progenitor
	Human herpesvirus 7	T cell	T cell
γ	Epstein-Barr virus	B cell and epithelial	B cell
	Kaposi's sarcoma-associated herpesvirus	Epithelial cell, macrophage, dendritic cell, B cell	B cell
	Murine herpesvirus 68	Epithelial cell, macrophage, dendritic cell, B cell	B cell, macrophage, dendritic cell, epithelial cell, plasma cell

of the EG proteins are transported to the nucleus, some of them remain in the cytoplasm. Viral DNA replication and recombination produces concatemeric DNA, which is the template of LGs. Most late mRNAs are transported to the cytoplasm to translate without splicing. The proteins encoded by LGs are primarily virion structural proteins and proteins for virus assembly and particle egress (Flint et al., 2009; reviewed in Weir, 2001).

Assembly and Egress

The packaging of DNA occurs in the cell nucleus. Newly synthesized viral DNA is replicated from concatemeric DNA and packaged into nucleocapsids which are transcribed from LGs. The DNA containing nucleocapsids, along with some tegument proteins, acquire primary envelopes from the nucleus when the new virions bud into perinuclear lumen from the inner nuclear membrane. Then the primary envelopes fuse with the outer leaflet of the nuclear membrane and the nucleocapsids are released into the cytoplasm, coupling with the loss of the primary envelopes. These structures are transported to a late Golgi-endosome compartment or an endosome where the tegument proteins and envelope proteins that are encoded by LGs are added onto the virions. The enveloped viruses then bud into vesicles transported to the plasma membrane and the virus particles are released by exocytosis (reviewed in Homa and Brown, 1997; reviewed in Mettenleiter, 2002).

1.1.3.2 Latent replication

Long term latency is a specific feature of herpesvirus infection. The mechanism usually involves restrained expression of the viral genome. Therefore, immunologically relevant molecules during the course of productive infection are not synthesized. Latent infection with HSV-1 occurs in ganglia of neurons in the peripheral nervous system. The primary steps of latent infection are similar to productive infection, where the DNA of the virion is released into the nucleus. However, during latency, the viral genome is transcriptionally silent, and latency-associated transcript (LAT) is the only viral gene that is abundantly transcribed. LAT RNA is spliced to a significantly smaller subset that either is maintained in the nucleus as a stable intron in the form of a lariat or is transported to the cytoplasm (Block and Hill, 1997). MicroRNA encoded by the LAT gene inhibits apoptosis in the infected cells that contribute to the persistence of HSV-1 in a latent form (Gupta et al., 2006).

1.1.3.3 Reactivation

In given conditions or stimuli in neuronal physiology induced by trauma, hormonal changes or stressful conditions, the reactivation process occurs in the latently infected cells as the entire genome is transcribed and replicated as productive infection. New progeny virions are produced resulting in recurrent infection. LAT is also essential for efficient reactivation of HSV-1 from sensory neurons, as the

reactivation is decreased in LAT deletion virus (Perng et al., 1994). Furthermore, products of VP16, infected-cell polypeptide 0 (ICP0) and ICP4 are required for the HSV-1 reactivation in latently infected trigeminal ganglion tissue culture (Halford et al., 2001).

1.2 Gammaherpesvirinae

The *Gammaherpesvirinae* are characterized by variable length of reproductive cycles and a lymphocyte-associated infection trend. They are subdivided into four genera: lymphocryptovirus (gamma-1 herpesvirus), rhadinovirus (gamma-2 herpesvirus), macavirus and percavirus (ICTV, http://www.ictvonline.org). The lymphocrypto-viruses include human herpesvirus 4 (also called Epstein-Barr virus (EBV)), callitrichine herpesvirus 3, cercopithecine herpesvirus 14, gorilline herpesvirus 1, and macacine herpesvirus 4; whereas the rhadinoviruses include saimiriine herpesvirus 2 (HVS), human herpesvirus 8 (also called Kaposi's sarcoma-associated herpesvirus (KSHV)), ateline herpesvirus 2 and 3, bovine herpesvirus 4 and murid herpesvirus 4 (also called murine gammaherpesvirus 68 (MHV-68)). Macavirus and percavirus are more recently defined genera. Macaviruses contain ovine herpesvirus 2, bovine herpesvirus 6, and suid herpesvirus 3-5; whereas percaviruses comprise equine herpesvirus 2 and 5, as well as mustelid herpesvirus 1. Host lymphocytes are the main location in which viruses establish latent infection. The infection of gammaherpesvirus is strongly associated with neoplastic diseases.

To date, there are two human gammaherpesviruses (EBV and KSHV) that are able to establish a lifelong, persistent infection with few or no clinical symptoms in immunocompetent hosts. Nonetheless, the infection can be lethal if the hosts are immunosuppressed or immunocompromised, such as chemotherapy drugs or other virus infections

1.2.1 EBV

EBV is about 172 kilobase (kb) and contains more than 85 genes. EBV was discovered in lymphoma cells cultured from Burkitt's lymphoma in 1964 (Epstein, Achong, and Barr, 1964). The infection of EBV can be transmitted through saliva or blood (Alfieri et al., 1996; Kieff, 1996; Magel, 2012), hence it is widespread in all human populations. In western countries, a high percentage of children and adolescents acquire immunity to EBV (Schuster and Kreth, 1992). The primary infection is usually accompanied by symptoms like upper respiratory tract infections. Infectious mononucleosis (IM), an acute and usually self-limiting lymphoproliferative disorder, is characterized by an expansion of EBV-infected B-lymphoid blasts and proliferation of activated T-cells. It can be found in 30-50% of the primary infected adolescents and adults. Splenomegaly is found in half of these people (reviewed in Hanto, 1995). Then the infection remains harmless unless the balance of the immunity between the host and EBV has changed. EBV infection results in a lifelong infection in the host's B lymphocytes and has been reported to be associated with several human cancers including Hodgkin's lymphoma (HL),

Burkitt's lymphoma (BL), nasopharyngeal carcinoma (NPC), and central nervous system lymphomas (Washington and Aiyar, 2012).

1.2.1.1 Entry of EBV and lytic infection

During a lytic infection, EBV lytically infects oral epithelial cells through saliva. Then the virus infects circulating B lymphocytes. Infection can be transferred between epithelial cells and B cells (Shannon-Lowe et al., 2006). A successful entry of EBV to B cells requires the complicated cooperation of several factors: viral envelope glycoprotein 350/220 protein binds to complement receptor CR2, the binding of glycoprotein (gp) 42 to human leukocyte antigen (HLA) class II, the interaction of gL/gH complex, gB and their receptors, which mediates the fusion with the cell membrane, as well as the binding of gB to the membrane directly (reviewed in Hutt-Fletcher, 2007). The entry mechanism of EBV to epithelial cells requires the B cells transfer infection, but without the binding of gp42 (Shannon-Lowe and Rowe, 2011).

During lytic infection, approximately 80 viral proteins are expressed (Kieff, 1996). BZLF1 and BRLF1 are the IEGs. Both are required for EGs and LGs expression and are essential for viral DNA replication during the lytic programme as they encode transcriptional activators that bind to and activate EBV EG promoters (Chevallier-Greco et al., 1986; Feederle et al., 2000). Meanwhile they are important mediators in the switch from latency to lytic replication (Zalani, Holley-Guthrie, and

Kenney, 1996). It has also been found that BZLF1 localizes to chromosomes of some cells including epithelial, fibroblast, and B cells during mitosis. As a result, it may affect mitotic chromosome architecture, normal cell function and viral replication and segregation (Adamson, 2005).

1.2.1.2 EBV persistent infection

The latent virus spreads throughout the lymphoid tissues via B cells. Most latently infected B cells are attacked and killed by natural killer (NK) cells or $CD8^+$ T cells, but a small proportion of the persistently infected small non-proliferating memory B cells survive in the blood (Babcock et al., 1999; Flint et al., 2009; Rickinson, Lee, and Steven, 1996). During latency, EBV gene expression profiles are distinct, which are termed Latency type 0, I, II, and III (Washington and Aiyar, 2012).

The gene expression of EBV which is observed in lymphoblastoid cell lines, AIDS-related immunoblastic lymphoma, central nervous system lymphoma and post-transplant lymphoma is referred to as Latency III. At least six nuclear antigens (EBV nuclear antigen (EBNA)-1, EBNA-2, EBNA-3A, EBNA-3B, EBNA-3C, and EBNA-leader protein (LP)), three membrane proteins (latent membrane protein (LMP)-1, LMP-2a, LMP-2b), non-coding RNA transcripts (Epstein-Barr virus-encoded RNA (EBER)-1, EBER-2, and BamHI A rightward frame (BARF)-0 and BARF-1) and BamHI H rightward frame (BHRF)-1 can be found in Latency III (reviewed in Rowe et al., 2009; Washington and Aiyar, 2012). These proteins and

expressed genes are required for immortalization of naïve B cells and are anti-apoptotic for B lymphocytes (Washington and Aiyar, 2012). For example, BHRF-1 is a B cell lymphoma-2 (Bcl-2) homologue known to be capable of protecting B cells from apoptosis (Henderson et al., 1993). Meanwhile, BARF1, as well as EBERs can induce the activation and expression of Bcl-2 (Komano et al., 1999; Wang et al., 2006).

EBNA-1, LMP-1, LMP-2a, LMP-2b, EBERs and BARTs, which are termed latency II, can be found in NPC, EBV-associated gastric carcinomas, T cell lymphomas and HL (Washington and Aiyar, 2012). LMP-1 up-regulates anti-apoptotic genes, such as Bcl-2 and A20, which interfere with p53-mediated apoptosis (Fries, Miller, and Raab-Traub, 1996; Laherty et al., 1992). Additionally, LMP-1 enhances growth and differentiation signals by mimicking CD40 signalling in B cells, leading to B-cell development, activation and immune responses (Rastelli et al., 2008).

During Latency I, EBNA-1 is the main EBV encoded protein in the majority of BL tumors. Moreover, EBERs and BARTs can also be detected in the tumors. Latency 0 is observed in infected memory B cells where only the expression of EBNA-1 is detectable during cell division.

Among these four latency patterns, only EBNA-1 can be found in all cells infected latently by EBV and EBV associated tumors. The presence of the EBNA-1 disturbs several host proteins and pathways that are related to apoptosis (reviewed in Frappier,

2012; Washington and Aiyar, 2012).

1.2.1.3 Reactivation of EBV

As mentioned in the lytic infection of EBV, the lytic transactivator BRLF1 and BZLF1 are essential for the reactivation of EBV. Moreover, the differentiation of peripheral memory B cells into plasma cells in the tonsil leads to the reactivation of EBV (Sun and Thorley-Lawson, 2007).

1.2.1.4 EBV associated diseases

It has been reported that the EBV genome and EBNA-1 are contained in a large number of lymphomas. The main EBV associated diseases are listed below.

BL

BL, first described by Dr. Dennis Burkitt in 1958, is the most common malignancy of children in Africa. BL cells were originally found to arise from germinal centre (GC) B cells. The cells express B-cell lymphoma 6 (Bcl-6) and have a high mitotic activity (Blum, Lozanski, and Byrd, 2004). Only EBNA-1 protein expression was found in EBV-positive BL. In this disease, the overexpression and rearrangement of the c-myc oncogene leads to deregulation of c-myc expression, thus inhibiting apoptosis (Blum, Lozanski, and Byrd, 2004). In areas of endemic BL, lymphomagenesis may be related to immunosuppression of EBV-specific T cell immunity and mitogenesis of B cells which are caused by *P.falciparum* malaria

(reviewed in Rowe et al., 2009). Another co-factor for BL is HIV infection, which activates the B cell system (reviewed in Rowe et al., 2009).

IM

IM is commonly found in adolescents and young adults. The majority of IM cases are reported during primary infection with EBV. This disease is characterized by lymphadenopathy, splenomegaly, hepatitis, hemolysis and an increase of $CD8^+$ T cells in the peripheral blood, coupled with an increase in cytokine release, such as interleukin (IL)-2, IL-6, interferon-gamma (IFN-γ) and tumour necrosis factor (TNF) (Andersson, 1996; reviewed in Luzuriaga and Sullivan, 2010; reviewed in Williams and Crawford, 2006). The symptoms last for several weeks, however, fatigue may persist for a longer time .

NPC

EBV infection is known to be an essential factor for the development of NPC. Other co-factors, such as dietary and genetic factors, are important etiological association. For example, NPC is more commonly found in certain regions such as southeast China, Alaska, and Greenland. According to epidemiology statistics, 95% of NPC tumors are EBV associated. NPC was classed in three types dependent on the degree of histopathologic differentiation. They are keratinizing squamous cell carcinoma (type 1), non-keratinizing carcinoma (type 2), and undifferentiated carcinoma (type 3) (reviewed in Raab-Traub, 2002).

HL

HL is a malignant tumor of the lymphatic system, but also affects the central and peripheral nervous systems. EBV genomes and gene products, such as LMP-1 and 2A, EBNA1, BARTs and EBERs, are detected in the Hodgkin and Reed-Sternberg cells, which are derived from crippled, pre-apoptotic GC B cells (Kanzler et al., 1996). Activation of programmed cell death protein 1 (PD-1)-PD-ligand (PD-L) signalling pathway inhibits T-cell effector functions in HL patients (Chemnitz et al., 2007; Yamamoto et al., 2008).

1.2.1.5 Immune response to EBV

Lytic antigens of EBV induce $CD8^+$ T cell responses against EBV infected cells (Callan et al., 1996). About 1-4% of the total $CD8^+$ T cells are activated by the IE and some E antigens during symptomic infection (reviewed in Hislop et al., 2007). Moreover, $CD8^+$ T cells also help to control EBV during latent infection (reviewed in Rickinson, Callan, and Annels, 2000). The increase of $CD4^+$ T cells is another key factor that contributes to the control of EBV replication because they react to the viral antigens and secrete IFN-γ (Landais et al., 2004). The number of virus-specific $CD4^+$ T cells reaches to its peak during acute IM, but the number of $CD4^+$ T cells declines quickly when the lytic and latent antigens are reduced (Amyes et al., 2003). Natural immunity is also a vital factor to control EBV infection. The number of NK cells is significantly increased after EBV infection and is inversely correlated to the

virus load. The mechanism used by NK cells to control EBV is the elimination of infected B cells, as well as the secretion of cytokines, like IFN-γ (Williams et al., 2005).

1.2.2 KSHV

KSHV has a 160 kb DNA genome. The Kaposi sarcoma (KS) was first described by Dr. Moritz Kaposi in 1872. However, the etiology of KS was unknown until a gammaherpesvirus, KSHV, was connected with this malignant cancer when KS biopsies were analysed in 1994 (Chang et al., 1994). KSHV has also been associated with two other neoplastic diseases: primary effusion lymphoma (PEL) and multicentric Castleman disease (MCD). The infection of KSHV can be found in sub-African and some Mediterranean countries, including Israel, Saudi Arabia, Italy and Greece.

1.2.2.1 Lytic infection

KSHV infection can be found in several cellular types in vivo, such as human B lymphocytes, macrophages, endothelial cells and epithelial cells. The IE genes, open reading frame (ORF) 45 and ORF50, were found to be transcribed during viral reactivation (Zhu, Cusano, and Yuan, 1999). ORF50 is a homologue of the EBV replication and transcription activation (RTA), which is the master regulator factor and is sufficient to induce KSHV gene expression. Moreover, the binding of ORF45 or ORF50 to interferon regulatory factor 7 disturbs the immune response as the

induction of type I IFN is reduced (Yu, Wang, and Hayward, 2005; Zhu et al., 2002). ORF50 can induce the expression of several E and L genes, such as K8, viral IL-6 (vIL-6) and viral CCL1 (vCCL1) (Sun et al., 1998). Some KSHV lytic genes have host/cellular regulation functions, including mitogenic and cell cycle-regulatory, anti-apoptotic and immunomodulating. For example, vIL-6 has a similar sequence and function to cellular IL-6. vIL-6 can induce cell proliferation and inhibit apoptosis and IFN signalling (Aoki et al., 1999; Chatterjee et al., 2002).

1.2.2.2 Latent infection

Expression of many KSHV-encoded latent genes, including Kaposin A, viral FLICE inhibitory protein (vFLIP), viral cyclin (vCyclin), latency-associated membrane protein (LAMP), and latency-associated nuclear antigen (LANA)-1 and -2, can be detected in KSHV associated tumors. These genes are indispensable for KSHV latency by the manipulation of cellular signalling pathways. For example, LANA-1 and LANA-2 are highly expressed in all latently infected tumour cells and are found to function as inhibitors of the tumor suppressors *p53* and *Rb*, as well as repressors of apoptosis (Friborg et al., 1999; Rivas et al., 2001; reviewed in Wen and Damania, 2010). In addition, vFLIP is also involved in the inhibition of apoptosis (Sarid et al., 1999; reviewed in Wen and Damania, 2010).

1.2.2.3 KSHV associated diseases

KS

KS lesions are characterized by poor differentiated and highly proliferating spindle-shaped endothelial cells. More than 95% of KS tumor cells contain KSHV viral DNA. According to epidemiology and clinical symptoms, KS can be classified into four subtypes: classic (sporadic), endemic (African), epidemic (AIDS-associated) and iatrogenic (post-transplant). The classic forms of KS are more commonly seen in elderly males whose skin has indolent and multiple pigmented sarcomas without much involvement with the lymph node and other organs. Endemic KS, which has more lymph node involvement, is more common in Eastern and Central Africa. AIDS-associated KS which affects internal organs, such as the lymph nodes or lungs, leads to a high fatality rate. Iatrogenic KS occurs when patients are under long-term immunosuppressive therapy after organ transplantation (reviewed in Wen and Damania, 2010).

MCD

MCD is an aggressive disease leading to a life-threatening consequence. it is closely associated with KS in the case of HIV-related MCD (Soulier et al., 1995). MCD is characterized by an overgrowth of B cells, GC expansion and vascular endothelial proliferation in the lymph nodes. It has been reported that vIL-6 are expressed in naïve B cells and overexpression of IL-6 and are found in MCD disease (Parravinci et al., 1997), which may induce the differentiation of KSHV-infected naïve B cells into plasmablasts without undergoing GC reaction (Du et al., 2001).

PEL

PEL, also termed body cavity-based lymphoma, was first described in 1989 (Knowles et al., 1989). It is a rare HIV-associated non-Hodgkin's lymphoma (NHL). The study of clinical cases has found that PEL is always accompanied by EBV co-infection (reviewed in Chen, Rahemtullah, and Hochberg, 2007). Molecular studies demonstrate that PEL originated from a B cell lineage and may be related to Bcl-6 dysregulation (Gaidano et al., 1999) and plasma cells (Jenner et al., 2003). In PEL tumor cells, only latent KSHV infection can be detected.

1.3 Murine gammaherpesvirus 68

Gammaherpesviruses have clinical influences in both the medical and the veterinary medical fields. However, investigation of the pathogenesis of human gammaherpesviruses is difficult and limited because of the asymptomatic characteristics of the initial EBV and KSHV infection. In addition, the latency establishment of EBV and KSHV cannot be directly assessed in humans. Moreover, the basic pathogenesis of EBV and KSHV cannot be reproduced in the experimental animals. Therefore, it was of great necessity and importance to find an animal model to fill these knowledge gaps. The study of MHV-68 was first reported by Blaskovic et al from a bank vole (*Clethrionomys glareolus*) in Slovakia (Blaskovic, 1980). And then in 2003, it was found in wood mice (*Apodemus sylvaticus*) (Blasdell et al., 2003). Although MHV-68 cannot be found in *Mus musculus*, including house mice,

in nature (Ehlers et al., 2007), it has an ability to infect laboratory mice (*Mus musculus*) through several infectious routes (Sunil-Chandra et al., 1992). The pathology of MHV-68 in mice is slightly different from the pathology of KSHV or EBV in humans (reviewed in Rickinson, 2001). Nevertheless, the study of MHV-68 is still significant because of the high similarity of genome and pathobiologies between MHV-68 infection of mice and EBV or KSHV infection of humans. Thus any MHV-68 infected mouse is a suitable animal model to study the pathogenesis of gammaherpesvirus and immune defense from the host. Additionally, MHV-68 infection associated fibrosis and vasculitis are important models to understand clinical pathologies of human diseases.

1.3.1 Genome

The MHV-68 genome contains 118237bp of unique sequence flanked by a variable number of a 1213bp terminal repeat (TR). The TR may be related to concatemer cleavage and assembled capsid packaging. (Efstathiou, Ho, and Minson, 1990; Virgin et al., 1997). The genome encodes 73 protein-coding ORFs (figure 1.1a). A number of these genes encoded by MHV-68 are closely related to EBV (Efstathiou, Ho, and Minson, 1990), while the genome organization of MHV-68 is more similar to that of HVS and KSHV (reviewed in Simas and Efstathiou, 1998; Virgin et al., 1997). Among these ORFs, there are several unique ORFs, termed M1-9, M10 a,b,c and M11-14, that have no obvious relationship with known virus or cellular genes (reviewed in Barton, Mandal, and Speck, 2011; reviewed in Mistríková and Rajčáni,

2008).

1.3.2 Left end of the genome

The left end of the MHV-68 genome, comprises M1-M4, 8 vtRNA like structures and 15 microRNAs, is implicated in lytic infection, latency, reactivation and immune evasion *in vivo* (Evans et al., 2006; Geere et al., 2006; Macrae et al., 2001; Macrae et al., 2003; Webb, Smith, and Alcami, 2004), although the function of microRNAs or vtRNAs is not known (Zhu et al., 2010). All M1-M4 genes are not required for virus replication in vitro (Bridgeman et al., 2001; Clambey, Virgin, and Speck, 2000; Evans et al., 2008; Macrae et al., 2003; Townsley, Dutia, and Nash, 2004). However, it has been reported that all the genes from the left end are expressed during the latency establishment phase (Bowden et al., 1997; Diebel, Smith, and van Dyk, 2010; Marques et al., 2003).

M1

M1 has sequence similarities to members of the poxvirus serpin family and encodes a secreted protein that is homologous to M3 protein. The function of M1 is believed to repress reactivation from latency in the spleen (Clambey, Virgin, and Speck, 2000) and reduce latency in $CD19^{+}$ immunoglobulin (Ig)D^{-} B cells during chronic infection (Krug et al., 2013). Moreover, in the absence of M1, the replication of persistent virus or the recrudescence of the virus were found in the lung (Krug et al., 2013). The repression function of M1 is opposite to the function of M11 (vBcl-2) and

ORF72 (vCyclin) (Gangappa et al., 2002). IM like-disease is a feature of MHV-68 infection, which is believed to be caused by a massive expansion of $V\beta4^+$ $CD8^+$ T cells (Tripp et al., 1997). M1 protein is required to drive the expansion of $V\beta4^+CD8^+$ T cells *in vivo* and induces $V\beta4^+$ TCR signaling *in vitro*, such as up-regulation of IFN-γ, TNF-α and IL-2 (Evans et al., 2008). Furthermore, the expansion of $V\beta4^+CD8^+$ T cells results in the increased expression of IFN-γ that controls MHV-68 reactivation without affecting the latent viral loads (Evans et al., 2008).

M2

M2 is strictly expressed during latent infection *in vitro* and in B cells in the spleen (Husain et al., 1999; Macrae et al., 2003). It is a target for $CD8^+$ T cells, as a $CD8^+$ T cell epitope was found in this protein (Husain et al., 1999). It has been shown that M2 can limit IFN-γ signaling by down-regulating STAT1/2 levels (Liang et al., 2004) and interfere with DNA damage responses (Liang et al., 2006). M2 expression induces the Vav1 proteins, which are related to phosphorylation- dependent Rho/RAc exchange factors that play critical roles in B-cell activation, proliferation and survival, hyperphosphorylation and exchange activity stimulation (Rodrigues et al., 2006). M2 protein is required for splenic follicle infection and latent infection of GC B cells. For example, M2-deficient MHV-68 may reduce the Vav1/Rac1 pathway that leads to a decreased latency in the spleen after intranasally infection (Pires de Miranda et al., 2008) and the failure of regulation of B cell differentiation (Siegel, Herskowitz, and Speck, 2008). Moreover, M2 protein induces the up-regulation of

IL-10 that drives B cell proliferation (Siegel, Herskowitz, and Speck, 2008). A recent study confirmed that M2 is essential for B cell development during MHV-68 infection by inducing that differentiation of plasma cells *in vitro* and *in vivo* (Liang et al., 2009; Siegel, Herskowitz, and Speck, 2008).

M3

M3 is a MHV-68 encoded chemokine binding protein. It is transcribed during productive infection in the lung and at early stages of latent infection in the spleen (Simas et al., 1999). It has been shown that M3 has an ability to bind to C-, CC-, CX_3C-chemokines and selected CXC-chemokines in vitro (Parry et al., 2000; van Berkel et al., 2000). Moreover, it can bind to CCL2, CCL21, CXCL10 and CXCL13 *in vivo* (Jensen et al., 2003; Martin et al., 2007; Martin et al., 2006). Study of the function of chemokines in the gut during inflammation found that M3 has low binding ability to several CXC-chemokines (Shang et al., 2009). The binding of M3 to chemokines directly interrupts the interaction of chemokines and their receptor as M3 interferes with the N-loop of chemokines which is necessary for the binding of their G-protein-coupled receptors (Alexander et al., 2002; Webb, Clark-Lewis, and Alcami, 2003). Moreover, M3 inhibits the binding of chemokine-GAGs, and thus disrupts the pre-formed chemokine gradients that are critical for cellular migration (Webb, Smith, and Alcami, 2004). Unexpectedly, no significant deficit of viral titer was observed in the lung, MLN or spleen following intranasal M3 deficient virus infection of BALB/c mice compared to wild type (WT) virus at acute or latent

infection (van Berkel et al., 2002). However, insertion of lacZ to ablate M3 leads to a decrease in viral load in the lung and latent virus in the spleen in BALB/C mice in a $CD8^+$ T cell dependent manner (Bridgeman et al., 2001). However, a study of the infection of MHV-68 in its natural host, *Apodemus sylvaticus*, has found that M3 is required for lytic infection because it reduces the inflammation in the lung. Furthermore, M3 is also involved in the efficient establishment of latency in the lung and spleen (Hughes et al., 2011). The conflicting results about the viral load and latency can be explained by different methods to make mutant viruses and infection of the different hosts. As a chemokine binding protein, M3 reduced the inflammatory response in the brain of the host, by intracerebral inoculation, compared to mice infected with M3 non-coding virus (van Berkel et al., 2002). M3 alters $CD8^+$ T cell subset accumulation in the lung and GC reaction in the wood mice, but the mechanism is still unknown (Hughes et al., 2011; Shang et al., 2009). Although the alignment comparison between M3 protein and M1 protein showed a high similarity between these two proteins (van Berkel et al., 1999), the M1 protein has not been shown as a chemokine binding protein.

The study of M3 not only focuses on MHV-68 immune evasion strategies and host responses, but also raises the possibility that M3 protein can be applied to reduce autoimmunity and inflammatory diseases in the medical field. For example, intimal hyperplasia is inhibited by M3 protein which may due to M3 protein stop the recruitment of bone marrow-derived cells in mice (Pyo et al., 2004). A recent study

found that an adenoviral vector encoding M3 protein can control the clinical severity of experimental autoimmune encephalomyelitis and reduce inflammation in the central nervous system of the mouse (Millward et al., 2010).

M4

The transcription of M4 has previously been shown to be expressed with IE kinetics during lytic infection in vitro. It encodes a secreted glycoprotein which can be detected in cell culture supernatant (Evans et al., 2006). M4 influences the establishment of splenic latency at early post infection days following intranasal infection by comparison of WT virus infection with M4-deficient-MHV-68 or MHV-76 virus infection compared with M4 insertion MHV-76 virus (Evans et al., 2006; Geere et al., 2006; Townsley, Dutia, and Nash, 2004), but M4 is not required for long-term latency *in vivo* (Evans et al., 2006). In contrast, a latency deficit was not found in peritoneal cells after intraperitoneal inoculation (Evans et al., 2006). The sequence of M4 protein showed a similarity to M3 protein (Alexander et al., 2002). To date, no published data has shown how M4 interacts with the host immune system.

Non-coding RNAs

The non-coding RNAs, including vtRNAs and microRNAs, play important roles in herpesvirus biology (Amen and Griffiths, 2011). These MHV-68 non-coding RNAs are encoded under the control of the cellular RNA polymerase III, and are predicted

to drive expression of the related microRNAs (Grey, Hook, and Nelson, 2008). The exact function of these non-structural RNAs is still undetermined.

The tRNA-like sequences are transcribed at high levels during lytic and latent infections, especially splenic GC (Bowden et al., 1997). vtRNAs are transcripted as IEs (Ebrahimi et al., 2003) and packaged within MHV-68 virions (Cliffe, Nash, and Dutia, 2009). They are predicted to have cloverleaf like secondary structures. Moreover, vtRNAs are found in higher levels in the cytoplasm of infected cells (Cliffe, Nash, and Dutia, 2009). The vtRNAs were shown not to be aminoacylated (Bowden et al., 1997), hence, they are unable to perform as tRNAs during protein synthesis.

MicroRNAs are post-transcriptional regulators that affect mRNA translation or stability in the cytoplasm, sharing hair-pin structures and a silencer function (Pfeffer et al., 2005). MHV-68 microRNAs are newly found non-coding RNAs (Pfeffer et al., 2005). The RNA polymerase III promoters is adjacent to viral tRNA-like sequence (Bogerd et al., 2010). Therefore, all the MHV-68 microRNA, except miRNA 11, can form co-linear structures with vtRNA, thus forming vtRNA-microRNA-microRNA or vtRNA-microRNA structures with unknown function (Grey, Hook, and Nelson, 2008; Zhu et al., 2010).

1.3.3 Mutant viruses

1.3.3.1 Natural mutants

Four other murine gammaherpesvirus strains (MHV-60, MHV-72, MHV-76, MHV-78) which are similar to MHV-68 were isolated in Slovakia at the same time as MHV-68 (Blaskovic, 1980). Some comparative studies of these strains with MHV-68 have been made that provide a wider view to understand the pathogenesis of EBV and KSHV infection. Among these mutants, MHV-76 and MHV-72 were followed with the most interest.

MHV-76

In comparison to MHV-68, MHV-76 was isolated from a different murid host, the yellow-necked mouse (*Apodemus flavicollis*). Later studies showed that MHV-76 is a naturally occurring deletion mutant of MHV-68 that lacks 9,538bp of the left end of the genome including M1-M4, 8 vtRNA like structures and also the microRNAs (Macrae et al., 2001). Despite the fact that the kinetics of replication of MHV-76 are identical to those of MHV-68 *in vitro*, there are several prominent alterations in the lytic and latent infection *in vivo* compared to MHV-68 infection. For example, no significant splenomegaly can be detected after MHV-76 infection (Macrae et al., 2001). Nevertheless, MHV-76 maintained long-term latency in the lungs and spleen as MHV-68 (Macrae et al., 2001), without tumors or the leukemia-like syndrome (Chalupková et al., 2008). The comparison of MHV-76 with MHV-68 infections

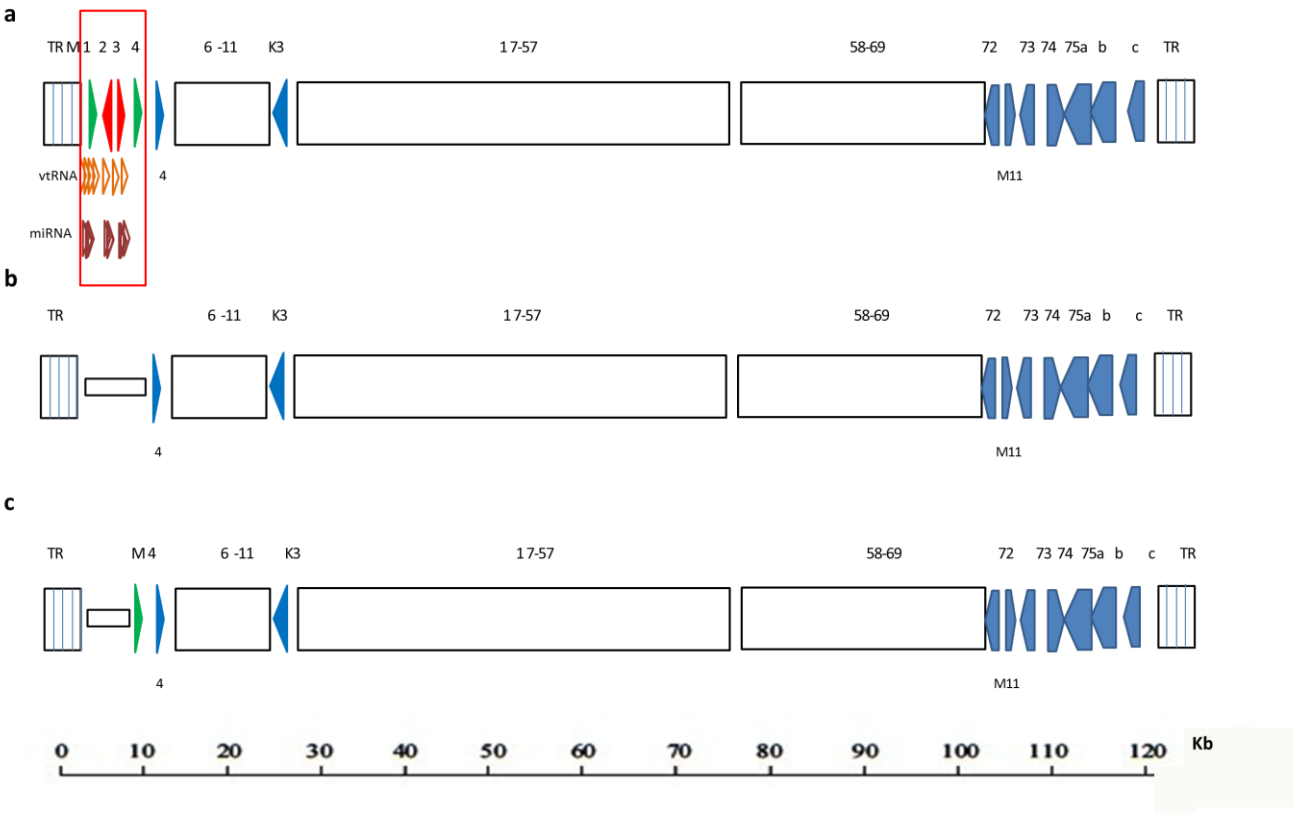

Figure 1.1 Schematic diagram of the genome of MHV-68 and its mutants. (a) MHV-68, (b) MHV-76, (c) MHV-72. The red square indicates the left-hand end region of MHV-68, which contains M1-M4, vtRNAs and microRNAs. The numbers above these boxes are related to the ORF designations.

reveals that the importance of the left end region of MHV-68. Moreover it gives a possibility to study the function of the individual genes in this region by making gene insertion mutant viruses.

MHV-72

MHV-72 was isolated from the same natural host as MHV-68, but is missing M1-M3 and 8 vtRNA-like genes (Oda et al., 2005). Splenomegaly is not observed after infection which is similar to MHV-76. However, unlike MHV-76, multi-organ lymphomas are found in the mice during long-term infection (Oda et al., 2005), therefore mice infected with MHV-72 are considered as an animal model to study tumorigenesis. Moreover, the transmission of MHV-72 is different from other isolates as it can infect mammary glands and infect new born mice through the mother's breast milk (Raslova et al., 2001).

1.3.3.2 Bacterial artificial chromosome (BAC) mutants

Nowadays, scientists study the function of MHV-68 ORFs by construction of a mutant genome with a deletion in its interesting part using a MHV-68 BAC (Adler, Messerle, and Koszinowski, 2003; Adler et al., 2000). To generate BAC mutant MHV-68, viral DNA and plasmid which contains BAC vector sequences are co-transfected into viral permissive cells. The BAC vector-containing viral DNA is isolated from infected cells and electroporated into an E. coli strain. Bacterial cells containing viral BACs can be selected based upon the antibiotic marker present in

the BAC vector. Then the mutated BAC plasmid is transfected into eukaryotic cells where recombinant viruses are expressed and new viruses propagate (Adler et al., 2000). BAC mutant viruses are used widely and by incorporating fluorescent protein may be used to identify infected cells *in vivo* (Adler et al., 2000; Collins and Speck, 2012; Dutia et al., 2009).

1.3.4 Virus infection and pathogenesis

Generally, scientists believe MHV-68 infection is transmitted due to the close contact between individuals in the wild. Intranasal and peritoneal inoculations are normally used for studying MHV-68 pathogenesis in the laboratory. However, these two different infection routes result in different pathogenesis because of the different viral reservoirs. The intranasal route of infection is regarded as a mimic of the natural route of infection with this virus. Importantly, the pathogenesis of MHV-68 infection of mice is similar to that of EBV, with symptoms such as splenomegaly developing when using an intranasal inoculation method.

After intranasal infection, replication of MHV-68 is first found in lung alveolar epithelial cells, then the lytic infection is cleared around day 10 p.i., whereas latency is found in epithelial cells and B cells during long term latency (Flano et al., 2005; Stewart et al., 1998). The infection of B cells requires the pre-infection of epithelial cells and macrophages (Frederico et al., 2012). From the lung, the productive viruses spread to the lung draining lymph node, the mediastinal lymph node (MLN) and

establish latency in B cells, macrophages and dendritic cells (DC) (Nash et al., 2001). The migration of B cells from the MLN to the spleen is exploited by MHV-68, through B cells, the virus traffick to the spleen at day 3 p.i.. In the spleen, latency is mainly established in B lymphocytes (Flano et al., 2000; Sunil-Chandra, Efstathiou, and Nash, 1992), although macrophages, splenic dendritic cells (Flano et al., 2000) and plasma cells (Collins, Boss, and Speck, 2009) have been shown to harbor the latent virus. The infection leads to a massive lymphoproliferation, thus the virus expands by a $CD4^+$ T cells dependent B lymphocyte proliferation (Stevenson and Doherty, 1999). Viral latency reaches peak levels at day 14 p.i. accompanied by a $CD4^+$ T cell (Usherwood et al., 1996) and cytokine (Lee et al., 2000; Siegel, Herskowitz, and Speck, 2008) dependent splenomegaly. Latent infection is preferentially associated with GC, as more viral genomes are harbored in GC B cells than non-GC B cell populations at early latency (Flano et al., 2002; Willer and Speck, 2003). Among the infected GC B cells, virus establishes latency mainly in the proliferating B cells (Collins and Speck, 2012). However, memory B cells are the long-term viral latency reservoir. Memory B cells can first differentiate into preplasma memory B cells under certain conditions, then develop into plasmablasts, finally becoming plasma cells which promotes viral reactivation (Shapiro-Shelef et al., 2003; Willer and Speck, 2003). Relatively high viral frequencies are found in memory B cells in the peripheral blood, macrophages, dendritic cells and B cells in the spleen and B cells in the lung during long-term latency. Moreover viruses are also

harbored in bone marrow, nasopharyngeal- associated lymphoreticular tissue and bronchus-associated lymphoid tissue (Flano et al., 2003; Kocks et al., 2009).

The study of MHV-68 replication is also established in tissue culture, which provides a good model to study early stages of gammaherpesvirus infection as well as mechanisms controlling viral replication during the lytic cycle. For example, MHV-68 can also infect and persist in mouse myeloma cell line NS0 without any cytopathic effect (Sunil-Chandra, Efstathiou, and Nash, 1993).

1.3.5 Immune response to MHV-68 infection

1.3.5.1 Adaptive immune response

The function of $CD4^+$ T cells in MHV-68 infection is studied in mice with $CD4^+$ T cell depletion. It has been found that the lack of $CD4^+$ T cells does not affect Ag-specific $CD8^+$ T cells or cytotoxicity (Belz et al., 2003; Stevenson et al., 1998), but the clearance of the virus in the lung is delayed (Ehtisham, Sunil-Chandra, and Nash, 1993). Moreover, $CD4^+$ T cells are an indispensable element for controlling MHV-68 latent infection. In transgenic mice lacking $CD4^+$ T cells, the virus spontaneously reactivated during long-term infection in the lung (Cardin et al., 1996). The study of MHC class II-deficient mice showed there was a high titer of virus in the lymphoid tissues including spleen, MLN, cervical lymphoid node and bone marrow during the long-term infection (Cardin et al., 1996). The increased viral load may be due to the suppression of immune responses by IL-10 overexpressed in $CD8^+$

T cells in CD4-deficient mice (Molloy, Zhang, and Usherwood, 2011). Another function of $CD4^+$ T cells is to help the activation of B cells during MHV-68 infection (Stevenson and Doherty, 1999).

Cytotoxic $CD8^+$ T cells are mainly charged with controlling viral replication in the lytic infection (Ehtisham, Sunil-Chandra, and Nash, 1993). The clearance of latent virus in the spleens of the $CD8^+$ T cell deficient mice is delayed and leads to dose and mouse strain dependent death (Ehtisham, Sunil-Chandra, and Nash, 1993; Stevenson et al., 1999). $CD8^+$ T cells also have a role in the $CD4^+$ T cell and IL-2 signalling dependent control of virus reactivation in the lung during latent infection (Dias et al., 2010; Molloy, Zhang, and Usherwood, 2009).

B cells not only play an important role for virus transmission and latency establishment during MHV-68 infection, but are also essential for regulating reactivation from latency and controlling the chronic stage of MHV-68 infection (Weck et al., 1999). MHV-68 latency is mainly established in GC B cells, especially centroblasts (Collins and Speck, 2012; Flano et al., 2002). The splenic activated B cells, which express CD69 on their surface, are the major B cell reservoir for the latent virus. It has been said that activated B cells may be related to GC reaction and long-lived memory cell differentiation (Flano et al., 2000; Krug et al., 2007).

1.3.5.2 Innate immune response

NK cells are known to mount a rapid response to several virus infections by secreting

interferons and perforin. Several studies have shown that NK cells play a major role in the control of early stages of alpha- or betaherpesvirus infection in humans and mice. Additionally, EBV is also controlled by NK cells. On the other hand, NK cells are dispensable in controlling the lytic infection, acute latency and long-term latency of MHV-68, although the population of NK cells has been found to be increased (Cartwright and Watkins, 2004; Thomson et al., 2008).

Macrophages also take part in the battle against the MHV-68 infection. For instance, MHV-68 infection leads to the up-regulation of CC-chemokines in the lung. These chemokines induce lymphocyte and macrophage infiltration that control virus infection (Sarawar et al., 2002).

The study of type 1 interferons was based on type 1 interferon receptor deficient mice (IFN-α/β $R^{-/-}$). IFN-α/β are important in controlling the lytic and latent phases of MHV-68 infection. However, there is splenic atrophy and splenomegaly during infection (Dutia et al., 1999). Further evidence for a role of IFN-α comes from a recent study which has found that a genetically modified IFN-α expressing MHV-68 has the ability to avoid virus reactivation (Aricò et al., 2011). Although the cytotoxicity of NK cells is activated by type 1 IFNs, there was no sign that NK cells are involved in the virus controlling mechanism.

IFN-γ is the only type 2 interferon and it is important for controlling human herpesvirus infection. During MHV-68 infection, high levels of IFN-γ are produced

in the lung and lymphoid tissues (Chou et al., 2008; Ganem, 2006). However, the study of MHV-68 infection of IFN-$\gamma^{-/-}$ and IFN-$\gamma R^{-/-}$ mice revealed that IFN-γ has no effect on the control of MHV-68 at the acute infection stage (Dutia et al., 1997; Sarawar et al., 1997). MHV-68 infected IFN-$\gamma^{-/-}$ or IFN-$\gamma R^{-/-}$ mice show an increase in latently infected cells in the MLN (Sarawar et al., 1997) and spleen accompanied by splenic architecture change (Dutia et al., 1997). Furthermore, IFN-γ is associated with T-cell-mediated control of MHV-68 recrudescence in the lung and spleen in B cell-deficient mice (Christensen et al., 1999; Sparks-Thissen et al., 2005). IFN-γ also helps to control the reactivation of MHV-68 and viral gene expression in long-term infection in a cell type-specific manner (Steed et al., 2007). For example, macrophages, but not B cells, are responsive to IFN-γ-mediated suppression of MHV-68 reactivation. (Steed et al., 2007).

1.3.6 Immune evasion

The MHV-68 genome encodes a number of genes that evolved strategies to allow it to persist for the lifetime of an infected animal, despite the presence of a strong immune response. Several immune evasion schemes which are important for MHV-68 infection are listed below.

Chemokine receptor homology

There are three strategies by which herpesvirus impairs the chemokine system: viral chemokine ligands, viral G-protein coupled receptors (vGPCRs), and chemokine-

binding proteins (Lalani, Barrett, and McFadden, 2000; Murphy, 2001). As previously mentioned (section 1.3.2), M3 protein plays an essential role in chemokine binding, chemokine gradient disruption and signalling blocking during MHV-68 infection. MHV-68 also encodes a vGPCR. The sequence of MHV-68 vGPCR has significant homology to the GPCRs of mammalian cells, the vGPCR of HVS (Nicholas, Cameron, and Honess, 1992), as well as the vGPCR of KSHV (Wakeling et al., 2001). The transcription of MHV-68 vGPCR can be examined in both lytic and latent infections (Wakeling et al., 2001). The main function of MHV-68 vGPCR is to act as a viral CXC-chemokine receptor on the surface of cells (Verzijl et al., 2004; Wakeling et al., 2001) and be involved in the replication and reactivation of MHV-68 from latency (Lee et al., 2003; Moorman, Virgin, and Speck, 2003). Moreover, MHV-68 vGPCR induces the activation of nuclear factor kappa-B (NFkB) and regulates several other pathways (Verzijl et al., 2004).

K3

MHV-68 K3 (mK3) is homologous with KSHV K3 and K5. The expression of mK3 can be detected during lytic infection in the lung and latent infection in the lymphoid tissue (Stevenson et al., 2002). mK3 modulates antigen presentation by degradation of MHC class 1 (Stevenson et al., 2000), which is related to the regulation of the cellular endoplasmic reticulum-associated degradation pathway (reviewed in Griffin, Verweij, and Wiertz, 2010). Moreover, mK3 restricts expression of MHC class I on lytically infected DC, thus reducing the priming of the $CD8^+$ T cells (Smith et al.,

2007). Consequently, the deletion of mK3 enhanced the activation of $CD8^+$ T cells (Stevenson et al., 2002). During latent infection, mK3 appears to inhibit MHC class I processing and maintain the number of latently infected spleen cells (Stevenson et al., 2002). Aside from these, the recruitment of DCs in the MLN is altered in the mice infected with mK3-deficient virus at early time points compared with that of WT virus infection (Mount et al., 2010).

Regulator of complement activation (RCA) protein

The ORF4 of MHV-68 encodes homologs of RCA protein. ORF4 is a late gene which is expressed during lytic replication in tissue culture in a cell membrane bound form and in a soluble form. The function of RCA protein is to down-regulate both classical and alternative pathways of murine complement activation (reviewed in Favoreel et al., 2003; Kapadia et al., 1999). Another function of RCA protein is to bind glycosaminoglycan (Gillet, Adler, and Stevenson, 2007). Moreover, it is essential for MHV-68 DNA synthesis in macrophages (Tarakanova et al., 2010). Other than that, RCA protein contributes to efficient infection by activating the protein kinase Akt (Steer et al., 2010).

Research into MHV-68 immune evasion is still ongoing. It has been reported that protein production of both ORF36 and ORF54 can inhibit IFN responses (Hwang et al., 2009; Leang et al., 2011). Therefore, by using these sophisticated immune evasion strategies, MHV-68 manages to escape from the host's immune recognition.

1.4 Chemokines and their receptors

Chemokines (chemotactic cytokines) are a family of small molecular weight proteins (approximately 7-14 kilodaltons (kDa)) that are secreted by cells (CXCL1 and CX3CL1 are membrane-bound chemokines (Moser et al., 2004)). Scientists started to draw certain attention to these molecules because chemokines promote migration of leukocytes, endothelial and epithelial cells. So far, approximately 48 chemokines and 23 chemokine receptors have been found. Among these, all the chemokine receptors have been found in both humans and mice. At least 45 chemokines are involved in chemokine network in humans, whereas approximately 38 chemokines have been found in mice. Chemokines have versatile functions which are associated with a variety of intercellular communication signals, such as cell migration, proliferation, differentiation and survival.

1.4.1 Chemokine classification

1.4.1.1 Structural classification

All chemokines share a similar and highly conserved three-dimensional structure containing a monomeric fold in the N-terminus, three β-strands and an α-helix in the C-terminus. Furthermore, chemokine molecules have four conserved cysteine residues of which the first and third cysteines are connected by a disulfide bond, the other two cysteines are connected by another disulfide bond. Based on the positioning of the N-terminal two cysteine residues and the number of amino acid

between them, chemokines are classified into: CXC-, CC-, C-, and CX3C-chemokines (reviewed in Zlotnik and Yoshie, 2000). X denotes the number of additional amino acids between the first and second cysteines. In the CC-chemokines, the first two cysteines are adjacent, whereas the C-chemokines are different from the other three kinds of chemokines, as their first and third cysteines are missing. Another chemokine structure, which lacks one of the first two cysteines but retains the others (CX-chemokine), has been reported in zebrafish but could not detected in mammals (Nomiyama et al., 2008). Human chemokines are designated in capital letters, whereas as mouse chemokines are designated in lowercase letters.

Lymphotactin (XCL1 and XCL2) and CX_3CL1 (fractalkine) are the only members so far described in C- and CX_3C- family, whereas the rest of the chemokines belong to CC- and CXC-chemokine families. The function of CXC-chemokines is the recruitment of neutrophils, granulocytes and the homing of endothelial cells. CXC-chemokines are divided into two sub-families. One has a tri-peptide sequence Glu-Leu-Arg which is attached to the first cysteine residue (ELR+CXC-chemokines). ELR+CXC- chemokines have an angiogenic function. The ELR+CXC-chemokine sub-family includes CXCL1, CXCL2, CXCL3, CXCL5, CXCL6, CXCL7 and CXCL8. In contrast, the CXC-chemokines without the ELR motif (ELR-CXC-chemokines) consist of CXCL4, CXCL4L1, CXCL9, CXCL10, and CXCL11. The ELR-CXC- chemokines have angiostatic activity. The ELR+CXC-chemokines specifically bind to CXCR1 and CXCR2 in humans and

only Cxcr2 in mice which are present on endothelial cells, whereas ELR-CXC-chemokines act through the chemokine receptors CXCR3, 4 and 5. The CC chemokines exert their action on dendritic cells, monocytes, macrophages and lymphocytes. However, CC-chemokines cannot attract neutrophils except murine neutrophils (Raman et al., 2007).

1.4.1.2 Functional classification

Leukocytes contain related chemokine receptors and are attracted and flow from lower to higher concentration of chemokines toward the relevant sites (Hoogewerf et al., 1997; Proudfoot et al., 2003). This progress is called chemotaxis. Chemokines are grouped into the functional sub-families termed homeostatic, inflammatory, or dual function chemokines.

Homeostatic chemokines are constitutively expressed at discrete locations in lymphoid and extra-lymphoid tissues. They have the ability to attract subsets of lymphocytes and dendritic cells. These chemokines are believed to be important for mediation of cellular recruitment at sites of hematopoiesis, initiation of adaptive immunity and immune surveillance. In secondary lymphoid organs, lymphocytes are attracted to the B cell zone or T cell zone under the control of chemokines. For example, both CCL19 and CCL21 induce CCR7-bearing cells, such as T cells, B cells and DC cells, to traffick into the T cell zone of secondary lymphoid tissues, then these cells promote lymphoid tissue formation (Luther et al., 2002). The homing of

$CD8^+$ T cells into small intestinal epithelium and lamina propria is induced by chemokines (Shang et al., 2009). The recruitment of B cells to Peyer's patches depends on several chemokine receptors, such as CCR6, CCR7, CXCR4 and CXCR5, and their ligands (Okada et al., 2002).

Inflammatory chemokines are induced by inflammatory stimuli and play pivotal roles in the control of leukocyte recruitment, including granulocytes, monocytes and effector T cells. Moreover, inflammatory chemokines regulate basal trafficking of resting B cells and T cells. Macrophages and neutrophils are the main cell types attracted by inflammatory chemokines and take part in inflammatory conditions, as they express various receptors for proinflammatory chemokines, then take part in inflammatory conditions. Moreover, the inflammatory function of chemokines was studied by the influx of neutrophils, eosinophils, macrophages and dendritic cells in the colon which was treated with dextran sulphate sodium. This study has proved that chemokines are critical for leukocyte accumulation in the gut during inflammation (Shang et al., 2009).

A number of chemokines which possess both inflammatory and homeostatic functions are called dual-function chemokines. CCL11, CCL17, CCL20, CCL22, and C-, CX_3C- family chemokines belong to dual-function chemokine family (reviewed in Zlotnik and Yoshie, 2012).

1.4.2 Chemokine receptor

Chemokine receptors are on cell surfaces, and they have the ability to bind to their chemokine ligands with high affinity. Because the receptors have a seven-membrane structure and are coupled to GTP-binding proteins, they are also called seven transmembrane GPCRs. The signal is delivered into the cells by a flux in intracellular Ca^{2+} calcium ions signalling when chemokine receptors interact with their chemokine ligands. Under chemokine signalling, cells traffic to desired locations. Chemokine receptors are classified as four sub-families according to the sub-family of their major ligands.

Homeostatic and dual-function chemokines bind to restricted receptors. Correspondingly, the homeostatic and dual-function chemokine receptors only interact with one or two related chemokines. In contrast, some inflammatory chemokines do not possess exclusive receptors. Meanwhile, inflammatory chemokine receptors have broad chemokine selectivity (reviewed in Zlotnik and Yoshie, 2012).

1.4.3 Chemokine and GAGs

GAGs are a group of long unbranched polysaccharides consisting of various disaccharide repeating units: chondroitin sulfates, dermatan sulfates, heparan sulfate, heparin, keratan sulfates, and hyaluronic acid are all belong to GAGs. The binding of chemokines to GAGs increases the local chemokine concentration on the

extracellular matrices or cell surface, which enhances the chance of recognition of chemokines and their GPCRs. Furthermore, the binding is believed to protect chemokines against proteolytic degradation (Middleton et al., 2002). It has been found that the GAG-chemokine and receptor-chemokine binding sites overlap for some chemokines, which indicates GAGs may disrupt cellular recruitment (Lau et al., 2004).

1.4.4 Chemokine gradient and cellular migration

During the inflammatory response, flowing leukocytes roll on the surface of the vascular wall. Then, leukocytes move to the relative tissues to aid the immune response. The migration of cells involves four steps, including rolling adhesion, tethering, diapedesis and migration (figure 1.3), which is reviewed in Rot and von Andrian's paper (2004). To explain this, neutrophils are taken as an example to demonstrate the migration of cells during the inflammation. In the first step, the circulating speed of neutrophils is slowed down via low-affinity and reversible interactions of L- and E-selectin which appear on blood vessel endothelium. Thus, neutrophils roll along endothelium. Then integrins LFA-1 and CR3 interact with ICAM-1 with a higher affinity than the binding of L- and E-selectin, alongside the binding of chemokine receptors and the endothelial cell-surface GAGs binding chemokines. As a result, the rolling of the neutrophils is stopped and the neutrophils firmly adhere to the endothelium. During the third step, neutrophils cross the endothelial wall by the assistance of LFA-1 and CR3, as well as a further adhesive

interaction involving an immunoglobulin-related molecule called CD31. Consequently, under the mediation of chemokines, neutrophils migrate through the tissue to the infection sites.

1.4.5 Chemokine and cellular differentiation

Chemokines are directly or indirectly involved in cellular differentiation. For example, the differentiation of T helper cell type 1 (Th1)/Th2 depends on several chemokines (reviewed in Luther and Cyster, 2001). CCL3-5 can directly stimulate $CD4^+$ T cells differentiation into the Th1 subtype (reviewed in Luther and Cyster, 2001; Roughan and Thorley-Lawson, 2009). Moreover, the binding of these chemokines and their receptor CCR5 induces IL-12 production in DC and indirectly induces Th1 differentiation (Alcami et al., 1998). On the other hand, CCL2 induces Th2 differentiation by enhancing IL-4 expression (Luther and Cyster, 2001). Moreover, CCL2, CCL7, CCL8 and CCL13 down-regulate the expression of IL-12 inducing Th2 development (Shukla and Spear, 2001; Spear, 1993). Aside from Th1/Th2 differentiation, the study of the function of CXCL4 found that it induces the differentiation of monocytes into macrophages (Scheuerer et al., 2000) and dendritic cells (Xia and Kao, 2003).

1.4.6 Chemokine and fibrosis

Fibrosis is a self-repair process in which excess fibrous connective tissue is formed in an organ or tissue. The development of fibrosis may be because of Th2

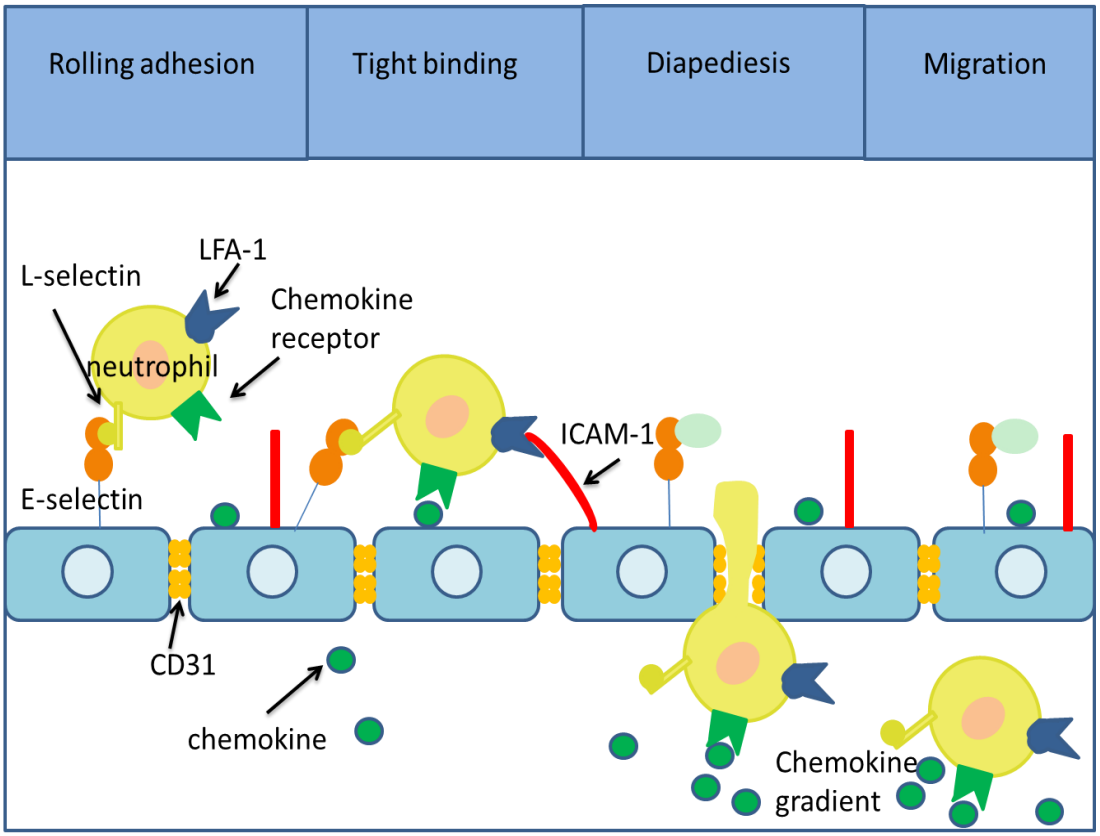

Figure 1.2 A diagrammatic sketch of the migration of neutrophils mediated by a chemokine gradient. The migration of neutrophils is described by four steps: rolling adhesion, tight binding, diapediesis and migration. Adapted from Janeway's Immunobiology, 7th edition.

inflammatory response contributes to the disruption of the normal tissue structure (reviewed in Keane, 2008). For example, CCL17 and CCL22 are associated with a Th2 profile and are significantly elevated in bleomycin-induced pulmonary fibrosis (Belperio et al., 2004). Moreover, the CC chemokine receptors which are expressed on the surface of Th2 T cells are found elevated and related to pulmonary fibrosis (reviewed in Keane, 2008). The balance of angiogenic and angiostatic CXC chemokine expression is also involved in chronic fibroproliferative disorder in the lung (reviewed in Strieter, Gomperts, and Keane, 2007). It has also been found that interaction of CXCL12 and CXCR4 is important for the trafficking and extravasation of fibrocytes into the lung when the pathogenesis of pulmonary fibrosis was studied (Phillips et al., 2004).

1.4.7 Chemokines manipulated by virus

It has been shown that certain chemokines are produced by tumor cells that are important for tumor growth and metastasis, because chemokines recruit proinflammatory cells and endothelial cells providing a superior environment for tumor growth and progression (reviewed in Raman et al., 2007). The study of KS has shown that the expression of CCL2 increased in KS cells *in vivo* and *in vitro* (Sciacca et al., 1994). Furthermore, EBV has been reported to induce chemokine receptors and cytokines during infection. For instance, CCR6, CCR7 and CCR10 are up-regulated in EBV infected cells, which may be important for homing these immortalized cells to secondary lymphoid tissues (Birkenbach et al., 1993; Nakayama et al., 2002).

1.4.8 Viral immune evasion by interrupting chemokine network

In the coevolution of viruses with the hosts' immune response, the hosts have strengthened their immune system to defend against viruses, meanwhile viruses have developed many immune-evasion strategies to limit immune control. The chemokine network is indispensable for controlling viral infection. For instance, CCR5 is involved in the recruitment of memory $CD8^+$ T cells to the lung during influenza infection, thus CCR5 leads to control of virus replication (Kohlmeier et al., 2008). Interestingly, large DNA viruses, particularly the poxviruses and herpesviruses can interrupt the host chemokine network to their advantage. For example, molluscum contagiosum virus encodes two chemokine like proteins which interfere with the chemotactic response to CXCL12 and CCL3 and block calcium fluxes induced by the CC- and CXC- chemokines (Damon, Murphy, and Moss, 1998; Jin et al., 2011). Aside from poxviruses, herpesviruses encode a large number of viral chemokines. For example, KSHV encodes three CC chemokine like genes (vCCL1, vCCL2 and vCCL3). VCCL2 can bind to and antagonize all four chemokine receptor sub-families to inhibit the binding and signalling of the leukocytes to their receptors. Thus it influences trafficking of leukocytes (Kledal et al., 1997; Luttichau et al., 2001; reviewed in Raman et al., 2007).

The virus subverts the immune system not only by secretion of viral chemokines, but also by mimicry of GPCR. The best studied herpesvirus vGPCRs are ORF74 encoded by KSHV and MHV-68, as well as US28 encoded by HCMV. KSHV

ORF74 have been shown to behave as broad-spectrum low-affinity receptor (Arvanitakis et al., 1997). KSHV ORF74 can activate oncogenic and angiogenic signalling pathways through a large number of G proteins (Bais et al., 1998; Smit et al., 2002) and influences the biology of vascular tissues by promoting the expression of angiogenic factor (Sadagopan et al., 2009).

Secretion of chemokine binding protein is another strategy exploited by DNA viruses to impair the host immune response. The best example of this is the broad spectrum chemokine binding protein M3 that was discussed in section 1.3.2. A newly characterized chemokine binding protein from pseudorabies virus only disrupts the chemokine-binding domain without affecting the GAG interactions (Viejo-Borbolla et al., 2010). Interestingly, Lalani et al (1997) has found that poxvirus chemokine binding protein M-T7 protein can bind to C-, CC- and CXC- chemokine, as well as rabbit IFN-γ. In contrast, HSV encoded glycoprotein G can enhance chemokine function *in vitro* and *in vivo* (Coscoy et al., 2012)

The main virus-encoded chemokines, chemokine receptors and chemokine binding proteins are summarized in Table 1.3.

1.5 GC and its regulators

GCs are formed in the B cell follicles of secondary lymphoid tissues during immune response to the viral infection. The infection of gammaherpesvirus exploits this structure for their benefit to establish long term latency in memory B cells

Table 1.3 Main chemokines, chemokine receptors and chemokine binding proteins that are encoded by herpesvirus and poxvirus.

virus	**Gene name**		
	chemokines	**vGPCRs**	**vCKBPs**
HSV-1,2			Glycoprotein G
HCMV	UL128, UL146 and UL147	UL33, UL78, US27 and US28	
HHV-6	U83	U12 and U51	
EBV		BILF	
KSHV	vCCL1, 2 and 3	ORF74	
MHV-68		ORF74	M3
Myxoma virus (MV)			M-T7 M-T1
Vaccinia virus			vCCI

(Babcock et al., 1998; Flano et al., 2002). Therefore, the study of GC is an important aspect to learn of gammaherpesvirus infection.

1.5.1 Formation and structure of GC

B cells which has membrane bound recombination of immunoglobulins (Ig) are generated from bone marrow. The naïve B cells aggregate at primary follicles in the secondary lymphoid tissue. During the immune response to antigens, foci of rapidly proliferating B blast cell begin to appear within the primary follicles of peripheral organs. Then this structure becomes the secondary follicle, surrounded by a mantle of concentrically packed, resting, small B-lymphocytes possessing both membrane-bound IgM and IgD, called GC. The differentiation of B cells occurs in the GC. First, B blast cells differentiate to centroblasts, which have downregulated surface immunoglobulins which undergo affinity maturation generated by somatic hypermutation (SHM) and class switch recombination in the dark zone. Thereafter, centroblasts develop into smaller and nondividing centrocytes in the light zone, where they contact the T follicular helper (T_{FH}) cells and follicular dendritic cells (FDCs) (Cyster, 2010). It has been found that most MHV-68 infected GC B cells are centroblasts, and only about 20% of GC B cells are centrocytes (Collins and Speck, 2012). Homeostatic chemokines are requisite for the formation of GC. The migration of centroblast and centrocyte is not a one way route, which involves two chemokine-receptor pairs, CXCL12-CXCR4 and CXCL13-CXCR5, playing a competitive role in homeostatic circulation of B cells. CXCL12 and CXCL13 are

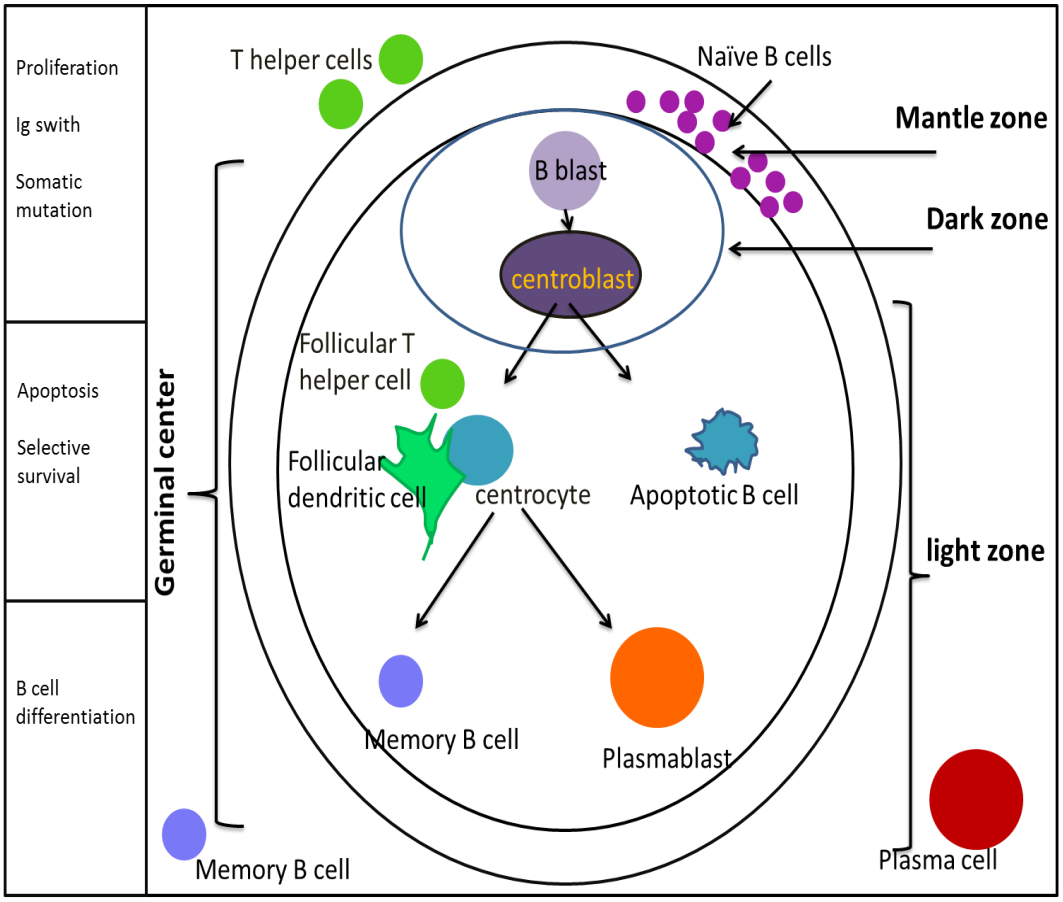

Figure 1.3 Diagrammatic stretch of GC and the development of B cells. Adapted from Roitt's Essential Immunology 11th Edition.

constitutively expressed by stromal cells in the follicular region. Centroblasts express higher CXCR4 than centrocytes. Meanwhile, CXCL12 was found to be more abundant in the dark zone than in the light zone. As a result, the upregulation of CXCL12 or CXCR4 drives the positioning of GC B cells to the dark zone (Allen et al., 2004). Higher levels of CXCL13 are found in the light zone and CXCR5 is expressed on centrocytes. However, CXCR5 is less likely to contribute to the GC dark zone and light zone polarization as shown by studies of CXCR5 deficient mice (Allen et al., 2004). Most centrocytes die from apoptosis without encountering antigens which are presented by FDC or without the help of T_{FH} cells. The rest of the centrocytes mature and differentiate into memory B cells or immunoblast plasma cells (reviewed in Victora and Nussenzweig, 2011) (figure 1.3). The memory B cells still maintain the ability to differentiate into plasma cells when they re-encounter antigens (Tarlinton, 2006).

1.5.2 GC reaction and its regulators

The GC reaction is helper T-cell-dependent and generates antigen-specific humoral immune responses in the secondary lymphoid organs. Proliferating B cells, T_{FH} cells and the specialized FDCs, which augment the latter stage of the primary immune response, are involved in the GC reaction. The function of the FDCs is to trap and retain unprocessed antigens through Fc and complement receptors, then present them to B cells. FDCs also provide signals to prevent apoptosis of GC B cells and stimulate cellular interaction and proliferation (reviewed in Ngo et al., 1999). In

addition, FDCs are a major source of CXCL13 in GC light zones, whereas T_{FH} cells express CXCR5. The intimate pairing of the GC B cells and T_{FH} cells is also apparent at the molecular level, at which both cell types require the transcription factors Bcl-6 and interferon regulatory factor 4 (IRF4) and the absence of the B lymphocyte-induced maturation protein-1 (Blimp-1). The GC reaction is suppressed by follicular regulatory T cells (Treg) (Chung et al., 2011).

The GC response is regulated by several sophisticated elements. Bcl-6 is reported to be a critical regulator for GC B cell phenotype (Basso and Dalla-Favera, 2010; reviewed in Victora and Nussenzweig, 2011). The transcription of Bcl-6 in B cells is up-regulated during the GC stage which is important for producing high-affinity antibodies (reviewed in Victora and Nussenzweig, 2011). The role of Bcl-6 has been studied in diffuse large B cell lymphoma. It has been shown that the expression of Bcl-6 in GC B cells requires the regulation of IL-21 (Linterman et al., 2010). Bach2 is another crucial transcriptional regulator that promotes GC formation and antibody class switch recombination (CSR) (Muto et al., 2004). Blimp-1 expression reduces both Bcl-6 mRNA and protein levels (Shaffer et al., 2002). Moreover, it is vital for B cell proliferation and antibody class switching. IRF4 has a dose-dependent function, in low concentrations promoting GC formation and CSR; whereas higher concentrations repress Bcl-6 and activate Blimp-1 (Klein et al., 2006; Sciammas et al., 2006).

Bcl-6 is also a master regulator of T_{FH} differentiation as it represses the expression of

microRNAs that target several key T_{FH} genes products, such as CXCR5 (Yu et al., 2009). Overexpression of Bcl-6 also regulates PD-1, but represses the master regulators like T-bet, RORγt and GATA-3 that are requisite for the development of other helper T cells (Kusam et al., 2003). T_{FH} cells are the key factor in GC formation and are potent inducers of affinity-matured antibody production during co-culture with B cells. Therefore, T_{FH} cells are designated as a T helper cell subset. After T helper cells are activated by antigens, CXCR5 expressing T_{FH} cells are relocated from the T zone into the B cell follicles. However, CXCR5 expression is transient and T_{FH} cells cease to exist during extended T cell expansion (Moser and Ebert, 2003). T_{FH} cells also express PD-1, which affects the development of T_{FH} cells and controls the function of T_{FH} cells, for example the reduced cytokine synthesis from T_{FH} is found in the lack of PD-1 signal environment (Good-Jacobson et al., 2010).

1.5.3 The differentiation of plasma cells

There are two types of plasma cell formation that are developed from activated B cells. Firstly, extrafollicular B cells that proliferate and terminate differentiation into short-lived plasma cells without somatically mutated immunoglobulin genes. These cells secrete antibodies and provide a rapid initial response to pathogens. Secondly, B cells move into B cell follicles and then proliferate, followed by a GC response. This is accompanied by affinity maturation and CSR of immunoglobulin. Afterwards, the B cells differentiate into long-lived plasma cells, then migrate to the bone

marrow where the subsets live for a long period (reviewed in Allen, Okada, and Cyster, 2007; reviewed in Shapiro-Shelef and Calame, 2005). When the B cells differentiate to plasma cells, the proliferation of B cells is stopped, the synthesis and secretion of Igs are increased. Meanwhile the CXCR4 is up-regulated which results in plasma cells leaving the GCs and homing to peripheral tissues (Tokoyoda et al., 2004). Several regulatory factors affect the differentiation of plasma cells. For example, Blimp-1 and Xbp-1 induce plasma cell differentiation, whereas Pax5, Bcl-6 and Bach2 promote the B cell programme that inhibits the development of plasma cells.

1.6 Project outline

The role of M4 protein has been examined *in vivo* by comparing viral latency in the spleens following infection with WT and M4stop virus (Evans et al., 2006; Geere et al., 2006), but how M4 protein benefits MHV-68 infection has not been fully understood from these publications. Therefore, the role of M4 was studied in this project. The main methods used in this study were: (1) investigation of the chemokine binding ability of M4 by ELISA using recombinant M4 protein; (2) comparison of host immune responses by flow cytometry; (3) understand the gene expression by PCR arrays and qPCR. The initial objective was to confirm whether M4 protein is a chemokine binding protein, and how it influences the interaction of chemokine and GAGs. A second objective was to study the effects of M4 protein on the activation of lymphocytes. The third aim was to investigate whether M4 protein

influence the GC development. The final objective was to assess whether M4 protein affect the pathogenesis of MHV-68 in IFN-$\gamma R^{-/-}$ mice.

Chapter 2

Materials and Methods

2 Materials and Methods

2.1 Cell Culture techniques

2.1.1 Cell lines and counting of cells

Cell lines were maintained in tissue culture plastic flasks (Nunc, UK). Baby hamster kidney fibroblast cells (BHK-21 cells) (Usherwood et al., 2005) were cultured at 37℃ with a humidified atmosphere of 5% CO_2. *Spodoptera frugiperda* insect cells (Sf9 cells) (Smith and Cherry, 1983) and *Trichoplusia ni* insect cells (High-Five cells) (Granados et al., 1994) were cultured at 27℃ and sub-cultured when the flask reached 90% confluence.

For quantification of the cell number, cells were 1 : 1 diluted (50μl of cells were mixed with 50μl 0.1% trypan blue (w/v)) or 1 : 9 diluted (10μl of cells were mixed with 90μl trypan blue) and the number of un-stained viable cells was counted using a haemocytometer under a microscope. The cell number was calculated by following calculation:

Cell number per ml= unstained cell count ×the dilution factor $\times 10^4$

2.1.2 Monolayer cultures

BHK-21 cells were maintained in Glasgow Modified Eagle's Medium (GMEM, Invitrogen, UK), supplemented with 2mM L-glutamine (Invitrogen, UK), 100U/ml penicillin (Invitrogen, UK), 100μg/ml streptomycin (Invitrogen, UK), 10% (v/v) new

born calf serum and 10% (v/v) tryptose phosphate broth (TPB, Invitrogen, UK) (complete GMEM). For sub-cultured cells, medium was discarded, and cells were washed with 0.02% (w/v) versene, followed by incubating with 10ml of 0.25% (w/v) trypsin (Invitrogen, UK) till the cells could be removed from the surface of the flask by gently tapping. An equal volume of complete GMEM was utilized to neutralize trypsin, and cells with medium were collected in a plastic universal tube and centrifuged at 450 × g for 5 minutes. The supernatant was discarded and the cell pellet was re-suspended in complete GMEM. 5×10^6 cells were re-seeded into a new 175cm^2 tissue culture (TC 175cm^2) flasks with 35-40 ml of medium.

Sf9 cells were grown in Sf-900 Ⅱ SFM medium (Invitrogen, UK), supplied with 100U/ml penicillin, 100U/ml streptomycin and 100μg/ml gentamycin (complete Sf-900 Ⅱ SFM medium). To sub-culture the Sf9 cells, 20ml of medium was removed from a total 25ml volume medium. The cells were dislodged by gently tapping the flask. 1×10^7 cells were re-seeded into a new TC 175cm^2 flask in 25ml of fresh complete Sf-900 Ⅱ SFM medium.

High-Five cells were grown in EXPRESS-FIVE™ SFM medium (Invitrogen, UK), supplemented with 18mM of L-glutamine and 100U/ml penicillin and 100U/ml streptomycin (complete EXPRESS-FIVE™ SFM medium). For passaging the cells, the monolayer was dislodged by tapping the flask. 9×10^6 cells were re-seeded into a fresh TC 175cm^2 flask with 25ml of complete EXPRESS-FIVE™ SFM medium.

2.1.3 Suspension cell cultures

The Sf9 cells were harvested from monolayer cell culture and then seeded in a spinner flask at a density of 10^6 cells/ml in complete Sf-900 Ⅱ SFM medium, incubated at 27℃ stirring rate at 75 rpm. An appropriate volume of the medium was added to maintain the density of the cells. For suspension culture, High-Five cells growth medium contained tissue culture grade heparin (Invitrogen, UK) at 10U/ml.

2.1.4 Cryopreservation and recovery of cells from liquid nitrogen

Cells were harvested when in exponential growth phase. BHK-21 cells and insect cells were centrifuged for 5 minutes at 450 × g and 200 × g respectively. The cell pellet was re-suspended with 10ml freezing media (10% (v/v) dimethylsulphoxide (DMSO) and 20% (v/v) fetal calf serum in medium) to allow 1ml per cryovial of cells at a density of 2-5 × 10^6 cells. These vials were then placed in liquid nitrogen storage tank for long-term storage. Insect cells were retained in -80℃ freezer for 24 hours before preserved in liquid nitrogen.

In order to recover the cells, the vials were taken out from liquid nitrogen storage tank and defrosted in a 37℃ water bath. Insect cells were half defrosted and a few droplets of warmed medium were added in the vial in order to equilibrate the osmotic pressure slowly. For the BHK-21 cells and High-Five cells, the DMSO was removed by centrifugation at 450 × g and 200 × g respectively. Cell pellets were re-suspended in 5 ml of warm growth medium and transferred into a TC 25cm^2 flask for routine

culture. For Sf9 cells, the cells which were maintained in freezing medium were cultured with 4ml of growth medium in a TC 25cm^2 flask and incubated at 27℃ for 1 hour to allow the cells attach the flask, and then the medium was replaced by fresh complete Sf-900 Ⅱ SFM medium.

2.2 Virological Methods

2.2.1 Preparation of virus stock

2.2.1.1 MHV-68 virus stock

Stocks of MHV-68 were generated in BHK-21 cells. 1 × 10^7/ml of cells were resuspended in complete GMEM and infected with MHV-68 at a multiplicity of infection (MOI) of 0.001. The cells and virus were incubated for 1.5 hours at 37℃ with shaking and seeded at 2 ×10^6 cells per flask in TC 175cm^2 flasks. The infected cells were incubated at 37℃ for 5-7 days. Then the cells were dislodged by scraping or gently tapping the flask and centrifuged in 2000 × g at 4℃ for 20min in universal tubes. The pellet was resuspended in 5-10ml of sterile phosphate buffered saline (SPBS) and homogenized with 20-30 strokes in a chilled Dounce homogenizer. The homogenate was transferred to a glass universal and sonicated in an iced water-bath for 15 minute. The homogenate was centrifuged in 2000 × g at 4℃ for 20 minutes and the supernatant was transferred to a clean universal tube. The pellet was resuspended in 1ml SPBS, re-homogenised and centrifuged in 2000 × g at 4℃ for 20min. The two supernatants were mixed, aliquoted and stored at -80℃.

2.2.1.2 Recombinant Baculovirus stock

Stock of baculovirus was produced in Sf9 cells. Sf9 cells were infected with baculovirus at a MOI=0.1 for 30 minutes at room temperature. Approximately 1.5 × 10^7 cells were re-seeded in a TC 175cm^2 flask with 25ml of medium and incubated for 72 hours at 27℃. The baculovirus was harvested by centrifuging the cells with medium in 2000 × g for 10min at 4℃. The supernatant was reserved as a virus stock covered with tin-foil at 4℃.

2.2.2 Titration of virus

2.2.2.1 Titration of MHV-68

Serial dilutions of the virus were prepared (10^{-2} to 10^{-9}) in 4ml medium in bijoux tubes. 200μl of BHK-21 cells at a density of 10^7 were added to each virus dilution and incubated for one hour at 37℃ with constant shaking. Each mixture was transferred to two 60mm culture plates (Falcon, Becton, Dickinson and Company, USA), followed by adding 3ml of complete GMEM on each plate. The infected cells were incubated at 37℃ supplied with 5% CO_2 for 4 days. Uninfected cells were also seeded at the same density in the plates as a negative control. After removal of medium, cells were fixed in 10% (v/v) neutral buffered formaldehyde (NBF, Leica Microsystems, Germany) for 30 minutes. After removing the NBF, 3ml of 0.1% (w/v) toluidine blue was added to stain the cells for 5 minutes. Then the dye was removed. Virus plaques were counted and virus titre was calculated as plaque forming units

(PFU/ml).

Titre=number of plaques × dilution/ final volume of virus plus cells added to the plate

2.2.2.2 Titration of baculovirus

Approximately 10^6 of Sf9 cells were seeded in duplicate 35mm culture plates with 2ml complete Sf-900 Ⅱ SFM medium, incubated at 27℃. The medium was removed 1 hour later and the serially diluted virus was added with 200μl medium to the plates. Meanwhile, 200μl medium was added to the control plates. The medium was discarded after 1 hour incubation and the plates were overlaid with 1ml 1 : 1 low-melt agarose (3% dissolved in water, steriled, Flowgen MicroSieve, UK) and Sf900 Ⅱ SFM medium mixture. The solidified agarose was covered with 2ml of medium and the cells were incubated at 27℃ for 5 days. After discarding the medium, the cells were stained with 2ml of 0.02% neutral red solution (diluted from 0.1% (w/v) stock and filtered, MP Biomedical, USA) and incubated for another 2 days at 27℃. The plaques were counted within 1 hour after removing the dye.

2.3 Recombinant baculovirus expressing system

2.3.1 Preparation of Bacmid

0.1M IPTG and X-gal were overlaid on 1.5% Luria-Bertani (LB) agar plates containing 50μg/ml kanamycin, 7μg/ml gentamicin, 10μg/ml tetracycline. E.coli

containing the M3 bacmid (a gift from Prof. J. Stewart) was streaked on the agar. They were cultured at 37℃ 12-16 hours and white colonies were picked and grown in 10ml LB broth with same concentration of antibiotics.

Plamid DNA was prepared by QIAprep Spin Miniprep Kit (Qiagen, Germany) according manufacturer's instructions. 1-5 ml overnight cultured E. coli was centrifuged at 6000 × g for 3 minutes and pellet was resuspended completely by vortexing in 250μl Buffer P1 contained RNase and lyseblue until cell clumps disappeared. The mixture was transfer to a microcentrifuge tube, followed by adding 250μl Buffer P2, and mixed thoroughly by inverting the tube 4-6 times. 350μl Buffer N3 was added and mixed immediately and thoroughly by inverting the tube 4-6 times. The mixture was centrifuged at 10000 × g for 10 minutes in a table-top microcentrifuge. The supernatant was loaded on a QlAprep spin column placed in a 2ml collection tube, and centrifuged at 6000 × g for 1 minute and the flow-through was discarded. The column was washed with 0.5ml Buffer PB and 0.75ml Buffer PE respectively by centrifuging at 6000 × g for 1 minute and flow-through was discarded. The column was dried by centrifuging for an additional 1 minute and then placed in a clean 1.5ml microcentrifuge tube. The plasmid was eluted by 50μl Buffer EB (10mM Tris-Cl, pH 8.5) which was added to the centre of the column standing for 1 minute and centrifuged the column at 6000 × g for 1 minute.

The concentration of plasmid DNA of each sample was quantified by using a spectrophotometer (NanoDrop 1000, Thermo Scientific, USA). For measurement of

the quantity of DNA, 1µl of each sample was evaluated. The concentrations of DNA samples were automatically calculated as in ng/µl and A260:A280 ratio was also recorded.

100ng of DNA was amplified by primer pair M3RTPCR For 5' and M3RTPCR Rev 3'. Polymerase chain reaction (PCR) was carried out using Invitrogen Taq DNA polymerase system (Invitrogen, UK). A typical reaction mixture consisted of 100ng of template DNA, PCR reaction buffer (20mM Tris (pH 8.4), 50mM KCl), 100 µM of each dATP, dCTP, dGTP and dTTP, 50pmol of each primer (MWG-biotech, Germany) and 5U of Taq DNA polymerase. The mixture was overlaid with approximately 40 µl of mineral oil to prevent evaporation. PCR conditions were 1 cycle of 3 minutes at 95 ℃, followed by holding at 80 ℃ to add Taq DNA polymerase, followed by 35 cycles of denaturation at 94 ℃ for 45 seconds, primer annealing at 55 ℃ for 45 seconds, and extension at 72 ℃ for 1 minute, and finishing with 7 minutes incubation at 72 ℃. The PCR product was analyzed by electrophoresis.

10µl of each PCR reaction product was mixed with 5 µl of the loading dye and electrophoresed through a 1.5% (w/v) agarose gel (Seakem® LE Agarose, Lonza, Switherland) in 50ml Tris-acetate-EDTA (TAE) buffer. 0.5 µg/ml (w/v) ethidium bromide (Sigma, UK) was added to the gel whilst molten to allow visualization of the DNA fragments. The appropriate volume of 10 × loading buffer (0.25% (w/v) orange G, 0.15% (w/v) Ficoll) was added to the DNA samples and 100bp DNA ladder (Invitrogen, UK) respectively, which were loaded into the set gel. Samples

and DNA ladder were then subjected to electrophoresis at 80 volts in TAE buffer for 60 minutes. The gel was placed in the documentation gel station (Alpha Innotech, Fluor Chem HD2, USA) and exposed under the ultra-violet light. The image was captured by the Innotech camera.

2.3.2 Transfection of baculovirus

The recombinant bacmid DNA was transfected into Sf9 cells by Effectene® Transfection Reagent (Qiagen, Germany). 9×10^5 Sf9 cells were seeded in a 6-well plate for 1 hour and then transfected by following the manufacture protocol. 0.4 µg DNA was dissolved in TE buffer with the DNA-condensation buffer EC, to a total volume of 100 µl. 3.2 µl Enhancer was added and mixed by vortexing for 1 minute. The mixture was incubated at room temperature for 2-5 minutes and centrifuged for a few seconds to remove the drops from the top of the tube, and then mixed with 10 µl Effectene Transfection Reagent by pipetting up and down five times. Transfection-complex was formed by incubating the mixture for 5-10 minutes at room temperature. After that, the Sf9 cells growth medium was replaced by 1.6ml fresh medium. 600 µl growth medium was mixed with the transfection complexes by pipetting up and down twice, and immediately added onto the cells. The mixture and medium were mixed by gently swirling. The cells were incubated with transfection complexes for three days under normal growth conditions. At that point, the M3 baculovirus containing medium was collected by centrifugation at 2000 × g for 5 minutes. To increase the titre of M3 virus, 100 µl of the supernatant was added in a

new 6-well plate which contained 9 × 10^5 Sf9 cells and 2ml growth medium each well. The cells were sub-cultured for another four generations till the plaques were observed easily and supernatant of each culture was harvested as M3 recombinant baculovirus.

2.3.3 Expression and purification of baculovirus recombinant protein (M1, M3 and M4)

500ml of High-Five cells were cultured to a density of 1 × 10^6/ml in a 1 liter spinner flask. 25ml cells were first infected by 1.25 × 10^9 recombinant M3 or M4 baculovirus (MOI=2.5 for the whole number of High-Five cells in the spinner flask) in 50ml tubes for 30 minutes, then the virus and infected cells were pipetted into a spinner flask containing the rest of cells at a spin rate of 60rpm and incubated for exactly 72 hours at 27℃. For M1 recombinant baculovirus, the cells were infected at MOI of 1. The supernatant was centrifuged at 2000 × g for 10 minutes and pooled. Proteases were inhibited by adding Pefabloc SC (Roche, Switzerland) to give a final concentration of 1mM. The supernatant was pipetted into snakeskin pleated dialysis tubing (Pierce, USA) and dialyzed at 4℃ against 5 litres of 20mM Na_2HPO_4, 500mM NaCl, 20mM imidazole, pH8.0 (adjusted by 1M NaH_2PO_4) for at least 4 hours and the dialysis was repeated twice. The supernatant was aliquoted into BD Falcon™ 50ml tubes (Becton, Dickinson and Company, USA) and centrifuged at 2000 × g for 10 minutes at 4℃. The supernatant was transferred to new BD Falcon™ 50ml tubes, followed by adding Pefabloc SC to give a final concentration

of 1mM. 1.5ml Ni-sepharose 6 fast flow resin (GE, Germany) was prepared by washing with H_2O twice and dialysis buffer three times. The resin was equally allocated to each tube and mixed with the supernatant. After rotating at 4℃ for 2 hours, the mixture was centrifuged at 200 × g for 5 minutes and the resin was pooled and poured into a 10ml Amersham column (GE healthcare, USA). The column was attached to a pump giving a fluid speed set to 1ml every 3 minutes. The protein was washed by dialysis buffer containing 1mM Pefabloc SC at 4℃ overnight. The protein fractions were collected in RNA-free non-stick tubes (Ambion, USA) by eluting with 10ml of 40mM imidazole buffer, 10ml of 125mM imidazole buffer and 5ml of 250mM imidazole buffer consecutively. The entire elution buffer contained 50mM Na_2HPO_4, 300mM NaCl, 5% glycerol and 1mM Pefabloc SC. Recombinant M3 and M4 protein contain a C-terminal penta-histidine (His) tag. The protein was stored in 4℃ in the dark.

2.4 Protein techniques

2.4.1 SDS-PAGE and western blotting

Proteins were separated by sodium dodecyl sulfate polyacrylamide gel electropheresis (SDS-PAGE) followed by western blotting. 20μl of each protein fraction was boiled with 5 × loading buffer (20% (v/v) glycerol; 2% (v/v) SDS; 0.125mM Tris pH 6.8; 0.4% (w/v) bromophenol blue; 5% (v/v) 2-ME for 5 minutes before loading onto the gel (resolving gel: 10% acrylamide/ bisacrylamide;

0.375M Tris pH 8.8; 0.1% (v/v) SDS; 0.1% (w/v) ammonium persulphate (AP); 0.01% (v/v) Tetramethylethylenediamine (TEMED). Stacking gel: 3.4% (w/v) acrylamide/ bisacrylamide; 140mM Tris pH 6.8; 0.1% (w/v) SDS; 0.05% AP; 0.01% (v/v) TEMED). One appropriate size of Amersham Hybond-E4 nitrocellulose membrane (GE healthcare, USA) was cut and rinsed with distilled H_2O. The nitrocellulose membrane and 9 pieces of same sized filter paper was soaked in semi-dry transfer buffer (25mM Tris base, 150mM glycine, 10% (v/v) methanol) with gentle agitation on a platform shaker for 5 minutes. 6 pieces of filter paper was placed on western blotting chamber, covered with nitrocellulose membrane, SDS gel, followed by 3 pieces of filter paper. The protein fractions were transferred to nitrocellulose membrane by 0.65mA/cm^2 for 90 minutes. Non-specific binding was blocked by TBS-milk (3g Marvel skimmed milk powder was dissolved in 100ml 1 × TBS (10 × TBS buffer, pH7.4, Severn Biotech Ltd.)). The 6 × His-tagged protein was probed with the mouse anti penta-His tag antibody (Qiagen, Germany) followed by washing with TBS. After that, rabbit anti-mouse IgG biotin (Sigma-Aldrich, USA) was used to detect the first antibody. Then, the membrane was washed with TBS-Tween (TBS with 4% Tween-20) and TBS only, followed by incubation with Streptavidin-Alkaline Phosphatase (Roche, Switzerland). Cxcl4 protein was detected with rat anti Cxcl4 (R & D System, UK) followed by biotinylated mouse anti rat antibody and Streptavindin-Alkaline Phosphatase. The membrane was washed as described for detection of His-tagged protein. At the final step, the membrane was

developed by SIGMAFAST BCIP/NBT (Sigma-Aldrich, USA). The dilution of each antibody was listed in Appendix I.

2.4.2 Coomassie staining

The purification of the protein fractions were determined by Coomassie staining. The SDS gel was incubated in Coomassie stain (0.25% (w/v) Coomassie Blue R250 (Sigma, UK); 40% (v/v) methanol; 7% (v/v) acetic acid) with shaking for at least 1 hour. After a brief rinse with de-stain (50% (v/v) methanol; 10% (v/v) acetic acid) gels were incubated in de-stain until bands were clear.

2.5 Enzyme-linked immunosorbent assay (ELISA)

2.5.1 The binding of recombinant protein and chemokines

ELISAs were performed in 96-well microtiter plates (Thermo, USA). The bottom of each well was coated with SPBS diluted Cxcl2, Cxcl5, CXCL8 (20ng each well, Pepro Tech, USA) respectively for 16 hours at 4℃. Weakly adherent chemokines were washed off three times with washing buffer (TBS, Severn Biotech, UK, containing 0.05% (v/v) Tween 20, 0.1% (w/v) bovine serum albumin (BSA)) rinses. After washing, the wells were blocked with the blocking buffer (TBS, containing 0.05% (v/v) Tween 20, 0.1% (w/v) BSA) for 8 hours at 4℃. After washing 3 times with washing buffer, the wells were incubated with blocking buffer diluted M4 protein for 16 hours at 4℃. M3 protein was used as a positive control, and imidazole buffer was used as a negative control. Then the solution was removed and the loosely

adherent proteins were washed off as before. To detect the bound M3 or M4 protein, a primary antibody (Qiagen, Germany) which would bind to 6 × His-tag produced in a mouse was diluted in blocking buffer and added to each well for 2 hours at 4℃. The plates were repeatedly washed three times with washing buffer. HRP conjugated goat anti mouse IgG (AbD Serotec, UK) was used as a secondary antibody that diluted in blocking buffer and incubated for additional 1 hour at 4℃ in the dark. The plates were washed three times with washing buffer to remove the unbound secondary antibody. At each step a volume of 100μl was added to the well. SIGMFAST™ OPD (Sigma-Aldrich, USA) which was used as a substrate at the final step was dissolved in 20ml H_2O. 200μl of SIGMFAST™ OPD solution was added in each well, and the plates were covered with tin-foil paper for 45 minutes. The reaction was stopped by addition of 50μl 3M H_2SO_4 and the absorbance at 492nm was measured using ELISA plate reader (Glomax, Promega, USA).

Alternatively, wells of microtiter plates were coated with SPBS diluted M4 protein for 14 hours at 4℃. M3 protein and imidazole were used as positive control and negative control respectively. After the protein was bound to the wells, the plates were washed three times with washing buffer and blocked with blocking buffer for 8 hours. After the plates were repeatedly washed for three times, 1ng, 10ng and 20ng of blocking buffer diluted Cxcl4 (R & D System, UK) was added and plates were incubated for 16 hours at 4℃. The unbound Cxcl4 was removed by washing three times with washing buffer. Blocking buffer diluted rat anti-Cxcl4 was used to detect

bound Cxcl4 by incubating for 2 hours at 4℃. The plates were repeatedly washed with washing buffer as before. Goat anti Rat IgG-HRP (AbD Serotec, UK) was used as secondary antibody and incubated for 1 hour at 4℃ in the dark. At each step, 100µl of agent was added. After washing off the unbound enzyme, SIGMFAST™ OPD (Sigma-Aldrich, USA) was dissolved in H_2O, and 200µl of solution was loaded in each well. The plate was covered with tin-foil paper for 45 minutes and the reaction was stopped by addition of 50µl 3M H_2SO_4 and the absorbance at 492nm was measured using ELISA plate reader. The dilution of the antibodies was listed in Appendix I.

2.5.2 The binding of M4 and heparin

Streptavidin coated plates (Thermo scientific, USA) were washed three times with washing buffer to rehydrate. Porcine intestinal mucosa biotin conjugated heparin (Calbiochem, USA) was added in each well. The plate was shaken constantly for 2 hours at room temperature and then shaken constantly for 1 hour on a shaker at 4℃. After 1 hour the unbound heparin was washed off with washing buffer. M4 was diluted with the blocking buffer and incubated with heparin coated plate for 14 hours at 4℃. For this step, 1ng or 20ng Cxcl4 was used as a positive control. After incubation, the plate was washed three times with washing buffer as before. Mouse anti-penta His antibody was used to detect bound M4 which was diluted in blocking buffer and incubated for 1 hour at 4℃. Goat anti mouse IgG HRP was diluted in blocking buffer and incubated with constantly shaking at room temperature for 1

hour in the dark. The reaction was stopped by addition of 50µl 3M H_2SO_4 and the absorbance at 492nm was measured using ELISA plate reader. As Cxcl4 was used as a positive control, rat anti Cxcl4, and HRP conjugated goat anti rat were used to detect bound Cxcl4.

2.5.3 Competitive ELISA

The binding of heparin-biotin to streptavidin coated plate was described above. The unbound biotinylated heparin was washed off, followed by adding blocking buffer diluted M4 protein which contained 1 or 10µl M4 protein, 14ng Cxcl4 was loaded and incubated. At this step, blocking buffer diluted M3 protein which contained 0.1, 1 or 10µl M3 protein and imidazole were used as positive control and negative control respectively. After incubation for 14 hours at 4℃, the plate was washed with washing buffer. To detect bound Cxcl4, rat anti-Cxcl4 was diluted and incubated for 2 hours at 4℃. After washing the plate as before, goat anti rat-HRP was diluted in blocking buffer and incubated for 1 hour at 4℃. 100µl of diluted agent was added for each step. After washing the plate three times, SIGMFAST™ OPD (Sigma-Aldrich, USA) was dissolved in H_2O, and 200µl of solution was added. The plate was covered with tin-foil paper for 45 minutes. The reaction was stopped by addition of 50µl 3M H_2SO_4 and the absorbance at 492nm was measured using ELISA plate reader.

2.6 Magnetic Cell Sorting (MACS) technique

2.6.1 Chemokine binding ability assayed by MACS

Monoclonal anti-6 × His antibodies were coupled to paramagnetic μMACS™ MicroBeads for specific isolation of His-tagged proteins. The magnetically labeled proteins were passed over and retained in μ Columns that provide a strong magnetic field when placed in a μMACS separator. After the non-labeled material was washed by wash buffer, the magnetically labeled material was eluted by suitable elution buffer. The anti-His MACS^{TM} MicroBeads beads kit, μ column and μMACS separator were bought from Miltenyi Biotec. M4 protein supernatant was collected from small scale M4 baculovirus infection which High-Five cells were infected in TC 25cm^2 flask (MOI=2.5) for 72 hours. 50μl of M4 protein supernatant or 50μl of 10 times diluted M4 protein supernatant (5μl of M4 protein supernatant containing 45μl imidazole mixture) was mixed with 40μl of beads, 250ng of Cxcl4 and 1mm Pefabloc in non-stick tubes respectively. To mix them, the tubes were rotated at 20rpm for 30 minutes at 4℃. During this procedure, the column was prepared by standing in the separator and washed with 200μl lysis buffer. After 30 minutes, the mixture was run through the columns and the flow through was collected. Later on, the columns were washed with four times with 200μl wash buffer I and 100μl wash buffer II once as described in the manufacturer's protocol. In the meantime, the elution buffer was prepared by heating at 95℃. To break the binding of anti His-tag beads and protein, 20μl of elution buffer was added to the columns, and incubated

for 5 minutes. Additional 50μl of elution buffer was added to the columns, and the flow-through was collected in a new non-stick tube. A mixture containing 45μl of 125mM imidazole elution buffer, 5μl M3 protein supernatant and same amount of Cxcl4 was used as a positive control. A mixture containing 50μl 125mM imidazole buffer with same amount of Cxcl4 was used as a negative control. The collections were loaded in duplicate and separated by Tris-HCL 4-20% precast gel (Biorad, USA) followed by western blotting as described before. One of the duplicated samples was probed with the mouse anti penta-His tag antibody followed by rabbit anti-mouse IgG biotin and Streptavidin-Alkaline Phosphatase. The membrane was developed by substrate SIGMAFAST BCIP/NBT (Sigma-Aldrich, USA). The other duplicated sample protein was detected by rat anti-Cxcl4, mouse anti rat-biotin and streptavidin-alkaline Phosphatase. The colour was generated by adding SIGMAFAST BCIP/NBT.

2.7 Infection and sampling of Mice

BALB/C mice, Wild type 129Sv mice and IFN-$\gamma R^{-/-}$ mice on the 129Sv mice background (Huang et al., 1993) were purchased from Bantin and Kingman, Hull, United Kingdom and bred in house. MacGreen mice (Sasmono et al., 2003) were a gift from Prof. David Hume. Age and sex matched mice were anaesthetized with isoflurane (Merial Animal Health Ltd.) and intranasally inoculated with 4×10^5 PFU of wild-type BAC-derived virus PHA4 (WT virus) or M4 mutant virus M4in2 (M4stop virus) in 40μl of sterile PBS.

At appropriate time point, the mice were sacrificed by CO_2 inhalation. Lungs from BALB/C, 129Sv and IFN-$\gamma R^{-/-}$ mice were removed and kept frozen. Lungs from MacGreen mice were infiltrated with 4% paraformaldehyde and immersed in the paraformaldehyde. Spleens from 129Sv and IFN-$\gamma R^{-/-}$ mice were placed in completed RPMI-1640 medium (Invitrogen, UK) supplemented with 2mM L-glutamine, 100U/ml penicillin, 100ug/ml streptomycin, 10% fetal calf serum, 2-ME and 25mM N-2-hydroxyethylpiperazine-N-ethane-sulphonicacid (HEPES) and weighed. Pieces of spleen from 129Sv mice were cut from the middle part of each spleen and placed in RNAlater® Soln (Ambion, USA) for PCR array or put into NBF for histology analysis. Spleens from MacGreen mice were fixed in 4% paraformaldehyde for section cutting.

In order to prepare cytospin, fresh splenocytes of MacGreen were isolated and red blood cells were lysed by adding 1ml H_2O, followed by mixing with 9ml SPBS immediately. The cells were counted and made to a concentration of 2×10^6 cells/ml. The slides (Wablemar Knittel, Germany) were prepared by mounting with the Shandon filter cards (Thermo Scientific, USA) and the cuvette in the metal holder. 500µl of PBS was loaded in each cuvette, followed by centrifugation with Shandon cytospin 2 (Thermo Scientific, USA) at 1000 rpm for 2 minutes. 200µl of cells were loaded and centrifuged at 1000 rpm for 5 minutes. The cells were dried at room temperature, then fixed in 4% paraformaldehyde for 15 minutes at room temperature. After dryness of these cytospins, they were stored in -80°C.

2.8 Measure of virus load

2.8.1 DNA extraction

Total DNA was isolated from spleen using the DNeasy blood and tissue kit (Qiagen, Germany). Up to 25mg of tissue was cut into small pieces, placed in a 1.5ml microcentrifuge tube with 180µl Buffer ATL and 20µl proteinase K and was mixed by vortexing for 15 seconds. The mixture was incubated at 56℃ and vortexed occasionally until the tissue was completely lysed. 200µl Buffer AL was added to the sample, and mixed thoroughly by vortexing, followed by adding 200µl ethanol (96–100% (v/v)), and vortexing again. All the mixture was pipetted into the DNeasy Mini spin column placed in a 2 ml collection tube. The column was centrifuged at 6000 × g for 1 minute. The collection tube with flow-through was replaced with a new 2ml collection tube, and 500µl Buffer AW1 was added in the column, and centrifuged for 1 minute at 6000 × g. The column was put in a new collection tube and 500µl Buffer AW2 was added in the column and centrifuged for 3 minutes at 20000 × g to dry the DNeasy membrane. The collection tube with flow-through was discarded. A clean 1.5ml microcentrifuge tube was provided to collect DNA and 200µl Buffer AE was pipetted directly onto the DNeasy membrane and incubated at room temperature for 1 minute, and then centrifuged for 1 min at 6000 × g to elute. The quantity of DNA was measured by spectrophotometry.

2.8.2 qPCR

Virus genome load was determined by qPCR from 100ng spleen DNA. qPCR was performed in 20µl reaction mixture containing PCR reaction buffer (50mM Tris-HCl, 10mM KCl, 5mM $(NH_4)_2SO_4$, 20mM $MaCl_2$, pH8.8), 40µM each of dATP, dCTP, dGTP and dTTP, 0.7µl intercalating dye SYBR green, 0.15U FastStartTM Taq DNA polymerase (Roche) and 50pmol of each primer (ORF 73, ORF73For 5'-CGTCTGTCTCTCCTACATCTAAACC-3' and ORF73qPCRRev , 5'-CACCAA CACTTCCCTCATCC-3'; or glyceraldehydes-3-phosphate dehydrogenase (GAPDH), GAPDHFor 5'-CCCACTCTTCCACCTTCG-3' and GAPDHRev 5'-GGTCCAGGG TTTCTTACTCC-3', MWG-Biotech, Germany), and 100ng of DNA by using a Corbett Rotorgene (Corbett Research, UK). In all reaction, an initial denaturation step was carried out by incubation at 95℃ for 10 minutes. 40 cycles of amplification were carried out, which consisted of denaturation at 95℃ for 15 seconds, annealing at 62℃ for 20 seconds and extension at 72℃ for 20 seconds. Samples were quantitated by using a standard curve generated from the serial dilution of plasmid DNA containing cloned ORF73 or GAPDH sequence. All products from the quantitative PCR were analysed by using a melting curve to confirm specificity and the results were normalized against GAPDH. Efficiency of quantitative PCR was ＞ 95%

2.8.3 Measurement of virus load in the lung

The virus titre in the lung was determined by culturing the lung homogenate with BHK-21 cells. The lungs were chopped into small pieces and homogenised in 1ml of complete GMEM, followed by another homogenizing with 0.8ml complete GMEM. The lung homogenate was kept in -80℃ to disrupt cell membranes. The samples were thawed and centrifuged at 2000 × g for 5min at 4℃. 4ml serially diluted lung supernatants were mixed with 200μl BHK-21 cells at a density of 10^7 cells/ml in a bijoux and incubated for 1 hour with continuously shaking at 37℃. Then the virus and cells in each bijou were transferred to two 60mm culture dishes followed by adding 3ml complete GMEM and incubated at 37℃ with 5% CO_2 for 4 days. The plaques were counted after being fixed and stained as described for the titration for the MHV-68.

2.9 Infectious centre assay

Splenocytes were isolated from the spleen casing with a scalpel blade, producing a single-cell suspension in 5ml of complete RPMI-1640. The cell suspension was transferred to a pre-rinsed 20ml universal tube and centrifuged at 450 × g for 5 minutes. The supernatant was discarded and the pellet was re-suspended in remaining liquid. Erythrocytes were lysed as described before. Cell debris was allowed to settle before transfer of the splenocytes suspension to a fresh pre-rinsed universal tube. The sample was centrifuged at 450 × g for 5 minutes. The supernatant was discarded and

the cell pellet re-suspended in 5ml of complete RPMI-1640. The viable cell count of suspension was determined. Infectious centre assay was carried out by incubating 10^7, 10^6 or 10^5 splenocytes with 10^6 BHK-21 cells in 60mm tissue culture plates with 5ml complete RPMI-1640 medium for 5 days at 37C with 5% CO_2. As previously described, the cells were fixed and stained and infectious centres were counted when the plates were dried. The remaining splenocytes were frozen and thawed 3 times, and the volume equal to 10^7, 10^6 or 10^5 splenocytes were incubated with 10^6 BHK-21 cells in 4ml complete GMEM for 1.5 hours with continuously shaking at 37℃ and then the cells and medium was transferred to 60mm tissue culture plates, followed by adding 3ml of complete GMEM. Plates were fixed and stained after 4 days and plaques were counted.

2.10 Fluorescence activated cell sorting (FCS)

2.10.1 Cell phenotyping

The percentages of the splenocytes or percentages of activated splenocytes were determined by flow cytometry. 2.5×10^5 fresh splenocytes were labeled directly with combinations of the following monoclonal antibodies for 15 minutes at 4°C in the dark. $CD4^+$ T cells: anti-CD69-FITC (AbD Serotec, UK), anti-CD38-APC (Biolegend, USA) and anti-CD4-PE (Invitrogen, UK); $CD8^+$ T cells: anti-CD69-FITC, anti-CD38-APC and anti-CD8-PE (Invitrogen, UK); B cells: anti-CD69-FITC, anti-CD38-APC and anti-CD19-PE; NK cells: anti-CD49-FITC; anti-CD69-FITC,

anti-CD38-APC and anti-CD49b-PE (Biolegend, USA), or anti-CD49b-FITC only; T_{FH} cells: anti-PD-1-FITC (Biolegend, USA), anti-Cxcr5-APC (Pharmingen BD Biosciences, USA) and anti-CD4-PE; plasma cells: anti-CD138-PE (Biolegend, USA) and anti-CD19-APC/Cy7 (Biolegend, USA); macrophages and neutrophils: anti-CD11b-APC (Miltenyi Biotec), anti-Ly6G-PE (Biolegend, USA), and anti-CD69-FITC. After incubation, the cells were washed three times with FACS buffer (PBS containing 0.5% BSA and 0.02% sodium azide) and then 400μl FACS buffer and 2% NBF mixture (1 : 1) was added. The tubes were preserved in the dark at 4℃. The labeled cells were analysed in a FACSCalibur cell sorter (Pharmingen BD Biosciences, USA). $V\beta4^+CD8^+$ T cells: anti-CD8-PE and biotinylated anti-TCR Vβ4 (BD Biosciences, USA) was used to label splenocytes for 20 minutes in the dark at 4℃, then the cells were washed three times with FACS buffer. The Vβ4 was detected by incubating with Streptavidin Alexaflour 647 for 15 minutes in the dark at 4℃. After that, the cells were washed, fixed and preserved as described before.

2.10.2 Intracellular IFN-γ staining

Spleens were dissected from WT virus or M4stop virus infected 129Sv mice at day 10, 12 and 14 p.i. and placed in 2ml RPMI containing 10μg/ml Brefeldin A (BFA, Sigma, UK). The splenocytes were released and erythrocytes were lysed as before. Lymphocytes were washed in staining wash buffer (SWB, 1 × PBS, 2% fetal calf serum 0.1% NaN_3) containing 10μg/ml BFA three times to remove the medium. 1×10^6 cells were stained per sample. FcR receptors were blocked by incubating with an

anti CD16/CD32 antibody (Pharmingen BD Biosciences, USA) for 15 minutes at 4℃, followed by a single wash in SWB + BFA. FITC-labeled CD49b (AbD Serotec, UK) was used as NK cell surface marker antibody. It was added and incubated for 20 minutes at room temperature. The cells were washed in PBS + BFA then fixed in 2% NBF. After fixing, the cells were permeabilised in permeabilisation buffer (SWB + 0.5% saponin (BDH Laboratory Supplies, UK)) for 10 minutes at room temperature. IFN-γ antibody, PE-labeled IFN-γ (Pharmingen BD Biosciences, USA), was added and incubated for 30 minutes on ice, washed in PBS and resuspended in SWB for flow cytometry analysis. As a positive control, 1×10^6 cells were incubated in RPMI containing 10ng/ml BFA, 50ng/ml phorbol 12-myristate 13-acetate (PMA, Sigma, UK) and 500ng/ml ionomycin (Sigma, UK) for 4 hours at 37℃ with 5% CO_2.

2.10.3 Detection of B cell proliferation

Splenocytes were stained with anti-CD19-PE antibody for 15 minutes in the dark at 4°C. After staining, the cells were washed and fixed with 50μl of 1% paraformaldehyde for 15 minutes at room temperature in the dark, then washed. Permeabilization of cells was performed by adding 50μl of 20% Tween-20 (diluted in SPBS (v/v)) for 10 minutes at room temperature in the dark. After washing, the cells were stained with rabbit poly-clonal anti-ki67 antibody (Abcam, UK) for 15 minutes in the dark at 4°C. Then the cells were washed for three times. Biotinylated goat anti rabbit IgG (H+L) (Vector Laboratories, USA) was used to stain the cells for 15 minutes in the dark at 4°C. The cells were washed for three times and were

stained with streptavindin Alexa Flour® 647 conjugated antibody (Invitrogen, UK) for 15 minutes in the dark at 4°C. Then the cells were washed and preserved as described before.

2.10.4 Isotype control and analysis

PE (Biolegend, USA), FITC (BD Pharmingen, USA or eBiosience, USA), APC (Biolegend, USA) isotype controls were used at the same concentration as each antibody. The concentrations of antibodies were listed in Appendix I. Flow cytometry was performed on a DakoCytomation using CyAn^{Tm} ADP with Summit^{TM} software (Dako, Danmark). For each sample, a minimum of 50000 events were counted. Further analysis was carried out using FCS express V3 (De Novo Software, USA)

2.11 RNA extraction and manipulation

2.11.1 RNA extraction from spleen

RNeasy Mini Kit (Qiagen, UK) was used for extraction of RNA. Spleens were dissected and preserved in RNAlater RNA Stabilization Reagent immediately to avoid RNA degradation. The samples were stored at -20℃ until use. The tissues were removed from RNAlater using forceps. Approximately 30mg of spleen was cut on a clean surface and placed in an RNA free eppendorf tube. The tissue was completely homogenised in 600µl Buffer RLT containing 2–ME using a mini pestle followed by centrifugation for 2 minutes at full speed in a QIAshredder spin column (Qiagen, UK) placed in a 2ml collection tube. The lysate was centrifuged again for

three minutes at full speed and the supernatant was transferred to a new microcentrifuge tube carefully. 600µl of 70% ethanol was added to the supernatant and mixed immediately by pipetting. 600µl of the sample including any precipitate was transferred to an RNeasy spin column placed in a 2ml collection tube and centrifuged for 15 seconds at 8000 × g to bind the total RNA to the column membrane. The remaining sample was centrifuged in the same RNeasy spin column. The flow-through after each centrifugation was discarded. At this point, DNA was removed by an on-column DNase digestion with the RNase-Free DNase Set (Qiagen, UK). 350µl of buffer RW1 was added to the RNeasy spin column, and centrifuged for 15 seconds at 8000 × g. After discarding the flow-through, 80µl of DNase 1 mixture (10µl DNase 1 stock solution + 70µl Buffer RDD) was added to the RNeasy spin column membrane. The column was incubated for 15 minutes at 20-30℃ followed by adding 350µl Buffer RW1 and centrifuged for 15 seconds at 8000 × g. The flow-through was discarded. The column was washed twice with 500µl of Buffer RPE at 8000 × g for 15 seconds and 2 minutes separately. To remove any Buffer RPE, the column was placed in a new 2 ml collection tube and centrifuged at full speed for 2 minutes. The column was placed in a new 1.5ml collection tube. RNA was eluted from the column by centrifugation at 10000 × g for 1 minute with 30µl of RNase-free water. RNA was stored at -80℃.

The RNA integrity was checked by gel electrophoresis and quantified by spectrophotometry and Agilent RNA 6000 Nano Assay.

2.12 Gene expression analysis by RT^2 first strand kit

2.12.1 Reverse Transcription of RNA

Genomic DNA Elimination Mixture (Qiagen, Germany) was made by mixing 0.8mg total RNA, 2μl 5 × g DNA Elimination Buffer (Qiagen, Germany) in an RNase free tube, and made up to 10μl by adding nuclease-free H_2O. The contents were gently mixed by a pipettor followed by centrifugation. After centrifugation, the mixture was incubated at 42℃ for 5 minutes, and then was chilled on ice immediately for at least one minute. The RT cocktail was prepared by mixing 4μl 5 × RT Buffer 3, 1μl Primer & External Control Mix, 2μl RT Enzyme Mix and 3μl H_2O. This RT cocktail was added to each 10μl Genomic DNA Elimination Mixture and was mixed gently with a pipettor. The mixture was incubated at 42℃ for exactly 15 minutes and the reaction was stopped by immediately putting in 95℃ condition for 5 minutes. The 20μl of cDNA synthesis reaction mixture was mixed well with 91μl of H_2O.

2.12.2 PCR Array

PAMM-12 PCR Array rings (Qiagen, Germany) were used to determine the expression levels of chemokines and their receptors. The genes containing in the PCR Array were listed in Appendix II. The PCR Array ring was carefully removed from its sealed bag and fitted into the Rotor-Disc 100 loading block using the tab at position A1 and the tube guide holes. 20μl of the RT^2 SYBR® Green qPCR mastermix was dispensed into each well of the PCR Array wheel by the PCR robot

(Qiagen, Germany). The Rotor-Gene Q 100 PCR Array was carefully sealed with the Rotor-Disc heat sealing film using the Rotor-Disc heat sealer. The excessive sealing film was removed when the film was cooled down. The Rotor-Gene Q 100 PCR Array was inserted into Rotor-Disc 100 rotor and locked by the Rotor-Disc 100 locking ring followed by inserting into Rotor-Gene Q real-time PCR machine. In all reaction, an initial denaturation step was carried out by incubation at 95℃ for 10 minutes. 40 cycles of amplification were carried out, which consisted of denaturation at 95℃ for 10 seconds, annealing at 60℃ for 30 seconds.

The data of each run was maintained in Rotor-gene software

2.13 Histology analysis

2.13.1 Production of paraformaldehyde

4g of paraformaldehyde (Sigma, UK) was dissolved in 50ml distilled deionized H_2O and then 1ml of 1M NaOH solution was added. The mixture was stirred gently on a heating block (about 65℃) in the fume hood. After the paraformaldehyde was totally dissolved, 10ml of 10 × PBS was added and allowed the mixture to cool to room temperature. The pH of the mixture was adjusted to 7.4 using HCl. The solution was filtered through a 0.25μm membrane filter to remove any particulate matter. The paraformaldehyde was allocated in 30ml universal, and stored at -20℃ until use. Repeated cycles of freeze-thawing were avoided.

2.13.2 Preparation of frozen section of Macgreen mice

The spleens of MacGreen mice were preserved into 4% paraformaldehyde for 2 hours on the ice in the dark. The tissues were washed with PBS and dropped into 18% sucrose solution (18g sucrose (Thermo Fisher Scientific, USA) in 100ml PBS). After keeping for 6-8 hours at 4℃ in the dark, the samples were transferred to 30% sucrose solution overnight. On the next day, the tissues were washed followed by embedding in OCT compound (Sakura Finetek, USA) in each plastic mould. The sample was frozen by dipping the plastic mould in liquid nitrogen using long forceps. When the sample was completely frozen, it was taken out from liquid nitrogen and pushed out from the plastic mode. The tissue was labeled and ready for sectioning. The remained tissue was preserved on dry ice or in -80℃ freezer.

2.13.3 Immunostaining

2.13.3.1 Detection of binding ability of M4 protein to splenocytes

20μl of recombinant M4 protein was incubated on MacGreen splenocyte cytospin over night at 4°C in the dark. Then slides were washed twice with PBS containing 4% Tween-20 at room temperature in the dark for 10 minutes. The His-tagged M4 protein was detected by incubation with mouse anti His-tag antibody, biotinylated rabbit anti mouse antibody and Alexa Fluor® 568 (Invitrogen, UK). To-Pro®-3 was used to stain the cell nucleus for 5 minutes. The slides were washed between each step as described. Then the slides were mounted and covered with cover slides (VWR international, USA). The fluorescent was observed by a confocal microscope.

2.13.4 Data analysis

Statistics: The results were investigated by the Mann-Whitney test at the 5% level.

PCR Array results: The RT^2 Profiler PCR Array results were analysed through web-based PCR Array Data Analysis webpage.

http://pcrdataanalysis.sabiosciences.com/pcr/arrayanalysis.php

Chapter 3
In vitro characterization of M4 protein

3 *In vitro* characterization of M4 protein

3.1 Introduction

MHV-68 contains the ORF M4 encoding a glycoprotein known as M4 protein. The transcripts can be detected during the lytic and latent establishment phase *in vivo* and the protein can be detected in the medium of infected cell cultures *in vitro* (Evans et al., 2006; Marques et al., 2003; Townsley, Dutia, and Nash, 2004). The M4 protein may have a role in down-regulating the immune response, leading to an increase in viral latency during a MHV-68 early latent infection in the spleen (Evans et al., 2006; Geere et al., 2006). However, the roles of the M4 protein of MHV-68 during infection are not yet fully understood. It was therefore of interest to further characterize the importance of the left end of the MHV-68 genome in pathogenesis by specifically investigating the role of the M4 protein *in vitro* and during infection.

The M4 protein has been shown to share a considerably close amino acid sequence similarity to the M3 protein. From the *in silico* analysis, it is indicated that M4 might share folding features with M3 (Alexander et al., 2002), suggesting M4 may have a similar function to M3. Large DNA viruses, such as herpesvirus and poxvirus, encode chemokine binding proteins to evade immune responses. The chemokine binding proteins have the potential to disrupt or alter chemokine signalling (reviewed in Webb and Alcami, 2005). M3 has an ability to bind to CC-, CXC-, C-, and CX_3X-chemokines, thus blocking the interaction of these chemokines with their

receptors *in vitro* (Parry et al., 2000; van Berkel et al., 2000). However, M3 binds to CXC-chemokines at a lower activity as compared to the other three chemokine families (Alcami, 2003). It has also been reported that M3 blocks certain CC- and CXC- chemokines *in vivo*, which interrupts leukocyte trafficking (Jensen et al., 2003; Martin et al., 2006).

A few experiments have been carried out in our lab using recombinant M4 protein to investigate the function of the M4 protein *in vitro*. The recombinant M4 protein was expressed using the baculovirus expression vector system (BEVS), because the expression of inserted foreign genes in this BEVS is facilitated by the powerful polyhedron promoter, and proteins are subsequently folded, modified, sorted and assembled correctly (Hara et al., 1986; Hitchman, Possee, and King, 2009). Although the recombinant M4 protein can also be produced by engineered *Escherichia coli,* the M4 protein proved difficult to produce in a soluble form even when expressed at various temperatures (Y. Ligertwood personal communication) (Mackay et al., 1997). Because poor solubility of a protein affects any high resolution structural studies and biochemical characterization of protein, BEVS is a better method of producing the M4 protein. Moreover, BEVS was also used to produce the M3 protein for studies of its chemokine binding function *in vitro* (Parry et al., 2000; van Berkel et al., 2000). The results of a cytokine and chemokine protein array showed that Cxcl4 levels were increased in the spleens of mice infected with M4stop virus compared to the WT virus infection, despite the transcription of Cxcl4 in spleens being the same following

M4stop and WT virus infections (Y Ligertwood personal communication). Therefore, we hypothesized that Cxcl4 in the WT virus infected spleens may be neutralized by the M4 protein. CXCL4 is involved in the migration of activated T lymphocytes which is mediated by CXCR3 (Mueller et al., 2008) and it has been shown to be involved in the control of a HIV-1 infection by interacting with gp120 which is essential for virus attachment and entry (Auerbach et al., 2012). Therefore, the neutralization of Cxcl4 in the spleen may be one of the immune evasion strategies used by MHV-68 during infection. In addition, Cxcl4, Cxcl9 and Ccl9-Ccl10 have been found to bind to the M4 protein *in vitro* (Y Ligertwood personal communication). Whether M4 has the ability to bind more chemokines is one of our interests and the results are shown in this chapter.

The interaction of chemokine binding proteins and their ligands may come about in two distinct ways. First, the chemokine binding protein may block the binding of chemokines to their receptors，thus inhibiting chemokine-induced chemotaxis. For example, vCCI protein binds to a large number of CC-chemokines, blocking the binding sites of receptor to reduce inflammation (Alcami et al., 1998; Beck et al., 2001; Dabbagh et al., 2000). Second, the binding of chemokines to GAGs may be blocked by a chemokine binding protein, therefore disturbing the local levels of chemokines. However, this binding mechanism is reversible. For example, the binding of A41 to chemokines was blocked by the overwhelming presence of sulphated GAGs (Bahar et al., 2008). Moreover, some chemokine binding proteins

also interact with GAGs. For example, M-T1 binds to GAGs; whereas the M3 protein and M-T7 do not bind to GAGs (Lalani et al., 1997; van Berkel et al., 2002; Webb, Smith, and Alcami, 2004). It has been reported that ORF M4 contains a heparin sulphate-binding domain (Ebrahimi et al., 2003), but the binding ability of M4 to heparin has not been determined. Therefore, whether the M4 protein can bind to GAGs and whether the M4 protein inhibits the binding of chemokine to GAGs were the questions that we wanted to understand in this study.

M4 may interact with the cell membrane via proteoglycan heparan sulphate, since it has a heparin sulphate-binding domain (Ebrahimi et al., 2003). Additionally, a previous study of M4 has shown that the M4 protein has the ability to bind a small quantity of mouse splenocytes, which have been shown not to be T or B lymphocytes (Y Ligertwood personal communication). It has been reported that some chemokine binding proteins can bind to cell surfaces. For example, M-T1 can remain on the cell surface as it simultaneously binds chemokines and GAGs (van Berkel et al., 2002). M4 protein may bind to cell surfaces to interrupt chemokine signalling. Therefore, we further explored the cell population which M4 protein may bind to.

In this chapter, we mainly focused on the function of the M4 protein *in vitro*. Moreover, we also wished to provide evidence of how M4 protein influences the chemokine network.

3.2 Results

3.2.1 The preparation of recombinant M3 and M4 protein

To study the function of M4 protein *in vitro*, a M4 recombinant baculovirus strain was constructed in our lab that expressed the M4 ORF and was confirmed to be M4 protein by protein mass spectrometry. A recombinant M4 protein which has a penta-His residues at its C terminal was secreted into the supernatant of an insect cell culture and purified by metal-affinity chromatography following standard protocols as described in Materials and Methods. Because it is known that M3 binds to human CXCL8, but not murine Cxcl1, Cxcl2 and Cxcl5 (Parry et al., 2000), M3 was selected to be used in my experiment as a positive (with CXCL8) and negative (with Cxcl2 and Cxcl5) control. M3 recombinant baculovirus was made from a baculovirus plasmid (a generous gift from Prof J.P Stewart) which contains the M3 gene under the control of a baculovirus promoter. The M3 coding sequence is preceded by an insect secretory signal which enables secretion into the medium and has a C terminal penta-His tag. Both M3 and M4 protein fractions were eluted from the affinity column with buffer containing 40mm, 125mm and 250mm imidazole. The fractions were characterized by SDS-PAGE and proteins were detected using an anti-Penta-His antibody (figure 3.1). From a western blot it can be seen that the concentration of M3 protein is much higher than for the M4 protein. The size of M3 is 44 kDa in the supernatant of cell culture, whereas the predicted size of M4 is 45 kDa (Evans et al., 2006; van Berkel et al., 1999). However, the observed molecular

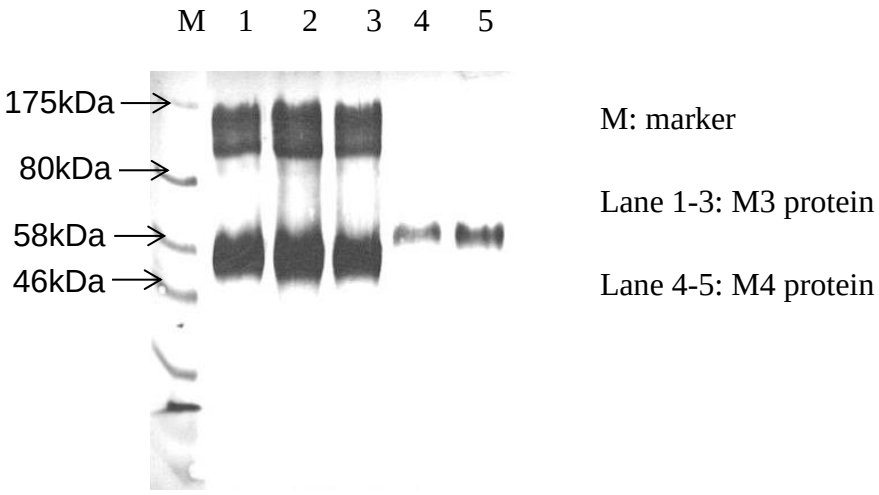

Figure 3.1 Western blotting detection of M3 and M4 proteins. Insect cells were infected with M3 or M4 baculovirus. The protein fractions were purified by metal affinity chromatography. 20μl of M3 or M4 protein fractions were loaded on a 10% SDS-polyacrylamide gel. Lane 1-3 are are M3 protein fractions, and lane 4 and 5 are different M4 protein fractions. The protein fractions were transferred to nitrocellulose membrane by western blotting. These His-tagged proteins were detected by mouse anti-His antibody, biotinylated rabbit anti mouse antibody, Streptavidin-AP and SIGMAFAST BCIP/NBT.

weight of M4 protein (60 kDa) may result from it being glycosylated, which may also interfere with the expression of M4 protein. The higher molecular size of M3 (55 kDa) was probably the result of protein aggregation, because the M3 protein is not glycosylated (van Berkel et al., 1999). M1 protein was also considered as a negative control since it has not been shown to bind to chemokines (Seet and McFadden, 2002). M1 baculovirus is available to infect insect cells and encode M1 protein in our lab. Unfortunately, the level of the M1 protein was low. Additionally, the M1 protein was degraded rapidly before further experiments could be carried out. Meanwhile, M4 protein was also difficult to produce at high concentration and maintain in a stable form. To characterize the binding ability of M4 protein, the binding of M3 protein and CXCL8 was used as a positive control; whereas the binding of imidazole elution buffer or M3 to Cxcl2 or Cxcl5 were used for negative controls.

3.2.2 Binding ability of M4 protein with chemokines

The binding of M4 protein to chemokines, which was mentioned in section 3.1, indicates that the M4 protein may be another chemokine binding protein secreted by MHV-68 infected cells. The results were confirmed by an ELISA carried out by coating chemokines onto plates. To reduce non-specific binding, the plates were blocked after coating. Because the concentration of M3 protein was much higher than M4 protein, 1μl or 10μl of M3 protein were used as controls, whereas 1μl, 10μl or 30μl of M4 protein were used in the ELISA. The absorbance values of 1μl and

10μl of M3 proteins with chemokines were the same (about 3.2). However, the background absorbance values of M3 protein (without coating with chemokines) was 2.22 for 1μl of M3 protein, 3.16 (the photometric measuring range of the ELISA reader is 0-5.0 OD, and the linear dynamic range of the ELISA reader is 0-4.0 OD) for 10μl of M3 protein which was much higher than the absorbance value of M4 protein (0.84), indicating that the M3 protein may have a higher binding ability to the plate compared to the M4 protein and/or the concentration of 1μl of M3 was much higher than 10 μl of M4 protein. The concentration of M3 and M4 proteins had not been quantified before the experiment; they were only predicted from the western blot result (figure 3.1). The ELISA results were corrected by subtracting background and are shown in figure 3.2. Unexpectedly, both M3 and M4 bound to murine Cxcl2, Cxcl5 and human CXCL8, but with various binding ability, as the binding ability of M4 to murine Cxcl2/Cxcl5 was higher than human CXCL8 which the M3 protein can bind with a high ability. In addition, the binding ability of the M3 protein to Cxcl2/Cxcl5 was weaker compared to CXCL8, which may explain why Cxcl2/Cxcl5 cannot replace M3 bound ^{125}I-CXCL8 in the cross-link assay (Parry et al., 2000).

To reduce the high background of M3 and M4 proteins, the plates were coated either with 2μl of M3 protein or 30μl of M4 protein. Murine Cxcl4 was used in this experiment since it has been shown to bind to the M4 protein and the antibodies which can detect the existence of Cxcl4 had been optimized in the lab. The non-specific binding of Cxcl4 was 0.233 which was lower than the background seen

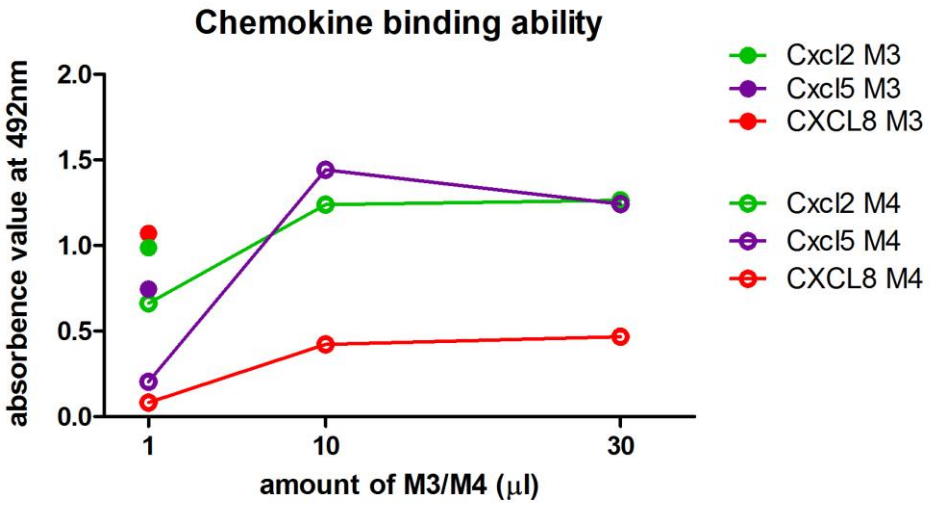

Figure 3.2 The chemokine binding ability of M4 was assayed by ELISA. The sandwich ELISA was performed by using recombinant M4. The wells were coated with or without Cxcl2, Cxcl5 and CXCL8. M3 protein was used as a positive and negative control. The M3/M4 protein was detected by anti penta-His antibody. The graph showed the absorbance value \above the protein non-specific binding background. The ○ represents the binding of M4 protein and Cxcl2, the ○ represnets the binding of M4 protein and Cxcl5, the ○ represents the binding of M4 protein and CXCL8. The ● represents the binding of M3 protein and Cxcl2, the ● represents the binding of M3 protein and Cxcl5, the ● represents the binding of M3 protein and CXCL8.

from M3 and M4 protein. The results are plotted in figure 3.3, which show both M4 and M3 protein can bind to Cxcl4. However, the binding ability of M4 was far less than for the M3 protein, possibly because the concentration of the M4 protein was lower than the M3 protein even though we diluted the latter before use.

The chemokine binding ability of the M4 protein was further investigated by using $MACS^{TM}$ Technology. The reagent, methods and equipments were described in Material and Methods. Cxcl4 was chosen for this experiment because it has been shown that there was a reduction in the spleen after a MHV-68 infection and it has been found to bind the M4 protein in an ELISA. The other reason for selecting Cxcl4 was because it can also be used for a competitive ELISA which will be described later in this chapter. The $MACs^{TM}$ beads have a high affinity for His-tagged proteins and will select the His-tagged M3 and M4 proteins in the supernatant of M3 or M4 baculovirus infected cell cultures. The supernatants were incubated with anti-His MACs beads, with or without Cxcl4 as described in Material and Methods. Eluted material was equally divided into two groups and both of them (20µl each) were loaded on a precast gradient gel followed by western blotting. Then the membrane was divided into two parts to detect either using the His-tagged proteins or the presence of Cxcl4. The M3 protein and imidazole containing elution buffer were used as a positive and negative control respectively. In order to detect the non-specific binding of Cxcl4 to the beads, Cxcl4 was incubated with $MACs^{TM}$ beads without M4 protein, then eluted and examined. Similar to the M3 protein

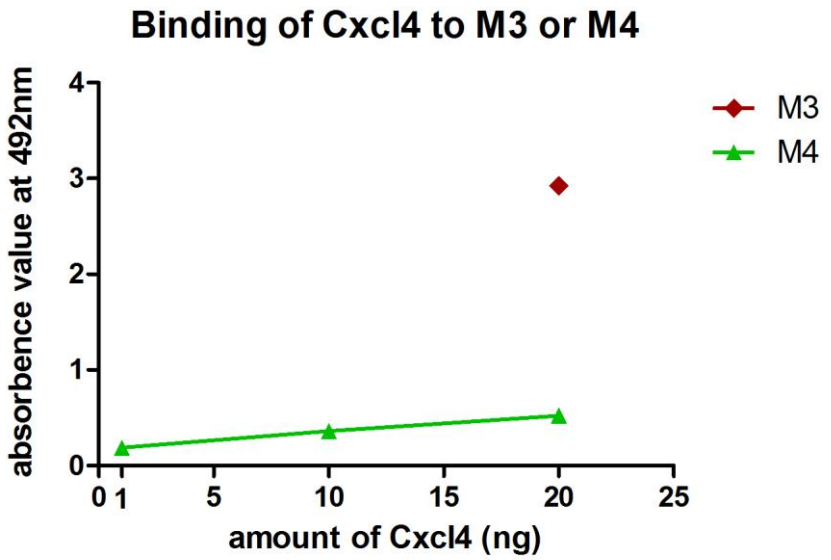

Figure 3.3 The chemokine binding ability of M4 was detected by ELISA. A sandwich ELISA was performed by coating recombinant M4 in the wells. M3 protein was used as a positive control and 125mM imidazole protein elution buffer was used as a negative control. The Cxcl4 which bound to proteins was detected by anti Cxcl4 antibody. The background absorbance value observed when no protein was coated onto the plate was deducted from the results. The red diamond refers to M3 protein positive control. The green triangle refers to M4 protein.

(figure 3.4, lane 1 and 4), Cxcl4 (about 10kDa) was found in the eluted M4 protein sample (figure 3.4, lane 2 and 5); whereas Cxcl4 was not found in the samples without M4 protein, indicating Cxcl4 does not bind the beads (figure 3.4, lane 3 and 6). The bound Cxcl4 in the M4 protein sample was less than in the M3 protein sample, which may be because the concentration of the M3 protein used in this experiment was higher than the M4 protein, as the band of the M3 protein was more intense than that of the M4 protein. Although we understand this, the concentration of M3 and M4 proteins contained in the supernatant of cell culture has to be measured. However, the concentration of the proteins could not be measured before MACs™, because M4 protein degrades and the protein quantification experiments take time to perform.

3.2.3 Quantitation of the M3 and M4 protein.

The binding of M3 and M4 protein to chemokines appears to be dose-dependent. We predicted the concentration of 20μl of M3 is 10-50 folds higher than the same volume of M4 protein from the western blot (figure 3.1). As the ELISA showed the absorbance value of 1μl of M3 protein with Cxcl2/Cxcl5 was lower than 10μl of M4 protein with Cxcl2/Cxcl5, it is possibly that the M4 protein binds to Cxcl2/Cxcl5 with a higher ability than M3 protein. Therefore, it was necessary to quantify the concentration of these proteins. In order to find out the concentration, the quantification of M3 and M4 was carried out by comparing band strengths with 2.5μl of a 6 x His-tagged protein ladder where the amount of each protein band was known

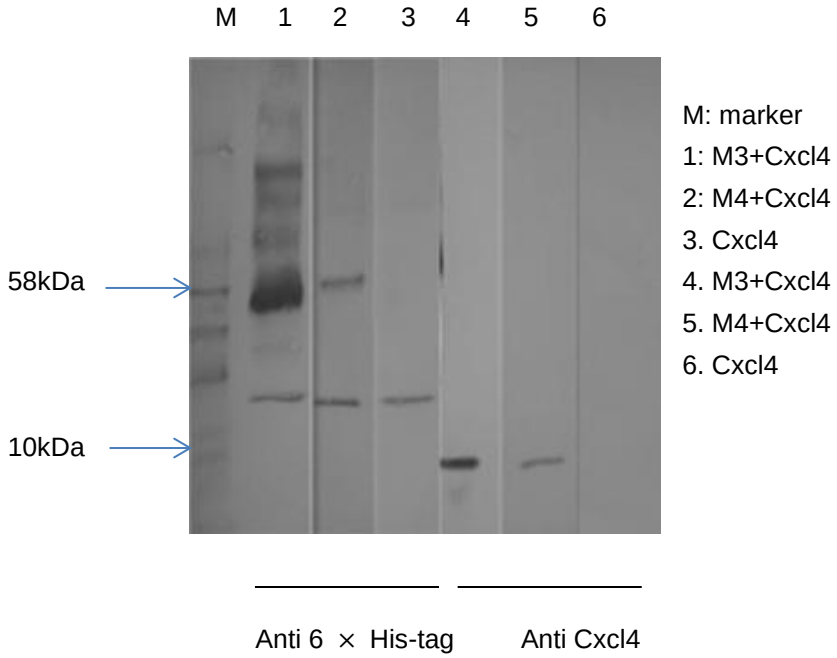

Figure 3.4 The chemokine binding ability of M4 was detected by MACS® Technology. Supernatant from M3 or M4 baculovirus infected cells was incubated with anti-His MACs beads in the presence of Cxcl4. Cxcl4 was also incubated with beads alone. After washing, 20μl of each eluted material was loaded on the gradient precast gel in duplicate, and the gel was run at the same time. Lane 1, 2, 3 were used to detect his-tagged protein by mouse anti-his antibody. Lane 4, 5, 6 were used to identify Cxcl4 by rat anti Cxcl4 antibody. Lane 1 and lane 4: eluted M3 mixture. Lane 2 and lane 5: eluted M4 mixture. Lane 3 and lane 6: eluted Cxcl4.

(figure 3.5). The M3 protein was serially diluted in imidazole containing elution buffer and the most diluted M3 protein sample contained 0.375μl M3 protein (figure 3.5, lane 1-5). Meanwhile, 20μl of neat M4 protein was loaded on the same gel (figure 3.5, lane 6). Then the density of the M3 protein (lower band) and M4 protein was analysed by ImageJ and compared to a 50 kDa marker band which is 50ng per 2.5μl. The marker was set to be 100%, thus the 20μl of M4 protein contained about 493% (246ng) and 0.375μl of M3 protein was about 1032% (516ng). Therefore, the concentration of 1μl of M3 protein was about 11 times that of 10μl of M4 protein. Therefore, it may explain the reason that 1μl or 2μl of M3 protein bound more chemokine than 10 μl or 30 μl of M4 protein in the ELISA assay. In order to compare the binding affinities between the M3 and M4 proteins, it would be better to dilute the M3 protein down to the same concentration as the M4 protein. Unfortunately, due to time constraints, and the poor stability of M4, this experiment has not been performed.

3.2.4 M4 protein cannot bind to GAGs

Some chemokine binding proteins also binds GAGs through the GAGs binding domain (van Berkel et al., 2002). It has been predicted that the M4 protein also contains this binding domain (Ebrahimi et al., 2003), therefore, it may have an ability to bind GAGs. In order to examine the binding ability of M4 protein to GAGs, an ELISA was performed using the M4 protein and heparin-biotin (a kind of highly sulfated GAGs and widely used as a GAGs substitute) as described in material and

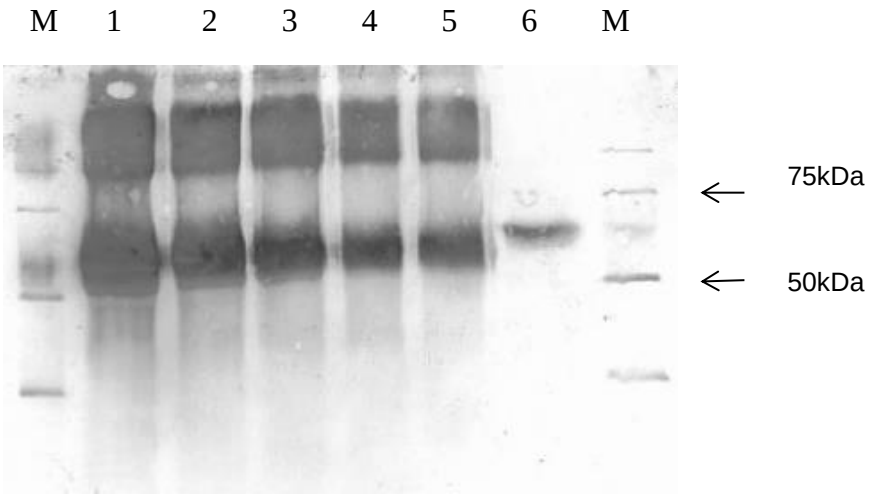

Figure 3.5 The quantity of M3 and M4 protein was measured by His-tagged protein ladder. Serially diluted M3 protein was loaded on lane 1-5, and the most diluted sample (lane 5) contained 0.375µl of M3 protein. The quantity of M4 protein was checked on lane 6 which contained 20µl of M4 protein. The ladder and proteins were detected by mouse anti-His antibody.

methods. For this experiment Cxcl4 was used as a positive control, because it is widely known that Cxcl4 has a high activity for binding with heparin (Mayo et al., 1995). Binding of M4 protein to GAGs could not be detected (data not shown), while the binding of the parallel positive control was successful (figure 3.6).

3.2.5 Competitive character of M4 protein

It has been reported that chemokine binding proteins, such as the M3 protein (Alexander-Brett and Fremont, 2007; Webb, Smith, and Alcami, 2004) and alphaherpesvirus gG (Bryant et al., 2003) inhibit the binding of chemokines to both chemokine receptors and GAGs. The binding activity of M3 protein to chemokines was stronger than the binding of chemokines to GAGs, because the M3 protein can displace chemokines from the pre-established chemokine-GAGs complex (Webb and Alcami, 2005). We have shown that the M4 protein has the ability to bind chemokines, and it would be interesting to investigate the ability of the M4 protein to inhibit binding of chemokine to GAGs.

To investigate whether the M4 protein inhibits the binding of chemokines and GAGs, heparin-biotin, Cxcl4 and the M4 protein were used in a competitive ELISA as described in Materials and Methods. The M3 protein was used as a positive control and imidazole containing elution buffer was used as a negative control in this experiment. The heparin-bound Cxcl4 was detected by rat anti Cxcl4 antibody and results are plotted in figure 3.7, which showed increasing the amount of M4 protein

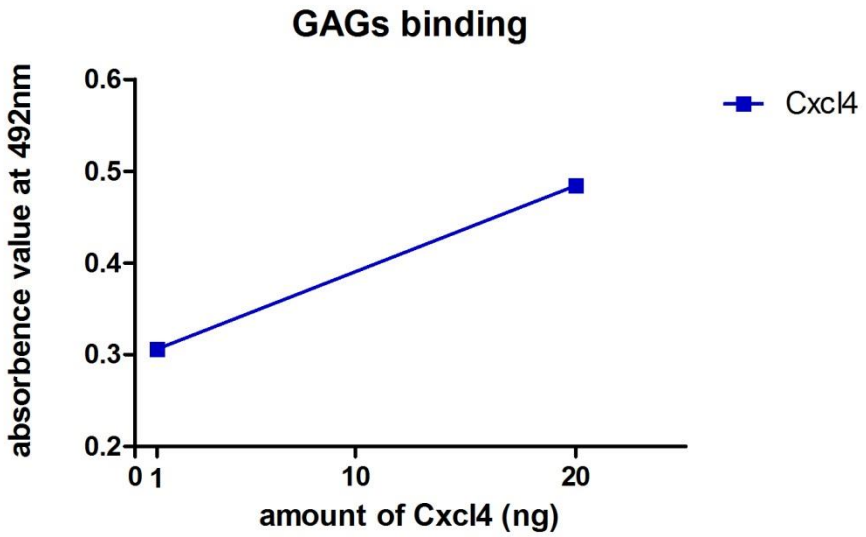

Figure 3.6 ELISA for detecting Cxcl4's GAGs binding ability. Heparin-biotin was used as a highly sulfated GAGs. A streptavidin plate was used to bind heparin-biotin onto the plate. After incubation with 1μl or 20μl Cxcl4, antibody against Cxcl4 was used to detect it.

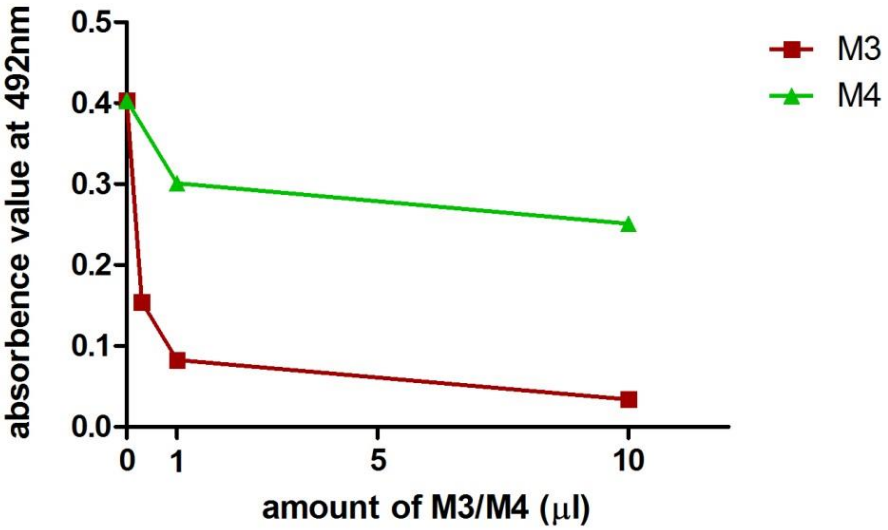

Figure 3.7 The ability of M4 protein to prevent binding of chemokine to GAGs was investigated by competitive ELISA. Diluted M4/M3/imidazole and Cxcl4 mixture was incubated in heparin coated wells overnight. The Cxcl4 which bound to the heparin was detected by anti-Cxcl4 antibody after washing. The purple square is imidazole negative control wells. The green triangle is M4 protein sample wells. The red square is M3 protein positive control.

led to a decrease in the heparin-bound Cxcl4, indicating the binding of Cxcl4 and heparin was interrupted by the M4 protein. As expected, the M3 protein largely reduced the binding of Cxcl4 to GAGs. Since we have shown that M4 protein does not bind GAGs, we can exclude the possibilities that (1) M4 protein blocks the binding site of GAGs for Cxcl4 and (2) M4 has different binding domains which can bind GAGs and Cxcl4 at the same time.

3.2.6 M4 protein binds to splenocytes

Some studies have found that the M4 protein can interact with a small population of splenocytes, which have been shown to be neither T cells nor B cells (Y. Ligertwood personal communication). Since M4 cannot bind GAGs, other mechanisms such as binding with the cell-membrane receptor or cell-membrane bound chemokines may be involved in. Cxcl2 and Cxcl5 are the ligands of Cxcr2, which is expressed on neutrophils and macrophages. As we showed M4 protein binds to Cxcl2 and Cxcl5, it is possible that the binding of Cxcl2/Cxcl5 to Cxcr2 mediates the binding of M4 protein to neutrophils and macrophages. Moreover, considering the size of the splenocytes to which the M4 protein binds, macrophages were thought to be the most likely cell population. Therefore, in order to investigate whether the M4 protein binds to macrophages or neutrophils, immunostaining was carried out using MacGreen mice which have enhanced green fluorescent protein (EGFP) expressed in macrophages and granulocytes (Sasmono et al., 2007; Sasmono et al., 2003). The spleens were harvested from uninfected MacGreen mice and the splenocytes were

prepared for cytospins. The M4 protein was incubated with the monolayer of splenocytes on a slide overnight then detected by rabbit anti M4 antibody. Imidazole containing elution buffer was used as a negative control. The results showed M4 can bind with a small population of cells, but they are not macrophages or granulocytes (figure 3.8). The cellular type to which the M4 protein binds still needs to be further investigated.

3.3 Discussion

This study confirmed that the M4 protein is a chemokine binding protein and further investigated the function of the M4 protein *in vitro*. We utilized recombinant M4 protein tagged with a C-terminal penta-His, made by a baculovirus expression system to study the function of M4. It showed that recombinant M4 protein has the ability to bind murine Cxcl2, Cxcl4, Cxcl5 and human CXCL8 with different binding affinities. Apparently, the binding activity of the M4 protein to human CXCL8 is much lower than the other two chemokines which the M3 protein binds poorly (Parry et al., 2000). Moreover, the binding activity of the M4 protein to CXC-chemokines is higher than with the M3 protein. A similar situation is found with M-T1 and M-T7,which are both secreted from the poxvirus myxoma and have different chemokine binding affinities (Graham et al., 1997; Lalani et al., 1997) and the binding sites of these two chemokine binding proteins are different (van Berkel et al., 2000). Therefore, it is not astonishing to find two chemokine binding proteins encoded from the same virus. The crystal structure of M3 protein showed that the

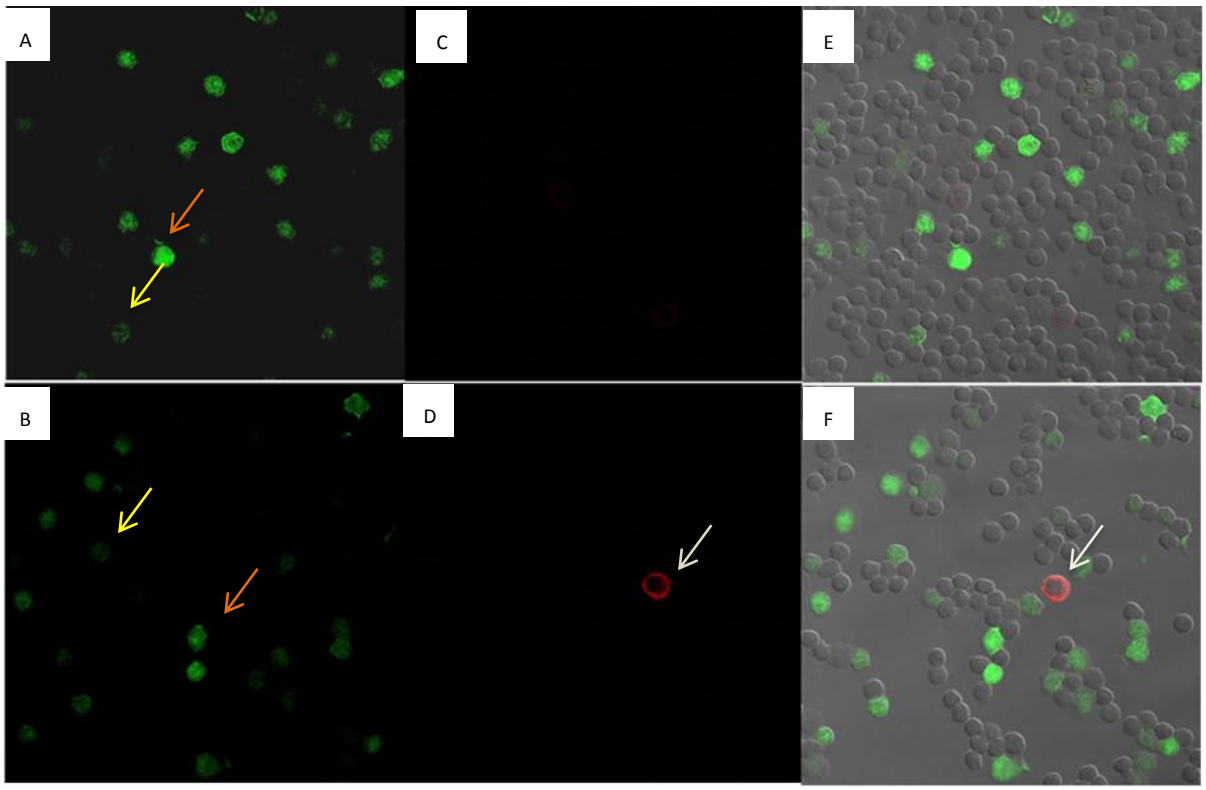

Figure 3.8 Staining for binding of M4 with splenocytes. Cytospins were made with splenocytes from uninfected MacGreen mice which have EGFP in the macrophages (bright green) and granulocytes. Orange arrows in A and B indicates macrophages, and yellow arrows in A and B indicate granulocytes. After incubation with M4 protein (B, D, F) or elution buffer control (A, C, E) the bound protein was detected by rabbit anti M4 antibody, a second biotinylated antibody and Alexa Fluor® 568 (C and D). E and F show the overlaid picture of the fluorescent and shape and location of the cells seen through white light. White arrows point to the M4 protein staining. Confocal microscope was used at 63x magnification.

dimerization of M3 generates a binding site for chemokines (Alexander et al., 2002), indicating that M4 may need a specific structure to maintain its function. Therefore, the experiments which were performed *in vitro* were limited, because at lower concentrations the M4 may lose the structure which benefits the binding of chemokines.

Moreover, we found that M4 can inhibit the binding of chemokine to GAGs, indicating that the M4 protein may influence the chemokine gradient which is established by GAG molecules on the surface of endothelial cells, thus reducing the chance of recruiting leukocytes to the inflammation sites. As we know, murine Cxcl2, Cxcl5 and human CXCL8 all have the same receptor, CXCR2, which is expressed on neutrophils and macrophages and is related to inflammation. Therefore, the decrease in latent virus load in the spleen during a M4stop virus infection at day 14 p.i. (Evans et al., 2006; Geere et al., 2006) may be because of the increase of leukocytes at the infected sites where the virus was cleared by phagocytosis and degranulation. The percentages of leukocytes have been described in the experiments in the later chapters of this thesis. There are several chemokine binding proteins involved in inhibiting the binding of chemokines and their receptors (Webb and Alcami, 2005). A recent study found some chemokine binding proteins can enhance chemotaxis (Coscoy et al., 2012). It would be interesting to know the function of M4 protein during chemotaxis.

This study also revealed that the M4 protein does not have a binding ability for

GAGs, which excluded the possibility that the M4 protein and Cxcl4 bind to the same site on GAGs so that the M4 protein can inhibit the binding of Cxcl4 to GAGs. It also excludes another possibility that M4 can bind with GAGs and Cxcl4 at the same time. This characteristic is like the M3 protein and vCCI (Parry et al., 2000; Webb and Alcami, 2005), but not like M-T1 which is the only known chemokine binding protein which can bind GAGs at the same time (van Berkel et al., 2002). M-T7 and heparin can both bind the C-terminal of CXCL8, whereas M-T7 utilized the N-terminal of CXCL8 to stop it binding with its receptor (Lalani et al., 1997). In addition, the M3 protein exploited the same binding domain (N-terminal) of CXCL8 (Webb, Clark-Lewis, and Alcami, 2003) as M-T7. But we cannot rule out the possibility that M4 protein binds to Cxcl4 through the same residues as the chemokine-GAG binding site presumably located within the lysine-rich, C-terminal region of the chemokine (Stuckey, Charles, and Edwards, 1992; Ziporen et al., 1998). Therefore, it would be interesting to know the binding domain of M4 protein to chemokines.

Interestingly, binding with chemokine and blockage of the chemokine-GAGs interaction seems not to be the only function of M4 protein, it may have other unknown functions, such as interacting with cells directly. At beginning, we hypothesised M4 may bind to neutrophils or macrophages. After examination, we found the cells were not neutrophils or even not granulocytes by staining the MacGreen mice splenocytes with bound M4 protein. As a chemokine binding protein,

M4 protein may have an ability to bind to cell membrane-bound chemokine, such as CX_3CL_1. However, the binding ability of M4 protein to CX_3CL_1 has not been determined. Moreover, it has been reported that vaccinia virus secreted viral IFN-α/β receptor can bind to both infected or uninfected cells (Alcamí, Symons, and Smith, 2000). Therefore it may possibly be that M4 protein binds to a certain cell surface to mimic the chemokine receptor, competitively attracts chemokines and stops the cellular signal transduction which is induced by chemokines.

The experiments described in this chapter point to some roles for the M4 protein *in vitro*. The binding ability of M4 is somewhat different from the M3 protein, which indicates that M4 appears to be complementary to the M3 protein. The decrease of Cxcl4 in the spleen of WT virus infection can be explained by the chemokine binding of the M4 protein, but we do not know the reason for this. In addition, we found that the M4 protein can break the gradient of chemokines by inhibiting the binding of chemokine-GAGs. This might reduce inflammation and provide a better environment for viral lytic and latent infections. Therefore, the inflammation following infection was investigated *in vivo* in the next chapter. The binding of M4 to splenocytes is another interesting observation which requires further investigation.

Chapter 4
M4 affects the viral lytic and latent infections

4 M4 affects the viral lytic and latent infections

4.1 Introduction

M4 is an IEG transcribed immediately after infection and independently of *de novo* protein synthesis *in vitro* (Ebrahimi et al., 2003; Townsley, Dutia, and Nash, 2004). The transcription of M4 can be detected in the lung and spleen during the lytic and acute-phases of latent infection up to day 14 p.i. (Marques et al., 2003; Townsley, Dutia, and Nash, 2004). Following infection with M4 expressing MHV-76 mutant virus (MHV-76inM4), there is an increase in viral load in the lungs and a higher level of viral DNA load in the spleens during early time points compared to MHV-76 infection (Townsley, Dutia, and Nash, 2004). To study the function of M4 protein further, a recombinant M4 non-coding (M4stop) virus was generated in our lab using BAC techniques with the insertion of three stop codons in the ORF (Geere et al., 2006). In M4stop virus, ORF M3, which is adjacent to ORF M4, is not disrupted as verified by real-time reverse transcription PCR (Geere et al., 2006). Moreover, the M4stop virus should have fully functional vtRNAs and miRNAs as they are not affected by the modification. Therefore, the pathogenic changes caused by M4stop virus are due to the lack of M4 protein. The same kinetics of replication have been reported among M4stop, WT and revertant viruses *in vitro* (Geere et al., 2006). Moreover, there is little difference in viral loads in the lungs of BALB/C mice following M4stop and WT virus infection at days 1, 3, 5, 7 and 10 p.i. (Geere et al., 2006). However, Evans et al (2006) find that M4stop virus decreased significantly in

the lung compared to WT virus infection at day 9 p.i.. (Evans et al., 2006). The conflicting results may be because the latter chose a different time point and/or a different mouse strain, since the immune response is different between strains. However, in both studies, the latency of viruses in the spleen is similar at day 10 p.i.. Thereafter, a rapid decline of the latent M4stop virus is detected in the spleen around day 14 p.i. as compared to WT virus infection (Evans et al., 2006; Geere et al., 2006). During long term latency, there is no difference in the viral DNA loads in the spleen or the number of splenic cells that have a reactivation ability between the two viral infections (Evans et al., 2006).

MHV-68 latent infection in the spleen is associated with splenomegaly (Usherwood et al., 1996). It has been reported that splenic lymphocytosis depends on the presence of an intact left end of the unique region of the MHV-68 genome (Chalupkov á et al., 2008; Macrae et al., 2001). M4 does not appear to be required for splenic lymphocytosis (Geere et al., 2006; Townsley, Dutia, and Nash, 2004). However, Evans et al (2006) have found that there is less splenomegaly in C57Bl/6 mice following infection with M4 mutant virus at a different time point. The relative proportions of splenic cell populations following M4stop virus infection has not been examined in these studies.

It has been demonstrated that the expression of chemokine binding protein M3 during MHV-68 infection in the central nervous system interferes with the trafficking of lymphocytes and macrophages (Jensen et al., 2003; van Berkel et al., 2002). In

Chapter 3, we showed that M4 protein binds to several neutrophil-, macrophage-, and T cell-trafficking associated chemokines, and M4 protein can prevent the formation of chemokine gradients. Therefore, M4 may influence the migration of neutrophils, macrophages and T cells from lymphatics to the spleen. It has been found that macrophages and B cells harbor MHV-68 in a latent form (Flano et al., 2000), therefore, the proliferation of B cells and macrophages would affect the viral burden. In this study, in order to understand whether splenomegaly was caused by the same cell populations and whether the decrease in the M4stop viral latency was due to a change in B cell and macrophage populations, the percentages of lymphocytes, macrophages and neutrophils were evaluated by flow cytometry during the early latency of M4stop and WT virus. MacGreen mice are c-fms transgenic mice, which express EGFP in macrophages and granulocytes of all tissues, although the EGFP is expressed in relatively lower levels in granulocytes compared to macrophages (Sasmono et al., 2003). In this chapter, MacGreen mice were used to examine the locations of macrophages and granulocytes in the spleens following M4stop and WT virus infections.

It has been reported that chemokines play an important role in T cell activation *in vitro* (Bacon et al., 1995; Taub et al., 1996). Chemokines and their receptors increase the basal motility of lymphocytes, increasing the chance for lymphocytes to encounter antigen presenting cells, such as dendritic cells. In addition, the interaction of dendritic cells with $CD4^+$ T cells or natural killer T (NKT) cells results in the

release of chemokines from dendritic cells which enhances the recruitment of $CD8^+$ T cells (Kurts et al., 2011). The activated lymphocytes are capable of responding to antigens and producing large quantities of cytokines or antibodies to control the infection. Moreover, the absence of CCL5 reduces the cytotoxicity of $CD8^+$ T cells and compromises cytokine production, leading to a higher viral load in chronic lymphocytic choriomeningitis virus infection (Douek et al., 2011). The activation of T-, B- and NK-lymphocytes, which are induced by M4stop virus infection during the early phase of latency, remains to be investigated. As M4 protein has the ability to bind chemokines, we hypothesized that the presence of M4 may reduce lymphocyte activation, resulting in increased WT viral latency in the spleen. Therefore, the percentages of activated $CD4^+$, $CD8^+$ T cells, B cells, NK cells and macrophages in the spleens following WT and M4stop virus infections were examined and compared.

The aims of this study were to (1) determine whether M4 affects MHV-68 infection in the lung; (2) examine whether M4 alters the proliferation or migration of splenocytes in the spleen; and (3) understand the mechanisms that control M4stop virus infection in the spleen.

4.2 Results

4.2.1 Acute viral infection in the lung

After intranasal MHV-68 infection, virus replicates in the alveolar epithelium and induces an inflammatory infiltrate in the lung. Afterwards, the virus is cleared around

day 10 p.i. by a T cell dependent mechanism (Cardin et al., 1996; Ehtisham, Sunil-Chandra, and Nash, 1993). The presence of chemokine binding protein M3 in the lung of wood mice supports lytic infection in the lung (Hughes et al., 2011). Since M4 was shown to possess the ability to bind to CXC-chemokines in Chapter 3 and the expression of M4 protein is detectable during acute infection (Marques et al., 2003; Townsley, Dutia, and Nash, 2004), it could possibly influence the host immune response in the lung. To investigate the function of M4 in the acute infection, age- and sex- matched BALB/c or 129Sv mice were intranasally infected with 4×10^5 PFU of either WT or M4stop virus. All experiments used three or four mice per group.

4.2.1.1 Viral loads in the Lung

The role of M4 during the lytic infection in the lung has been examined by Evans et al (2006) and Geere et al (2006). The results were not comparable possibly because of the different mouse strains, various time points, and distinct infection dose. Hence, the viral loads in the lungs following M4stop and WT virus infections were examined in this study during the lytic stage of the infections. To compare the viral replication kinetics in the lung, lungs were harvested at (1) days 7 and 10 p.i.; (2) day 8 p.i. after M4stop and WT virus infections and homogenised. The diluted lung homogenate was co-cultured with BHK-21 cells as described in Materials and Methods. The plaques were counted and the results are plotted in figure 4.1. At day 7 p.i., the viral loads in lungs of mice infected with M4stop were indistinguishable

from those infected with WT virus (figure 4.1a). However, the viral loads of M4stop virus infected mice decreased at day 8 p.i. as compared to WT infection (figure 4.1b). By day 10 p.i., the infected mice had so little virus in the lungs that they were below the detection limit of the plaque assay (figure 4.1a). The results of days 7 and 10 p.i. were consistent with Geere et al (2006)'s finding, which showed that WT and M4stop virus had similar replication kinetics in the lungs of BALB/c mice. It indicated that during lytic infection in the lung, by day 7 p.i., M4 is completely dispensable for MHV-68 replication. The results of day 8 p.i. were more close to the finding of Evans et al (2006) that the loss of M4 protein caused a more rapid clearance of virus during the late lytic phase of the infection in the lung. However, this time point was only examined once in this study. It would therefore be necessary to repeat this experiment to confirm the result, however due to time constraints, this was not possible.

4.2.1.2 Inflammation of the lung following infection

The decrease in M4stop viral loads may be related to overwhelming host inflammation, since M4 protein was shown to bind macrophage- and neutrophil-migration chemokines in the Chapter 3 and the lack of M4 protein may trigger an increase of neutrophils and macrophages. Therefore, more neutrophils and macrophages may be found in the BAL of the mice infected with M4stop compared to WT. To determine whether M4 protein altered inflammation of the lung, BAL samples were taken and sampled at day 3, 7 and 10 p.i. from BALB/c mice, which

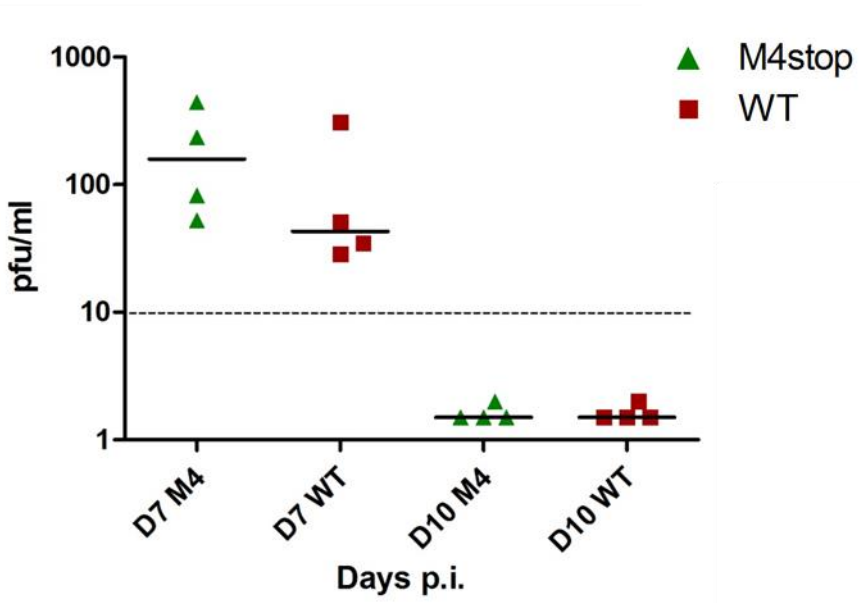

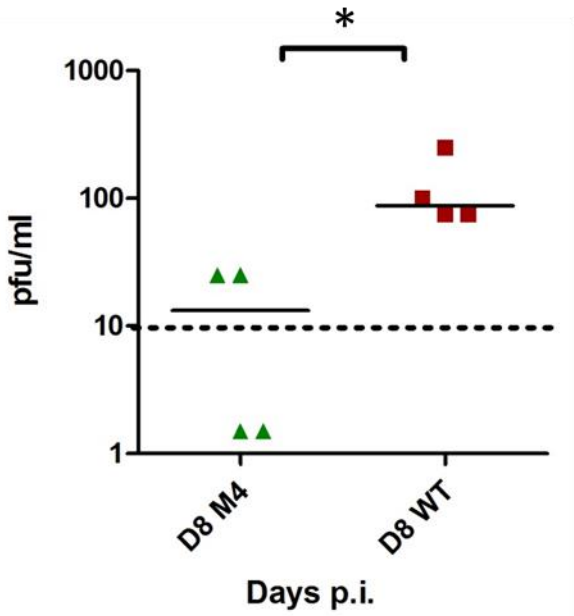

Figure 4.1 Viral loads in the lungs of M4stop or WT-inoculated mice. 129Sv mice were intranasally infected with 4×10^5 PFU of either WT or M4stop. Lungs were harvested at days 7 and 10 p.i. (a) or day 8 p.i. (b). The amount of virus is quantitated by plaque assay on BHK-21 monolayers. The black bars donate the median; dotted line represents the limit of detection of the assay; D represents day. Each symbol denotes an individual animal. Groups that have mean values that vary significantly ($p<0.05$) by Mann-Whitney test are indicated by *.

were infected with either M4stop or WT virus. The BAL was fixed on the slides and examined by hematoxylin and eosin (HE) staining. Similar inflammation was detected in the lungs of BALB/c mice infected with either M4stop or WT virus at defined time points (data not shown). Unfortunately, we did not have the BAL samples at day 8 p.i. when the viral loads were significantly different. Moreover, it would be more accurate to determine the percentage of the neutrophils and macrophages in the BAL by flow cytometry.

4.2.2 Latent infection in the mediastinal lymph nodes

MHV-68 spreads to the lung draining lymph nodes, MLNs, then establishes latency in B cells, macrophages and dendritic cells in the MLNs (Nash et al., 2001). The latent virus can be detected from day 6 p.i. and is maintained until late time points (Cardin et al., 1996).

Cellular activation in the MLNs reflects the host immune response to the initial seeding of virus and viral latency. CD69 is an early activation marker, which is transiently expressed on activated lymphocytes. It can, therefore, indicate the activation and/or differentiation of T cells and the activation of NK cells (Hara et al., 1986; Lanier et al., 1988; Testi, Phillips, and Lanier, 1989). An increased expression of CD69 is found on B cells in the draining lymph nodes and spleens, which was dependent on the presence of $CD4^+$ T cells (Stevenson and Doherty, 1999). To assess whether M4stop infection changes the cellular activation of $CD4^+$, $CD8^+$ T cells, B

cells and NK cells in the MLNs, MLNs were harvested at days 3 and 7 p.i.. The size of MLNs at day 7 p.i. was greater than at day 3 p.i., which may be due to the proliferation of lymphocytes (data not shown). The cells from MLNs were directly double-stained with fluorescent conjugated anti-CD69 and anti-CD4, anti-CD8, anti-CD19 (CD19 is a B-cell-specific marker whose expression is detectable as early as the pro-B-cell stage and subsequently in all further stages of B-cell development until the plasma cell stage), or anti-CD49b (pan-NK cells antibody) antibodies and examined by flow cytometry. There was no difference in the percentages of $CD4^+$, $CD8^+$ T cells, B cells and NK cells in the MLNs between M4stop and WT virus infection groups at each time point (figure 4.2). An increase in the percentages of $CD4^+$ T cells was found at day 7 p.i. compared to the result of day 3 p.i. (figure 4.2a) that may be because the number of $CD4^+$ T cells in the MLNs was increased following infection with MHV-68 (Christensen and Doherty, 1999). However, because the total cell number in MLNs was not determined in this experiment, the difference in total numbers of $CD4^+$, $CD8^+$ T cells, B cells and NK cells between the two viral infections was unclear. The activation percentage is assessed by the percentage of CD69 expressing $CD4^+$, $CD8^+$ T cells and B cells and the percentage of the specific cell population. Figure 4.3 shows the percentage of activated $CD4^+$, $CD8^+$ T cells and B cells were comparable in the MLN between M4stop and WT virus infections. However, the proportion of activated $CD4^+$, $CD8^+$ T-cells and B-cells was significantly decreased in the MLNs at day 7 p.i. when compared to day

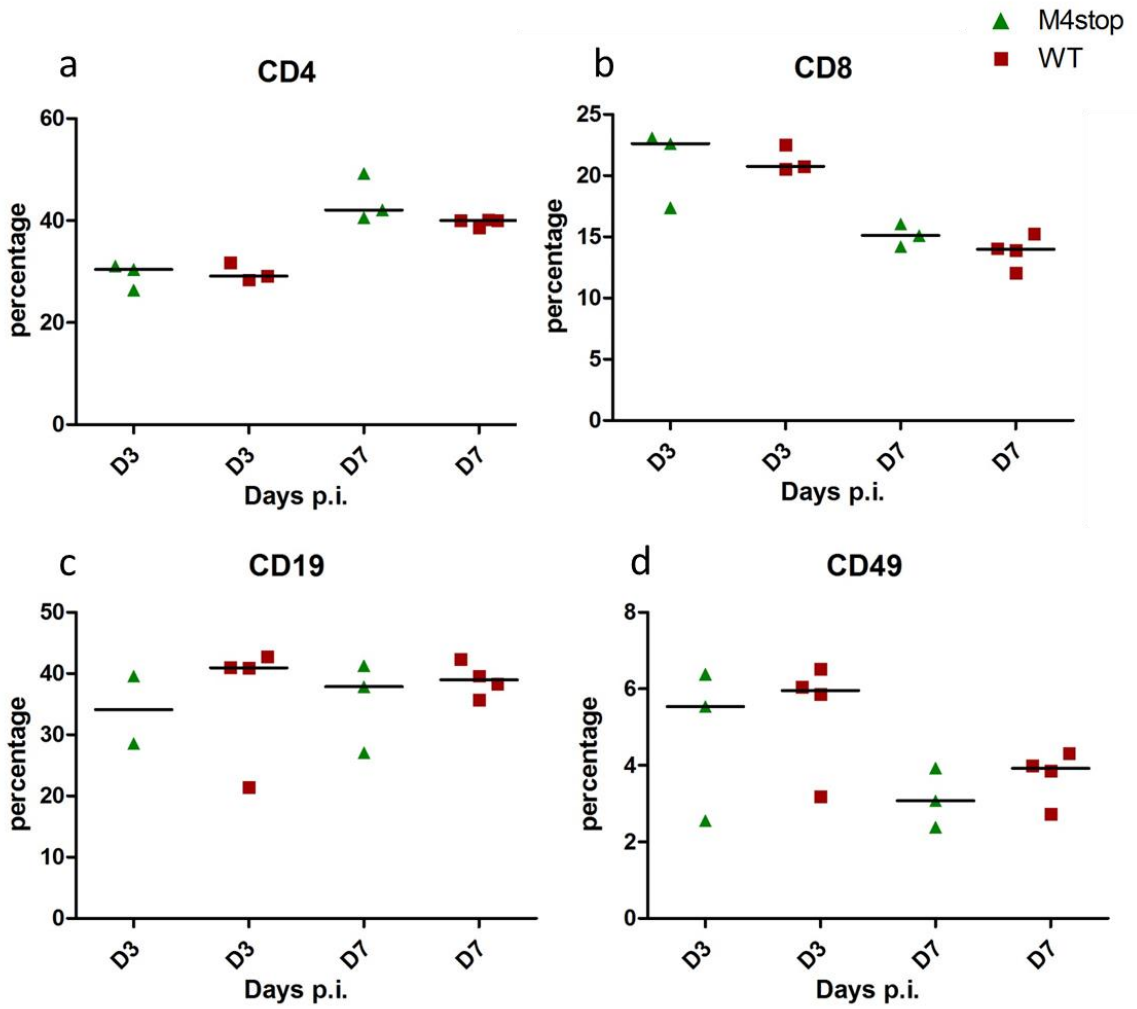

Figure 4.2 Percentages of lymphocytes in the MLNs of M4stop or WT virus infected mice. BALB/c mice were infected with 4×10^5 PFU of WT or M4stop virus intranasally. The percentages of $CD4^+$, $CD8^+$ T cells, $CD19^+$ B cells and $CD49^+$ NK cells in mediastinal lymph node were determined by flow cytometry at days 3 and 7 p.i. (a) $CD4^+$ T cells (b) $CD8^+$ T cells (c) B cells (d) NK cells. Each bar shows the median of two to four mice replicates, D refers to day.

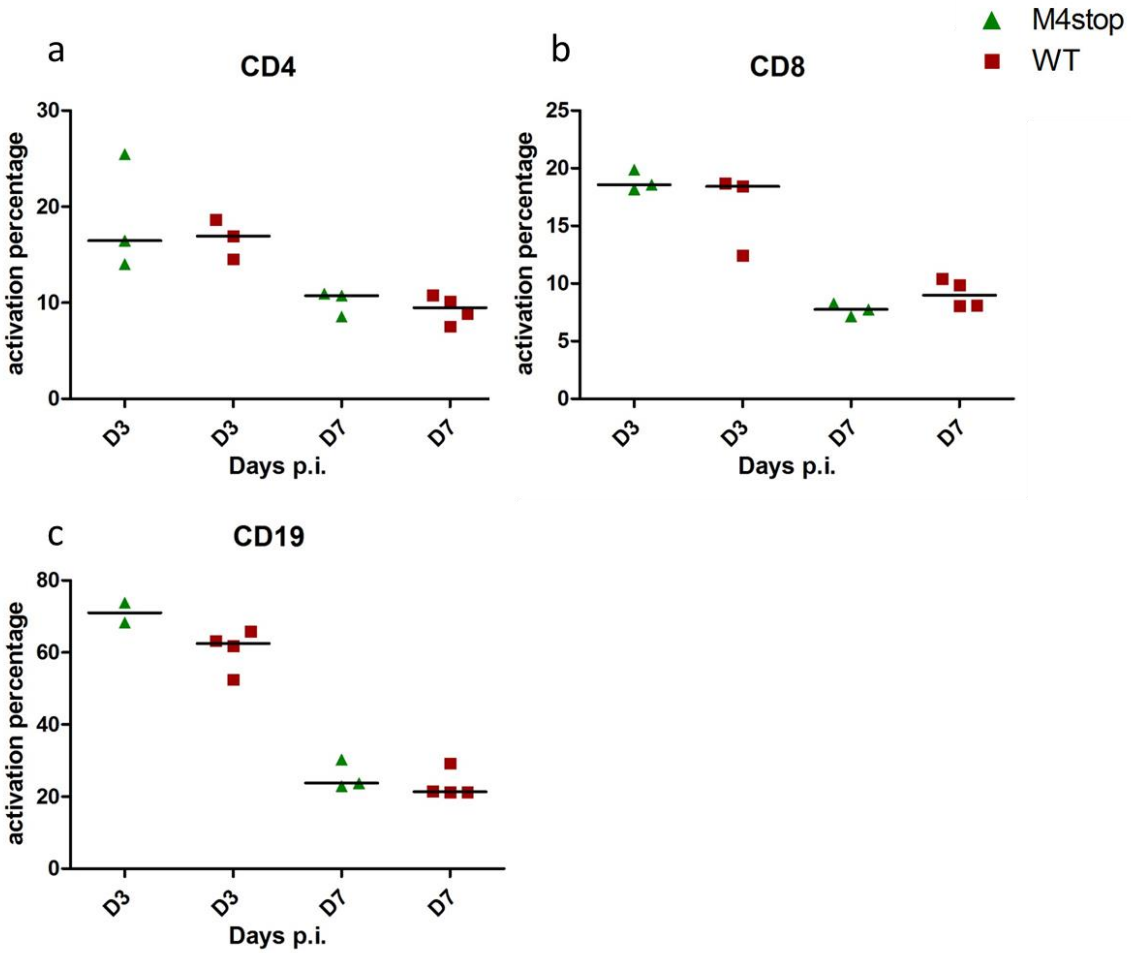

Figure 4.3 Percentages of activated $CD4^+$, $CD8^+$ T cells and B lymphocytes in the total population of each cellular subset. BALB/C mice were infected with 4×10^5 PFU of WT or M4stop intranasally. The percentages of activated $CD4^+$ T cells, $CD8^+$ T cells and CD19 B cells in mediastinal lymph node were identified by surface marker $CD69^+$ using flow cytometry at days 3 and 7 p.i. (a) $CD4^+$ T cells (b) $CD8^+$ T cells (c) B cells. The black bar shows the median of two to four mice replicates, D represents day.

3p.i..The percentages of $CD69^+$ B cells were consistent with Stevenson et al (1999)'s report. The decrease in the percentages of activated lymphocytes may be due to high proliferation of the lymphocytes or may be because of decreased cellular activation following the decrease in viral loads in the MLNs. Moreover, it would be quite interesting to know the percentages of these lymphocytes, the level of cellular activation and the viral loads in the MLNs during the M4stop and WT infections at day 8 p.i., when the increased WT viral loads were found in the lungs. However, the difference in the viral loads in the lung at day 8 p.i. was obtained from my last experiment, and no further study has been done.

4.2.3 The role of M4 during the early phase of the latent infection in the spleen

As no clear difference in host immune response was detected in the MLNs of mice infected with either M4stop or WT virus at the indicated time points, it was unlikely that M4stop infection was controlled by activated T cells. Therefore, the study of M4 protein was moved to the next infection stage, the early latent phase of infection in the spleen. M4 protein is also essential for the establishment of the acute latency, because it has been shown that the latency of M4stop in the spleens is comparable to the WT at day 10 p.i., then decreased suddenly by day 14 p.i. (Evans et al., 2006; Geere et al., 2006). The functions of M4 during early latency were examined in this study.

To assess the role of M4 in the early latent infection, age- and sex- matched 129Sv were intranasally infected with 4 x 10^5 PFU of WT or M4stop virus. Mice were sacrificed at (1) days 7, 10, 14 and 17 p.i.; (2) days 10, 12 and 14 p.i.; and (3) days 8, 10, 12 and 14 p.i.. Three or four mice were used in each group. Because it would be interesting to understand the change of host immune response after infection, a negative control group, which was inoculated with same amount of PBS, was used and named mock in this study. Only the 129Sv strain was used in this experiment, because IFN-$\gamma R^{-/-}$ 129Sv mice were allocated to use in other experiments in the future, thus results from IFN-$\gamma R^{-/-}$ mice could be compared with the results of 129Sv infection.

4.2.3.1 Viral DNA loads in the spleens

The viral loads in the spleens of the mice infected with M4stop and WT virus were examined by Geere et al (2006) from day 10 p.i.. The reduction of the M4stop viral load was found in the spleens around day 14 p.i. (Evans et al., 2006; Geere et al., 2006). In my study, viral loads were also determined to correlate with the results of cellular percentages and cellular activation. The viral loads were quantified by examining the amount of viral DNA by qPCR. Then, the results were normalized to GAPDH realtime PCR results. The results from all three experiments were combined and are shown in figure 4.4.

The virus loads were consistent with Geere et al (2006)'s results that a significant

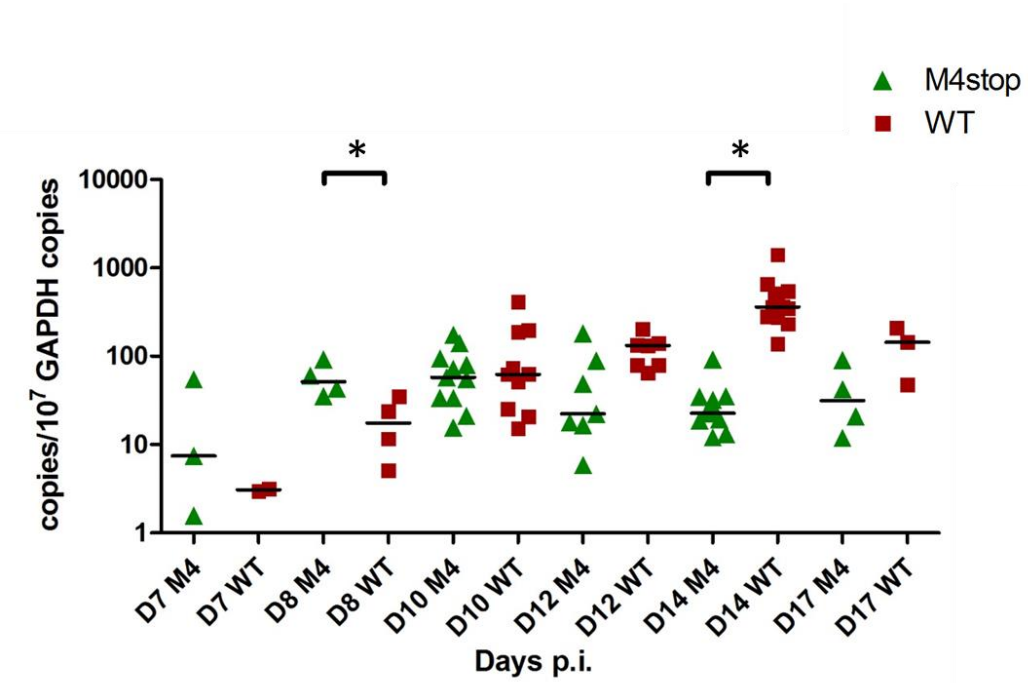

Figure 4.4 Viral DNA loads in the spleen. The results were combined from three different experiments. Viral DNA of WT and M4stop obtained from latently infected splenocytes, analysed by Realtime PCR at (1) days 7, 10, 14 and 17 p.i. and (2) days 8, 10, 12 and 14 p.i. and normalized to GAPDH. The genomic load in the spleens of MHV-68 infected animals was measured by quantitative PCR of the ORF73 gene. Each symbol represents a mouse. The black bar shows the median of two to twelve mouse replicates, and D denotes day. Groups that have mean values that vary significantly ($p<0.05$) by Mann-Whitney test are indicated by *.

decrease ($p<0.0001$) of viral loads was found in the spleens infected with M4stop virus at day 14 p.i. compared to that of WT virus infection. That aside, a significantly increased ($p<0.05$) viral load was found in the M4stop-infected spleens at day 8 p.i. at the first time.

4.2.3.2 Infectious centre of the infected splenic cells

In previous reports the number of infectious centres of WT-infected splenic cells is significantly higher than M4stop virus infection when examined at days 14 and 16 p.i. (Evans et al., 2006; Geere et al., 2006). Because the kinetics of viral pathogenesis may be different between mouse strains, splenic cells, which are able to reactivate MHV-68, were examined by infectious centre assay and compared between viral infections. 129Sv mice were sacrificed at days 7, 10, 14 and 17 p.i.. The spleens were harvested and the latent virus in the spleens was determined as described in Materials and Methods. The results are plotted in figure 4.5, which shows a significant decrease in number of infectious centres of M4stop in the spleens of 129Sv mice at days 14 and 17 p.i. ($P<0.05$). Similar to the results of viral DNA loads, WT virus infection exhibited approximately a 10-fold higher number of latently infected cells at day 14 p.i. compared to M4stop virus infection. This indicates the decrease in M4stop latency is not due to a reduced reactivation ability of this mutant virus. The increased viral latency during the M4stop infection at days 8 p.i. suggested that M4stop may stimulate a more aggressive anti-viral response than WT infection, which may control the M4stop virus during latency.

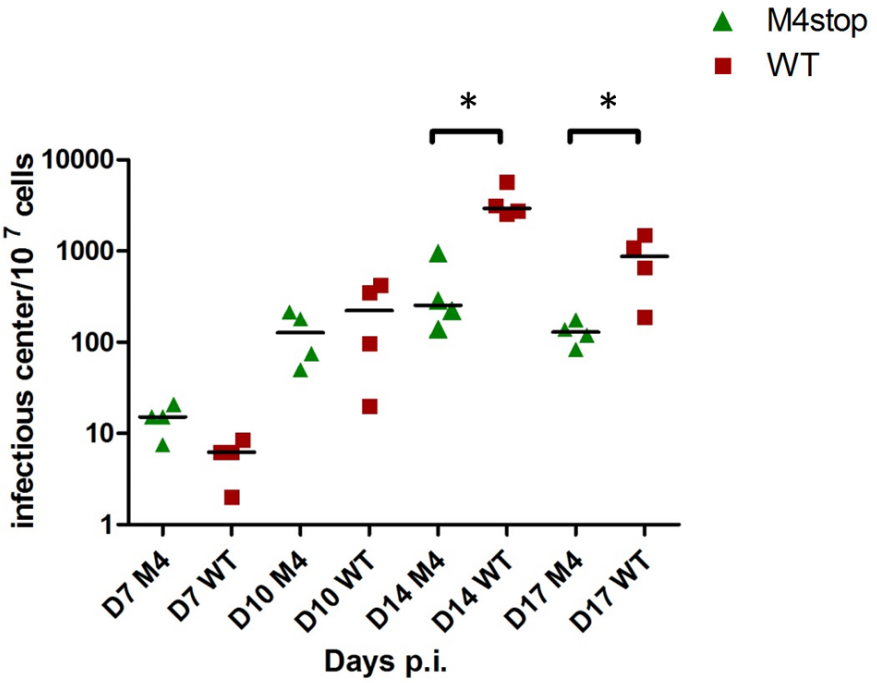

Figure 4.5 Infectious centre in the spleen. 129SV mice were infected with 4×10^5 PFU of M4Stop or WT virus intranasally. Spleens were removed at days 7, 10, 14 and 17 p.i. and virus load was determined by infectious center assay. The black bar shows the median of four mouse replicates, and D denotes day. Groups that have mean values that vary significantly ($p<0.05$) by Mann-Whitney test are indicated by *.

4.2.3.3 Viral induced splenomegaly

The weight of the spleens was measured at days 7, 10, 14 and 17 p.i.. An expansion of lymphocyte numbers which causes the splenomegaly was observed in both viral infections after day 7 p.i., compared to the spleen weight of the negative control. Evans et al (2006) reported significantly less splenomegaly in animals infected with M4stop at day 16 p.i. as compared to WT. In this study, less splenomegaly was found in the mice infected with M4stop at days 14 p.i. and 17 p.i. compared to that of mice infected with WT virus, however, this was not significant ($p=0.057$ and 0.1 respectively) (figure 4.6). The different results may be due to the different time points. Moreover, the virus titre used for my *in vivo* experiment was different from Evans's et al (2006) published data.

4.2.3.4 Percentages of lymphocyte subsets

The splenomegaly induced by MHV-68 is mainly caused by the proliferation of $CD4^+$, $CD8^+$ T cells and B cells (Usherwood et al., 1996). The infection of mice with M4stop virus leads to a similar splenomegaly to WT, but it is still unknown whether the same cellular types lead to the splenomegaly during M4stop infection. In order to identify this, the percentages of $CD4^+$, $CD8^+$ T cells, and B cells were determined in all three experiments by flow cytometry, whereas the percentages of NK cells were measured in the first two experiments. The percentages of cellular subsets in the spleens were recorded by flow cytometry and are presented in figure 4.7. Compared to day 7 p.i., decreased percentages of $CD4^+$ T cells and B cells were found after

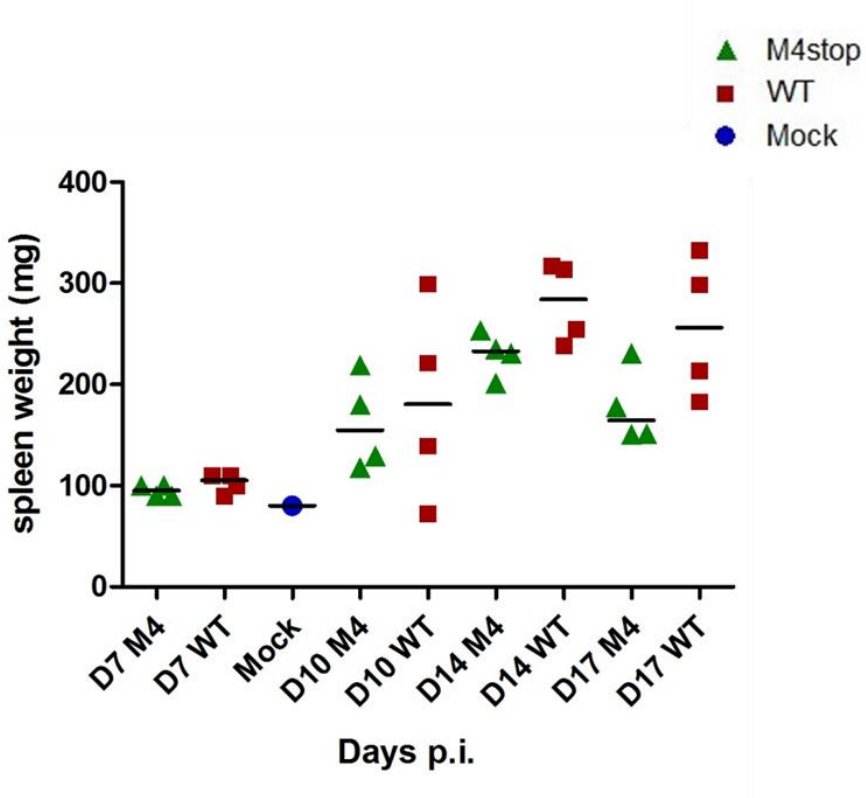

Figure 4.6 Viral induced splenomegaly. 129Sv mice infected with 4×10^5 PFU of WT and M4stop virus were sacrificed at days 7, 10, 14 and 17 p.i., and the spleens weighed. Splenomegaly was found following infection with both viruses after day 7 p.i.. The black bar shows the median of four mice, D denotes day.

viral infection (figure 4.7a and 4.7c), which may be because the proliferation rate of these cell types was not as high as the other cellular types during splenomegaly, therefore the percentages were reduced. In contrast, an expansion in the percentage of $CD8^+$ T cells in the spleens was observed from day 12 p.i. (figure 4.7b). The percentages of $CD4^+$ and $CD8^+$ T cells in the spleens of the WT-infected mice were higher than that of M4stop-infected mice ($p<0.05$) at day 14 p.i. when the difference in latency was detected (figure 4.7a). Therefore, $CD4^+$ and $CD8^+$ T cells may play an important role during MHV-68 infection.

4.2.3.4 Percentages of macrophages and neutrophils

Cxcl2 and Cxcl5 are potent neutrophil chemoattractants in mice (Lin et al., 2007; Walz et al., 1991). In Chapter 3, M4 protein was shown to bind Cxcl2 and Cxcl5, suggesting that the migration of neutrophils may be affected by M4 protein during infection. To investigate this assumption, the percentages of neutrophils were examined in the spleens after M4stop and WT virus infection. Because MHV-68 establishes latency in macrophages (Flano et al., 2000), increased proliferation of macrophages could increase viral latency. Moreover, macrophages express Cxcr2, which is the receptor for Cxcl2 and Cxcl5. Therefore, it is important to know if there are any differences in the percentage of macrophages during viral infections. To examine the percentages of neutrophils and macrophages, 129Sv mice were infected and sacrificed at (1) days 10, 12 and 14 p.i.; (2) days 8, 10, 12 and 14 p.i.. The

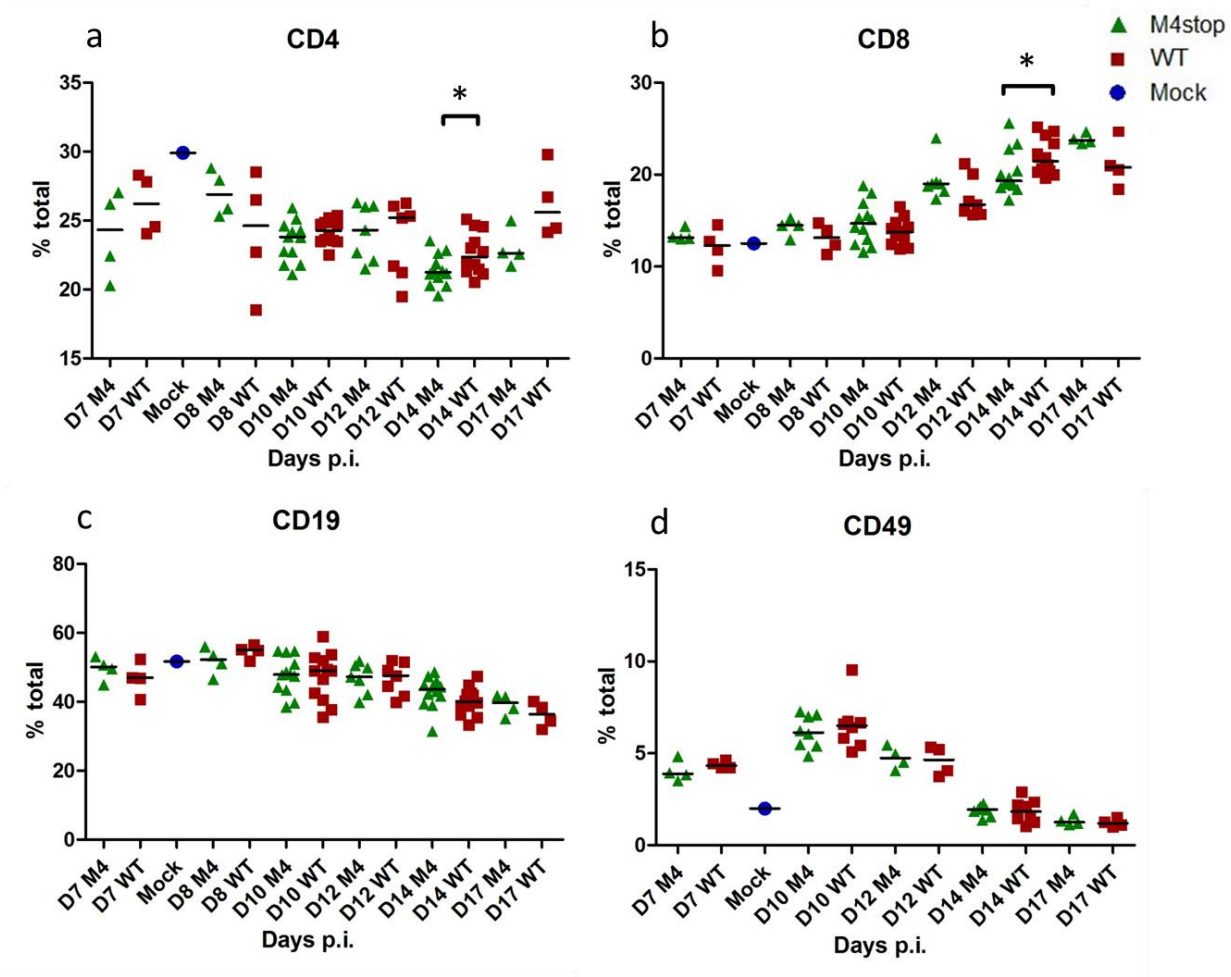

Figure 4.7 Percentages of cell types in the spleens. Samples of splenocytes from the mice which were infected with either M4stop or WT virus were stained by anti-CD4, CD8, CD19 and CD49b antibodies and analysed by flow cytometry to determine the percentage of each population. (a) $CD4^+$ T cells (b) $CD8^+$ T cells (c) $CD19^+$ B cells (d) $CD49b^+$ NK cells. One mouse was used as a negative control. The black bar shows the median of four to twelve mice replicates, D denotes day. Groups that have mean values that vary significantly ($p<0.05$) by Mann-Whitney test are indicated by *.

splenocytes were double-stained with anti-CD11b and anti-Ly6G antibodies. Then the percentages were examined by flow cytometry. Neutrophils were defined as $CD11b^{+}Ly6G^{+}$, whereas macrophages were gated as $CD11b^{+}Ly6G^{-}$. The percentages of neutrophils and macrophages in the spleens are shown in figure 4.8. Comparison of the percentage of neutrophils indicated no differences between M4stop-infected and WT-infected mice (figure 4.8a).

One chemotaxis study has found that the reduction of Cxcl2 and Cxcl5 did not completely inhibit the recruitment and migration of neutrophils, because other neutrophil chemoattractants, such as Cxcl1, also contributed to the recruitment of neutrophils (Lin et al., 2007). This may explain why M4 protein can bind Cxcl2 and Cxcl5, but the lack of M4 protein does not influence the recruitment of neutrophils.

Interestingly, there was a significant decrease in the percentage of macrophages in the spleens of the mice infected with M4stop at day 14 p.i. in comparison to that of WT infection ($p<0.05$) (figure 4.9b). As splenic macrophages are reservoirs of latent MHV-68, the decrease in macrophages may be related to the decreased M4stop viral loads.

In order to know the location of the macrophages in the spleen following M4stop and WT virus infection, MacGreen mice were infected and then sacrificed at days 10, 12 and 14 p.i.. The spleens were manipulated as described in Materials and Methods and frozen sections were cut using a cryostat microtome. Fluorescent macrophages and

granulocytes in the spleens were observed using a confocal microscope. The results are shown in figure 4.9. The B follicles were enlarged and started to form GCs after infection. The GCs of the WT-infected mice exhibited more macrophages at days 10 and 12 p.i. compared to M4stop virus infection. Unfortunately, the expansion of the GC macrophages was not clear on day 14 p.i., due to the green fluorescence being too faint. It would be better to stain the GC B cells to study the interaction of macrophages and B cells. M4 protein may influence the migration of macrophages.

4.2.3.5 Cellular activation in the spleens

The activation of T lymphocytes reflects the control of infection by the host immune system (Gredmark-Russ et al., 2008). $CD8^+$ T cells play a key role in controlling MHV-68 acute infection in the lung (Ehtisham, Sunil-Chandra, and Nash, 1993) and both $CD4^+$ and $CD8^+$ T cells control MHV-68 reactivation during persistent infection (Cardin et al., 1996; Ehtisham, Sunil-Chandra, and Nash, 1993). Increased NK cell percentage were found after MHV-68 infection, therefore, the activation status of NK cells was also compared between the two viral infections, although NK cells may not be associated with the virus clearance mechanism in the spleen (Thomson et al., 2008; Usherwood et al., 2005). The infection of MHV-68 also triggers latency associated B cell activation ($CD19^+CD69^+$) in the spleen (Moser et al., 2005; Stevenson and Doherty, 1999). Therefore, the detection of activated B cells reflects the infection of B cells. There were two hypotheses about how WT virus successfully escapes immune responses and establishes latency at day 14 p.i.. One hypothesis was that M4

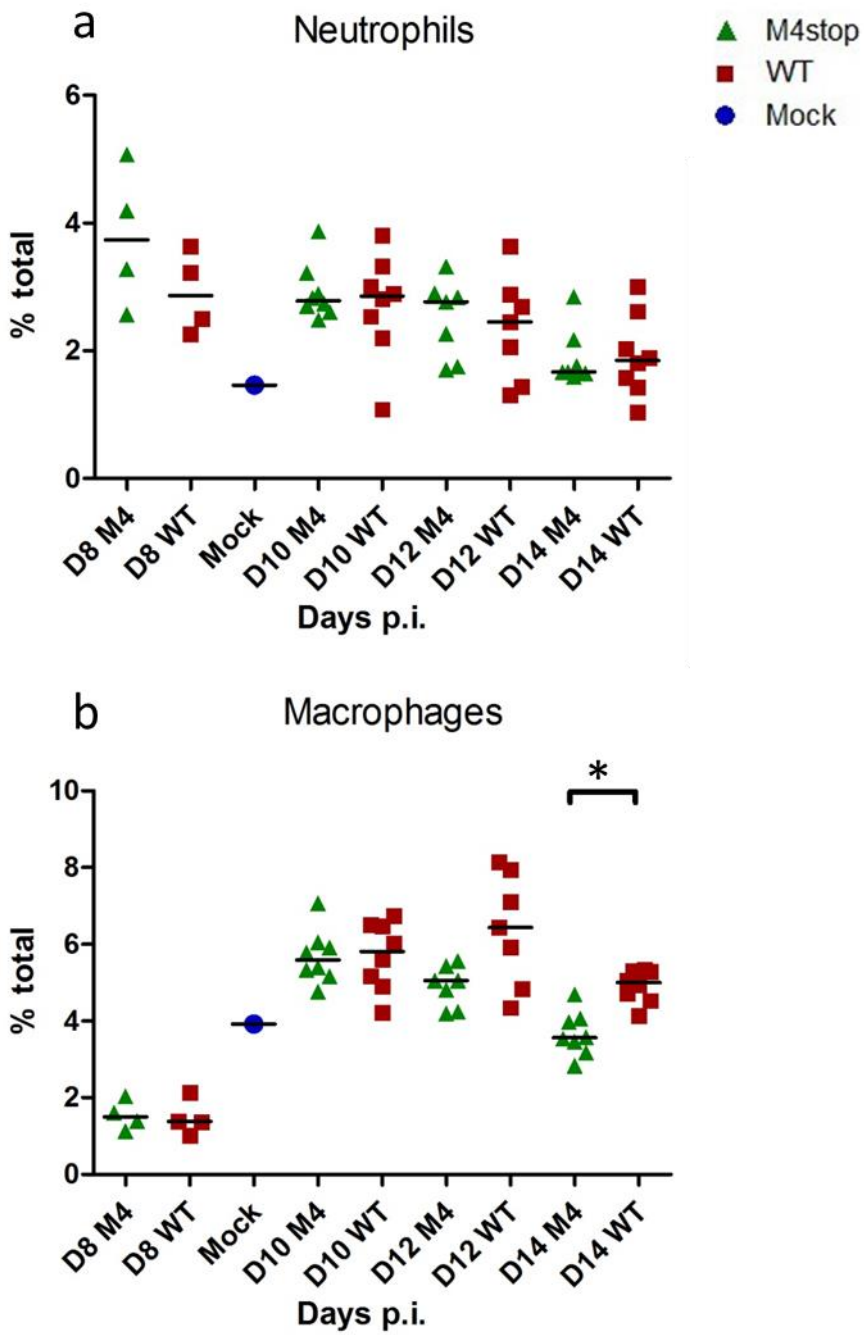

Figure 4.8 The percentages of neutrophils and macrophages. Mice were infected with 4×10^5 PFU of either M4stop or WT virus. Spleens were harvested at days 8, 10, 12 and 14 p.i. and lymphocytes were extracted and double stained with cell surface marker $CD11b^+$ and $Ly6G^+$ (a) neutrophils ($CD11b^+$ $Ly6G^+$) (b) macrophages ($CD11b^+$ $Ly6G^-$). One mouse was used as a negative control. The black bar shows the median of four to eight mice replicates, D represents day. Groups that have mean values that vary significantly ($p<0.05$) by Mann-Whitney test are indicated by *.

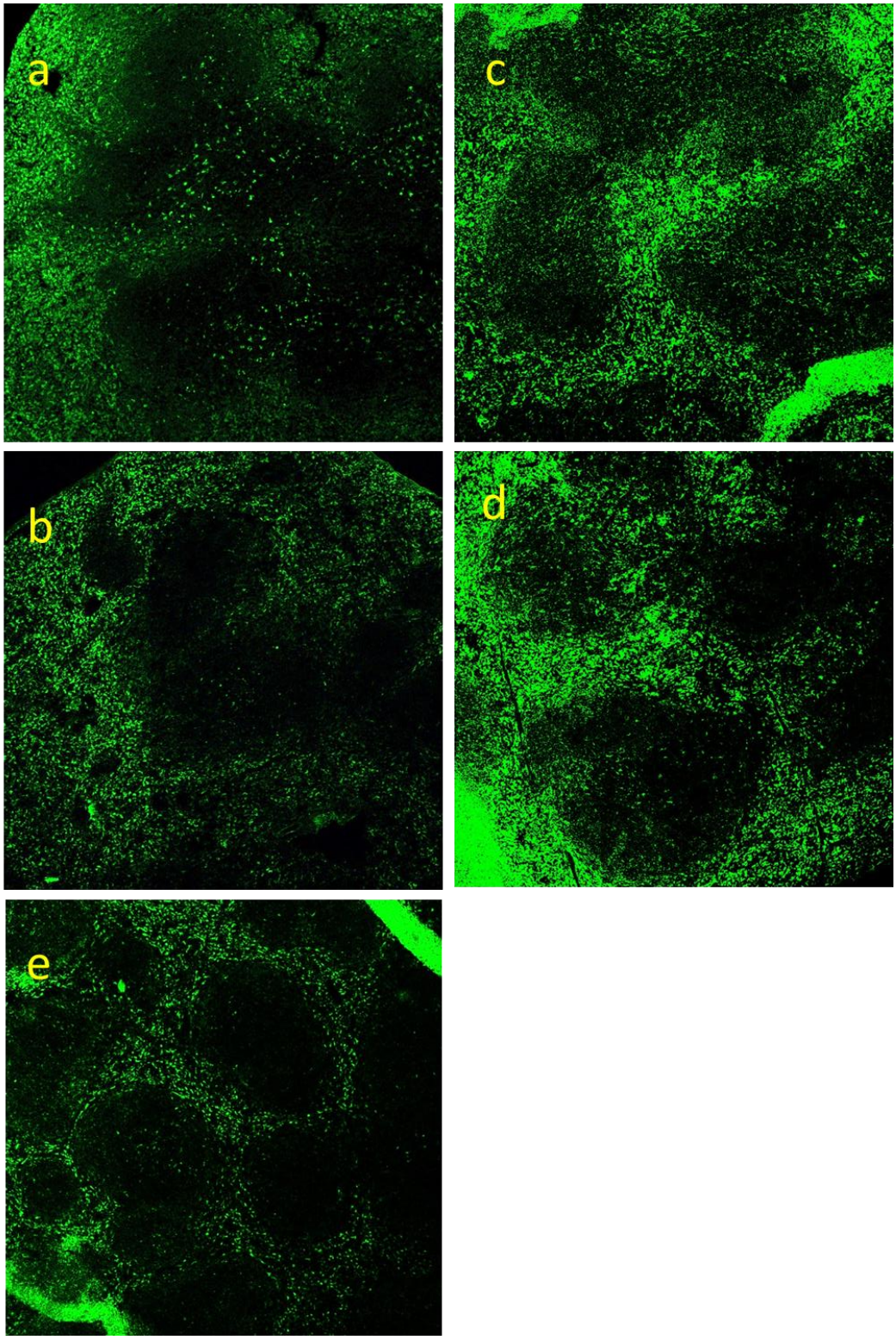
a
c
b
d
e

Figure 4.9 Macrophages and granulocytes in the spleens of MacGreen Mice following M4stop or WT virus infections. Mice were infected with 4×10^5 PFU of either M4stop or WT virus. Spleens were harvested at days 10 and 12 p.i. and sections were cut using a cryostat microtome. Fluorescent macrophages and granulocytes in the spleens were observed using a confocal microscope. A mock-infected mouse was sacrificed and the spleen sections were prepared as for the viral infection groups. The confocal microscope was used at 20 x magnification. (a) WT virus infected spleen at day 10 p.i., (b) M4stop virus infected spleen at day 10 p.i., (c) WT virus infected spleen at day 12 p.i., (d) M4stop virus infected spleen at day 12 p.i., (e) mock-infected spleen.

protein may reduce cellular activation during the establishment of latency in the spleen and therefore the WT virus would be cleared less rapidly. The other is that the higher M4stop viral load may induce more cellular activation in the spleens at day 7 or 8 p.i., and that this controls M4stop virus.

In order to test the two possibilities, cellular activation in the spleen was examined using the early activation marker CD69 (Caruso et al., 1997; Ziegler et al., 1993) in combination with the splenic $CD4^+$, $CD8^+$ T cells, B cells and NK cells markers. The activation percentages of $CD4^+$, $CD8^+$ T cells and B cells were investigated at (1) days 10, 12 and 14 p.i. and (2) days 8, 10, 12 and 14 p.i., whereas the activation percentages of NK cells were determined at days 10, 12 and 14 p.i.. The infected spleens, as well as a spleen from a mock-infected mouse were examined and significantly higher activation percentages of $CD4^+$ T cells ($p<0.05$), $CD8^+$ T cells ($p<0.001$) and B cells ($p<0.05$) were detected in the spleens of WT-infected mice at day 14 p.i. (figure 4.10). The increased cellular activation in the WT-infected spleens correlated with the increased WT viral DNA loads in the spleen at day 14 p.i.. However, the percentage of activated NK cells in the spleens of the mice infected with WT virus was higher than M4stop virus infection, as shown in figure 4.10d, although this was not significant ($p=0.2$). As the percentage of NK cells was reduced suddenly at day 14 p.i., the detection of activated NK cells ($CD69^+$) was limited by the number of cells present.

It is known that NK cells respond to activation by producing IFN-γ. In order to

confirm the percentage of activated NK cells, the ability of NK cells to produce IFN-γ was analysed by double staining of splenocytes with anti-CD49b and anti-IFN-γ intracellular antibody at days 10, 12 and 14 p.i. The percentage of splenocytes expressing IFN-γ is shown in figure 4.11a. There was a significant increase in the IFN-γ expressing splenocytes in the WT virus infected mice at day 14 p.i. compared to the M4stop infection ($p<0.05$). However, no difference was found between the percentages of IFN-γ expressing NK cells following infection with either M4stop or WT virus.

CD38 is another surface marker used to determine the activation status of $CD4^+$, $CD8^+$ T cells, macrophages, etc. (Sandoval-Montes and Santos-Argumedo, 2005). In my study, the percentages of activated $CD4^+$ and $CD8^+$ T cells were also determined by an anti-CD38 antibody. To determine T cell activation in the spleen, splenocytes were double-stained with anti-CD38 and anti-CD4 antibodies or anti-CD38 and anti-CD8 antibodies at (1) days 7, 10, 14 and 17 p.i., and (2) days 10, 12 and 14 p.i.. The gating strategy is shown in figure 4.12 and results are plotted in figure 4.13.

A significant increase in the percentages of $CD4^+$ $CD38^+$ ($P<0.05$) and $CD8^+CD38^+$ ($P<0.001$) T cells were found in the spleens of the mice infected with WT virus at day 14 p.i. compared to M4stop virus, supporting the increase in activating found by CD69 staining in figure 4.10 at day 14 p.i.. It also has been shown that $CD38^+$ T cells have an ability to produce higher levels of cytokines, like IL-2 and IFN-γ, but

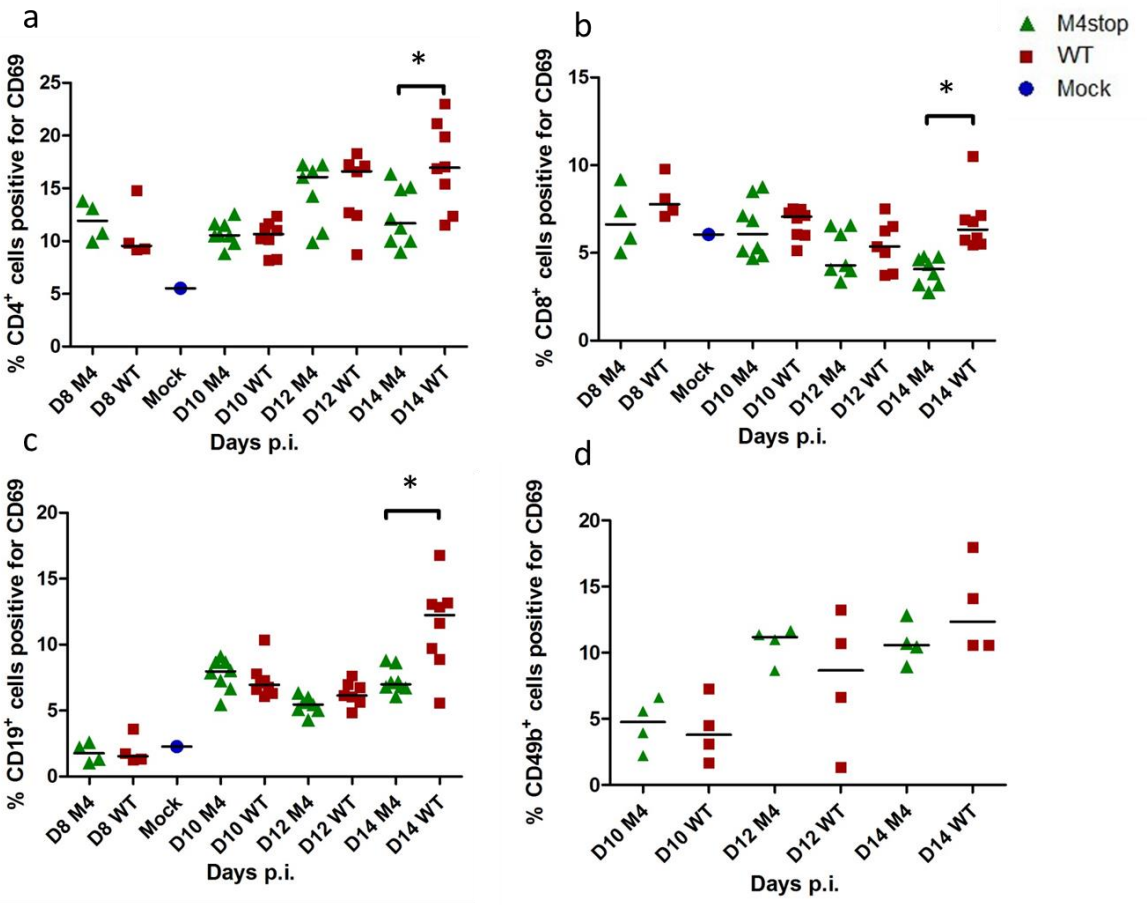

Figure 4.10 Percentage of activated lymphocytes in the spleen. 129Sv mice were infected with 4 x10^5 PFU of either M4stop or WT virus and the spleens were harvested at (1) days 8, 10, 12 and 14 p.i., or (2) days 10, 12 and 14 p.i.. Lymphocytes were double stained with anti-CD69 antibody, accompanied with anti-CD4 T-cell, CD8 T-cell, CD19 B-cell or CD49 NK-cell antibody. The results were analysed by flow cytometry. (a) CD4, (b) CD8, (c) CD19, (d) CD49. Each symbol represents a mouse. D represents day. The black bar shows the median of four to eight mouse replicates. Groups that have mean values that vary significantly ($p<0.05$) by Mann-Whitney test are indicated by *.

undergo less proliferation (Sandoval-Montes and Santos-Argumedo, 2005; Spence and Green, 2008).

The significant increase in percentage of activated cells was only found in $CD4^+$, $CD8^+$ T cells (CD38 and CD69) and B cells (CD69) of the spleens which were infected with WT virus at day 14 p.i., when the viral load of WT virus was significantly higher than M4stop virus. However, there was no difference in the percentages of activated cells at day 7 or 8 p.i., when a significantly higher viral load and cellular reactivation of M4stop were detected.

T cell activation results in the up-regulation of inhibitory molecules, such as PD-1. The expression of PD-1 has been characterized as a negative regulator of T cells, which inhibits T-cell proliferation, cytokine production and autoimmunity (Francisco, Sage, and Sharpe, 2010; Latchman et al., 2001). The increase of PD-1 expression is related to cellular activation during a primary immune response, as well as during persistent immune activation (Keir, Francisco, and Sharpe, 2007; Sun et al., 1998). Therefore, fluorescent conjugated anti-PD-1 antibody was used to define the percentage of activated T cells during early latent infection in the spleen. The percentages of $PD1^+CD4^+$ over the total $CD4^+$ T cells were calculated and compared between the two infection groups (figure 4.14). A significantly higher percentage of $PD1^+CD4^+$ T cells was found in the spleen of the mice infected with WT at day 14 p.i. ($p<0.05$), which was comparable to the CD69 and CD38 results. Additionally, there was a significant increase in the level of $PD\text{-}1^+CD4^+$ T cells in the spleens infected

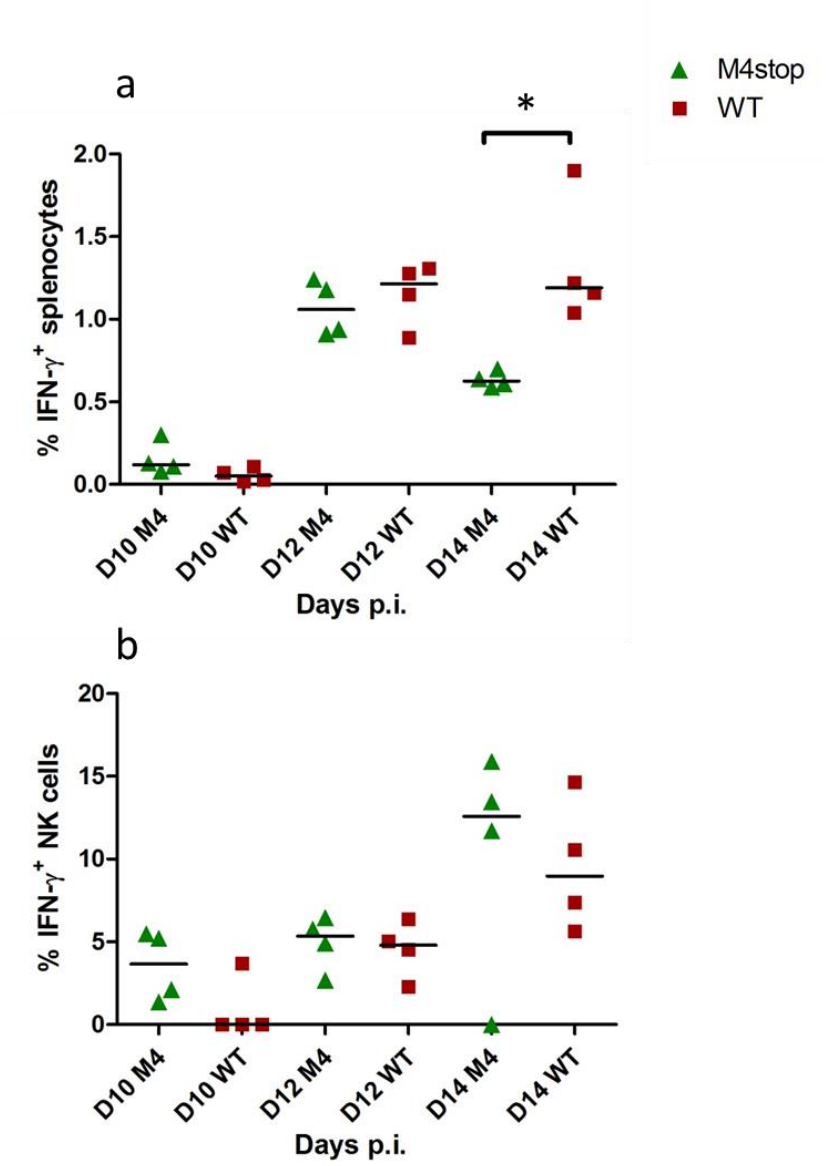

Figure 4.11 IFN-γ expression. 129Sv mice were infected with 4 x 10^5 PFU of either M4stop or WT virus and the spleens were harvested at days 10, 12 and 14 p.i.. Lymphocytes were stained with anti-CD49, accompanied with intracellular staining of IFN-γ. (a) Percentage of splenocytes which expressed IFN-γ. (b) The percentage of the activated NK cells which have the ability to express IFN-γ. The black bar shows the median of four mouse replicates, D presents day. Each shape indicates one mouse. Groups that have mean values that vary significantly ($p<0.05$) by Mann-Whitney test are indicated by *.

with M4stop virus at day 8 p.i. ($p<0.05$). It has been reported that herpesviruses, such as HCMV, MCMV and EBV, induce the PD-1-PD-L pathway that suppress T cell activation (Benedict et al., 2008; Green et al., 2012; Zhang et al., 2008). The absence of increased $CD69^+$ or $CD38^+$ lymphocytes in the M4stop-infected spleen at day 7 or 8 p.i. may due to the immunosuppressive activity of PD-1. Although this experiment was only carried out once, it supported our hypothesis that the higher viral DNA load in the spleen following M4stop infection at day 7 and 8 p.i. stimulates earlier cellular activation. Interestingly, a higher percentage of total $PD\text{-}1^+$ cells were found in WT virus infected spleens compared to that of M4stop virus infected spleen at day 14 p.i. (14.5 ± 2.5 versus 8.9 ± 1.7). This indicates cellular activation had also occurred in other cells in the spleen at day 14 p.i.. In addition, it has been reported that PD-1 is involved in GC B cell formation and differentiation, as well as T_{FH} cell development and function (Good-Jacobson et al., 2010). Therefore, the increase in PD-1 at day 8 p.i. in the spleens of M4stop-infected mice and day 14 p.i. in the spleens of WT-infected mice may be related to the development of GC B cells.

Cytokines secreted from activated T cells have an ability to induce macrophage activation. As the activation of macrophages is crucial for control of herpesvirus (Heise and Virgin, 1995), we were keen to know whether macrophages play a part in M4stop virus infection. To assess the activation of macrophages, splenocytes were triple stained with anti-CD11b, Ly6G, and CD69 antibodies. As described before, the

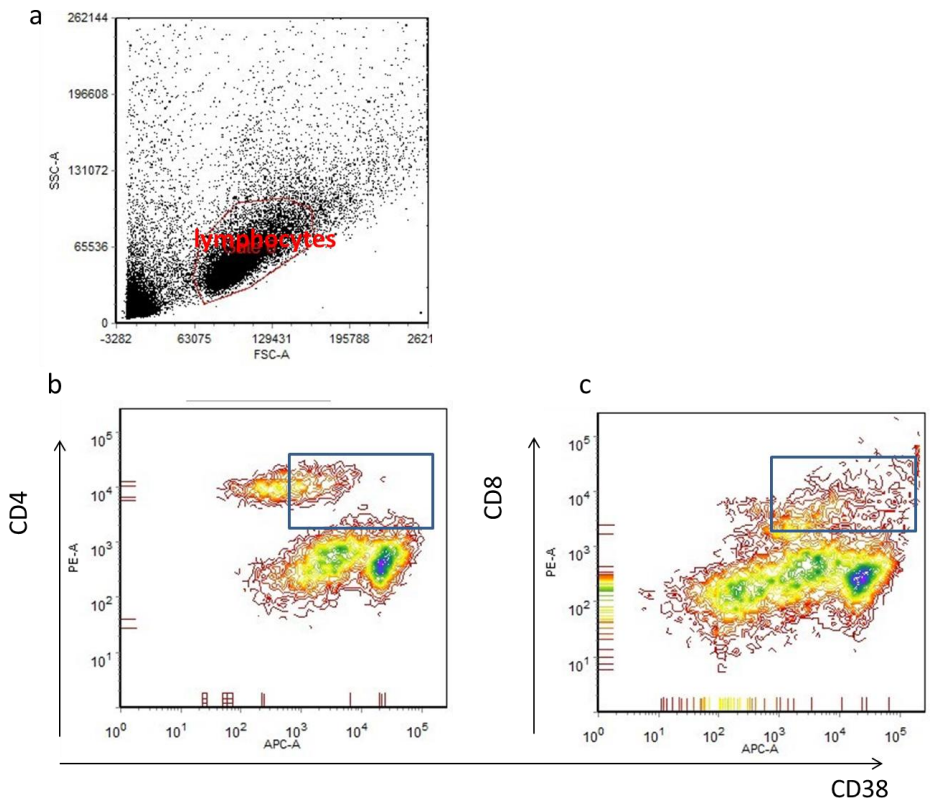

Figure 4.12 Gating strategies for CD38 expressing $CD4^+$ and $CD8^+$ T cells. (a) The gate was set on the lymphocytes. (b) Gating for $CD38^+CD4^+$ T cells. (c) Gating for $CD38^+CD8^+$ T cells.

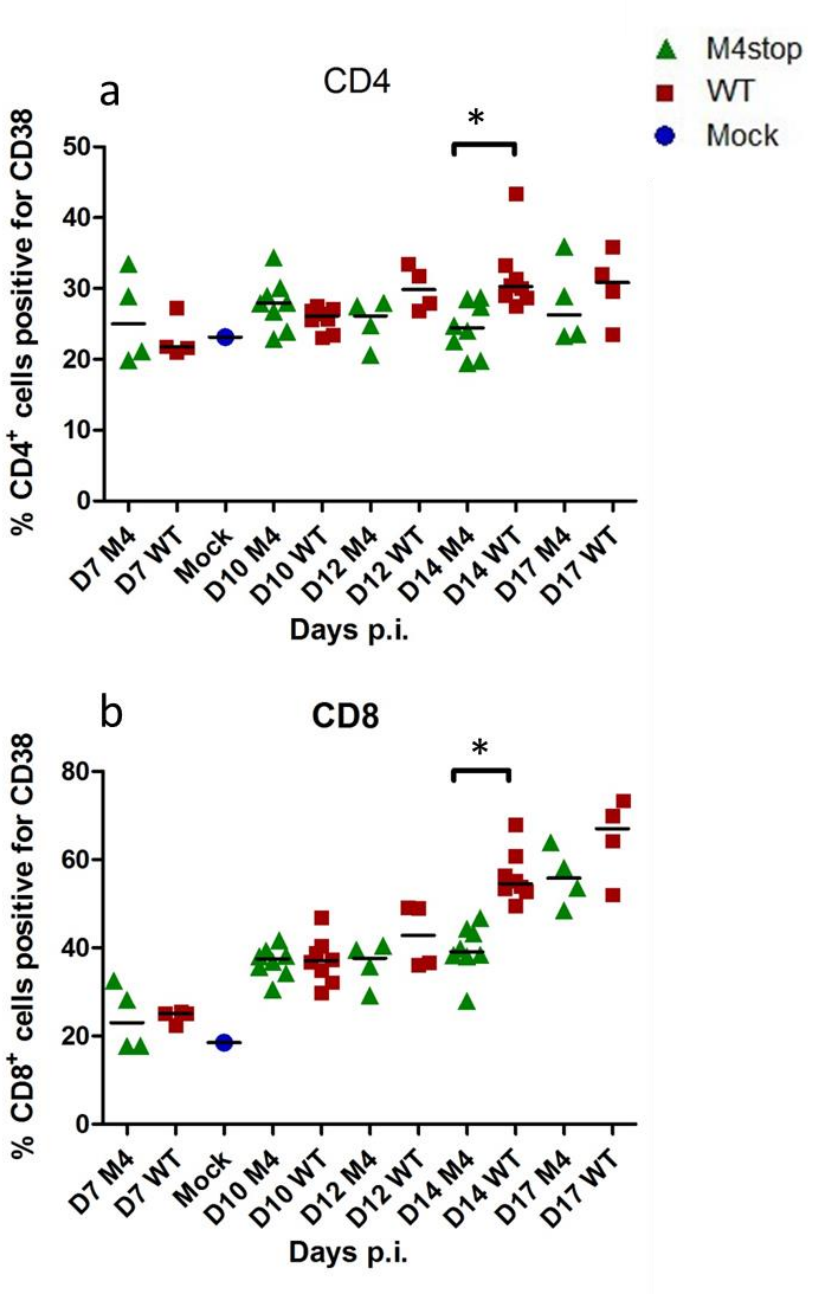

Figure 4.13 Percentage of activated ($CD38^+$) $CD4^+$ and $CD8^+$ T cells in the spleens following infection with M4stop or WT. 129Sv mice were infected with 4×10^5 PFU of M4stop or WT virus and sacrificed at days 7, 10, 14 and 17 p.i., and days 10, 12 and 14 p.i.. Splenocytes which were double stained with $CD38^+$ and (a) $CD4^+$ or (b) $CD8^+$ antibodies were determined the activated of T cells. D represents day. Each symbol indicates one mouse. The black bar shows the median of four to eight mouse replicates Groups that have mean values that vary significantly ($p<0.05$) by Mann-Whitney test are indicated by *.

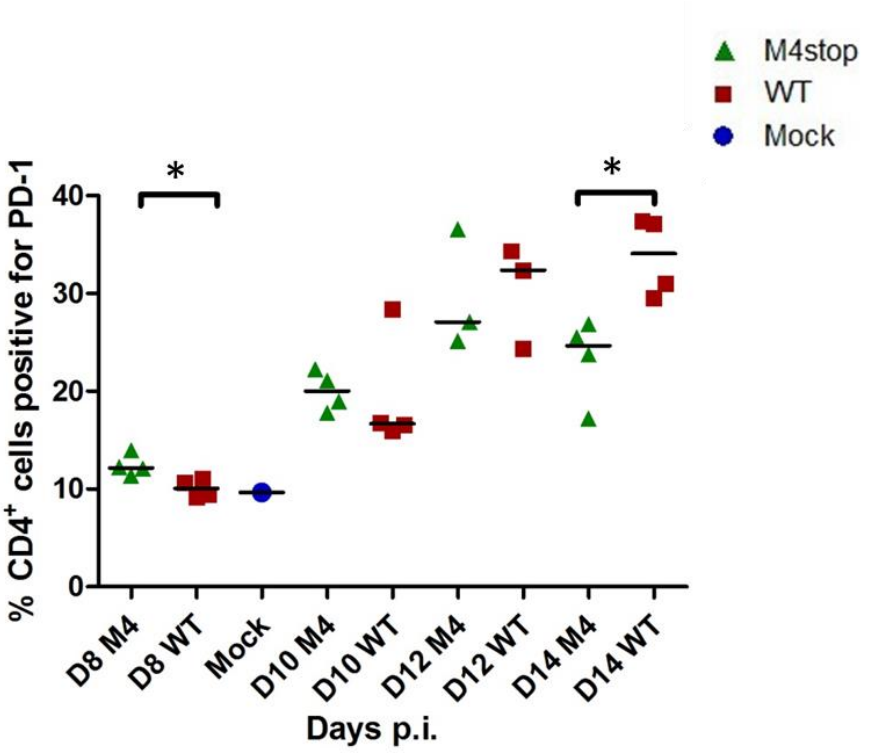

Figure 4.14 Percentage of PD-1^+ $CD4^+$ T cells. 129Sv mice were infected with 4×10^5 PFU of M4stop or WT virus and sacrificed at days 8, 10, 12 and 14 p.i. The splenocytes were double stained with anti-CD4 and anti-PD-1 antibodies. D represents day. Each symbol indicates one animal. The black bar shows the median of three to four mouse replicates, D denotes day. Groups that have mean values that vary significantly ($p<0.05$) by Mann-Whitney test are indicated by *.

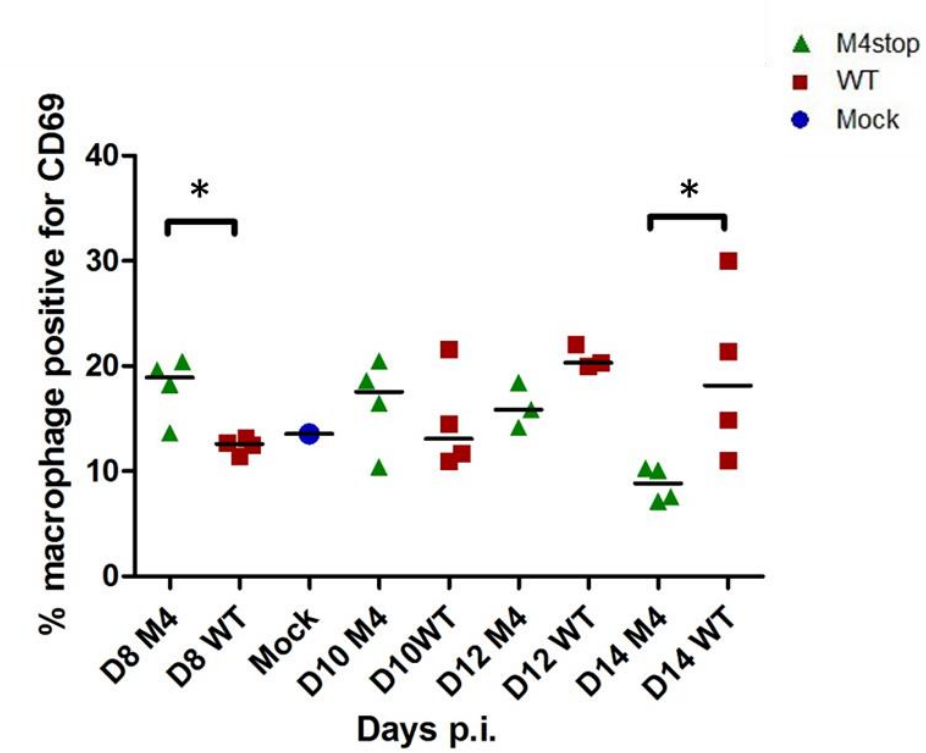

Figure 4.15 The percentage of activated macrophages. The $CD11b^{+}$ $Ly6G^{-}$ macrophages were gated and the percentage of activated macrophages ($CD69^{+}$ $CD11b^{+}$ $Ly6G^{-}$) over the total macrophage ($CD11b^{+}Ly6G^{-}$) population was calculated. One mouse was mock-infected with the same amount of PBS and was used as a negative control. The black bar shows the median of three to four mouse replicates, D represents day. Groups that have mean values that vary significantly ($p<0.05$) by Mann-Whitney test are indicated by *.

$CD11b^{+}Ly6G^{-}$ cells were gated as the macrophage population, then the percentage of activated ($CD69^{+}$) macrophages in the whole macrophage population was calculated (figure 4.15). Significantly higher ($p<0.05$) percentages of activated macrophages were found in M4stop-infected spleens at day 8 p.i. when compared to WT infection. The percentage of activated macrophages dropped sharply in the M4stop-infected spleen at day 14 p.i. compared to WT virus infection ($p<0.05$). The difference in macrophage activation between M4stop and WT virus infections may be associated with the production of proinflammatory cytokines (Sancho, Gómez, and Sánchez-Madrid, 2005).

4.2.4 The transcription of immune molecules during infection

Activated leukocytes can up-regulate the synthesis of chemokines, cytokines and chemokine/cytokine receptors. These immune molecules and receptors are involved in the regulation of immune responses, such as T cell activation, and the trafficking of immune cells. To gain insight into what mechanisms play a part in controlling M4stop infection, the expression of cytokines, chemokines and their receptors was analyzed and compared in the spleens of either M4stop or WT virus infected mice. RT² Profiler™ PCR arrays (PAMM-011) were performed using splenic cDNA which was reverse transcribed from splenic RNA that was isolated from mice culled at days 10, 12 and 14 p.i.. The results were normalized using one house keeping gene that was simultaneously run with the samples. The names of the inflammatory genes, which are contained in PAMM-011, are listed in the Appendix II. Due to the limited

number of PCR array wheels, each of the eight spleen samples from day 12 p.i. was examined individually, whereas the samples of each infection group from day 10 or 14 p.i. were pooled and examined as a single sample. The expression of genes in each sample was analysed on the manufacturer's website (http://pcrdataanalysis.sabiosciences.com/pcr/arrayanalysis.php). The normalized $2^{-Avg\Delta Ct}$ values of these genes in the spleens of the mice following WT virus infection at day 10 p.i. were considered as controls. Then the other normalized $2^{-Avg\Delta Ct}$ values for M4stop virus infected samples and WT virus infected samples from days 10, 12 and 14 p.i. were compared to the WT virus infected sample at day 10 p.i.. Genes with fold changes in expression >2 or <0.5 at day 10, 12 or 14 p.i. were chosen and presented in figure 4.16. Significant increases in IL-16, Ccr4, Cxcr2 and LTβ expression were detected in the spleens of mice infected with M4stop virus at day 12 p.i., compared to WT virus at the same time point ($p<0.05$). Several inflammatory chemokines, such as Ccl2 (figure 4.16b), Ccl7 (figure 4.16d), Ccl8 (figure 4.16d), Ccl11 (figure 4.16c) and Ccl12 (figure 4.16b), were apparently up-regulated in spleens which were infected with WT virus at day 14 p.i. based on the fold changes. These results were consistent with T cell activation ($CD69^+$) results at day 14 p.i., since the activated T cells may generate more chemokines.

As the RNA samples from days 10 and 14 p.i. were pooled, we did not know whether the differences in gene transcription between M4stop and WT virus infections were significant. Therefore, Ccl7, Ccl8, Ccl17 and Ccr4, whose transcripts were very

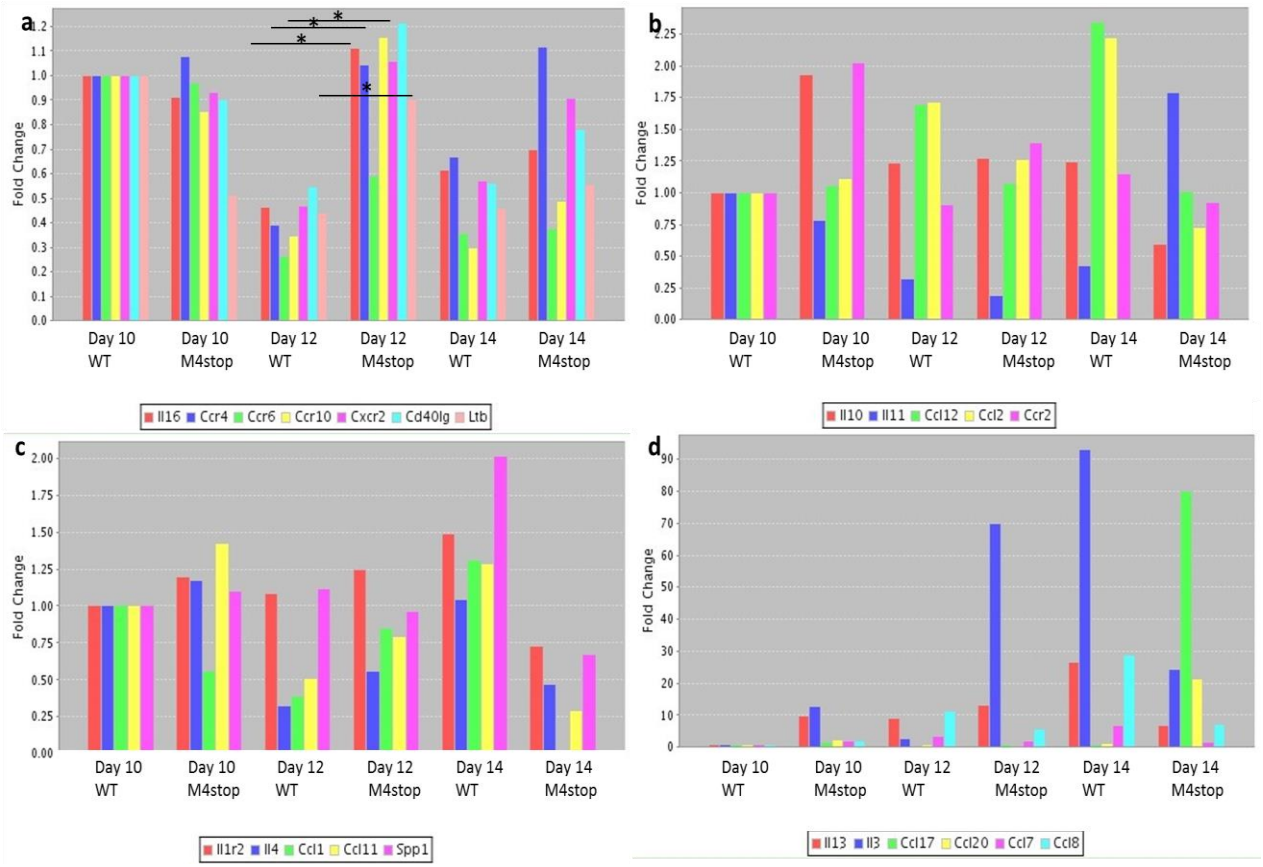

Figure 4.16 Fold changes in gene expression. The mice, infected with 4×10^5 PFU of M4stop or WT virus, were sacrificed at days 10, 12 and 14 p.i.. RNA was extracted from the spleens and transcribed into cDNAs. PCR arrays (PAMM-011) were carried out to examine gene expressions in the spleen. The samples from day 12 p.i. were examined individually, whereas the samples from days 10 and 14 p.i. were pooled. 23 genes, which have differences between M4stop and WT virus infections, are shown. The results of gene expression in the spleens infected with WT at day 10 p.i. were set as the controls (fold change=1), and up- or down-regulation of the other results are presented as fold changes. (a) IL-16, Ccr4, Ccr6, Ccr10, Cxcr2, CD40lg and LTβ. (b) IL-10, IL-11, Ccl12, Ccl2 and Ccr2. (c) IL-1r2, IL-4, Ccl1, Ccl11 and Spp1. (d) IL-13, IL-3, Ccl17, Ccl20, Ccl7 and Ccl8. Groups that have mean values that vary significantly ($p<0.05$) are indicated by *, which was calculated by the Sabiosciences online statistics programme.

different between viral infections and involved in cellular activation, were selected and qPCR primers for these genes were purchased to examine the cDNA samples from days 10 and 14 p.i.. The results of the WT infected mice at day 10 p.i. were set as the controls as in the earlier experiment showed. Then the normalized $2^{-Avg\Delta Ct}$ values of M4stop and WT infection from days 10, 12 and 14 p.i. were compared to the controls and the fold changes are presented in figure 4.17. Ccl7 was significantly up-regulated ($p<0.05$) in the spleens of the mice infected with M4stop virus at day 10 p.i. in comparison to WT virus. The expression of Ccr4 was significantly increased ($p<0.05$) in the spleens following M4stop infection at days 12 and 14 p.i. compared to WT virus infection. A great variability in the values of Ccl8 was found at day 12 and 14 p.i..

4.3 Discussion

In this chapter, several changes have been found during the course of the lytic infection in the lung and early latent infection in the spleen in the absence of M4 compared to WT infection: (1) The viral load of the M4stop virus infection was lower in the lungs at day 8 p.i. which was consistent with the results of Evan et al (2006) at day 9 p.i.; (2) the number of latently infected was higher at 8 p.i. respectively; (3) higher percentages of $PD1^+$ $CD4^+$ T cells and activated macrophages were found in the spleens of the mice infected with the M4stop virus at day 8 p.i.; (4) significantly lower percentage of activated ($CD69^+$, $CD38^+$ or $PD\text{-}1^+$) $CD4^+$, $CD8^+$ T cells and B cells were found in the spleens infected with M4stop virus

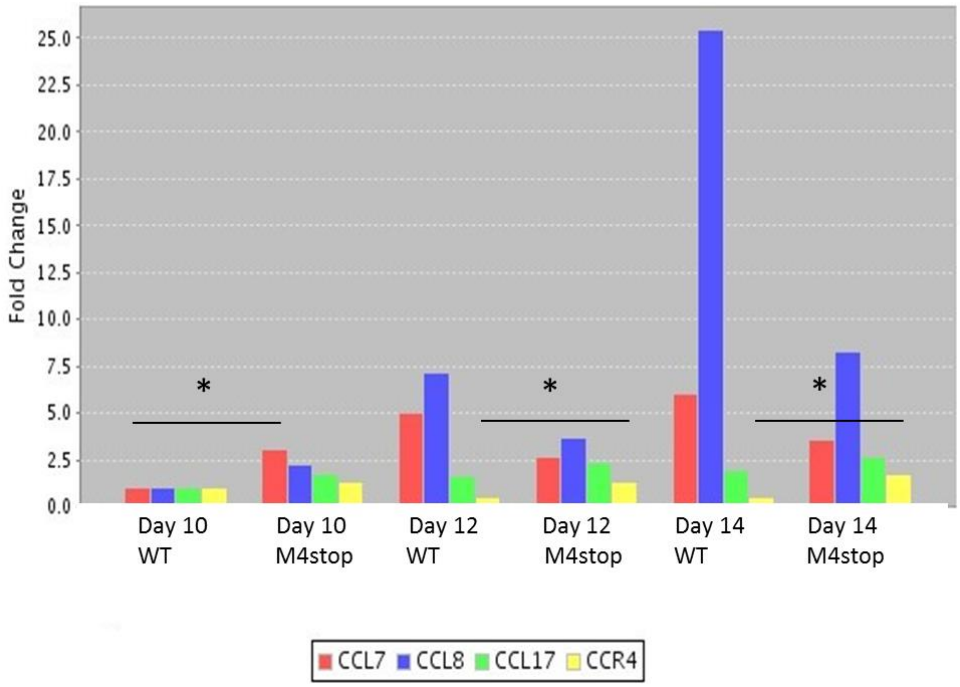

Figure 4.17 Fold change in gene expression. Mice were infected with 4×10^5 PFU of M4stop or WT virus and were sacrificed at days 10, 12 and 14 p.i.. The RNA was extracted from the spleen and transcribed to cDNAs. The qPCR was performed on selected genes. The results of gene expression in spleens infected with WT at day 10 p.i. were set as the controls (fold change=1), and up- or down-regulation of the other results are presented in the fold changes. The results were compared between M4stop and WT virus infections at each time point. The results of day 10 and 14 p.i. were got from qRT-PCR and the results of day 12 p.i. were from RT-PCR array. Groups that have mean values that vary significantly ($p<0.05$) are indicated by *, which was calculated by the Sabiosciences online statistics programme.

at day 14 p.i.; (5) The transcription of IL-16, Ccr4, Cxcr2 and LTβ was shown to up-regulated in the spleens of M4stop infected mice at days 12 p.i., while the expression of Ccl7 was detected to be up-regulated in the spleens of M4stop infected mice at day 10 p.i.. In the Chapter 4, M4 was shown to be a chemokine binding protein. The faster clearance of M4stop viral loads in the lungs and spleen might be caused by M4 having the same function as Equine herpesvirus type 1 (EHV-1) gG which reduces the migration of neutrophils and macrophages to the lung (Vigne et al., 2011). The transmission of the MHV-68 from lung to MLN requires the help of dendritic cells and macrophages. If M4 can slow down the trafficking of dendritic cells and/or macrophages, the virus may take longer to reach the MLN. Therefore, in the absence of M4 protein, there may possibly be more M4stop virus entering the MLN by day 8 p.i., accompanied by higher M4stop viral loads in the spleens at early latent infection. As the different viral loads in the lungs were found in the final experiment, it was a pity that there was no follow up studies looking at the chemokine levels, percentages of dendritic cells and/or macrophages in the lung, as well as the viral loads or latency in the MLNs at day 8 p.i.. The reduction in M4stop viral loads in the lung may also be caused by the increased inflammation in the lung during the M4stop virus infection. Therefore, the M4stop was cleared more quickly than WT in the lung at day 8 p.i.. However, this idea cannot explain the increase of M4stop viral load in the spleen at day 8 p.i..

It has been shown for the first time that viral DNA loads and the number of

infectious centre in the spleens of mice infected with M4stop virus were higher than WT infection early after infection. This is associated with an increase of the percentages of activated $CD4^+$ T cells ($PD1^+$) and activated macrophages ($CD69^+$) at day 8 p.i.. Afterwards, a decrease in the $PD1^+CD4^+$ T cells and activated macrophages was seen in the M4stop-infected spleens at day 14 p.i.. PD-1 is essential for GC B cell development and the affinity of plasma cells antibody (Good-Jacobson et al., 2010). GC B cells are the reservoir of MHV-68 (Marques et al., 2003) and plasma cells are the main cells that induce MHV-68 reactivation (Liang et al., 2009). In addition, blockage of PD-1 and PD-L1 pathway influences the virus reactivation (Dias et al., 2010). Therefore, the down-regulation of PD-1 on $CD4^+$ T cells at day 14 p.i. in the M4stop-infected spleens may impair the GC response, thereby, influence the M4stop latency and reactivation. In addition, as PD-1 is an immunoinhibitory receptor, it is beneficial for MHV-68 to exploit this inhibitory pathway. However, it is unclear whether the presence of M4 protein is essential for up-regulation of PD-1.

The increase in the percentage of activated B cells ($CD69^+$) in the WT infected spleens was consistent with the higher viral loads and latency. EBV infection drives B-cell differentiation that results in the accumulation of EBV (Calender et al., 1987). This can be measured by activation markers. This raises the possibility that M4 protein may trigger the proliferation of B cells, leading to an increased WT viral load at day 14 p.i. compared to M4stop virus infection. However, the percentage of

$CD19^+$ B cells in the spleen showed no difference following the two viral infections.

The results of PCR arrays and PCR showed that there was an increase in the transcription of Ccl7 at day 10 p.i., and IL-16, Cxcr2 and LTβ at day 12 p.i. in the spleens infected with M4stop virus. Ccl7 is secreted by macrophages and is able to attract a variety of leukocytes including monocytes, eosinophils, basophils, DC, NK cells and activated T cells (Fukuda et al., 1997). The increased expression of Ccl7 suggests that the macrophages were highly activated in the spleens. It is known that IL-16 is a repressor for HIV replication (Maciaszek et al., 1997). The production of IL-16 is decreased after co-infection with HIV-1 and HHV-7, when HHV-7 replication expands rapidly (Lisco et al., 2007). Therefore, HHV-7 infection may help to down-regulate the expression of IL-16 to help the virus evade the immune response. The up-regulation of IL-16 in M4stop virus infection may impair viral latency. Cxcr2 is expressed on endothelial cells, neutrophils and macrophages and is the receptor for Cxcl1, Cxcl2 and Cxcl5. Cxcr2 has a role in neutrophil and macrophage trafficking during several infections (Del Rio et al., 2001; Herbold et al., 2010; Wareing et al., 2007). However, there was no difference in the percentage of neutrophils or macrophages at day 12 p.i.. MHV-68 and KSHV encoded ORF74 is a homologue of CXCR2 (Bais et al., 1998; Virgin et al., 1997). Meanwhile, M4 protein was shown to bind Cxcr2 ligands in Chapter 3. As the function of Cxcr2 is impaired by ORF74, it may explain why there was no difference in the percentage of neutrophils and macrophages in the spleens following M4stop and WT virus

infection, although the expression of Cxcr2 was increased in the M4stop virus infection. The up-regulation of LTα was also found in the spleen of the mice infected with M4stop virus at day 12 p.i., with a 1.95 fold increase in expression compared to WT ($p<0.05$) (data not shown). LTα and LTβ are members of the tumor necrosis factor (TNF) family and they are important factors for immune responses. For example, LTα is required for the control of Mycobacterium tuberculosis infection (Roach et al., 2001) and LTβ can enhance immune responses of lymphocytes, boost antigen presentation by antigen-presenting cells, and inhibit the exhaustion or apoptosis of $CD8^+$ T cells (Junt et al., 2006). Moreover, LTα and LTβ are involved in the normal development of GC (Alimzhanov et al., 1997; Lee et al., 2000). Interestingly, we found more genes related to the development of GC were up-regulated when they were examined by qPCR. This result will be introduced in the next chapter.

Compared to M4stop virus infected mice, more IFN-γ^+ cells were found in the spleens at day 14 p.i., and may be responsible for the activation of the macrophages. Interestingly, IFN-γ may not be the only factor that induces the activation of macrophages. The up-regulation of IL-4 and IL-13 was found in the spleens infected with WT virus at day 14 p.i. (figure 4.16 c and d), which may drive alternative activation of macrophages at days 12 and 14 p.i.. Moreover, Ccr4 is the receptor for Ccl2, Ccl3, Ccl5 and Ccl17, and it expressed on activated T cells. CCr4 is important in proinflammatory macrophage differentiation, as the features of alternatively

activated macrophages were found in Ccr4 deficient mice (Ness et al., 2006). Therefore, decreased transcription of Ccr4 and the increased expression of IL-13 and IL-4 indicate that macrophages may be alternatively activated during WT virus infection. Therefore, both classical and alternative activation of macrophages may be stimulated simultaneously at day 14 p.i. It has been found that MHV-68 results in alternative activation of macrophages and fibrosis in IFN-γ unresponsive mice (IFN-γR$^{-/-}$ mice) (Gangadharan et al., 2008). This may be due to the blockage of the IFN-γ pathway, leading to a dominant of Th2 immune response. In this case, the M4stop virus may induce less fibrosis in the IFN-γR$^{-/-}$ mice since M4stop infection may trigger reduced Th2 responses.

Chapter 5

M4 may change the GC development

5 M4 may change the GC development

5.1 Introduction

GCs exist in secondary lymphoid organs and develop when naïve B cells are activated through stimulation of antigen receptors on their surface and receive stimulatory signals from immune helper cells, such as T_{FH} cells. This procedure is dynamic, for example, newly activated B cells have an ability to enter existing GCs (Schwickert et al., 2009). During GC development, B cells transform into centroblasts that proliferate within the dark zone of the GC. Centroblasts revise their antigen receptors through somatic hypermutation of IgV region genes, a process that introduces mainly single nucleotide substitutions into the IgV gene to generate antibodies with a higher or lower affinity to the respective antigen. Centroblasts migrate to the light zone under the influence of chemoattractants, then develop to centrocytes, which express high-affinity antibody mutants and eventually differentiate into plasma cells or memory B cells. T_{FH} cells provide help to B cells during GC development by secreting IL-21. IL-21 interacts with the IL-21R which is expressed on B cells, then B cells differentiate into plasma cells which have the ability to secrete antibodies (Bryant et al., 2007; Linterman et al., 2010). Moreover, IL-21 can modulate expression of CXCR5 and CCR7 on activated T cells (reviewed in King, Tangye, and Mackay, 2008).

Homeostatic chemokines and some cytokines can promote lymphoid tissue

organization. For example, CCL19 and CCL21, the ligands of CCR7, can induce the expression of LTα-LTβ complex, LTα1β2, which precipitates secondary lymphoid organ formation (Luther et al., 2002). Moreover, IL-2, -4, -7, -15 are all able to enhance the level of LTα1β2 on activated $CD4^+$ and $CD8^+$ T cells (Luther et al., 2002). On the other hand, CXCR5 is the receptor for CXCL13 and it is required for B cell homing to the spleen (Ansel et al., 2000). Therefore, the mice with deficiency of both Cxcr5 and Ccr7 exhibit severely disturbed architecture in the spleen (Ohl et al., 2003). CXCL12 mediates the trafficking of CXCR4-expressing B cells, dendritic cells and plasma cells (Hargreaves et al., 2001; Luther et al., 2002). Thus, the interaction of CXCR5-CXCL13 and CXCR4-CXCL12 is essential for the migration of centroblast and centrocytes (Allen et al., 2004).

Aside from chemokines and cytokines, transcription factors also influence GC formation. For example, Bcl-6 is expressed highly in GC B cells and is selectively expressed in T_{FH} cells. It has been reported that Bcl-6 knockout mice fail to develop GCs and do not produce high-affinity antibodies (Fukuda et al., 1997; Ye et al., 1997). Bcl-6 is also required for programming of T_{FH} cell generation. For example Bcl-6 represses the expression of several microRNAs that target several key T_{FH} genes (Yu et al., 2009), therefore a deficiency in Bcl-6 results in impaired T_{FH} cell development and GC development (Nurieva et al., 2009).

Gammaherpesvirus infection is related to GC formation. For example, EBV infects naïve B cells and drives their activation and proliferation, which is regulated by

expression of viral growth transcription programmes, such as EBNA-2 (Sinclair et al., 1994). EBV establishes latency in the GC when the GC reaction occurs (Roughan, Torgbor, and Thorley-Lawson, 2010). Most B cells die as a result of apoptosis during the GC reaction. However, LMP-1 and LMP-2A regulate NFκB activation, which provides survival signals (reviewed in Spender and Inman, 2011). In the GC, virus has access to resting memory B cells, where persistent infection of EBV is found (Roughan and Thorley-Lawson, 2009). KSHV also infects B cells during infection. It may preferentially infect naïve B cells in the absence of EBV infection, but during co-infection with EBV, KSHV infects GC or post-GC B cells (Hamoudi et al., 2004). Moreover, KSHV-positive macrophages were detected only within GC (Valmary, Richard, and Brousset, 2005). MHV-68 establishes latency mainly in GC B cells, especially in the centroblasts (Collins and Speck, 2012; Flano et al., 2002). It has been found that plasma cells contain latent MHV-68 and the differentiation of plasma cells is important to maintain MHV-68 latency (Collins, Boss, and Speck, 2009; Siegel et al., 2010). Moreover, the M2 protein encoded by MHV-68 drives plasma cell differentiation and this regulates viral reactivation (Liang et al., 2009). Therefore, the dysregulation of GC development during viral infection may affect MHV-68 latency.

In Chapter 4, the analysis of PCR arrays demonstrated the up-regulation of inflammatory genes in the spleens of mice following M4stop virus infection compared to WT virus infection. Moreover, the arrays showed some transcripts

which are involved in the development of GC were up-regulated in the M4stop virus infection compared to WT virus infection. For example, LTα and LTβ were found to be significantly up-regulated in the M4stop-infected spleens at day 12 p.i. compared to WT virus infection (figure 4.16a and in the discussion of chapter 4). LTα and LTβ are important in the development of stromal cells, which secrete T cell and B cell homing chemokines (Ngo et al., 1999). Without LTα and/or LTβ, the spleen structure or the development of GC is abnormal. For instance, MHV-68 induced splenomegaly is absent in LTα-deficient mice (Lee et al., 2000), probably because the mice fail to develop GC. In order to understand whether the development of GC were distinct in the spleen following M4stop and WT virus infections, the transcripts involved in the development of GC were analyzed. Furthermore, we analyzed key cell populations which are important in GC development and virus infection.

5.2 Results

5.2.1 M4stop infection increases gene expressions

In Chapter 4, PAMM-11 PCR arrays were carried out to examine the expression of inflammatory genes in the spleen following M4stop and WT virus infections at days 10, 12 and 14 p.i.. As described in Chapter 4, the samples from days 10 and 14 p.i. were pooled and examined, whereas the samples from day 12 p.i. were studied individually. In this chapter, the analysis was focused on the mRNA transcripts which are essential for GC development. As described in the Chapter 4, the results of the WT infection at day 10 p.i. were set as the control, while the other results from days

12 and 14 p.i. were compared with the control. PCR array results showed Cxcl12, Ccr7 and Bcl-6 were significantly up-regulated in the spleens of mice infected with M4stop virus ($p<0.05$, figure 5.1) at day 12 p.i. as compared to the WT virus infection. Moreover, the expression of Ccl19 and Cxcr5 was 2.1 and 2.3 fold up-regulated in the M4stop-infected spleen compared to WT virus infected at day 12 p.i., but this was not significantly different ($p=0.07$ and 0.08 respectively). All five gene transcripts are known to be important in GC development. Since we could not perform statistical tests on the difference between the M4stop and WT virus infections at days 10 and 14 p.i. from the PCR arrays, RT-PCR analysis of the expression of Ccl19, Cxcl12, Cxcr5 and Bcl-6 mRNA was carried out to understand the change between viral infections at these two time points. Additionally, the transcription of Ccl19 was barely detected in the M4stop-infected spleens at day 14 p.i. from the RT-PCR arrays and this may have been due to technical error. It was therefore necessary to confirm this result by qPCR. The results were analysed as in the Chapter 4, in which the gene transcription levels of WT virus infection at day 10 p.i. were set as the control (fold change=1), then the other results were compared with the controls. Figure 5.2 shows transcript levels of Ccl19, Cxcl12, Cxcr5 and Bcl-6 in the spleens following M4stop and WT virus infections at days 10 and 14 p.i.. Additionally, the results of these four transcripts from RT-PCR arrays were also included in order to give a panorama of changes during infections (figure 5.2). Interestingly, all four genes were found to be up-regulated in the spleens of M4stop

virus infection when compared to WT virus infection at least at one time point. At days 10 and 14 p.i., the expression of Ccl19 in the spleens of M4stop infection was increased significantly ($p<0.001$ and <0.05 respectively). The transcription of Cxcl12 was increased significantly at day 12 and 14 p.i. ($p<0.05$ in both time points), accompanied by a significant increase in the levels of Bcl-6 and Cxcr5 mRNA at days 12 and 14 p.i. respectively ($p<0.05$ in both gene transcription). In contrast, the transcription of Ccl19, Cxcl12 and Cxcr5 in the spleens of mice following WT virus infection was significantly down-regulated at days 12 and 14 p.i., compared to the transcripts in the WT-infected spleens at day 10 p.i. ($p<0.05$ for Cxcr5 at day 14 p.i, and $p<0.001$ for Ccl19 and Cxcl12 at days 12 and 14 p.i.). Because of the importance of GC development during MHV-68 infection (Flano et al., 2002; Liang et al., 2009), the down-regulation of expression of Ccl19, Cxcl12, Cxcr5 and Bcl-6 mRNA in the WT-infected spleens could be involved in the successful establishment of WT virus latency.

The up-regulation of Cxcr5 and Cxcl12 mRNA in the spleen during M4stop virus infection may affect the differentiation of GC B cells, because the localization of GC B cells in the dark and light zone may be altered by Cxcr5 and Cxcl12 induced chemotaxis. Because Bcl-6 can trigger the differentiation of follicular B helper T (T_{FH}) cells (Yu et al., 2009), the up-regulation of Bcl-6 may suggest an increase of T_{FH} cells in the spleens following M4stop virus infection. Therefore, we proposed a hypothesis that there were differences in GC formation and B cell differentiation

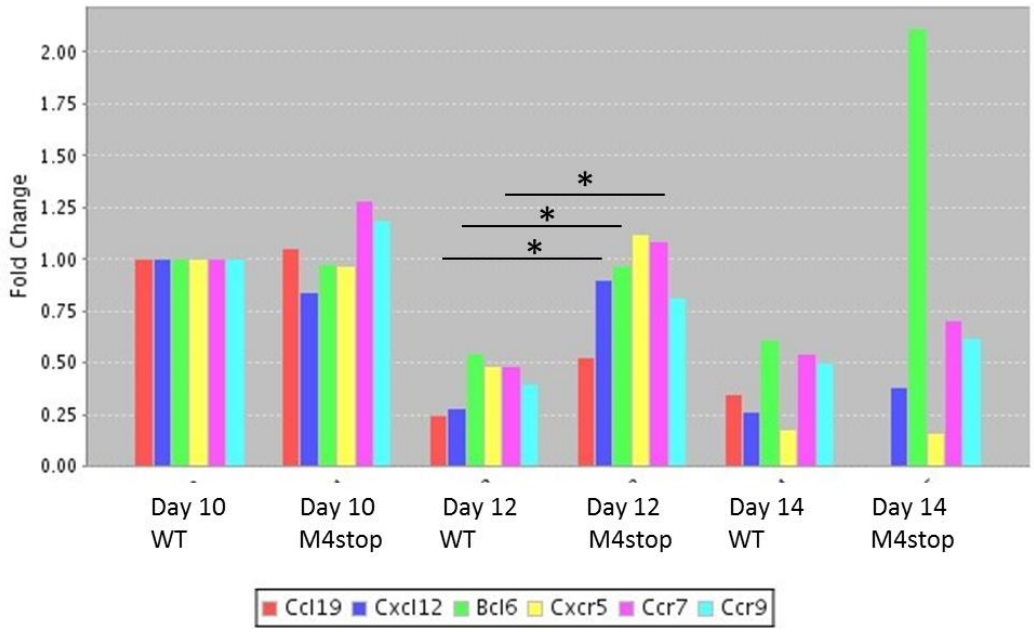

Figure 5.1 Fold change of gene transcription. 129Sv mice were intranasally infected with 5 × 10^4 PFU of M4stop or WT virus. The mice were sacrificed at days 10, 12 and 14 p.i., and the spleen RNA of each sample was reverse-transcribed to cDNA. The samples from day 12 p.i. were examined individually on PCR arrays, while the others were pooled and assessed. The results of the WT infection at day 10 p.i. were set as the control (fold change=1), then the levels of other results were compared to the control. Groups that have mean values that vary significantly ($p<0.05$) by student T test are indicated by *, which was calculated by the Sabiosciences online statistics programme.

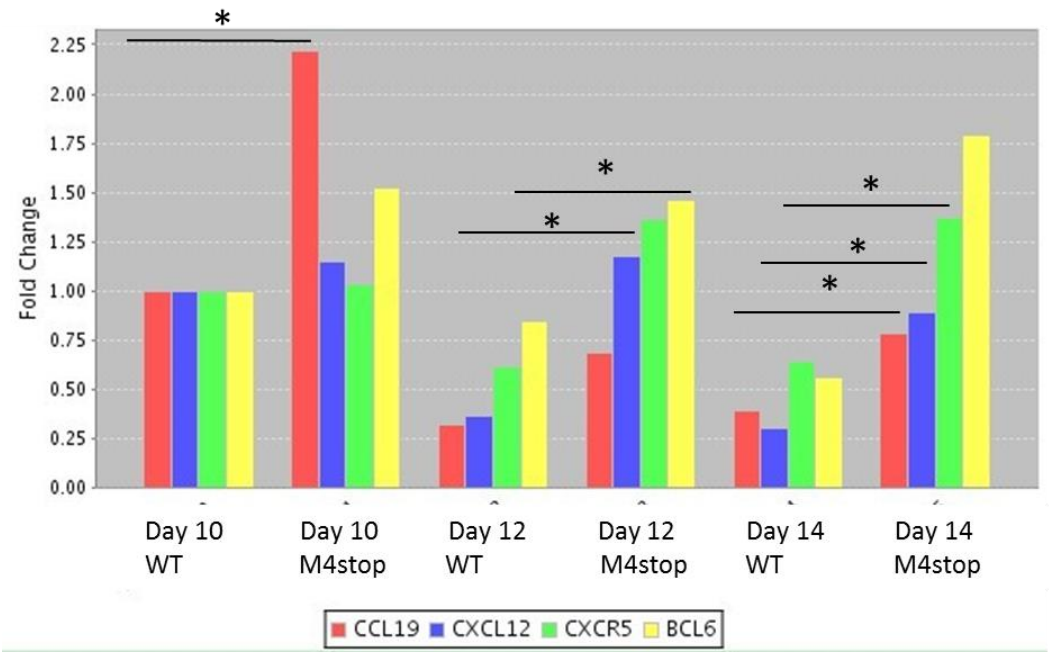

Figure 5.2 Fold changes of gene expression. 129Sv mice were intranasally infected with 5 × 10^4 PFU of M4stop or WT virus. The mice were sacrificed at days 10, 12 and 14 p.i., and the spleen RNA of each sample was reverse-transcribed to cDNA. The gene transcription of Ccl19, Cxcl12, Cxcr5 and Bcl-6 were examined by RT-PCR. The results of the WT infection at day 10 p.i. were set as the control (fold change=1), then the levels of the other results were compared to the control. The results of day 10 and 14 p.i. were got from qRT-PCR and the results of day 12 p.i. were from RT-PCR array. Groups that have mean values that vary significantly ($p<0.05$) by student T test are indicated by *, which was calculated by the Sabiosciences online statistics programme.

between M4stop and WT virus infections which led to a decrease in M4stop latency.

5.2.2 The percentage of GC B cells

The up-regulation of Bcl-6, Ccl19 and LTβ in the spleens of the mice which were infected with M4stop virus suggested M4stop virus infection caused different development of GC. Because B cells are the main cellular types in the GC and GC B cells are essential for MHV-68 latency (Flano et al., 2002), the percentage of GC B cells was determined during M4stop and WT infections. Furthermore, the increase in PD-1 may help to maintain the number of GC B cells (Good-Jacobson et al., 2010). To examine GC B cells in the spleen, the splenocytes of M4stop or WT infected 129Sv mice were double-stained with fluorescent conjugated anti-CD38 and anti-CD19 antibodies. The expression of CD38 is down-regulated ($CD38^{dim}$) on GC B cells and mature plasma cells in the mice (Oliver, Martin, and Kearney, 1997). Moreover, mature plasma cells lose the surface marker CD19. Therefore, gating on $CD19^{+}CD38^{dim}$ represents GC B cells. The gating strategy is shown in figure 5.3. A number of resting B cells and memory cells ($CD38^{high}$) were found at day 7 p.i.. Then GC B cells were shown to be generated from day 10 p.i. (figure 5.3).

The determination of GC B cells proportions following viral infections was carried out three times, where the mice were sacrificed at (1) days 7, 10, 14 and 17 p.i.; (2) days 10, 12 and 14 p.i.; (3) days 8, 10, 12 and 14 p.i.. The percentages of GC B cells are presented in figure 5.4. A significant increase ($p<0.05$) in the percentage of GC

B cells occurred in the spleens infected with M4stop virus at day 10 p.i. (figure 5.4), compared to WT virus infection at the same time point. This result may be associated with the rise of PD-1 positive $CD4^+$ T cells in the M4stop-infected spleen (figure 4.13). Or the increased M4stop viral latency (figure 4.4) induced naïve B cells to migrate to GC. After day 10 p.i., the levels of GC B cells are increased in both infections, but there was no difference between the two viral infection groups at any later time points, even at day 14 p.i. when PD-1 positive $CD4^+$ T cells and viral latency were found to be decreased in M4stop infected spleens (figure 4.14 and 4.4). The increase in the percentage of GC B cells during M4stop infection at day 10 p.i. may be because the increased M4stop viral latency at earlier time points (figure 4.4) induced the development of naïve B cells and formation of GC.

Down-regulation of Cxcl12 and Cxcr5 was found in spleens following WT virus infection at days 12 and 14 p.i., which could have influenced the development of centroblasts (Allen et al., 2004). Furthermore, latent MHV-68 is mainly found in centroblasts (Collins and Speck, 2012) which are reported to have a high proliferation rate. In this case, we would like to examine whether the reducion in M4stop latency was due to a low proliferation rate of B cell. The expression of Ki-67 antigen occurs preferentially during late G1, S, G2 and M phases of the cell cycle, while it cannot be detected in G0 phase. Therefore, to investigate the proliferation of B cells, splenocytes were double-stained with florescent conjugated

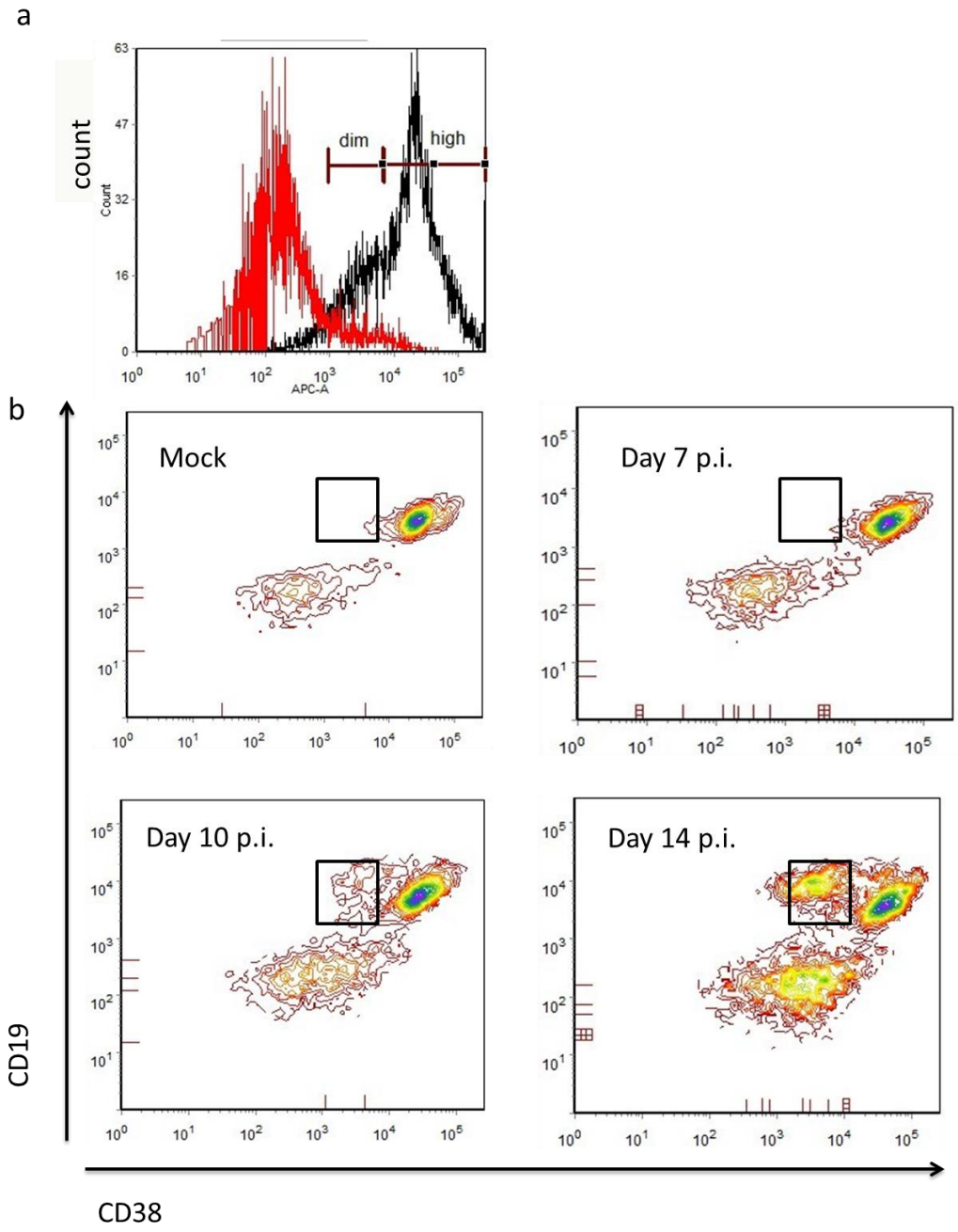

Figure 5.3 The gating strategy of GC B cells after MHV-68 infection. The GC B cells are characterized as $CD19^{+}CD38^{dim}$ B cells. (a) Histogram of the infected $CD19^{+}$ B cells stained with anti-CD38 antibody (black) and unstained cells (red). The $CD38^{high}$ and $CD38^{dim}$ are defined by the two peaks and the unstained control. (b) the generation of $CD38^{dim}CD19^{+}$ GC B cells after infection.

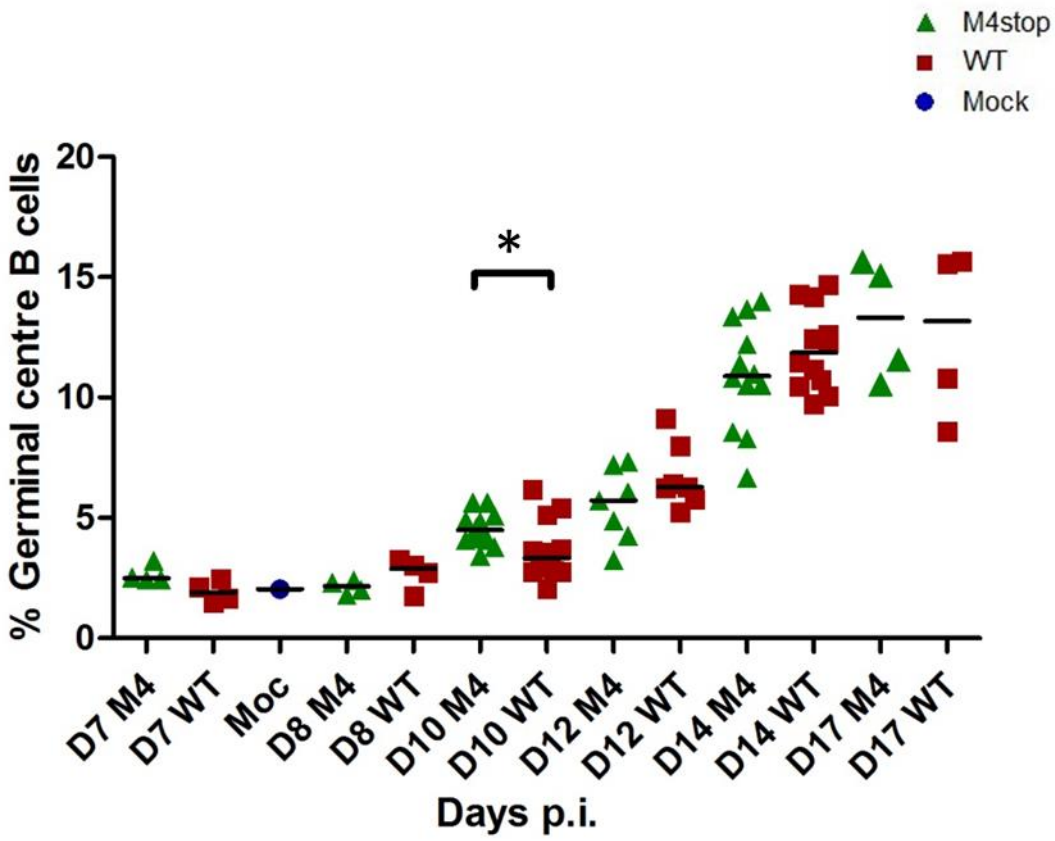

Figure 5.4 The percentage of GC B cells after infection. 129Sv mice were intranasally infected with 5×10^4 PFU of M4stop or WT virus. The mice were sacrificed at days (1) 7, 10, 14 and 17 p.i.; (2) 10, 12 and 14 p.i.; (3) 8, 10, 12 and 14 p.i.. The GC B cells were gated on $CD19^+CD38^{dim}$ B cells, and the percentage was calculated by the ration of percentage of GC B cells and percentage of $CD19^+$ B cells. Each symbol represents an animal, and D presents day. The black bar shows the median of four to twelve mice replicates. Groups that have mean values that vary significantly ($p<0.05$) by Mann-Whitney test are indicated by *.

anti-CD19 and anti-intracellular antigen Ki-67 antibodies and examined by flow cytometry. The proliferation of B cells in WT-infected spleen was slightly higher at day 10 p.i., compared to M4stop infection, but not significantly (p=0.052) (figure 5.5). This result confirmed that the M4 protein does not have an ability to induce the proliferation of B cells during infection. This result was consistent with previous results showing that the percentage of B cells was the same during M4stop and WT virus infections (figure 4.7c).

The percentage of GC B cells and proliferation of B cells were the same at days 12 and 14 p.i. between M4stop and WT virus infections, indicating that the decrease in the level of M4stop viral latency did not appear to be related to the number of GC B cells or proliferating B cells.

5.2.3 Levels of T_{FH} cells during M4stop and WT infections

Increased levels of transcripts of Bcl-6 and Cxcr5 in M4stop-infected spleens at days 12 or 14 p.i. (figure 5.2) suggests M4stop virus infection might induce a higher level of T_{FH} cells, because Bcl-6 is required for the development of T_{FH} cells and Cxcr5 is expressed on T_{FH} cells (reviewed in Fazilleau et al., 2009). To determine the percentage of T_{FH} cells in the spleen, $Cxcr5^+PD1^+$ T_{FH} cells were gated on $CD4^+$ live lymphocytes from the spleens following M4stop and WT virus infections by flow cytometry. The proportion of T_{FH} cells was calculated by the ratio of the percentage of T_{FH} cells and the percentage of $CD4^+$ T cells (figure 5.6).

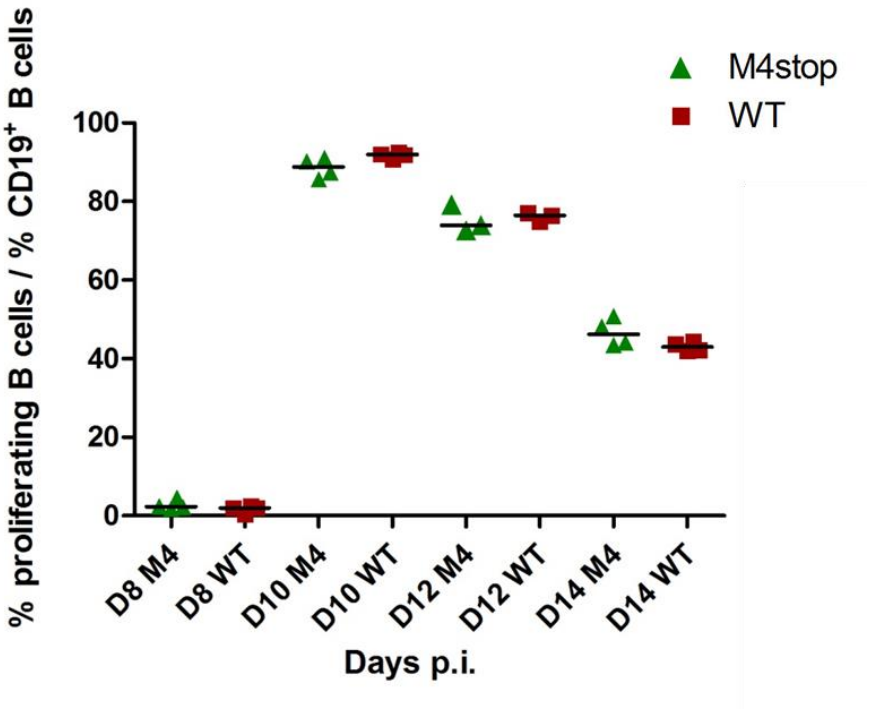

Figure 5.5 The percentage of proliferating B cells after infection. 129Sv mice were intranasally infected with 5×10^4 PFU of M4stop or WT virus. The mice were sacrificed at days 8, 10, 12 and 14 p.i.. The splenocytes were double stained with anti-CD19 and anti-intracellular proliferation marker Ki-67 antibodies. The percentage of proliferating B cells was calculated from the total $CD19^+$ B cell population. Each symbol represents an animal, and D presents day. The black bar shows the median of three to four mice replicates.

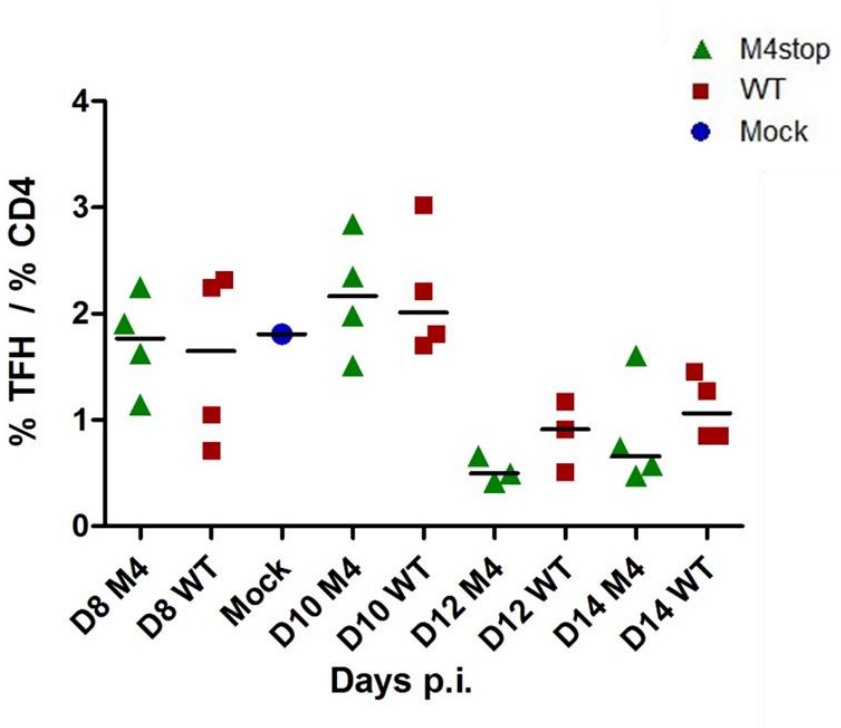

Figure 5.6 The percentages of T_{FH} cells in the spleen. 129Sv mice were intranasally infected with 5×10^4 PFU of M4stop or WT virus. The mice were sacrificed at days 8, 10, 12 and 14 p.i., and splenocytes were triple-stained with anti-CD4, anti-Cxcr5 and anti-PD-1 antibodies, then selected by FACS. The percentage of T_{FH} was calculated from percentage of $CD4^+$ T cells. Each symbol represents an animal, and D presents day. The black bar shows the median of three to four mice replicates.

No difference in percentage of T_{FH} cells was found in the spleens between M4stop and WT virus infections. Therefore, the increase in Bcl-6 and Cxcr5 in the spleens of M4stop infection did not result in increased proportions of T_{FH} cells at days 12 and 14 p.i..

5.2.4 The percentages of plasma cells during M4stop and WT infections

Increased levels of Cxcr5 in the M4stop-infected spleens did not result in an increased percentage of T_{FH} cells at least at days 12 or 14 p.i.. However, it has been shown that Cxcr5 and Ccr7 are down-regulated in mouse plasma cells (Hargreaves et al., 2001). The increase in Ccr7 at day 12 p.i. (figure 5.1) and Cxcr5 at day 14 p.i. (figure 5.2) in the M4stop-infected spleens suggests less plasma cell may have developed in the spleens compared to WT virus infection. Moreover, Bcl-6 is a repressor of plasma cells differentiation as it represses the expression of Blimp-1, which has a role in promoting plasma cell formation and immunoglobulin secretion (Shapiro-Shelef et al., 2003). Plasma cells are vital for MHV-68 latency (Collins, Boss, and Speck, 2009; Liang et al., 2009), therefore, the decrease in the number of plasma cells can lead to reduced viral latency and reactivation. Additionally, M2 protein has been shown to play an important role in the differentiation of plasma cells (Liang et al., 2009). The absence of PD-1-PD-L interaction impairs plasma cell development. As we found an increase in PD-1 expression at day 8 p.i. and a decrease in PD-1 at day 14 p.i. in the spleen of M4stop virus infection when

compared to WT virus infection, we hypothesized that plasma cell development was different between M4stop and WT virus infections, thus the reduction in M4stop latency and M4stop viral reactivation may be due to impaired differentiation of plasma cells in the absence of M4 protein. In order to test this hypothesis, the percentage of plasma cells at days 8, 10, 12 and 14 p.i. following M4stop and WT virus infection was determined by double-staining splenocytes with anti-CD19 and anti-CD138 antibodies and examined by flow cytometry. No difference in percentage of plasma cells was found between M4stop and WT infection at these indicated time points (figure 5.7). However, there was non-significant ($p=0.2$) increase in the percentage of plasma cells in the M4stop-infected spleen at day 10 p.i. compared to WT infection. This experiment should be repeated to confirm whether the difference observed is real using a larger group number.

Similar to the T_{FH} cells result, the up-regulation of mRNA expression of Bcl-6, Cxcr5 and Ccr7 in the M4stop virus infection did not result in the development of plasma cells at days 12 and 14 p.i.. It might be because other cells that are involved in the GC reaction. For example, a subset of Treg cells can highly express Bcl-6 and Cxcr5. And they can inhibit the development of GC (Chung et al., 2011). However, due to the time limitation, we have not examined the population of Treg cells.

5.2.5 Histological examination of spleens

The difference in the expression of Bcl-6 and Ccl19 between M4stop and WT virus

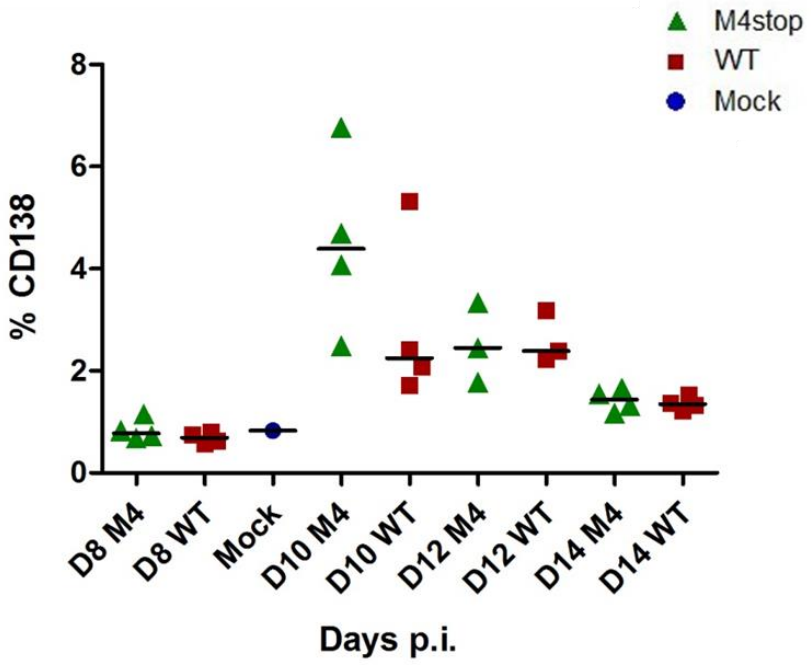

Figure 5.7 The percentage of plasma cells after infection. 129Sv mice were intranasally infected with 5×10^4 PFU of M4stop or WT virus. The mice were sacrificed at days 8, 10, 12 and 14 p.i.. The splenocytes were double stained with anti-CD19 and anti-138 antibodies. Plasma cells are $CD19^{dim/-}CD138^{+}$ cells. Each symbol represents an animal, and D presents day. The black bar shows the mean of two to four mice replicates, error bars represent the standard deviation,

infections may induce distinct GC formation (Luther et al., 2002; Nurieva et al., 2009). The spleens following M4stop and WT virus infections were examined by histology. The mice were sacrificed at days (1) 10, 12 and 14 p.i., and (2) 8, 10, 12 and 14 p.i., and the spleens were harvested and stained with H&E. Sections were examined, but no clear difference in the GC structure was detected by light microscopy, when comparing the two viral infection groups (data not shown). Since the H&E staining only showed the shape of GCs, we are not clear about what cell populations contained in the GC and what the distribution of these cells. It would be more useful to determine the GC structure further.

5.3 Discussion

Levels of viral latency of M4stop were decreased in the spleen at day 14 p.i. compared to WT infection (figure 4.4) (Geere et al., 2006). In this chapter, we examined the transcript levels of Cxcl12, Cxcr5, Ccr7, Ccl19 and Bcl-6, which have been shown to be involved in development of GC, and were up-regulated in the spleens of mice infected with M4stop virus when compared to that of WT virus infection. Moreover, these genes were down-regulated in the WT-infected spleens at days 12 and 14 p.i. compared to that of WT infection day 10 p.i. (figure 5.1 and figure 5.2). Because these genes are involved in GC B cell formation and B cell proliferation, the up-regulation of these genes in the M4stop-infected spleens may interfere with the development of GC B cells, which are known to be related to viral latency. The examination of percentage of GC B cells showed a difference at day 10

p.i. during M4stop and WT viral infections, but levels were similar at days 12 and 14 p.i., indicating GC B cells and the proliferative ability of B cells were not related to the decrease in M4stop viral latency in the spleen at day 14 p.i..

As Cxcr5, Ccr7 and Bcl-6 are indicators of the development of T_{FH} cells and plasma cells, which are two important factors for GC development, the percentages of these two cellular types were investigated between the two viral infections. However, no difference was observed. Therefore, the levels of T_{FH} cells and plasma cells appear not to be related to the failure of M4stop latency at day 14 p.i.. These experiments have only been carried out once; therefore the results require confirmation. It seems like the increase in the PD-1 and decrease in these gene transcripts work in opposite ways, which may maintain the levels of T_{FH} cells and plasma cells during WT virus infection. Furthermore, although the percentage of T_{FH} cells and plasma cells was the same during infection, we do not know whether the functions of these cells are the same between the two viral infections. It would be interesting to examine the level of cytokines, such as IL-4 and IL-21, expressed by T_{FH} cells and the antibodies that secreted from plasma cells to assess the functions of these cells.

The up-regulation of Ccl19, Cxcl12, Cxcr5 and Bcl-6 during M4stop virus infection was not due to changes in the percentages of GC B cells, proliferating B cells, T_{FH} cells or plasma cells. Some other possibilities that may be related to the up-regulation of these transcripts, such as (1) other cellular types in the spleen may be involved in controlling M4stop virus infection. For example, FDC can also express Cxcr5. The

latency of MHV-68 in FDC is unknown, but other herpesvirus infections have been found in FDC (El-Daly, Bower, and Naresh, 2010). Moreover, FDC interact with B cells in the GC light zone; therefore, the disruption of FDC can affect the development of B cells. Treg cells might also be involved in the up-regulation of Bcl-6 and Cxcr5 during the M4stop infection (Chung et al., 2011). Therefore, the down-regulation of CD69 on splenic lymphocytes might be due to the increase in Treg following M4stop virus infection. (2) Other mechanisms may induce transcripts in the M4stop infection. For example, Bcl-6 can repress the microRNAs that modulate several genes of T_{FH} cells and Cxcr5 (Yu et al., 2009). Therefore, the decrease in Bcl-6 may result in the down-regulation of expression of other genes.

Antigen-specific B cells go through somatic hypermutation in the dark zone during the GC response. Plasma cells producing high affinity antibodies are important for the control of viral infections. Although the percentages of plasma cells were the same between the two viral infections, antibody affinity for antigen remains unclear. Moreover, it has been found that immune sera cannot block MHV-68 infection of macrophages and dendritic cells, instead the virus exploits the IgG Fc receptor to increase their infection (Rosa et al., 2007). Therefore, it would be interesting to compare the levels of antibodies, such as IgG, in the peripheral blood during M4stop and WT infections.

It is worth noticing that the changes in gene expression during viral infections are involved in Th1/Th2 polarization. LTα has been characterized as a Th1 cytokine.

LTα1β2 is absent on Th2 cells (Gramaglia et al., 1999). Moreover, the expression of Bcl-6 represses GATA-1 and STAT-6, thus Bcl-6 down-regulates expression of IL-4 and IL-13 (Dent et al., 1997; Harris et al., 1999; Kusam et al., 2003). Bcl-6 deficient mice develop a Th2-mediated inflammatory response, as the expression of Th2 cytokines was increased (Dent et al., 1997; Ye et al., 1997). Moreover, Bcl-6 is an antagonist of Blimp-1, which can repress Th1 genes and reinforce Th2 differentiation (Cimmino et al., 2008). Therefore, Th2 differentiation may be more likely to occur in an environment which contains lower level of Bcl-6, such as in the spleens of mice infected with WT virus. IL-4 and IL-13 signals are required for the differentiation of Th2 cells (Mora et al., 2006). Higher levels of Bcl-6 in the spleens of M4stop-infected mice may impair Th2 differentiation. In addition, it would be interested to examine the transcription of IL-4 and IL-13 in the spleens at day 14 p.i.. Moreover, it has been reported that Bcl-6 can repress the proliferation of macrophages (Yu et al., 2005). Thus, the lower levels of macrophages in M4stop-infected spleens compared to WT infection may due to negative regulation of Bcl-6.

The development of GC might be different between M4stop and WT virus infections, but does not appear to be related to the proportions of GC B cells, T_{FH} cells and plasma cells. Therefore, more experiments are required to determine whether cell populations are changed during the two viral infections.

Chapter 6

Role of M4 in MHV-68 pathogenesis in IFN-γR$^{-/-}$ mice

6 Role of M4 in MHV-68 pathogenesis in IFN-γR$^{-/-}$ Mice

6.1 introduction

IFN-γ, which is produced predominantly by NK, NKT cells, CD4^{+} (Th1) and CD8^{+} T cells, is critical for innate and adaptive immunity during many viral infections. It has been reported to be involved in protective immune responses to several herpesviruses (Bodaghi et al., 1999; Christensen et al., 1999; Orange et al., 1995; Smith et al., 1994). During the acute phase of MHV-68 infection, IFN-γ is produced at high levels in the MLN, cervical lymph node and spleen. Nevertheless, this cytokine is not essential for control of this viral infection in the lungs using MHV-68-infected IFN-γR$^{-/-}$ mice (Dutia et al., 1997; Nash et al., 2001; Sarawar et al., 1997; Sarawar et al., 1996) and IFN-γ$^{-/-}$ mice (Sarawar et al., 1997). However, an expansion of latent virus and chronic infection is reported in the spleens of MHV-68-infected IFN-γ$^{-/-}$ mice and IFN-γR$^{-/-}$ mice (Dutia et al., 1997; Weck et al., 1997). In Chapter 4, we showed that the M4 protein of MHV-68 played an important role in the establishment of latent infection in the spleen of immunocompetent 129Sv mice. The study of the role of IFN-γ in MHV-68 infection shows that it can inhibit reactivation from latency and control viral gene expression during latency (Steed et al., 2006). The transcription of M4 can be found in the spleen during the early latency stage following infection (Marques et al., 2003; Townsley, Dutia, and Nash, 2004). Therefore, I investigated whether the M4 protein has a role in the pathogenesis that

occurs in the absence of IFN-γ.

Multi-organ, including mediastinal lymph node, lung and liver, fibrosis has been found in IFN-γR$^{-/-}$ mice following intranasal infection with MHV-68 (Dutia et al., 1997; Ebrahimi et al., 2001; Lee et al., 2009). The most obvious changes of lymphoid pathology in IFN-γR$^{-/-}$ mice are the decrease in the number of splenocytes, which lead to an increase in leukocytes, lymphocytes and neutrophils in venous blood, and splenic atrophy after day 14 p.i., coupled with the generation of collagen and fibrosis by day 23 p.i. (Ebrahimi et al., 2001). It has also been considered that the change of splenic structure was related to the left-end gene of MHV-68 since MHV-76 fails to induce atrophy (Dutia et al., 2004). A further study reported that the changes are related to the expansion of Vβ4^{+}CD8^{+} T cells after day 18 p.i., which are activated by the M1 protein (Evans et al., 2008). Therefore, this is why the loss of the splenic structure did not occur in CD8^{+} T cell depleted mice (Dutia et al., 1997) or M1 deficient MHV-68 infected mice (Dutia et al., 2004). Aside from Vβ4^{+}CD8^{+} T cells, alternatively activated macrophages, which are driven by the Th2 response, are involved in the generation of fibrosis during MHV-68 infection (Gangadharan et al., 2008). The histology of M4stop-infected spleens in IFN-γR$^{-/-}$ mice has not been studied yet, therefore the differences of the histology were studied and comparisons were made following M4stop and WT virus infections in this chapter.

In order to determine whether the M4 gene product plays a role in the development of fibrosis in the spleen of IFN-γR$^{-/-}$ mice, IFN-γR$^{-/-}$ mice were infected with the WT

and M4stop viruses. Comparisons were made between the spleen weights, percentages of splenocyte subsets, viral DNA loads, viral reactivations, and the percentages of activated of lymphocytes between two viral infections.

6.2 Results

To study whether M4stop influences the development of fibrosis in the absence of IFN-γ during MHV-68 infection, IFN-γR$^{-/-}$ mice were intranasally infected with 4 x 10^5 pfu of M4stop or WT virus. The experiments were performed during the early latency stage of MHV-68 infection when M4 transcripts can be detected. In four separate experiments, the mice were sacrified at (1) days 7, 10, 14 and 18 p.i.; (2) days 10, 14, 18 and 25 p.i.; (3) days 18 and 25 p.i.; and (4) days 18 and 25 p.i.. There were four mice in each group. A mock-infected mouse which was intranasally infected with the same amount of SPBS was sacrificed to get a better understanding of the pathological changes during both virus infections.

6.2.1 Viral DNA loads and viral reactivation in the spleen

Previous studies of MHV-68 infection of IFN-γR$^{-/-}$ mice showed that MHV-68 infection resulted in significantly higher viral latent loads in IFN-γR$^{-/-}$ mice than in immunocompetent mice (Dutia et al., 1997; Dutia et al., 2004). In order to assess whether there is any difference in the viral DNA loads and viral reactivation during M4stop and WT virus infections, qPCR and infectious centre assays were carried out as described in Materials and Methods, and the results are presented in figure 6.1 and

6.2 respectively. The number of the infectious centres reflects the reactivation of the virus from infected cells. The viral DNA loads of WT virus in the spleens were higher than M4stop virus at days 7, 18 and 25 p.i. ($p<0.05$). The number of infectious centres caused by WT virus infection was significantly higher at day 18 p.i. ($p<0.05$) than that of M4stop-infected spleen of IFN-γR$^{-/-}$ mice. Compared to levels of viral latency and reactivation in the spleens of 129Sv mice (figure 4.4 and 4.5), viral DNA loads and the number of infectious centres were higher. The delay in the viral clearance from the spleen reflects the importance of IFN-γ in the control of MHV-68 latency in the spleen. However, the decrease in viral DNA loads and the ability of the virus to reactivate from latency in the spleens of IFN-γR$^{-/-}$ mice following M4stop virus infection was similar to the decrease in that of M4stop-infected 129Sv mice, therefore the lack of response to IFN-γ did not stop the decrease in M4stop virus latency.

6.2.2 Viral induced changes of splenic morphology

MHV-68 infection leads to splenic fibrosis in IFN-γR$^{-/-}$ mice; however, the splenic morphology in M4stop-infected IFN-γR$^{-/-}$ mice was unknown. Therefore, the weight of spleens from three different experiments is presented in figure 6.3. Splenomegaly with an increase in the number of splenocytes was found at the initial stage of spleen infection at days 7 and 10 p.i. in both viral infections. Then spleens from WT virus infected IFN-γR$^{-/-}$ mice became pale, shrunken and fibrous from day 14 p.i. onwards, and decreased in weight at day 18 p.i. when compared to the spleens

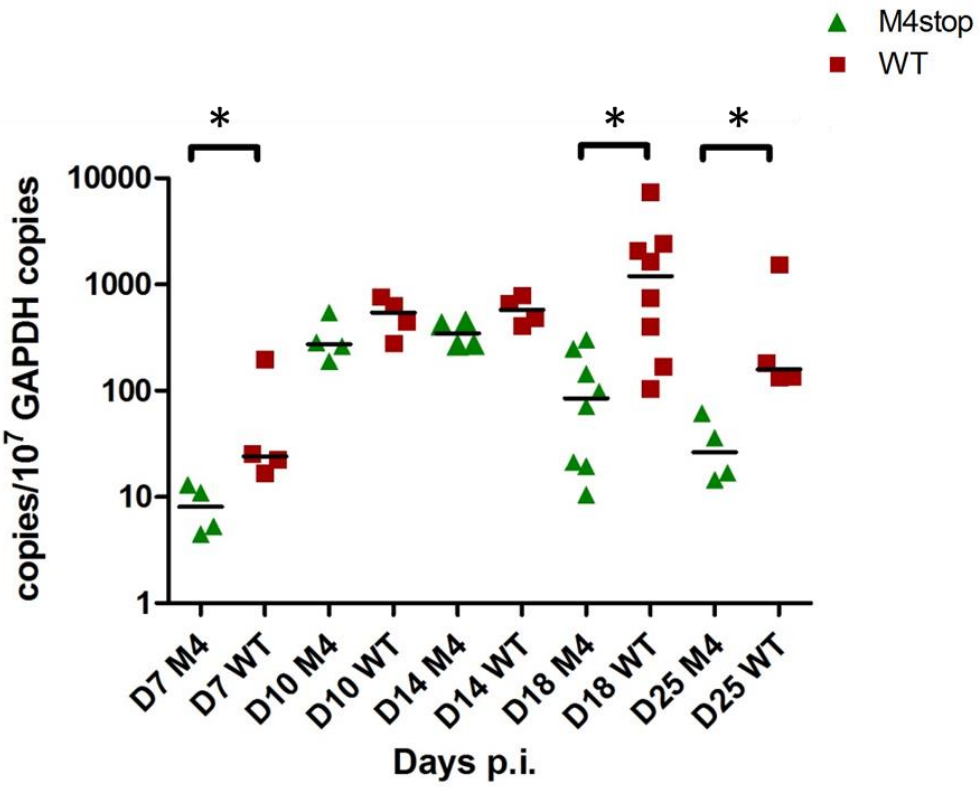

Figure 6.1 Viral DNA loads in spleens. IFN-γR$^{-/-}$ mice were infected with 4 × 10^5 PFU of M4Stop or WT virus by the intranasal route. Viral DNA loads of WT and M4stop obtained from latently infected splenocytes were analysed by qPCR at days (1) 7, 10, 14 and 18 p.i. and (2) 18 and 25 p.i., all normalized to GAPDH. Each symbol represents an animal and D represents day. The black bars denote the median of each group. Groups that have mean values that vary significantly ($p<0.05$) by Mann-Whitney test are indicated by *.

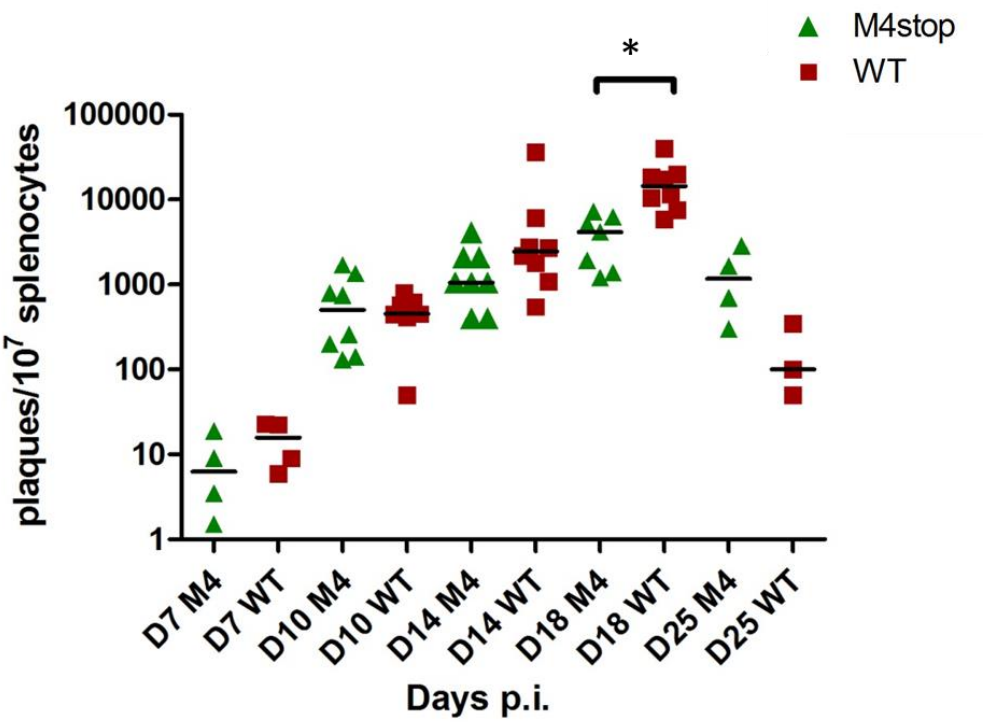

Figure 6.2 Latent virus in spleen. IFN-γR$^{-/-}$ mice were infected with 4 × 10^5 PFU of M4Stop or WT virus by the intranasal route. Spleens were removed at (1) days 7, 10, 14 and 18 p.i. and (2) days 10, 14, 18 and 25 p.i.. The levels of latent virus were quantified by an infectious center assay. Each symbol represents an animal and D represents day. The black bars denote the median of each group. Groups that have mean values that vary significantly ($p<0.05$) by Mann-Whitney test are indicated by *.

infected with M4stop virus ($p<0.05$). Fibrosis was found in the M4stop-infected spleens at day 25 p.i., and the texture of the spleens was similar to the WT-infected spleens at day 18 p.i.. Therefore, the generation of fibrosis may be delayed in the absence of M4 protein.

To determine fibrosis and architectural changes in the spleens after viral infection, the spleens were harvested at days 18 and 25 p.i. and examined by H&E staining and Masson's trichrome staining (figure 6.4). A mock-infected mouse was sacrificed and the spleen was stained as a negative control. Compared to the negative control H&E staining (figure 6.4a), the white pulps were enlarged, merged with each other and GCs were generated by day 18 p.i. during M4stop and WT virus infections (figure 6.4c and e). However, the GC structure was not clear at day 25 p.i. (figure 6.4g and i). The staining clearly showed that collagen fibers, seen in blue, were starting to be generated in the WT-infected spleens at day 18 p.i. (figure 6.4f), but were absent from the M4stop-infected spleens (figure 6.4d). The fibrosis level was defined by measuring the area of blue staining using imageJ. The area of fibrosis in the spleen which infected with WT virus was 10 times larger than M4stop virus infection at day 18 p.i.. At day 25 p.i., more fibrosis was seen in the spleens of mice infected with WT compared to day 18 p.i. (figure 6.4j). As we expected, fibrosis was found in the M4stop-infected spleen at day 25 p.i., but to a lesser degree when compared to WT virus infection. The area of fibrosis in WT virus infected spleen was about 2 times larger than M4stop virus infection at day 25 p.i.. Therefore, M4stop virus infection

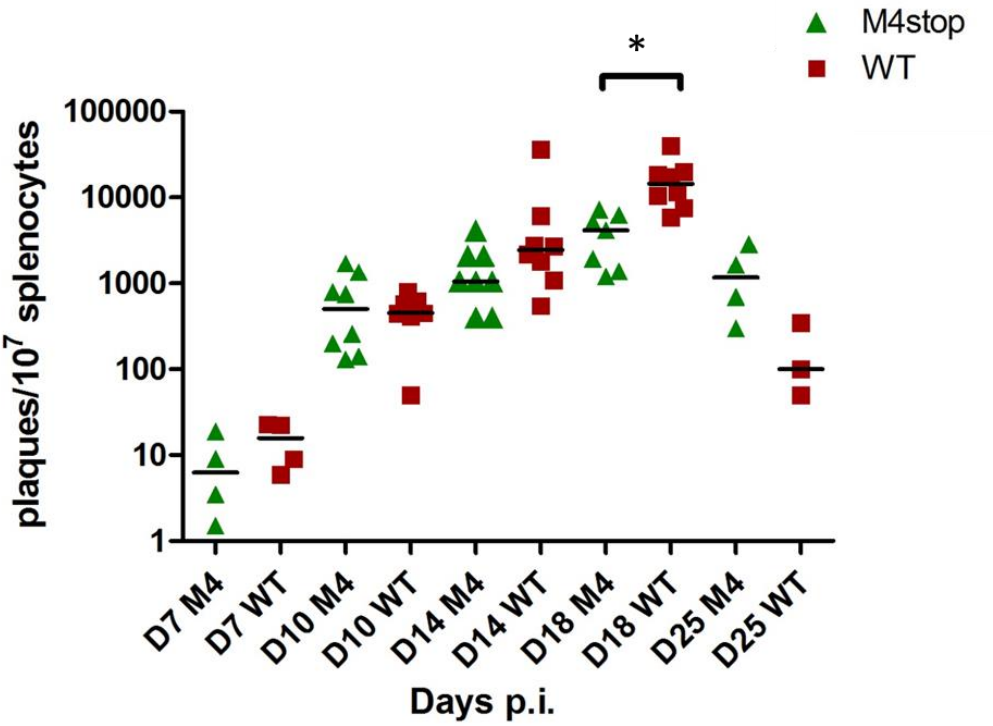

Figure 6.3 Splenomegaly and atrophy occurred in IFN-γR$^{-/-}$ mice infected with WT or M4stop virus. IFN-γR$^{-/-}$ mice were intranasally infected with 4 × 10^5 PFU of either WT or M4stop virus. Then the mice were sacrificed at (1) days 7, 10, 14 and 18 p.i.; (2) days 10, 14, 18 and 25 p.i.; and (3) days 18 and 25 p.i.. The spleens were weighed and recorded. Each symbol represents an individual animal, D represents day. The black bars denote the median of each group. Groups that have mean values that vary significantly ($p<0.05$) by Mann-Whitney test are indicated by *.

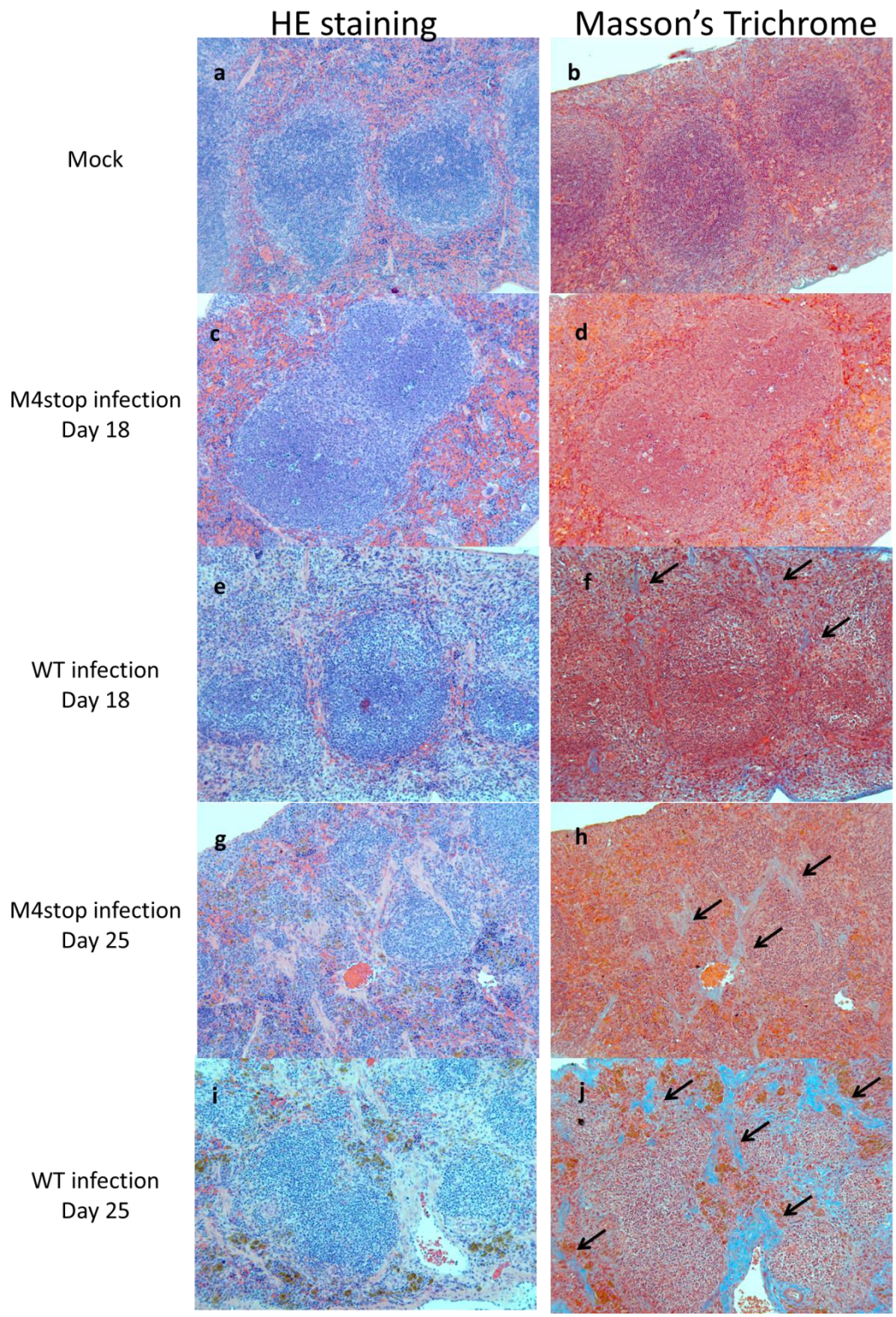

Figure 6.4 Detection of splenic structure and fibrosis by H&E and Masson's trichrome staining. The spleens were harvested at days 18 and 25 p.i. after being infected with M4stop and WT virus. One mock-infected mouse was sacrificed and the spleen was stained. (a), (c), (e), (g) and (i) are H&E staining. (b), (d), (f), (h)and (j) are Masson's trichrome staining.

can also cause fibrosis in the spleen, but the fibrosis is delayed.

6.2.3 Proportion of different cell populations in spleens

In order to determine whether the splenomegaly in the IFN-γR$^{-/-}$ mice following M4stop and WT infections was caused by proliferation of the same lymphocytes, the percentages of CD4^{+}, CD8^{+} T cells, B cells and NK cells in the spleens of IFN-γR$^{-/-}$ mice infected with M4stop or WT were studied by flow cytometry. CD4^{+} and CD8^{+} T cells are essential for the structural change and fibrosis in IFN-γR$^{-/-}$ spleens caused by MHV-68 as depletion of these two subsets reduces the pathology (Dutia et al., 1997) and they are essential in controlling virus infection in the acute and latent stages. MHV-68 establishes a latent infection in B lymphocytes of the spleen in mice (Sunil-Chandra, Efstathiou, and Nash, 1992). Therefore, a change in the number of B cells could influence levels of virus latency. During infection, a large amount of IFN-γ is produced by NK cells. It has been found that IFN-γ is elevated in a MHV-68 infection in IFN-γR$^{-/-}$ mice; therefore, it would be interesting to monitor the percentage and numbers of NK cells. Macrophages are associated with the generation of fibrosis induced by MHV-68 infections in IFN-γR$^{-/-}$ mice through their alternative activation pathway (Gangadharan et al., 2008), thus they were considered as another main target to study. At the beginning of a latent infection in the spleen, an increase in neutrophils in IFN-γR$^{-/-}$ mice was found (Ebrahimi et al., 2001). Therefore, the percentages of neutrophils in the spleen following WT virus infection

were compared to that of M4stop virus infection.

Figure 6.5 presents the percentages of CD4^{+}, CD8^{+} T cells, B cells and NK cells. Among these subsets the percentages of CD19^{+} B cells remained at the same level during infections between M4stop and WT infections except at day 14 p.i. ($p<0.05$) (figure 6.5c). The percentages of CD4^{+} T cells were increased in the WT-infected IFN-γR$^{-/-}$ mice at day 18 and 25 p.i. as compared to the M4stop virus infection (figure 6.5a) ($p<0.05$). The proportions of CD8^{+} T cells were decreased in WT-infected spleens as compared to M4stop infections at day 10 and 18 p.i. (figure 6.5b) ($p<0.05$). The percentages of NK cells were also decreased at day 18 p.i. in the WT-infected spleens compared to M4stop infection (figure 6.5d) ($p<0.05$). An increase in the percentage of CD4^{+} T cells was also found in the 129Sv mice following infection with WT virus compared to M4stop virus at day 14 p.i. (figure 4.5). Therefore, CD4^{+} T cells may be important for MHV-68 latency. IFN-γR$^{-/-}$ mice have a bias toward Th2-type responses with impaired Th1 responses. It is possible that the CD4^{+} T cells in the WT virus infection are Th2 cells. Furthermore, MHV-68 infection in Th2-biased mice causes splenic fibrosis (Ebrahimi et al., 2001; Gangadharan et al., 2008). Therefore, the increased percentage of CD4^{+} T cells in the spleen may be related to the higher level of fibrosis in the WT-infected mice as compared to M4stop virus infection.

To determine the changes in proportion of macrophages and neutrophils, anti-CD11b and anti-Ly6G antibodies were used for double staining. The CD11b^{+}Ly6G^{+} cell

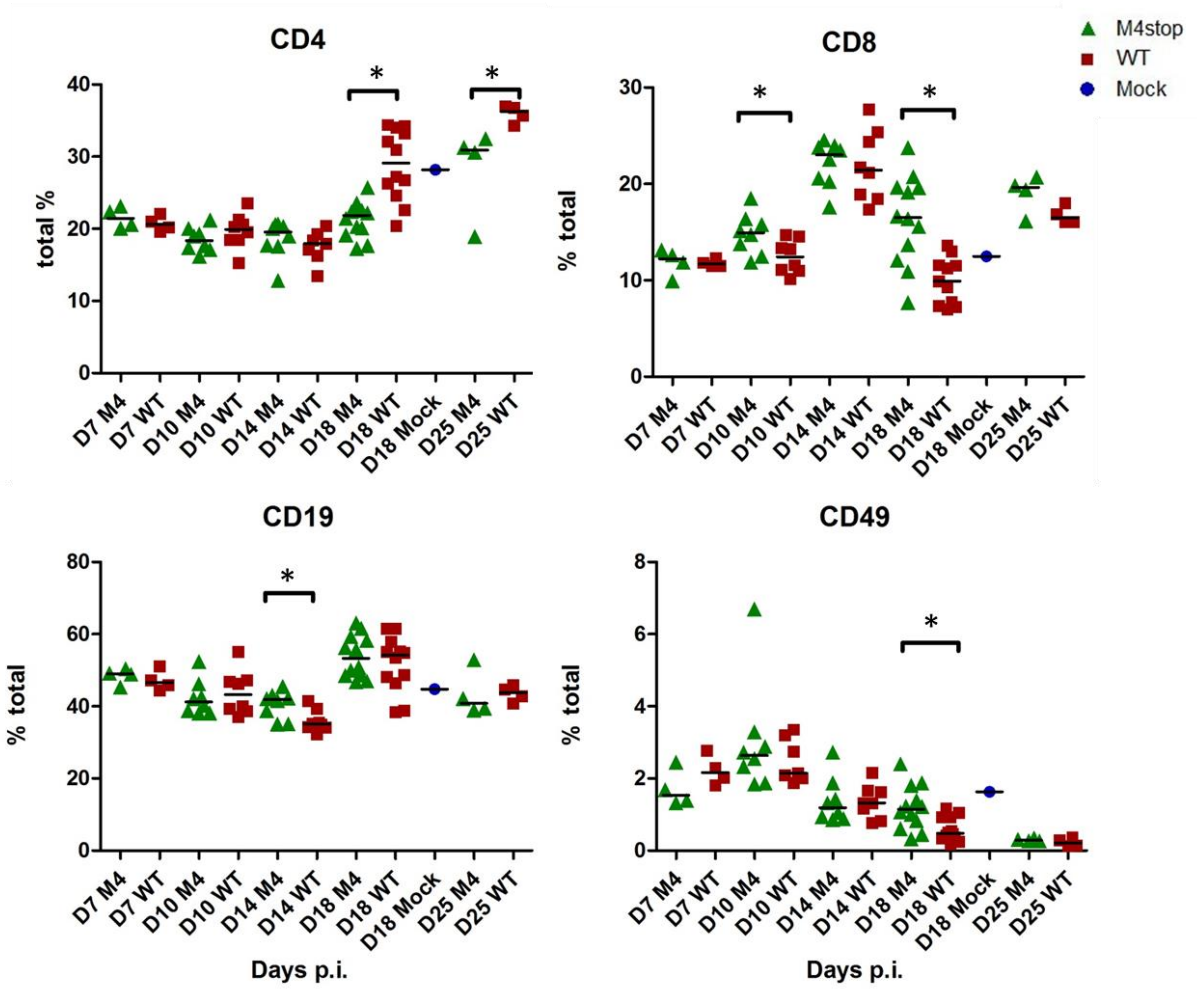

Figure 6.5 Changes in percentages of lymphocytes in the spleen. IFN-γR$^{-/-}$ mice were infected with 4 × 10^5 PFU of either M4stop or WT virus and the splenocytes were stained with fluorescent conjugated anti-CD4, -CD8, -CD19 and -CD49b antibodies and analysed by flow cytometry to determine the percentage of each population in the spleen. (a) CD4$^+$ T cells. (b) CD8$^+$ T cells. (c) B cells. (d) NK cells. Each symbol represents an animal, and D represents day. The black bars denote the median of each group. Groups that have mean values that vary significantly ($p<0.05$) by Mann-Whitney test are indicated by *.

population was defined as neutrophils, and the CD11b^{+}Ly6G^{-} was determined as macrophages. The percentages of neutrophils and macrophages are presented in figure 6.6. There was non-significant increase ($p=0.057$) in the percentages of macrophages in the WT-infected spleens at day 10 and 14 p.i. (figure 6.6b). In contrast, there was a significantly ($P<0.05$) increased percentage of neutrophils in the spleens of the mice infected with WT at day 25 p.i. as compared to M4stop virus infection (figure 6.6a).

6.2.4 The percentage of Vβ4^{+}CD8^{+} T cells in the spleens

An increase of Vβ4^{+}CD8^{+} cells is related to IM-like syndrome and fibrosis in MHV-68-infected IFN-γR$^{-/-}$ mice by day 21 p.i., and is induced by the M1 protein (Evans et al., 2008; Tripp et al., 1997). Although M4 protein was shown not to trigger the increase of Vβ4^{+}CD8^{+} T cells from day 28 p.i. (Evans et al., 2008), the ability of the M4 protein to induce this cellular type during earlier time points has not been examined. Because M4 protein can be detected during acute latency and the fibrosis pathogenesis was delayed in M4stop virus infection, it is possible that the M4 protein was involved in inducing Vβ4^{+}CD8^{+} cells in the spleen of IFN-γR$^{-/-}$ mice at the earlier time points. In order to assess this hypothesis, the percentage of Vβ4^{+} expressing CD8^{+} T cells was calculated by comparing to total CD8^{+} T cells in the spleens during M4stop and WT infections at days 18 and 25 p.i.. The percentage of Vβ4 expressing CD8^{+} T cells among the total CD8^{+} T cell population was the same at day 18 p.i., suggesting the development of fibrosis in the WT-infected spleens at

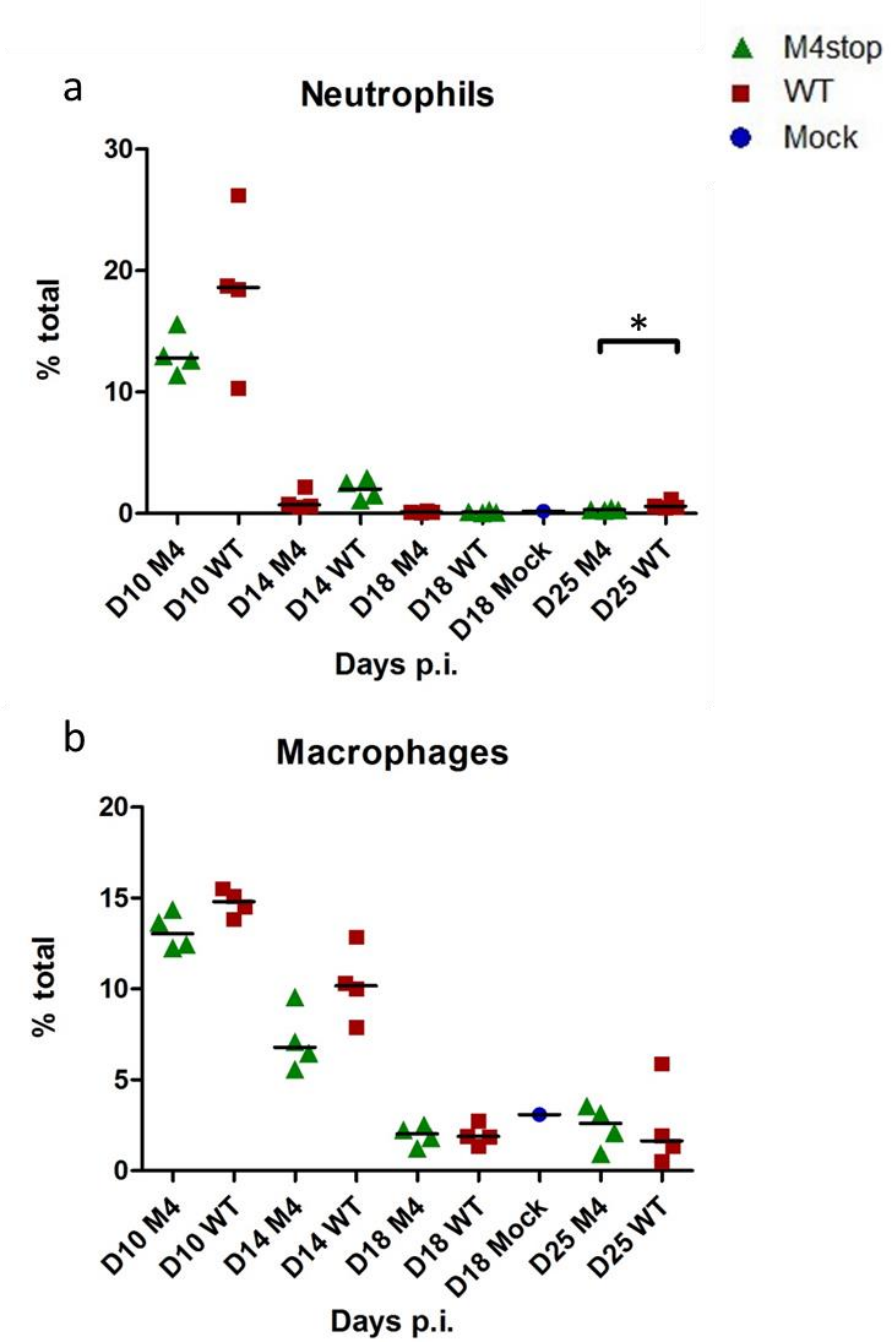

Figure 6.6 Changes in the percentage of neutrophils and macrophages in the spleens after infection. IFN-γR$^{-/-}$ mice were infected with 4 × 10^5 PFU of M4stop or WT virus and the neutrophils and macrophages were characterized as CD11b$^+$Ly6G$^+$ and CD11b$^+$Ly6G$^-$ respectively by fluorescent-conjugated antibodies in the FACS. (a) The percentages of neutrophils. (b) The percentages of macrophages. Each symbol represents one mouse and D represents day. The black bars denote the median of each group. Groups that have mean values that vary significantly ($p<0.05$) by Mann-Whitney test are indicated by *.

day 18 p.i. was not associated with the increase of Vβ4^{+}CD8^{+} T cells. Moreover, the development of fibrosis in the WT-infected spleens of IFN-γR$^{-/-}$ mice at day 18 p.i. may be due to some other reasons, such as the Th2 response. However, at day 25 p.i., the proportion of Vβ4^{+}CD8^{+} T cells was lower ($p<0.05$) in the M4stop-infected spleens when compared to WT virus infection (figure 6.7), which may be due to decreased expression of M1 protein in spleens which harbored less M4stop latent virus than WT virus infection.

6.2.5 Cellular activation

It has been found in Chapter 4 that a high level of latency in the spleen of WT-infected 129Sv mice correlated with a higher percentage of activated lymphocytes at day 14 p.i.. To examine whether there was a difference between the cellular activation observed in IFN-γR$^{-/-}$ mice from that found in WT mice, the percentage of activated CD4^{+}, CD8^{+} T cells, B cells and NK cells was monitored by flow cytometry. Because the changes of splenic pathology were mainly found between day 10 and day 25 p.i., days 10, 14, 18 and 25 p.i. were chosen. The results are shown in figure 6.8. Non-significant ($p=0.057$) increase in activated lymphocytes was found in all four lymphocyte subsets in the spleens of WT-infected mice at day 18 p.i., when the notable increase in the latency was found in the WT-infected spleen. It would be interesting to repeat this experiment to determine whether a higher WT viral latency induces a higher level of cellular activation in IFN-γR$^{-/-}$ mice.

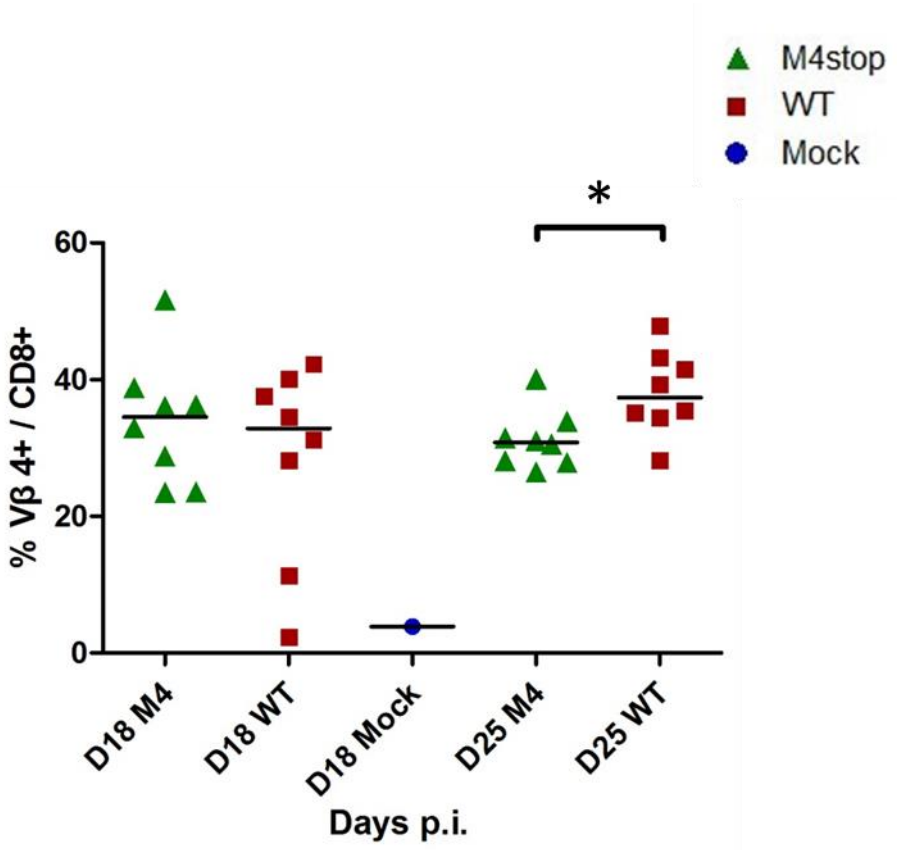

Figure 6.7 The change in Vβ4 expressing CD8 T cells. IFN-γR$^{-/-}$ mice were infected with 4 × 10^5 PFU M4stop or WT virus and the splenocytes were stained with anti-Vβ4 and CD8 fluorescent-conjugated antibodies at days 18 and 25 p.i.. The percentage of Vβ4$^+$CD8$^+$ T cells was calculated by comparing with the percentage of CD8$^+$ T cells. The black bars denote the median of each group; each symbol represents one mouse and D represents day. Groups that have mean values that vary significantly ($p<0.05$) by Mann-Whitney test are indicated by *.

6.2.6 Changes in GC B cells

MHV-68 is mainly latent in the GC B cells; therefore, a change in level of the GC B cells could influence viral latency. The expression of CD38 on B cells is an indicator of B-cell differentiation in the spleen (Oliver, Martin, and Kearney, 1997). Hence, to determine the percentage of GC B cells, splenocytes were double-stained with anti-CD38 and anti-CD19 antibodies. The histogram and density plots in figure 6.9a show the gating strategies used to determine CD38^{high}, CD38^{dim} and CD38^{low} expression in these populations. Figure 6.9b illustrates that the proportion of CD38^{dim}CD19^{+} B cells was increased after M4stop and WT infection, but this population disappeared in the spleens of IFN-γR$^{-/-}$ mice infected with WT virus at day 25 p.i.. The percentage of GC B cells in the WT-infected spleens was significantly higher than for M4stop ($p<0.05$) at day 18 p.i. , then the GC B cell population which was found in M4stop virus infection was not seen in the spleens of WT-infected mice at day 25 p.i. ($p=0.05$) (figure 6.10). This result is consistent with the previous results, which showed the GC structure was disturbed during a MHV-68 infection around day 23 p.i. (Ebrahimi et al., 2001). The disruption of the GC structure may influence the population of plasma cells in which the reactivation of MHV-68 occurs.

It has been shown in Chapter 5 that the difference in viral latency between WT and M4stop virus infections at days 14 and 17 p.i. was not related to the percentage of

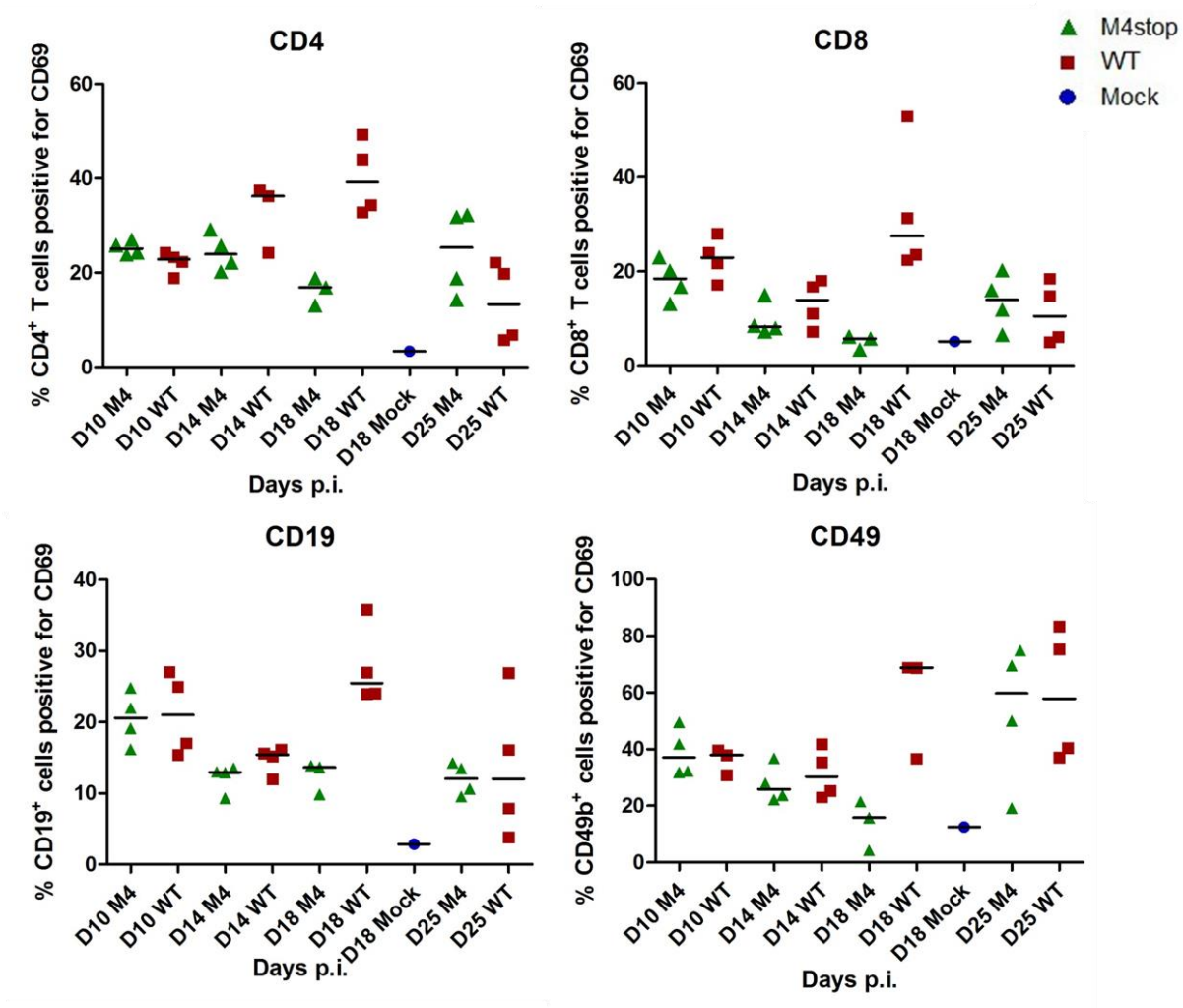

Figure 6.8 Percentages of activated lymphocytes in the spleens following infection with M4stop or WT virus. IFNγR$^{-/-}$ mice were infected with 4 × 10^5 PFU of either M4stop or WT virus. Spleens were harvested at days 10, 14, 18 and 25 p.i.. Lymphocytes were double stained with anti-CD69 and CD4, CD8, CD19 or CD49b antibodies, followed by analysis using flow cytometry. The black bars denote the median of each group. Each symbol represents one mouse and D represents day.

splenic GC B cells during the 129Sv mice infection, because the percentage of GC B cells was the same between the two viral infections at day 12, 14 and 17 p.i.. Interestingly, the percentages of B cells that were GC B cells in the WT-infected IFN-γR$^{-/-}$ mice spleens was higher than that seen in M4stop virus infection at day 18 p.i.. However, the increase in splenic GC B cells is possibly related, but not the only reason for the higher level of WT viral latency at day 18 p.i., because the sudden disappearance of GC B cells at day 25 p.i. did not reduce the latency difference between M4stop and WT, indicating the decrease in M4stop latency at day 18 p.i. is not due to the lower GC B.

6.3 Discussion

In this chapter, pathological changes were compared between the immune response and kinetics of virus replication that occur in IFN-γR$^{-/-}$ mice following infection with WT and M4-mutant viruses. As described in the results part of this chapter, there was a notable pathological change in the WT-infected IFN-γR$^{-/-}$ mice, whereas a delay in the loss of splenocytes and the formation of fibrosis were found to occur in M4stop virus infection. Compared to 129Sv mice infection, the peak of WT latency was postponed to day 18 p.i.. M4stop virus infection showed a reduced ability to establish latency in both mouse strains. It is indicated that although IFN-γ is essential for the control of viral latency in the spleen, it does not appear to be modulated by the M4 protein.

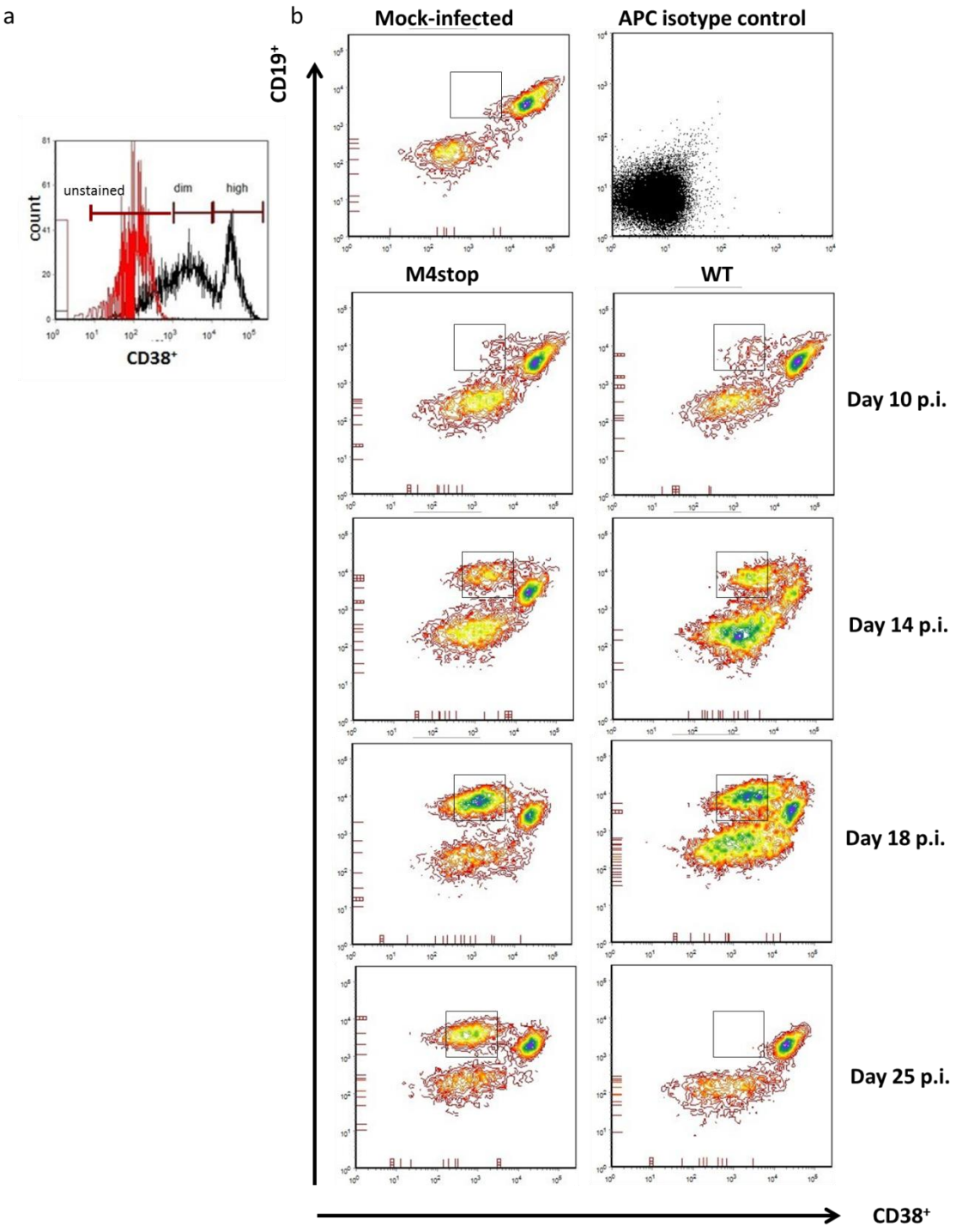

Figure 6.9 Gating strategies of GC B cells. IFN-γR$^{-/-}$ mice were infected with 4 × 10^5 PFU of either M4stop or WT virus and sacrificed at days 10, 14, 18 and 25 p.i.. Splenocytes were double stained with anti-CD38 and anti-CD19 antibodies. (a) The histogram shows how to define CD38^{high}, CD38^{dim} and CD38^{negative}. The red peak indicates the unstained cells, the middle peak represents the CD38^{dim}, and the right peak represents the CD38^{high} cells. (b) The change in proportion of CD38^{dim} cells during M4stop and WT virus infections. The cells in the black square are defined as CD38^{dim}CD19$^+$ B cells.

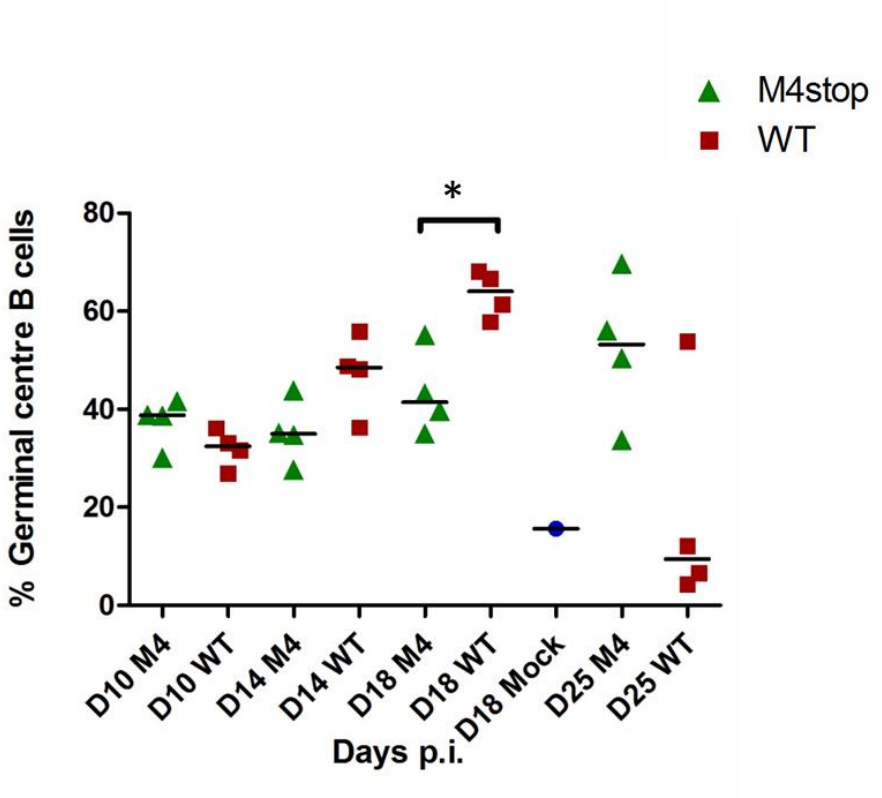

Figure 6.10 The percentages of GC B cells. IFN-γR$^{-/-}$ mice were infected with 4 × 10^5 PFU of either M4stop or WT virus and sacrificed at days 10, 14, 18 and 25 p.i.. Splenocytes were double stained with anti-CD38 and anti-CD19 antibodies. The GC B cells were gated as CD38^{dim}CD19^{+} B cells. The median from each group of animals are shown. Each symbol represents one mouse and D represents day. Groups that have mean values that vary significantly ($p<0.05$) by Mann-Whitney test are indicated by *.

It has been shown that Vβ4^{+}CD8^{+} T cells, which are induced by the M1 protein, are involved in the generation of fibrosis in the IFN-γR$^{-/-}$ mice during MHV-68 infection (Evans et al., 2008). Although the M4 protein has been shown not to be related to the expansion of Vβ4^{+}CD8^{+} T cells from day 28 p.i., there was no evidence to show that the M4 protein did not induce the Vβ4^{+}CD8^{+} T cells at earlier time points. Therefore, the percentages of Vβ4^{+}CD8^{+} T cells were monitored during infection. A slight but significant ($p<0.05$) increase in the percentage of Vβ4^{+}CD8^{+} T cells was found in WT-infected spleens at day 25 p.i. as compared to that found during M4stop virus infection. However, the results of M4stop virus infection are unlike those seen in a M1-deficient virus infection, where the percentage of Vβ4^{+}CD8^{+} T cells is decreased dramatically in the IFN-γR$^{-/-}$ mice at day 28 p.i. compared to that seen in a WT infection (Evans et al., 2008). The number of splenocytes in M1-deficient virus infected IFN-γR$^{-/-}$ mice is maintained at a similar level during infection, whereas the number decreased in WT virus infection (Dutia et al., 2004). Moreover, no fibrosis is found in M1-mutant virus infected IFN-γR$^{-/-}$ mice (Evans et al., 2008), whereas M4stop virus infection induced a delayed fibrosis in the spleens at day 25 p.i.. These indicate that the increase of Vβ4^{+}CD8^{+} T cells in WT virus infection is not the only reason for inducing the splenic fibrosis.

IFN-γR$^{-/-}$ mice develop a Th2 biased response after MHV-68 infection (Gangadharan et al., 2008). Transcription of chemokines and cytokines in IFN-γR$^{-/-}$ mice following MHV-68 infection is different from that seen in WT mice (Ebrahimi et al., 2001;

Gangadharan et al., 2008). For example, the transcription of Cxcl9 were significantly reduced during infection (Ebrahimi et al., 2001). The M4 protein has been shown be a Cxcl9 binding protein, therefore, the M4 protein may reduce these Th1 chemokines and enlarge the Th2 response. In this case, it would be interesting to assess and compare the levels of Th1 chemokines in the spleens of M4stop-infected IFN-γR$^{-/-}$ mice with WT virus infection.

An increased percentage of macrophages was found in WT infected IFN-γR$^{-/-}$ mice at day 10 and 14 p.i.. It has been reported that MHV-68 infection of IFN-γR$^{-/-}$ mice leads to the activation of F4/80^{+} macrophages via the alternative pathway, and the alternatively activated macrophages migrate to the GC at day 12 p.i. (Gangadharan et al., 2008), which is related to the development of fibrosis in the spleen. We do not know what the kinetics of the macrophage migration in the M4stop virus infection of IFN-γR$^{-/-}$ mice are, but it would be interesting to compare it to that of a WT infection. The splenic transcripts of Th2 cytokines and chemokine receptor, such as IL-4, IL-5, IL-13, IL-21 and CCR4, were significantly higher in IFN-γR$^{-/-}$ mice as compared to WT mice around day 20 p.i. (Gangadharan et al., 2008). These Th2 biased cytokines and chemokine receptor are involved in the alternative activation of macrophages (Gordon, 2003), which induce fibrosis in the spleen in IFN-γR$^{-/-}$ mice (Gangadharan et al., 2008). Transcripts of IL-13, IL-4 and Ccr4 were found to be expanded in the spleens of the 129Sv mice infected with WT virus as compared to M4stop virus infection at day 14 p.i., whereas the levels of transcripts of these chemokines in the

M4stop infected IFN-γR$^{-/-}$ were unknown. IFN-γ is an anti-fibrogenic cytokine, and it may control the fibrosis formation mechanism in 129Sv mice. Therefore, in the non-responsive IFN-γ mice, the over-expansion of the Th2 chemokines and cytokines may induce fibrosis. Therefore, to understand the generation of spleen fibrosis through the chemokines, cytokines and their receptors, it would be interesting to examine and compare the transcripts of Th2 chemokines and cytokine in M4stop-infected IFN-γR$^{-/-}$ mice.

The loss of the splenocytes and the change of spleen structure during WT virus infection in the IFN-γR$^{-/-}$ mice did not impact on viral latency at day 18 p.i.. Moreover, the decrease in GC B cells (CD38^{dim}CD19^{+} B cells) at day 25 p.i. only reduced viral reactivation in comparison to M4stop virus infection. However, WT viral DNA loads were higher than that seen in M4stop virus infection, indicating GC B cells are not the only main site of MHV-68 latency in the IFN-γR$^{-/-}$ mice at day 25 p.i.. The mechanism of GC B cell loss is still unknown, but it is probably one way to defend the host from viral infection, or latent virus could trigger the differentiation of B cells into memory B cells or plasma cells. However, the percentage of memory B cells has been shown to be reduced at the same time (S Li's personal communication). Due to the decrease in the number of infectious centres in the WT-infected spleen at day 18 p.i.. The number of infectious centres in WT-infected spleens decreased at day 25 p.i., but the viral DNA loads of WT virus were higher than M4stop suggesting that it is unlikely that the decrease in the M4stop viral

latency was because of the disruption of plasma cells differentiation (which are the major cell involves in reactivation).

Chapter 7

Conclusion

7 Conclusion

The left end of the MHV-68 genome, which encodes M1-M4, vtRNAs and microRNAs, plays an important role during viral lytic and latent infections. The M4 gene encodes a secreted glycoprotein which is predicted to have modulatory functions, because the viral DNA load and reactivation of virus are decreased after infection with a virus lacking a functional M4 gene compared to WT virus infection. In this study, we investigated the function of M4 protein of MHV-68 by examining the chemokine binding ability of the recombinant M4 protein *in vitro* and by comparing the host responses following M4stop virus and WT virus infections.

The recombinant M4 protein was shown to bind to Cc- and Cxc-chemokines. Moreover, the binding of M4 protein and chemokine inhibited the chemokine-GAGs interaction. Interestingly, the binding ability of M4 protein to Cxcl2 and Cxcl5 was higher than M3 protein. In contrast, M4 protein showed lower binding activity to CXCL8, which has been shown to bind to M3 protein with a high activity (Parry et al., 2000). Therefore, it could be possible that MHV-68 secretes two chemokine binding proteins, which bind to different chemokines. It would be interesting to examine the binding activity of M4 with more chemokines which M3 protein does not bind or binds with a low affinity.

M3 protein modulates the immune response in the lungs of wood mice (Hughes et al., 2011), but there is no change in the lung inflammation in the laboratory mice

following M3 mutant virus (Sarawar et al., 2002). Similarly, there was no difference in the lung inflammation during M4stop infection as compared with WT infection. This might be due to a difference between the natural host environment and the laboratory mouse. Alternatively, the timing post infection might be very important for MHV-68 infection.

We noticed that the M4stop viral titres in the lung were lower at day 8 p.i.. Furthermore, M4stop virus had a higher viral load in the spleens at the same time point compared to WT viral infection, suggesting the spread of M4stop virus is faster. It has been found that MHV-68 is passed to macrophages through the infected epithelial cells, then the B cells are infected only after the infection of macrophages (Frederico et al., 2012). Although, the kinetics of viral transportation are not clear during M4stop viral infection, it is possible that the infected macrophages in the lung are able to migrate faster to the MLN in the absence of M4 protein. Hence, more B cells might be infected in the MLN and transported to the spleen. However, more experiments, such as investigating the viral DNA loads of M4stop and WT virus and the number of macrophages in the MLN, are required to confirm our hypothesis.

The absence of M4 protein led to a decrease in viral DNA load and reactivation of viral latency at day 14 p.i., accompanied by less activation of T cells, B cells and macrophages compared to WT infection. The activation of B cells depends on the assistance of $CD4^+$ T cells (Stevenson and Doherty, 1999). Then the activated B cells migrate to the GC and develop to centroblasts (reviewed in Nutt and Tarlinton, 2011;

Schwickert et al., 2009). However, there was no difference in the percentage of proliferating B cells or the percentage of GC B cells in the spleens of 129Sv mice infected with M4stop and WT viral infections. Interestingly, more GC B cells were found in the spleens of WT-infected IFN-$\gamma R^{-/-}$ mice at day 18 p.i., accompanied by a higher WT viral load. However, at day 25 p.i., the disappearance of GC B cells during WT virus infection did not influence the fact that WT virus latency was still higher than M4stop virus. This evidence suggests GC B cells are not responsible for the decreased M4stop virus latency.

The expression of Ccl19, Cxcl12, Cxcr5 and Bcl-6 mRNA, which are related to the development of GC, was found to be decreased in the WT-infected spleen when compared to M4stop viral infection at various time points. Moreover, these transcripts were down-regulated at day 12 or 14 p.i. in the spleens of WT-infected 129Sv mice compared to WT viral infection at day 10 p.i.. Therefore, we believed the development of GC was different between M4stop and WT infection. However, the percentages of GC B cells, T_{FH} cell and plasma cells in the spleens of two viral infections did not support our hypothesis. Although we noticed that there was no difference in the percentage of macrophages in the spleen following M4stop and WT virus infection at days 10 and 12 p.i., the distribution of macrophages in the GC were distinct. Therefore, it would be interesting to examine the distribution of T_{FH} cells and plasma cells, as M4 protein may affect the trafficking of these cells.

An increase in the transcripts of IL-4 and IL-13 and a decrease in the transcripts of

LTα, LTβ, Bcl-6 and Ccr7 in the spleen indicate there was a strong Th2 response during WT infection. Th2 cytokines, such IL-4 and IL-13, can downregulate the Th1 response, which suggests WT virus infection induced a reduced Th1 immune reaction. Several viruses modulate the immune system by inhibition of the biological activity of Th1 cytokines, thus the immune response shifts from Th1 response to Th2 response and the viruses increase their chance to survive. For example, EBV encodes an IL-10 homolog (Swaminathan et al., 1993) and Myxoma virus encodes a homolog of IFN-γ receptor (Upton, Mossman, and McFadden, 1992), which both inhibit the Th1 response. Additionally, KSHV encodes a vCCL2 homolog, which drives a Th2-type immune response in vivo and avoids a Th1 response (Weber et al., 2001). On the contrary, immune responses in M4stop viral infection seem to be less Th2 skewed than in WT viral infection. M4 protein has an ability to bind to Cxcl2 and Cxcl9, which are Th1 chemokines. Therefore, the chemokine binding ability of M4 protein might be involved in the Th1/Th2 equilibrium by binding the Th1 chemokines. We also found that M4 protein can bind to Cxcl4 and prevent the Cxcl4-GAGs interaction. However, Cxcl4 inhibits the production of IFN-γ and promotes the development of Th2 cytokines (Fleischer et al., 2002; Romagnani et al., 2005). However, it has been found that chemokine binding protein can enhance the function of chemokines (Coscoy et al., 2012). Therefore, it is necessary to examine the ability of these chemokines to mediate chemotaxis after binding with M4 protein.

The development of fibrosis was delayed in the M4stop-infected spleen compared to

WT viral infection in the IFN-γR$^{-/-}$ mice. It is believed that fibrosis is related to the alternative activation of macrophages, involving Th2 cells secreting IL-4 and IL-13 (Gangadharan et al., 2008; Gordon, 2003; Stein et al., 1992). Therefore, the earlier generation of fibrosis in the WT-infected IFN-γR$^{-/-}$ mice might be due to the severe imbalance of Th1/Th2 response. Moreover, we found the difference in the levels of viral load in the absence of M4 protein is not related to the IFN-γ response.

Although we know M4 protein has an ability to bind chemokines, the mechanism of successful latency establishment of WT virus in the spleens of immunocompetent mice at day 14 p.i. is still unsure. Our study helps to shed some light on the possibilities of what roles M4 protein might be involved in. However, to fully understand the function of M4 protein, we still have some goals to achieve. Firstly, as we know M4 protein interrupts the chemokine-GAGs interaction, we further want to investigate whether M4 protein modulates chemotaxis. Supposing M4 protein can affect chemotaxis, whether it inhibits or enhances cell migration or the function of chemokines is another question. Secondly, we know that GC regulatory factors and PD-1 expression are different between the two viral infections. We would like to study GC development further to find out whether the distribution of cells is distinct after infection by histological methods. Thirdly, Th1 and Th2 responses will be studied during M4stop and WT viral infections to confirm that WT virus induces a Th2 response which is absent from M4stop infection. Lastly, the laboratory mouse strain we selected has distinct immune responses during MHV-68 infection from its

natural host. Therefore, the influence of M4 protein in the wood mice will be examined in future experiments.

8 Appendix

Appendix I

Antibody	Dilution	Technique
Mouse anti His-tag	1:500	ELISA, Western Blot
Rabbit anti mouse biotin	1:1000	Western Blot
Rat anti Cxcl4	1:500	Western Blot
Rat anti Cxcl4	1:1000	ELISA
Streptavidin-AP	1:500	Western Blot
Goat anti rat HRP	1:1000	ELISA
Goat anti mouse HRP	1:500	ELISA
CD4-PE	1:666	Flow cytometry
CD8-PE	1:130	Flow cytometry
CD19-PE	1:230	Flow cytometry
CD19-APC/Cy7	1:160	Flow cytometry
CD38-APC	1:666	Flow cytometry
CD49b-PE	1:100	Flow cytometry
CD49b-FITC	1:20	Flow cytometry
CD138-PE	1:1000	Flow cytometry

Cxcr-5-APC	1:68	Flow cytometry
PD-1-FITC	1:68	Flow cytometry
CD11b-APC	1:34	Flow cytometry
Ly6G-PE	1:42	Flow cytometry
Ki-67	1:200	Flow cytometry
IFN-γ-PE	1:1000	Flow cytometry
Goat anti rabbit biotin	1:300	Flow cytometry
Alexa Fluor® 647	1:500	Flow cytometry
Alexa Fluor® 568	1:1000	Immunostaining
To-Pro®-3	1:1000	Immunostaining

Appendix II

Position	Symbol	Position	Symbol	Position	Symbol
A01	Abcf1	C05	Ccr7	E09	Il1b
A02	Bcl6	C06	Ccr8	E10	Il1f6
A03	Cxcr5	C07	Ccr9	E11	Il1f8
A04	C3	C08	Crp	E12	Il1r1
A05	Casp1	C09	Cx3cl1	F01	Il1r2
A06	Ccl1	C10	Cxcl1	F02	Il20
A07	Ccl11	C11	Cxcl10	F03	Il2rb
A08	Ccl12	C12	Cxcl11	F04	Il2rg
A09	Ccl17	D01	Cxcl12	F05	Il3
A10	Ccl19	D02	Cxcl13	F06	Il4
A11	Ccl2	D03	Cxcl15	F07	Il5ra
A12	Ccl20	D04	Pf4	F08	Il6ra
B01	Ccl22	D05	Cxcl5	F09	Il6st
B02	Ccl24	D06	Cxcl9	F10	Cxcr2
B03	Ccl25	D07	Cxcr3	F11	Itgam
B04	Ccl3	D08	Ccr10	F12	Itgb2
B05	Ccl4	D09	Ifng	G01	Lta
B06	Ccl5	D10	Il10	G02	Ltb
B07	Ccl6	D11	Il10ra	G03	Mif
B08	Ccl7	D12	Il10rb	G04	Aimp1
B09	Ccl8	E01	Il11	G05	Spp1
B10	Ccl9	E02	Il13	G06	Tgfb1
B11	Ccr1	E03	Il13ra1	G07	Tnf
B12	Ccr2	E04	Il15	G08	Tnfrsf1a
C01	Ccr3	E05	Il16	G09	Tnfrsf1b
C02	Ccr4	E06	Il17b	G10	Cd40lg
C03	Ccr5	E07	Il18	G11	Tollip
C04	Ccr6	E08	Il1a	G12	Xcr1

9 References

Adamson, A. L. (2005). Epstein-Barr virus BZLF1 protein binds to mitotic chromosomes. *J Virol* **79**(12)**,** 7899-904.

Adler, H., Messerle, M., and Koszinowski, U. H. (2003). Cloning of herpesviral genomes as bacterial artificial chromosomes. *Reviews in medical virology* **13**(2)**,** 111-121.

Adler, H., Messerle, M., Wagner, M., and Koszinowski, U. H. (2000). Cloning and mutagenesis of the murine gammaherpesvirus 68 genome as an infectious bacterial artificial chromosome. *J Virol* **74**(15)**,** 6964-74.

Alcami, A. (2003). Viral mimicry of cytokines, chemokines and their receptors. *Nat Rev Immunol* **3**(1)**,** 36-50.

Alcami, A., Symons, J. A., Collins, P. D., Williams, T. J., and Smith, G. L. (1998). Blockade of chemokine activity by a soluble chemokine binding protein from vaccinia virus. *J Immunol* **160**(2)**,** 624-33.

Alcamí, A., Symons, J. A., and Smith, G. L. (2000). The Vaccinia Virus Soluble Alpha/Beta Interferon (IFN) Receptor Binds to the Cell Surface and Protects Cells from the Antiviral Effects of IFN. *Journal of virology* **74**(23)**,** 11230-11239.

Alexander-Brett, J. M., and Fremont, D. H. (2007). Dual GPCR and GAG mimicry by the M3 chemokine decoy receptor. *The Journal of Experimental Medicine* **204**(13)**,** 3157-3172.

Alexander, J. M., Nelson, C. A., van Berkel, V., Lau, E. K., Studts, J. M., Brett, T. J., Speck, S. H., Handel, T. M., Virgin, H. W., and Fremont, D. H. (2002). Structural basis of chemokine sequestration by a herpesvirus decoy receptor. *Cell* **111**(3)**,** 343-56.

Alfieri, C., Tanner, J., Carpentier, L., Perpete, C., Savoie, A., Paradis, K., Delage, G., and Joncas, J. (1996). Epstein-Barr virus transmission from a blood donor to an organ transplant recipient with recovery of the same virus strain from the recipient's blood and oropharynx. *Blood* **87**(2)**,** 812-817.

Alimzhanov, M. B., Kuprash, D. V., Kosco-Vilbois, M. H., Luz, A., Turetskaya, R. L., Tarakhovsky, A., Rajewsky, K., Nedospasov, S. A., and Pfeffer, K. (1997). Abnormal development of secondary lymphoid tissues in lymphotoxin β-deficient mice. *Proceedings of the National Academy of Sciences* **94**(17)**,** 9302-9307.

Allen, C. D., Ansel, K. M., Low, C., Lesley, R., Tamamura, H., Fujii, N., and Cyster, J. G. (2004). Germinal center dark and light zone organization is mediated by CXCR4 and CXCR5. *Nat Immunol* **5**(9)**,** 943-52.

Allen, C. D. C., Okada, T., and Cyster, J. G. (2007). Germinal-Center Organization and Cellular Dynamics. *Immunity* **27**(2)**,** 190-202.

Amen, M. A., and Griffiths, A. (2011). Packaging of non-coding RNAs into herpesvirus virions: comparisons to coding RNAs. *Frontiers in genetics* **2**.

Amyes, E., Hatton, C., Montamat-Sicotte, D., Gudgeon, N., Rickinson, A. B., McMichael, A. J., and Callan, M. F. (2003). Characterization of the CD4+ T cell response to Epstein-Barr virus during primary and persistent infection. *J Exp Med* **198**(6)**,** 903-11.

Andersson, J. (1996). Clinical and immunological considerations in Epstein-Barr virus-associated diseases. *Scand J Infect Dis Suppl* **100,** 72-82.

Ansel, K. M., Ngo, V. N., Hyman, P. L., Luther, S. A., Forster, R., Sedgwick, J. D., Browning, J. L., Lipp, M., and Cyster, J. G. (2000). A chemokine-driven positive feedback loop organizes lymphoid follicles. *Nature* **406**(6793)**,** 309-314.

Aoki, Y., Jaffe, E. S., Chang, Y., Jones, K., Teruya-Feldstein, J., Moore, P. S., and Tosato, G. (1999). Angiogenesis and hematopoiesis induced by Kaposi's sarcoma-associated herpesvirus-encoded interleukin-6. *Blood* **93**(12)**,** 4034-4043.

Aricò, E., Monque, D. M., D'Agostino, G., Moschella, F., Venditti, M., Kalinke, U., Allen, D. J., Nash, A. A., Belardelli, F., and Ferrantini, M. (2011). MHV-68 producing mIFNα1 is severely attenuated in vivo and effectively protects mice against challenge with wt MHV-68. *Vaccine* **29**(23)**,** 3935-3944.

Arvanitakis, L., Geras-Raaka, E., Varma, A., Gershengorn, M. C., and Cesarman, E. (1997). Human herpesvirus KSHV encodes a constitutively active G-protein-coupled receptor linked to cell proliferation. *Nature* **385**(6614)**,** 347-350.

Auerbach, D. J., Lin, Y., Miao, H., Cimbro, R., DiFiore, M. J., Gianolini, M. E., Furci, L., Biswas, P., Fauci, A. S., and Lusso, P. (2012). Identification of the platelet-derived chemokine CXCL4/PF-4 as a broad-spectrum HIV-1 inhibitor. *Proceedings of the National Academy of Sciences* **109**(24)**,** 9569-9574.

Babcock, G. J., Decker, L. L., Freeman, R. B., and Thorley-Lawson, D. A. (1999). Epstein-barr virus-infected resting memory B cells, not proliferating lymphoblasts, accumulate in the peripheral blood of immunosuppressed patients. *J Exp Med* **190**(4)**,** 567-76.

Babcock, G. J., Decker, L. L., Volk, M., and Thorley-Lawson, D. A. (1998). EBV Persistence in Memory B Cells In Vivo. *Immunity* **9**(3)**,** 395-404.

Bacon, K. B., Premack, B. A., Gardner, P., and Schall, T. J. (1995). Activation of dual T cell signaling pathways by the chemokine RANTES. *Science* **269**(5231)**,** 1727-30.

Bahar, M. W., Kenyon, J. C., Putz, M. M., Abrescia, N. G., Pease, J. E., Wise, E. L., Stuart, D. I., Smith, G. L., and Grimes, J. M. (2008). Structure and function of A41, a vaccinia virus chemokine binding protein. *PLoS Pathog* **4**(1)**,** e5.

Bais, C., Santomasso, B., Coso, O., Arvanitakis, L., Raaka, E. G., Gutkind, J. S., Asch, A. S., Cesarman, E., Gershengorn, M. C., and Mesri, E. A. (1998). G-protein-coupled receptor of Kaposi's sarcoma-associated herpesvirus is a viral oncogene and angiogenesis activator. *Nature* **391**(6662)**,** 86-9.

Barton, E., Mandal, P., and Speck, S. H. (2011). Pathogenesis and host control of gammaherpesviruses: lessons from the mouse. *Annu Rev Immunol* **29,** 351-97.

Basso, K., and Dalla-Favera, R. (2010). BCL6: master regulator of the germinal center reaction and key oncogene in B cell lymphomagenesis. *Adv Immunol* **105,** 193-210.

Beck, C. G., Studer, C., Zuber, J. F., Demange, B. J., Manning, U., and Urfer, R. (2001). The viral CC chemokine-binding protein vCCI inhibits monocyte chemoattractant protein-1 activity by masking its CCR2B-binding site. *Journal of Biological Chemistry* **276**(46)**,** 43270-43276.

Belperio, J. A., Dy, M., Murray, L., Burdick, M. D., Xue, Y. Y., Strieter, R. M., and Keane, M. P. (2004). The Role of the Th2 CC Chemokine Ligand CCL17 in Pulmonary Fibrosis. *The Journal of Immunology* **173**(7)**,** 4692-4698.

Belz, G. T., Liu, H., Andreansky, S., Doherty, P. C., and Stevenson, P. G. (2003). Absence of a functional defect in CD8+ T cells during primary murine gammaherpesvirus-68 infection of I-A(b-/-)

mice. *J Gen Virol* **84**(Pt 2)**,** 337-41.

Benedict, C. A., Loewendorf, A., Garcia, Z., Blazar, B. R., and Janssen, E. M. (2008). Dendritic cell programming by cytomegalovirus stunts naive T cell responses via the PD-L1/PD-1 pathway. *J Immunol* **180**(7)**,** 4836-47.

Birkenbach, M., Josefsen, K., Yalamanchili, R., Lenoir, G., and Kieff, E. (1993). Epstein-Barr virus-induced genes: first lymphocyte-specific G protein-coupled peptide receptors. *J Virol* **67**(4)**,** 2209-20.

Blasdell, K., McCracken, C., Morris, A., Nash, A. A., Begon, M., Bennett, M., and Stewart, J. P. (2003). The wood mouse is a natural host for Murid herpesvirus 4. *Journal of general virology* **84**(1)**,** 111.

Blaskovic, D. (1980). Isolation of five strains of herpesviruses from two species of free living small rodents. *Acta Virol* **24,** 468.

Block, T. M., and Hill, J. M. (1997). The latency associated transcripts (LAT) of herpes simplex virus: still no end in sight. *J Neurovirol* **3**(5)**,** 313-21.

Blum, K. A., Lozanski, G., and Byrd, J. C. (2004). Adult Burkitt leukemia and lymphoma. *Blood* **104**(10)**,** 3009-3020.

Bodaghi, B., Goureau, O., Zipeto, D., Laurent, L., Virelizier, J. L., and Michelson, S. (1999). Role of IFN-gamma-induced indoleamine 2,3 dioxygenase and inducible nitric oxide synthase in the replication of human cytomegalovirus in retinal pigment epithelial cells. *J Immunol* **162**(2)**,** 957-64.

Bogerd, H. P., Karnowski, H. W., Cai, X., Shin, J., Pohlers, M., and Cullen, B. R. (2010). A mammalian herpesvirus uses noncanonical expression and processing mechanisms to generate viral MicroRNAs. *Mol Cell* **37**(1)**,** 135-42.

Bowden, R. J., Simas, J. P., Davis, A. J., and Efstathiou, S. (1997). Murine gammaherpesvirus 68 encodes tRNA-like sequences which are expressed during latency. *J Gen Virol* **78 (Pt 7),** 1675-87.

Bridgeman, A., Stevenson, P. G., Simas, J. P., and Efstathiou, S. (2001). A secreted chemokine binding protein encoded by murine gammaherpesvirus-68 is necessary for the establishment of a normal latent load. *J Exp Med* **194**(3)**,** 301-12.

Bryant, N. A., Davis-Poynter, N., Vanderplasschen, A., and Alcami, A. (2003). Glycoprotein G isoforms from some alphaherpesviruses function as broad-spectrum chemokine binding proteins. *The EMBO journal* **22**(4)**,** 833-846.

Bryant, V. L., Ma, C. S., Avery, D. T., Li, Y., Good, K. L., Corcoran, L. M., de Waal Malefyt, R., and Tangye, S. G. (2007). Cytokine-mediated regulation of human B cell differentiation into Ig-secreting cells: predominant role of IL-21 produced by CXCR5+ T follicular helper cells. *J Immunol* **179**(12)**,** 8180-90.

Calender, A., Billaud, M., Aubry, J. P., Banchereau, J., Vuillaume, M., and Lenoir, G. M. (1987). Epstein-Barr virus (EBV) induces expression of B-cell activation markers on in vitro infection of EBV-negative B-lymphoma cells. *Proc Natl Acad Sci U S A* **84**(22)**,** 8060-4.

Callan, M. F. C., Steven, N., Krausa, P., Wilson, J. D. K., Moss, P. A. H., Gillespie, G. M., Bell, J. I., Rickinson, A. B., and McMichael, A. J. (1996). Large clonal expansions of CD8+ T cells in acute infectious mononucleosis. *Nature medicine* **2**(8)**,** 906-911.

Campbell, E. M., and Hope, T. J. (2003). Role of the cytoskeleton in nuclear import. *Advanced Drug*

Delivery Reviews **55**(6)**,** 761-771.

Cardin, R. D., Brooks, J. W., Sarawar, S. R., and Doherty, P. C. (1996). Progressive loss of CD8+ T cell-mediated control of a gamma-herpesvirus in the absence of CD4+ T cells. *J Exp Med* **184**(3)**,** 863-71.

Cartwright, R. A., and Watkins, G. (2004). Epidemiology of Hodgkin's disease: a review. *Hematol Oncol* **22**(1)**,** 11-26.

Caruso, A., Licenziati, S., Corulli, M., Canaris, A. D., De Francesco, M. A., Fiorentini, S., Peroni, L., Fallacara, F., Dima, F., Balsari, A., and Turano, A. (1997). Flow cytometric analysis of activation markers on stimulated T cells and their correlation with cell proliferation. *Cytometry* **27**(1)**,** 71-6.

Chalupková, A., Hricová, M., Hrabovská, Z., and Mistríková, J. (2008). Pathogenetical Characterization of MHV-76: a Spontaneous 9.5-Kilobase-Deletion Mutant of Murine Lymphotropic Gammaherpesvirus 68. *Acta Veterinaria Brno* **77**(2)**,** 231-237.

Chang, Y., Cesarman, E., Pessin, M., Lee, F., Culpepper, J., Knowles, D., and Moore, P. (1994). Identification of herpesvirus-like DNA sequences in AIDS-associated Kaposi's sarcoma. *Science* **266**(5192)**,** 1865 - 1869.

Chatterjee, M., Osborne, J., Bestetti, G., Chang, Y., and Moore, P. S. (2002). Viral IL-6-induced cell proliferation and immune evasion of interferon activity. *Science Signalling* **298**(5597)**,** 1432.

Chemnitz, J. M., Eggle, D., Driesen, J., Classen, S., Riley, J. L., Debey-Pascher, S., Beyer, M., Popov, A., Zander, T., and Schultze, J. L. (2007). RNA fingerprints provide direct evidence for the inhibitory role of TGFbeta and PD-1 on CD4+ T cells in Hodgkin lymphoma. *Blood* **110**(9)**,** 3226-33.

Chen, Y.-B., Rahemtullah, A., and Hochberg, E. (2007). Primary Effusion Lymphoma. *The Oncologist* **12**(5)**,** 569-576.

Chevallier-Greco, A., Manet, E., Chavrier, P., Mosnier, C., Daillie, J., and Sergeant, A. (1986). Both Epstein-Barr virus (EBV)-encoded trans-acting factors, EB1 and EB2, are required to activate transcription from an EBV early promoter. *EMBO J* **5**(12)**,** 3243-9.

Chou, J., Lin, Y.-C., Kim, J., You, L., Xu, Z., He, B., and Jablons, D. M. (2008). Nasopharyngeal carcinoma--review of the molecular mechanisms of tumorigenesis. *Head & Neck* **30**(7)**,** 946-963.

Christensen, J. P., Cardin, R. D., Branum, K. C., and Doherty, P. C. (1999). CD4(+) T cell-mediated control of a gamma-herpesvirus in B cell-deficient mice is mediated by IFN-gamma. *Proc Natl Acad Sci U S A* **96**(9)**,** 5135-40.

Christensen, J. P., and Doherty, P. C. (1999). Quantitative analysis of the acute and long-term CD4(+) T-cell response to a persistent gammaherpesvirus. *J Virol* **73**(5)**,** 4279-83.

Chung, Y., Tanaka, S., Chu, F., Nurieva, R. I., Martinez, G. J., Rawal, S., Wang, Y. H., Lim, H., Reynolds, J. M., Zhou, X. H., Fan, H. M., Liu, Z. M., Neelapu, S. S., and Dong, C. (2011). Follicular regulatory T cells expressing Foxp3 and Bcl-6 suppress germinal center reactions. *Nat Med* **17**(8)**,** 983-8.

Cimmino, L., Martins, G. A., Liao, J., Magnusdottir, E., Grunig, G., Perez, R. K., and Calame, K. L. (2008). Blimp-1 Attenuates Th1 Differentiation by Repression of ifng, tbx21, and bcl6 Gene Expression. *The Journal of Immunology* **181**(4)**,** 2338-2347.

Clambey, E. T., Virgin, H. W. t., and Speck, S. H. (2000). Disruption of the murine gammaherpesvirus

68 M1 open reading frame leads to enhanced reactivation from latency. *J Virol* **74**(4)**,** 1973-84.

Cliffe, A. R., Nash, A. A., and Dutia, B. M. (2009). Selective uptake of small RNA molecules in the virion of murine gammaherpesvirus 68. *J Virol* **83**(5)**,** 2321-6.

Collins, C. M., Boss, J. M., and Speck, S. H. (2009). Identification of Infected B-Cell Populations by Using a Recombinant Murine Gammaherpesvirus 68 Expressing a Fluorescent Protein. *Journal of virology* **83**(13)**,** 6484-6493.

Collins, C. M., and Speck, S. H. (2012). Tracking murine gammaherpesvirus 68 infection of germinal center B cells in vivo. *PLoS One* **7**(3)**,** e33230.

Coscoy, L., Viejo-Borbolla, A., Martinez-Martín, N., Nel, H. J., Rueda, P., Martín, R., Blanco, S., Arenzana-Seisdedos, F., Thelen, M., Fallon, P. G., and Alcamí, A. (2012). Enhancement of Chemokine Function as an Immunomodulatory Strategy Employed by Human Herpesviruses. *PLoS Pathogens* **8**(2)**,** e1002497.

Cyster, J. G. (2010). B cell follicles and antigen encounters of the third kind. *Nat Immunol* **11**(11)**,** 989-96.

Dabbagh, K., Xiao, Y., Smith, C., Stepick-Biek, P., Kim, S. G., Lamm, W. J. E., Liggitt, D. H., and Lewis, D. B. (2000). Local blockade of allergic airway hyperreactivity and inflammation by the poxvirus-derived pan-CC-chemokine inhibitor vCCI. *The Journal of Immunology* **165**(6)**,** 3418-3422.

Damon, I., Murphy, P. M., and Moss, B. (1998). Broad spectrum chemokine antagonistic activity of a human poxvirus chemokine homolog. *Proc Natl Acad Sci U S A* **95**(11)**,** 6403-7.

Davison, A. J., Eberle, R., Ehlers, B., Hayward, G. S., McGeoch, D. J., Minson, A. C., Pellett, P. E., Roizman, B., Studdert, M. J., and Thiry, E. (2009). The order Herpesvirales. *Arch Virol* **154**(1)**,** 171-7.

Del Rio, L., Bennouna, S., Salinas, J., and Denkers, E. Y. (2001). CXCR2 deficiency confers impaired neutrophil recruitment and increased susceptibility during Toxoplasma gondii infection. *The Journal of Immunology* **167**(11)**,** 6503-6509.

Dent, A. L., Shaffer, A. L., Yu, X., Allman, D., and Staudt, L. M. (1997). Control of inflammation, cytokine expression, and germinal center formation by BCL-6. *Science* **276**(5312)**,** 589-92.

Dias, P., Giannoni, F., Lee, L. N., Han, D., Yoon, S., Yagita, H., Azuma, M., and Sarawar, S. R. (2010). CD4 T-cell help programs a change in CD8 T-cell function enabling effective long-term control of murine gammaherpesvirus 68: role of PD-1-PD-L1 interactions. *J Virol* **84**(16)**,** 8241-9.

Diebel, K. W., Smith, A. L., and van Dyk, L. F. (2010). Mature and functional viral miRNAs transcribed from novel RNA polymerase III promoters. *RNA* **16**(1)**,** 170-85.

Douek, D. C., Crawford, A., Angelosanto, J. M., Nadwodny, K. L., Blackburn, S. D., and Wherry, E. J. (2011). A Role for the Chemokine RANTES in Regulating CD8 T Cell Responses during Chronic Viral Infection. *PLoS Pathogens* **7**(7)**,** e1002098.

Du, M. Q., Liu, H., Diss, T. C., Ye, H., Hamoudi, R. A., Dupin, N., Meignin, V., Oksenhendler, E., Boshoff, C., and Isaacson, P. G. (2001). Kaposi sarcoma-associated herpesvirus infects monotypic (IgM lambda) but polyclonal naive B cells in Castleman disease and associated lymphoproliferative disorders. *Blood* **97**(7)**,** 2130-6.

Dutia, B. M., Allen, D. J., Dyson, H., and Nash, A. A. (1999). Type I interferons and IRF-1 play a critical role in the control of a gammaherpesvirus infection. *Virology* **261**(2)**,** 173-9.

Dutia, B. M., Clarke, C. J., Allen, D. J., and Nash, A. A. (1997). Pathological changes in the spleens of gamma interferon receptor-deficient mice infected with murine gammaherpesvirus: a role for CD8 T cells. *Journal of virology* **71**(6)**,** 4278-83.

Dutia, B. M., Reid, S. J., Drummond, D. D., Ligertwood, Y., Bennet, I., Rietberg, W., Silvia, O., Jarvis, M. A., and Nash, A. A. (2009). A novel Cre recombinase imaging system for tracking lymphotropic virus infection in vivo. *PLoS One* **4**(8)**,** e6492.

Dutia, B. M., Roy, D. J., Ebrahimi, B., Gangadharan, B., Efstathiou, S., Stewart, J. P., and Nash, A. A. (2004). Identification of a region of the virus genome involved in murine gammaherpesvirus 68-induced splenic pathology. *J Gen Virol* **85**(Pt 6)**,** 1393-400.

Ebrahimi, B., Dutia, B. M., Brownstein, D. G., and Nash, A. A. (2001). Murine gammaherpesvirus-68 infection causes multi-organ fibrosis and alters leukocyte trafficking in interferon-gamma receptor knockout mice. *Am J Pathol* **158**(6)**,** 2117-25.

Ebrahimi, B., Dutia, B. M., Roberts, K. L., Garcia-Ramirez, J. J., Dickinson, P., Stewart, J. P., Ghazal, P., Roy, D. J., and Nash, A. A. (2003). Transcriptome profile of murine gammaherpesvirus-68 lytic infection. *J Gen Virol* **84**(Pt 1)**,** 99-109.

Efstathiou, S., Ho, Y. M., and Minson, A. C. (1990). Cloning and molecular characterization of the murine herpesvirus 68 genome. *Journal of general virology* **71**(6)**,** 1355-1364.

Ehlers, B., Kuchler, J., Yasmum, N., Dural, G., Voigt, S., Schmidt-Chanasit, J., Jakel, T., Matuschka, F. R., Richter, D., Essbauer, S., Hughes, D. J., Summers, C., Bennett, M., Stewart, J. P., and Ulrich, R. G. (2007). Identification of novel rodent herpesviruses, including the first gammaherpesvirus of Mus musculus. *J Virol* **81**(15)**,** 8091-100.

Ehtisham, S., Sunil-Chandra, N. P., and Nash, A. A. (1993). Pathogenesis of murine gammaherpesvirus infection in mice deficient in CD4 and CD8 T cells. *J Virol* **67**(9)**,** 5247-52.

El-Daly, H., Bower, M., and Naresh, K. N. (2010). Follicular dendritic cells in multicentric Castleman disease present human herpes virus type 8 (HHV8)-latent nuclear antigen 1 (LANA1) in a proportion of cases and is associated with an enhanced T-cell response. *European Journal of Haematology* **84**(2)**,** 133-136.

Epstein, M. A., Achong, B. G., and Barr, Y. M. (1964). Virus particles in cultured lymphoblasts from burkitt's lymphoma. *Lancet* **15,** 702-703.

Evans, A., Moorman, N., Willer, D., and Speck, S. (2006). The M4 gene of γHV68 encodes a secreted glycoprotein and is required for the efficient establishment of splenic latency. *Virology* **344**(2)**,** 520-531.

Evans, A. G., Moser, J. M., Krug, L. T., Pozharskaya, V., Mora, A. L., and Speck, S. H. (2008). A gammaherpesvirus-secreted activator of Vbeta4+ CD8+ T cells regulates chronic infection and immunopathology. *J Exp Med* **205**(3)**,** 669-84.

Favoreel, H. W., Van de Walle, G. R., Nauwynck, H. J., and Pensaert, M. B. (2003). Virus complement evasion strategies. *Journal of general virology* **84**(1)**,** 1-15.

Fazilleau, N., Mark, L., McHeyzer-Williams, L. J., and McHeyzer-Williams, M. G. (2009). Follicular helper T cells: lineage and location. *Immunity* **30**(3)**,** 324-35.

Feederle, R., Kost, M., Baumann, M., Janz, A., Drouet, E., Hammerschmidt, W., and Delecluse, H. J. (2000). The Epstein-Barr virus lytic program is controlled by the co-operative functions of two transactivators. *EMBO J* **19**(12)**,** 3080-9.

Flano, E., Husain, S. M., Sample, J. T., Woodland, D. L., and Blackman, M. A. (2000). Latent murine

gamma-herpesvirus infection is established in activated B cells, dendritic cells, and macrophages. *J Immunol* **165**(2)**,** 1074-81.

Flano, E., Jia, Q., Moore, J., Woodland, D. L., Sun, R., and Blackman, M. A. (2005). Early establishment of gamma-herpesvirus latency: implications for immune control. *J Immunol* **174**(8)**,** 4972-8.

Flano, E., Kim, I. J., Moore, J., Woodland, D. L., and Blackman, M. A. (2003). Differential gamma-herpesvirus distribution in distinct anatomical locations and cell subsets during persistent infection in mice. *J Immunol* **170**(7)**,** 3828-34.

Flano, E., Kim, I. J., Woodland, D. L., and Blackman, M. A. (2002). Gamma-herpesvirus latency is preferentially maintained in splenic germinal center and memory B cells. *J Exp Med* **196**(10)**,** 1363-72.

Fleischer, J., Grage-Griebenow, E., Kasper, B., Heine, H., Ernst, M., Brandt, E., Flad, H. D., and Petersen, F. (2002). Platelet factor 4 inhibits proliferation and cytokine release of activated human T cells. *J Immunol* **169**(2)**,** 770-7.

Flint, S. J., Racaniello, V. R., Enquist, L. W., and Skalka, A. M. (2009). "Principles of Virology." Pattens of Infection, 1. 2 vols. ASM press, Washington, DC, Washington.

Francisco, L. M., Sage, P. T., and Sharpe, A. H. (2010). The PD-1 pathway in tolerance and autoimmunity. *Immunol Rev* **236,** 219-42.

Frappier, L. (2012). Contributions of Epstein‐Barr Nuclear Antigen 1 (EBNA1) to Cell Immortalization and Survival. *Viruses* **4**(9)**,** 1537-1547.

Frederico, B., Milho, R., May, J. S., Gillet, L., and Stevenson, P. G. (2012). Myeloid infection links epithelial and B cell tropisms of murid herpesvirus-4. *PLoS Pathog* **8**(9)**,** e1002935.

Friborg, J., Jr., Kong, W., Hottiger, M. O., and Nabel, G. J. (1999). p53 inhibition by the LANA protein of KSHV protects against cell death. *Nature* **402**(6764)**,** 889-94.

Fries, K. L., Miller, W. E., and Raab-Traub, N. (1996). Epstein-Barr virus latent membrane protein 1 blocks p53-mediated apoptosis through the induction of the A20 gene. *J Virol* **70**(12)**,** 8653-9.

Fukuda, T., Yoshida, T., Okada, S., Hatano, M., Miki, T., Ishibashi, K., Okabe, S., Koseki, H., Hirosawa, S., Taniguchi, M., Miyasaka, N., and Tokuhisa, T. (1997). Disruption of the Bcl6 gene results in an impaired germinal center formation. *J Exp Med* **186**(3)**,** 439-48.

Gaidano, G., Capello, D., Cilia, A. M., Gloghini, A., Perin, T., Quattrone, S., Migliazza, A., Lo Coco, F., Saglio, G., Ascoli, V., and Carbone, A. (1999). Genetic characterization of HHV-8/KSHV-positive primary effusion lymphoma reveals frequent mutations of BCL6: implications for disease pathogenesis and histogenesis. *Genes Chromosomes Cancer* **24**(1)**,** 16-23.

Ganem, D. (2006). KSHV infection and the pathogenesis of Kaposi's sarcoma. *Annu Rev Pathol* **1,** 273-96.

Gangadharan, B., Hoeve, M. A., Allen, J. E., Ebrahimi, B., Rhind, S. M., Dutia, B. M., and Nash, A. A. (2008). Murine gammaherpesvirus-induced fibrosis is associated with the development of alternatively activated macrophages. *Journal of leukocyte biology* **84**(1)**,** 50-58.

Gangappa, S., van Dyk, L. F., Jewett, T. J., Speck, S. H., and Virgin, H. W. (2002). Identification of the In Vivo Role of a Viral bcl-2. *The Journal of Experimental Medicine* **195**(7)**,** 931-940.

Geere, H. M., Ligertwood, Y., Templeton, K. M., Bennet, I., Gangadharan, B., Rhind, S. M., Nash, A. A., and Dutia, B. M. (2006). The M4 gene of murine gammaherpesvirus 68 modulates latent

infection. *J Gen Virol* **87**(Pt 4)**,** 803-7.

Gillet, L., Adler, H., and Stevenson, P. G. (2007). Glycosaminoglycan interactions in murine gammaherpesvirus-68 infection. *PLoS One* **2**(4)**,** e347.

Good-Jacobson, K. L., Szumilas, C. G., Chen, L., Sharpe, A. H., Tomayko, M. M., and Shlomchik, M. J. (2010). PD-1 regulates germinal center B cell survival and the formation and affinity of long-lived plasma cells. *Nat Immunol* **11**(6)**,** 535-542.

Gordon, S. (2003). Alternative activation of macrophages. *Nat Rev Immunol* **3**(1)**,** 23-35.

Graham, K. A., Lalani, A. S., Macen, J. L., Ness, T. L., Barry, M., Liu, L. Y., Lucas, A., Clark-Lewis, I., Moyer, R. W., and Mcfadden, G. (1997). The T1/35kDa family of poxvirus-secreted proteins bind chemokines and modulate leukocyte influx into virus-infected tissues. *Virology* **229**(1)**,** 12-24.

Gramaglia, I., Mauri, D. N., Miner, K. T., Ware, C. F., and Croft, M. (1999). Lymphotoxin alphabeta is expressed on recently activated naive and Th1-like CD4 cells but is down-regulated by IL-4 during Th2 differentiation. *J Immunol* **162**(3)**,** 1333-8.

Granados, R. R., Guoxun, L., Derksen, A. C. G., and McKenna, K. A. (1994). A new insect cell line from< i> Trichoplusia ni</i>(BTI-Tn-5B1-4) susceptible to< i> Trichoplusia ni</i> single enveloped nuclear polyhedrosis virus. *Journal of Invertebrate Pathology* **64**(3)**,** 260-266.

Gredmark-Russ, S., Cheung, E. J., Isaacson, M. K., Ploegh, H. L., and Grotenbreg, G. M. (2008). The CD8 T-cell response against murine gammaherpesvirus 68 is directed toward a broad repertoire of epitopes from both early and late antigens. *J Virol* **82**(24)**,** 12205-12.

Green, M. R., Rodig, S., Juszczynski, P., Ouyang, J., Sinha, P., O'Donnell, E., Neuberg, D., and Shipp, M. A. (2012). Constitutive AP-1 activity and EBV infection induce PD-L1 in Hodgkin lymphomas and posttransplant lymphoproliferative disorders: implications for targeted therapy. *Clin Cancer Res* **18**(6)**,** 1611-8.

Grey, F., Hook, L., and Nelson, J. (2008). The functions of herpesvirus-encoded microRNAs. *Med Microbiol Immunol* **197**(2)**,** 261-7.

Griffin, B. D., Verweij, M. C., and Wiertz, E. J. (2010). Herpesviruses and immunity: the art of evasion. *Vet Microbiol* **143**(1)**,** 89-100.

Gupta, A., Gartner, J. J., Sethupathy, P., Hatzigeorgiou, A. G., and Fraser, N. W. (2006). Anti-apoptotic function of a microRNA encoded by the HSV-1 latency-associated transcript. *Nature* **442**(7098)**,** 82-85.

Halford, W. P., Kemp, C. D., Isler, J. A., Davido, D. J., and Schaffer, P. A. (2001). ICP0, ICP4, or VP16 expressed from adenovirus vectors induces reactivation of latent herpes simplex virus type 1 in primary cultures of latently infected trigeminal ganglion cells. *J Virol* **75**(13)**,** 6143-53.

Hamoudi, R., Diss, T. C., Oksenhendler, E., Pan, L., Carbone, A., Ascoli, V., Boshoff, C., Isaacson, P., and Du, M.-Q. (2004). Distinct cellular origins of primary effusion lymphoma with and without EBV infection. *Leukemia Research* **28**(4)**,** 333-338.

Hanto, D. W. (1995). Classification of Epstein-Barr virus-associated posttransplant lymphoproliferative diseases: implications for understanding their pathogenesis and developing rational treatment strategies. *Annu Rev Med* **46,** 381-94.

Hara, T., Jung, L. K., Bjorndahl, J. M., and Fu, S. M. (1986). Human T cell activation. III. Rapid induction of a phosphorylated 28 kD/32 kD disulfide-linked early activation antigen (EA 1) by 12-o-tetradecanoyl phorbol-13-acetate, mitogens, and antigens. *J Exp Med* **164**(6)**,**

1988-2005.

Hargreaves, D. C., Hyman, P. L., Lu, T. T., Ngo, V. N., Bidgol, A., Suzuki, G., Zou, Y. R., Littman, D. R., and Cyster, J. G. (2001). A coordinated change in chemokine responsiveness guides plasma cell movements. *J Exp Med* **194**(1)**,** 45-56.

Harris, M. B., Chang, C. C., Berton, M. T., Danial, N. N., Zhang, J., Kuehner, D., Bihui, H. Y., Kvatyuk, M., Pandolfi, P. P., and Cattoretti, G. (1999). Transcriptional Repression of Stat6-Dependent Interleukin-4-Induced Genes by BCL-6: Specific Regulation of Iε Transcription and Immunoglobulin E Switching. *Molecular and cellular biology* **19**(10)**,** 7264-7275.

Heise, M. T., and Virgin, H. W. (1995). The T-cell-independent role of gamma interferon and tumor necrosis factor alpha in macrophage activation during murine cytomegalovirus and herpes simplex virus infections. *Journal of virology* **69**(2)**,** 904-9.

Henderson, S., Huen, D., Rowe, M., Dawson, C., Johnson, G., and Rickinson, A. (1993). Epstein-Barr virus-coded BHRF1 protein, a viral homologue of Bcl-2, protects human B cells from programmed cell death. *Proc Natl Acad Sci U S A* **90**(18)**,** 8479-83.

Herbold, W., Maus, R., Hahn, I., Ding, N., Srivastava, M., Christman, J. W., Mack, M., Reutershan, J., Briles, D. E., Paton, J. C., Winter, C., Welte, T., and Maus, U. A. (2010). Importance of CXC chemokine receptor 2 in alveolar neutrophil and exudate macrophage recruitment in response to pneumococcal lung infection. *Infect Immun* **78**(6)**,** 2620-30.

Herold, B. C., Visalli, R. J., Susmarski, N., Brandt, C. R., and Spear, P. G. (1994). Glycoprotein C-independent binding of herpes simplex virus to cells requires cell surface heparan sulphate and glycoprotein B. *J Gen Virol* **75 (Pt 6),** 1211-22.

Hislop, A. D., Taylor, G. S., Sauce, D., and Rickinson, A. B. (2007). Cellular responses to viral infection in humans: lessons from Epstein-Barr virus. *Annu Rev Immunol* **25,** 587-617.

Hitchman, R. B., Possee, R. D., and King, L. A. (2009). Baculovirus expression systems for recombinant protein production in insect cells. *Recent Pat Biotechnol* **3**(1)**,** 46-54.

Homa, F. L., and Brown, J. C. (1997). Capsid assembly and DNA packaging in herpes simplex virus. *Reviews in medical virology* **7**(2)**,** 107-122.

Honess, R. W., and Roizman, B. (1974). Regulation of herpesvirus macromolecular synthesis I. Cascade regulation of the synthesis of three groups of viral proteins. *Journal of virology* **14**(1)**,** 8-19.

Hoogewerf, A. J., Kuschert, G. S., Proudfoot, A. E., Borlat, F., Clark-Lewis, I., Power, C. A., and Wells, T. N. (1997). Glycosaminoglycans mediate cell surface oligomerization of chemokines. *Biochemistry* **36**(44)**,** 13570-8.

Huang, S., Hendriks, W., Althage, A., Hemmi, S., Bluethmann, H., Kamijo, R., Vilcek, J., Zinkernagel, R. M., and Aguet, M. (1993). Immune response in mice that lack the interferon-gamma receptor. *Science* **259**(5102)**,** 1742-1745.

Hughes, D. J., Kipar, A., Leeming, G. H., Bennett, E., Howarth, D., Cummerson, J. A., Papoula-Pereira, R., Flanagan, B. F., Sample, J. T., and Stewart, J. P. (2011). Chemokine binding protein M3 of murine gammaherpesvirus 68 modulates the host response to infection in a natural host. *PLoS Pathog* **7**(3)**,** e1001321.

Husain, S. M., Usherwood, E. J., Dyson, H., Coleclough, C., Coppola, M. A., Woodland, D. L., Blackman, M. A., Stewart, J. P., and Sample, J. T. (1999). Murine gammaherpesvirus M2 gene is latency-associated and its protein a target for CD8+ T lymphocytes. *Proceedings of the*

National Academy of Sciences **96**(13)**,** 7508.

Hutt-Fletcher, L. M. (2007). Epstein-Barr Virus Entry. *Journal of virology* **81**(15)**,** 7825-7832.

Hwang, S., Kim, K. S., Flano, E., Wu, T.-T., Tong, L. M., Park, A. N., Song, M. J., Sanchez, D. J., O'Connell, R. M., Cheng, G., and Sun, R. (2009). Conserved Herpesviral Kinase Promotes Viral Persistence by Inhibiting the IRF-3-Mediated Type I Interferon Response. *Cell Host & Microbe* **5**(2)**,** 166-178.

Jenner, R. G., Maillard, K., Cattini, N., Weiss, R. A., Boshoff, C., Wooster, R., and Kellam, P. (2003). Kaposi's sarcoma-associated herpesvirus-infected primary effusion lymphoma has a plasma cell gene expression profile. *Proc Natl Acad Sci U S A* **100**(18)**,** 10399-404.

Jensen, K. K., Chen, S. C., Hipkin, R. W., Wiekowski, M. T., Schwarz, M. A., Chou, C. C., Simas, J. P., Alcami, A., and Lira, S. A. (2003). Disruption of CCL21-induced chemotaxis in vitro and in vivo by M3, a chemokine-binding protein encoded by murine gammaherpesvirus 68. *Journal of virology* **77**(1)**,** 624-630.

Jin, Q., Altenburg, J. D., Hossain, M. M., and Alkhatib, G. (2011). Role for the conserved N-terminal cysteines in the anti-chemokine activities by the chemokine-like protein MC148R1 encoded by Molluscum contagiosum virus. *Virology* **417**(2)**,** 449-456.

Junt, T., Tumanov, A. V., Harris, N., Heikenwalder, M., Zeller, N., Kuprash, D. V., Aguzzi, A., Ludewig, B., Nedospasov, S. A., and Zinkernagel, R. M. (2006). Expression of lymphotoxin beta governs immunity at two distinct levels. *Eur J Immunol* **36**(8)**,** 2061-75.

Kanzler, H., Kuppers, R., Hansmann, M. L., and Rajewsky, K. (1996). Hodgkin and Reed-Sternberg cells in Hodgkin's disease represent the outgrowth of a dominant tumor clone derived from (crippled) germinal center B cells. *J Exp Med* **184**(4)**,** 1495-505.

Kapadia, S. B., Molina, H., van Berkel, V., Speck, S. H., and Virgin, H. W. t. (1999). Murine gammaherpesvirus 68 encodes a functional regulator of complement activation. *J Virol* **73**(9)**,** 7658-70.

Keane, M. P. (2008). The role of chemokines and cytokines in lung fibrosis. *European Respiratory Review* **17**(109)**,** 151-156.

Keir, M. E., Francisco, L. M., and Sharpe, A. H. (2007). PD-1 and its ligands in T-cell immunity. *Curr Opin Immunol* **19**(3)**,** 309-14.

Kieff, E. (1996). "Epstein-Barr virus and its replication." B.N. Fields, D.M. Knipe, and P.M. Howley (F. Virology, Ed.) Lippincott-Raven

Philadelphia.

King, C., Tangye, S. G., and Mackay, C. R. (2008). T follicular helper (TFH) cells in normal and dysregulated immune responses. *Annu Rev Immunol* **26,** 741-66.

Kledal, T. N., Rosenkilde, M. M., Coulin, F., Simmons, G., Johnsen, A. H., Alouani, S., Power, C. A., Luttichau, H. R., Gerstoft, J., Clapham, P. R., Clark-Lewis, I., Wells, T. N., and Schwartz, T. W. (1997). A broad-spectrum chemokine antagonist encoded by Kaposi's sarcoma-associated herpesvirus. *Science* **277**(5332)**,** 1656-9.

Klein, U., Casola, S., Cattoretti, G., Shen, Q., Lia, M., Mo, T., Ludwig, T., Rajewsky, K., and Dalla-Favera, R. (2006). Transcription factor IRF4 controls plasma cell differentiation and class-switch recombination. *Nat Immunol* **7**(7)**,** 773-82.

Knowles, D. M., Inghirami, G., Ubriaco, A., and Dalla-Favera, R. (1989). Molecular genetic analysis of three AIDS-associated neoplasms of uncertain lineage demonstrates their B-cell derivation

and the possible pathogenetic role of the Epstein-Barr virus. *Blood* **73**(3)**,** 792-9.

Kocks, J. R., Adler, H., Danzer, H., Hoffmann, K., Jonigk, D., Lehmann, U., and Forster, R. (2009). Chemokine receptor CCR7 contributes to a rapid and efficient clearance of lytic murine gamma-herpes virus 68 from the lung, whereas bronchus-associated lymphoid tissue harbors virus during latency. *J Immunol* **182**(11)**,** 6861-9.

Kohlmeier, J. E., Miller, S. C., Smith, J., Lu, B., Gerard, C., Cookenham, T., Roberts, A. D., and Woodland, D. L. (2008). The Chemokine Receptor CCR5 Plays a Key Role in the Early Memory CD8+ T Cell Response to Respiratory Virus Infections. *Immunity* **29**(1)**,** 101-113.

Komano, J., Maruo, S., Kurozumi, K., Oda, T., and Takada, K. (1999). Oncogenic role of Epstein-Barr virus-encoded RNAs in Burkitt's lymphoma cell line Akata. *J Virol* **73**(12)**,** 9827-31.

Krug, L. T., Evans, A. G., Gargano, L. M., Paden, C. R., and Speck, S. H. (2013). The absence of M1 leads to higher establishment of murine gammaherpesvirus 68 latency in IgD negative B cells. *Journal of virology*.

Krug, L. T., Moser, J. M., Dickerson, S. M., and Speck, S. H. (2007). Inhibition of NF-κB Activation In Vivo Impairs Establishment of Gammaherpesvirus Latency. *PLoS Pathog* **3**(1)**,** e11.

Kurts, C., Wagner, H., Franken, L., Semmling, V., and Thaiss, C. A. (2011). Chemokines: A New Dendritic Cell Signal for T Cell Activation. *Frontiers in Immunology* **2**.

Kusam, S., Toney, L. M., Sato, H., and Dent, A. L. (2003). Inhibition of Th2 Differentiation and GATA-3 Expression by BCL-6. *The Journal of Immunology* **170**(5)**,** 2435-2441.

Laherty, C. D., Hu, H. M., Opipari, A. W., Wang, F., and Dixit, V. M. (1992). The Epstein-Barr virus LMP1 gene product induces A20 zinc finger protein expression by activating nuclear factor kappa B. *J Biol Chem* **267**(34)**,** 24157-60.

Lalani, A. S., Barrett, J. W., and McFadden, G. (2000). Modulating chemokines: more lessons from viruses. *Immunology Today* **21**(2)**,** 100-106.

Lalani, A. S., Graham, K., Mossman, K., Rajarathnam, K., Clark-Lewis, I., Kelvin, D., and McFadden, G. (1997). The purified myxoma virus gamma interferon receptor homolog M-T7 interacts with the heparin-binding domains of chemokines. *Journal of virology* **71**(6)**,** 4356-4363.

Landais, E., Saulquin, X., Scotet, E., Trautmann, L., Peyrat, M.-A., Yates, J. L., Kwok, W. W., Bonneville, M., and Houssaint, E. (2004). Direct killing of Epstein-Barr virus (EBV)–infected B cells by CD4 T cells directed against the EBV lytic protein BHRF1. *Blood* **103**(4)**,** 1408-1416.

Lanier, L. L., Buck, D. W., Rhodes, L., Ding, A., Evans, E., Barney, C., and Phillips, J. H. (1988). Interleukin 2 activation of natural killer cells rapidly induces the expression and phosphorylation of the Leu-23 activation antigen. *J Exp Med* **167**(5)**,** 1572-85.

Latchman, Y., Wood, C. R., Chernova, T., Chaudhary, D., Borde, M., Chernova, I., Iwai, Y., Long, A. J., Brown, J. A., Nunes, R., Greenfield, E. A., Bourque, K., Boussiotis, V. A., Carter, L. L., Carreno, B. M., Malenkovich, N., Nishimura, H., Okazaki, T., Honjo, T., Sharpe, A. H., and Freeman, G. J. (2001). PD-L2 is a second ligand for PD-1 and inhibits T cell activation. *Nat Immunol* **2**(3)**,** 261-8.

Lau, E. K., Paavola, C. D., Johnson, Z., Gaudry, J. P., Geretti, E., Borlat, F., Kungl, A. J., Proudfoot, A. E., and Handel, T. M. (2004). Identification of the glycosaminoglycan binding site of the CC chemokine, MCP-1: implications for structure and function in vivo. *J Biol Chem* **279**(21)**,** 22294-305.

Leang, R. S., Wu, T.-T., Hwang, S., Liang, L. T., Tong, L., Truong, J. T., and Sun, R. (2011). The

Anti-interferon Activity of Conserved Viral dUTPase ORF54 is Essential for an Effective MHV-68 Infection. *PLoS Pathog* **7**(10)**,** e1002292.

Lee, B. J., Koszinowski, U. H., Sarawar, S. R., and Adler, H. (2003). A gammaherpesvirus G protein-coupled receptor homologue is required for increased viral replication in response to chemokines and efficient reactivation from latency. *J Immunol* **170**(1)**,** 243-51.

Lee, B. J., Santee, S., Von Gesjen, S., Ware, C. F., and Sarawar, S. R. (2000). Lymphotoxin-α-deficient mice can clear a productive infection with murine gammaherpesvirus 68 but fail to develop splenomegaly or lymphocytosis. *Journal of virology* **74**(6)**,** 2786-2792.

Lee, K. S., Groshong, S. D., Cool, C. D., Kleinschmidt-DeMasters, B. K., and van Dyk, L. F. (2009). Murine gammaherpesvirus 68 infection of IFNγ unresponsive mice: a small animal model for gammaherpesvirus-associated B-cell lymphoproliferative disease. *Cancer research* **69**(13)**,** 5481.

Liang, X., Collins, C. M., Mendel, J. B., Iwakoshi, N. N., and Speck, S. H. (2009). Gammaherpesvirus-driven plasma cell differentiation regulates virus reactivation from latently infected B lymphocytes. *PLoS Pathog* **5**(11)**,** e1000677.

Liang, X., Pickering, M. T., Cho, N. H., Chang, H., Volkert, M. R., Kowalik, T. F., and Jung, J. U. (2006). Deregulation of DNA damage signal transduction by herpesvirus latency-associated M2. *J Virol* **80**(12)**,** 5862-74.

Liang, X., Shin, Y. C., Means, R. E., and Jung, J. U. (2004). Inhibition of interferon-mediated antiviral activity by murine gammaherpesvirus 68 latency-associated M2 protein. *J Virol* **78**(22)**,** 12416-27.

Lin, M., Carlson, E., Diaconu, E., and Pearlman, E. (2007). CXCL1/KC and CXCL5/LIX are selectively produced by corneal fibroblasts and mediate neutrophil infiltration to the corneal stroma in LPS keratitis. *J Leukoc Biol* **81**(3)**,** 786-92.

Linterman, M. A., Beaton, L., Yu, D., Ramiscal, R. R., Srivastava, M., Hogan, J. J., Verma, N. K., Smyth, M. J., Rigby, R. J., and Vinuesa, C. G. (2010). IL-21 acts directly on B cells to regulate Bcl-6 expression and germinal center responses. *J Exp Med* **207**(2)**,** 353-63.

Lisco, A., Grivel, J.-C., Biancotto, A., Vanpouille, C., Origgi, F., Malnati, M. S., Schols, D., Lusso, P., and Margolis, L. B. (2007). Viral Interactions in Human Lymphoid Tissue: Human Herpesvirus 7 Suppresses the Replication of CCR5-Tropic Human Immunodeficiency Virus Type 1 via CD4 Modulation. *Journal of virology* **81**(2)**,** 708-717.

Luther, S. A., Bidgol, A., Hargreaves, D. C., Schmidt, A., Xu, Y., Paniyadi, J., Matloubian, M., and Cyster, J. G. (2002). Differing Activities of Homeostatic Chemokines CCL19, CCL21, and CXCL12 in Lymphocyte and Dendritic Cell Recruitment and Lymphoid Neogenesis. *The Journal of Immunology* **169**(1)**,** 424-433.

Luther, S. A., and Cyster, J. G. (2001). Chemokines as regulators of T cell differentiation. *Nat Immunol* **2**(2)**,** 102-7.

Luttichau, H. R., Lewis, I. C., Gerstoft, J., and Schwartz, T. W. (2001). The herpesvirus 8-encoded chemokine vMIP-II, but not the poxvirus-encoded chemokine MC148, inhibits the CCR10 receptor. *Eur J Immunol* **31**(4)**,** 1217-20.

Luzuriaga, K., and Sullivan, J. L. (2010). Infectious Mononucleosis. *New England Journal of Medicine* **362**(21)**,** 1993-2000.

Maciaszek, J. W., Parada, N. A., Cruikshank, W. W., Center, D. M., Kornfeld, H., and Viglianti, G. A.

(1997). IL-16 represses HIV-1 promoter activity. *The Journal of Immunology* **158**(1)**,** 5-8.

Mackay, F., Majeau, G. R., Lawton, P., Hochman, P. S., and Browning, J. L. (1997). Lymphotoxin but not tumor necrosis factor functions to maintain splenic architecture and humoral responsiveness in adult mice. *European journal of immunology* **27**(8)**,** 2033-2042.

Macrae, A. I., Dutia, B. M., Milligan, S., Brownstein, D. G., Allen, D. J., Mistrikova, J., Davison, A. J., Nash, A. A., and Stewart, J. P. (2001). Analysis of a novel strain of murine gammaherpesvirus reveals a genomic locus important for acute pathogenesis. *J Virol* **75**(11)**,** 5315-27.

Macrae, A. I., Usherwood, E. J., Husain, S. M., Flaño, E., Kim, I. J., Woodland, D. L., Nash, A. A., Blackman, M. A., Sample, J. T., and Stewart, J. P. (2003). Murid herpesvirus 4 strain 68 M2 protein is a B-cell-associated antigen important for latency but not lymphocytosis. *Journal of virology* **77**(17)**,** 9700-9709.

Magel, G. D., Ed. (2012). Herpesviridae - A Look Into This Unique Family of Viruses. Contributions of the EBNA1 Protein of Epstein-Barr Virus Toward B-Cell Immortalization and Lymphomagenesis,. Edited by A. T. W. a. A. Aiyar.

Marques, S., Efstathiou, S., Smith, K. G., Haury, M., and Simas, J. P. (2003). Selective gene expression of latent murine gammaherpesvirus 68 in B lymphocytes. *J Virol* **77**(13)**,** 7308-18.

Martin, A. P., Alexander-Brett, J. M., Canasto-Chibuque, C., Garin, A., Bromberg, J. S., Fremont, D. H., and Lira, S. A. (2007). The Chemokine Binding Protein M3 Prevents Diabetes Induced by Multiple Low Doses of Streptozotocin. *The Journal of Immunology* **178**(7)**,** 4623-4631.

Martin, A. P., Canasto-Chibuque, C., Shang, L., Rollins, B. J., and Lira, S. A. (2006). The chemokine decoy receptor M3 blocks CC chemokine ligand 2 and CXC chemokine ligand 13 function in vivo. *The Journal of Immunology* **177**(10)**,** 7296.

Mayo, K. H., Ilyina, E., Roongta, V., Dundas, M., Joseph, J., Lai, C. K., Maione, T., and Daly, T. J. (1995). Heparin binding to platelet factor-4. An NMR and site-directed mutagenesis study: arginine residues are crucial for binding. *Biochem J* **312 (Pt 2),** 357-65.

MC WEBB, L., Smith, V. P., and Alcami, A. (2004). The gammaherpesvirus chemokine binding protein can inhibit the interaction of chemokines with glycosaminoglycans. *The FASEB journal* **18**(3)**,** 571-573.

Mettenleiter, T. C. (2002). Herpesvirus assembly and egress. *Journal of virology* **76**(4)**,** 1537-1547.

Middleton, J., Patterson, A. M., Gardner, L., Schmutz, C., and Ashton, B. A. (2002). Leukocyte extravasation: chemokine transport and presentation by the endothelium. *Blood* **100**(12)**,** 3853-3860.

Millward, J. M., Holst, P. J., Hogh-Petersen, M., Thomsen, A. R., Christensen, J. P., and Owens, T. (2010). The murine gammaherpesvirus-68 chemokine-binding protein M3 inhibits experimental autoimmune encephalomyelitis. *J Neuroimmunol* **224**(1-2)**,** 45-50.

Mistríková, J., and Rajčáni, J. (2008). Comparison of pathogenic properties of the murid gammaherpesvirus (MuHV 4) strains: a role for immunomodulatory proteins encoded by the left (5′-)end of the genome. *Central European Journal of Biology* **3**(1)**,** 19-30.

Molloy, M. J., Zhang, W., and Usherwood, E. J. (2009). Cutting edge: IL-2 immune complexes as a therapy for persistent virus infection. *J Immunol* **182**(8)**,** 4512-5.

Molloy, M. J., Zhang, W., and Usherwood, E. J. (2011). Suppressive CD8+ T cells arise in the absence of CD4 help and compromise control of persistent virus. *J Immunol* **186**(11)**,** 6218-26.

Moorman, N. J., Virgin, H. W. t., and Speck, S. H. (2003). Disruption of the gene encoding the

gammaHV68 v-GPCR leads to decreased efficiency of reactivation from latency. *Virology* **307**(2)**,** 179-90.

Mora, A. L., Torres-Gonzalez, E., Rojas, M., Corredor, C., Ritzenthaler, J., Xu, J., Roman, J., Brigham, K., and Stecenko, A. (2006). Activation of alveolar macrophages via the alternative pathway in herpesvirus-induced lung fibrosis. *Am J Respir Cell Mol Biol* **35**(4)**,** 466-73.

Moser, B., and Ebert, L. (2003). Lymphocyte traffic control by chemokines: follicular B helper T cells. *Immunology Letters* **85**(2)**,** 105-112.

Moser, B., Wolf, M., Walz, A., and Loetscher, P. (2004). Chemokines: multiple levels of leukocyte migration control. *Trends Immunol* **25**(2)**,** 75-84.

Moser, J. M., Upton, J. W., Allen, R. D., 3rd, Wilson, C. B., and Speck, S. H. (2005). Role of B-cell proliferation in the establishment of gammaherpesvirus latency. *J Virol* **79**(15)**,** 9480-91.

Mount, A. M., Masson, F., Kupresanin, F., Smith, C. M., May, J. S., van Rooijen, N., Stevenson, P. G., and Belz, G. T. (2010). Interference with dendritic cell populations limits early antigen presentation in chronic gamma-herpesvirus-68 infection. *J Immunol* **185**(6)**,** 3669-76.

Mueller, A., Meiser, A., McDonagh, E. M., Fox, J. M., Petit, S. J., Xanthou, G., Williams, T. J., and Pease, J. E. (2008). CXCL4-induced migration of activated T lymphocytes is mediated by the chemokine receptor CXCR3. *Journal of leukocyte biology* **83**(4)**,** 875-882.

Murphy, P. M. (2001). Viral exploitation and subversion of the immune system through chemokine mimicry. *Nat Immunol* **2**(2)**,** 116-22.

Muto, A., Tashiro, S., Nakajima, O., Hoshino, H., Takahashi, S., Sakoda, E., Ikebe, D., Yamamoto, M., and Igarashi, K. (2004). The transcriptional programme of antibody class switching involves the repressor Bach2. *Nature* **429**(6991)**,** 566-71.

Nakayama, T., Fujisawa, R., Izawa, D., Hieshima, K., Takada, K., and Yoshie, O. (2002). Human B cells immortalized with Epstein-Barr virus upregulate CCR6 and CCR10 and downregulate CXCR4 and CXCR5. *J Virol* **76**(6)**,** 3072-7.

Nash, A. A., Dutia, B. M., Stewart, J. P., and Davison, A. J. (2001). Natural history of murine gamma-herpesvirus infection. *Philos Trans R Soc Lond B Biol Sci* **356**(1408)**,** 569-79.

Ness, T. L., Ewing, J. L., Hogaboam, C. M., and Kunkel, S. L. (2006). CCR4 is a key modulator of innate immune responses. *J Immunol* **177**(11)**,** 7531-9.

Ngo, V. N., Korner, H., Gunn, M. D., Schmidt, K. N., Sean Riminton, D., Cooper, M. D., Browning, J. L., Sedgwick, J. D., and Cyster, J. G. (1999). Lymphotoxin α/β and Tumor Necrosis Factor Are Required for Stromal Cell Expression of Homing Chemokines in B and T Cell Areas of the Spleen. *The Journal of Experimental Medicine* **189**(2)**,** 403-412.

Nicholas, J., Cameron, K. R., and Honess, R. W. (1992). Herpesvirus saimiri encodes homologues of G protein-coupled receptors and cyclins. *Nature* **355**(6358)**,** 362-5.

Nicola, A. V., McEvoy, A. M., and Straus, S. E. (2003). Roles for endocytosis and low pH in herpes simplex virus entry into HeLa and Chinese hamster ovary cells. *J Virol* **77**(9)**,** 5324-32.

Nomiyama, H., Hieshima, K., Osada, N., Kato-Unoki, Y., Otsuka-Ono, K., Takegawa, S., Izawa, T., Yoshizawa, A., Kikuchi, Y., and Tanase, S. (2008). Extensive expansion and diversification of the chemokine gene family in zebrafish: identification of a novel chemokine subfamily CX. *BMC genomics* **9**(1)**,** 222.

Nurieva, R. I., Chung, Y., Martinez, G. J., Yang, X. O., Tanaka, S., Matskevitch, T. D., Wang, Y. H., and Dong, C. (2009). Bcl6 mediates the development of T follicular helper cells. *Science*

325(5943)**,** 1001-5.

Nutt, S. L., and Tarlinton, D. M. (2011). Germinal center B and follicular helper T cells: siblings, cousins or just good friends? *Nat Immunol* **12**(6)**,** 472-7.

Oda, W., Mistrikova, J., Stancekova, M., Dutia, B. M., Nash, A. A., Takahata, H., Jin, Z., Oka, T., and Hayashi, K. (2005). Analysis of genomic homology of murine gammaherpesvirus (MHV)-72 to MHV-68 and impact of MHV-72 on the survival and tumorigenesis in the MHV-72-infected CB17 scid/scid and CB17+/+ mice. *Pathology International* **55**(9)**,** 558-568.

Ohl, L., Henning, G., Krautwald, S., Lipp, M., Hardtke, S., Bernhardt, G., Pabst, O., and Förster, R. (2003). Cooperating Mechanisms of CXCR5 and CCR7 in Development and Organization of Secondary Lymphoid Organs. *The Journal of Experimental Medicine* **197**(9)**,** 1199-1204.

Okada, T., Ngo, V. N., Ekland, E. H., Forster, R., Lipp, M., Littman, D. R., and Cyster, J. G. (2002). Chemokine requirements for B cell entry to lymph nodes and Peyer's patches. *J Exp Med* **196**(1)**,** 65-75.

Oliver, A. M., Martin, F., and Kearney, J. F. (1997). Mouse CD38 is down-regulated on germinal center B cells and mature plasma cells. *J Immunol* **158**(3)**,** 1108-15.

Orange, J. S., Wang, B., Terhorst, C., and Biron, C. A. (1995). Requirement for natural killer cell-produced interferon gamma in defense against murine cytomegalovirus infection and enhancement of this defense pathway by interleukin 12 administration. *J Exp Med* **182**(4)**,** 1045-56.

Parravinci, C., Corbellino, M., Paulli, M., Magrini, U., Lazzarino, M., Moore, P. S., and Chang, Y. (1997). Expression of a virus-derived cytokine, KSHV vIL-6, in HIV-seronegative Castleman's disease. *The American journal of pathology* **151**(6)**,** 1517.

Parry, C. M., Simas, J. P., Smith, V. P., Stewart, C. A., Minson, A. C., Efstathiou, S., and Alcami, A. (2000). A broad spectrum secreted chemokine binding protein encoded by a herpesvirus. *J Exp Med* **191**(3)**,** 573-8.

Penkert, R. R., and Kalejta, R. F. (2011). Tegument protein control of latent herpesvirus establishment and animation. *Herpesviridae* **2**(1)**,** 3.

Perng, G. C., Dunkel, E. C., Geary, P. A., Slanina, S. M., Ghiasi, H., Kaiwar, R., Nesburn, A. B., and Wechsler, S. L. (1994). The latency-associated transcript gene of herpes simplex virus type 1 (HSV-1) is required for efficient in vivo spontaneous reactivation of HSV-1 from latency. *J Virol* **68**(12)**,** 8045-55.

Pfeffer, S., Sewer, A., Lagos-Quintana, M., Sheridan, R., Sander, C., Grasser, F. A., van Dyk, L. F., Ho, C. K., Shuman, S., Chien, M., Russo, J. J., Ju, J., Randall, G., Lindenbach, B. D., Rice, C. M., Simon, V., Ho, D. D., Zavolan, M., and Tuschl, T. (2005). Identification of microRNAs of the herpesvirus family. *Nat Methods* **2**(4)**,** 269-76.

Phillips, R. J., Burdick, M. D., Hong, K., Lutz, M. A., Murray, L. A., Xue, Y. Y., Belperio, J. A., Keane, M. P., and Strieter, R. M. (2004). Circulating fibrocytes traffic to the lungs in response to CXCL12 and mediate fibrosis. *J Clin Invest* **114**(3)**,** 438-46.

Pires de Miranda, M., Alenquer, M., Marques, S., Rodrigues, L., Lopes, F., Bustelo, X. R., and Simas, J. P. (2008). The Gammaherpesvirus m2 protein manipulates the Fyn/Vav pathway through a multidocking mechanism of assembly. *PLoS One* **3**(2)**,** e1654.

Proudfoot, A. E., Handel, T. M., Johnson, Z., Lau, E. K., LiWang, P., Clark-Lewis, I., Borlat, F., Wells, T. N., and Kosco-Vilbois, M. H. (2003). Glycosaminoglycan binding and oligomerization are

essential for the in vivo activity of certain chemokines. *Proc Natl Acad Sci U S A* **100**(4)**,** 1885-90.

Pyo, R., Jensen, K. K., Wiekowski, M. T., Manfra, D., Alcami, A., Taubman, M. B., and Lira, S. A. (2004). Inhibition of intimal hyperplasia in transgenic mice conditionally expressing the chemokine-binding protein M3. *Am J Pathol* **164**(6)**,** 2289-97.

Raab-Traub, N. (2002). Epstein-Barr virus in the pathogenesis of NPC. *Semin Cancer Biol* **12**(6)**,** 431-41.

Raman, D., Baugher, P. J., Thu, Y. M., and Richmond, A. (2007). Role of chemokines in tumor growth. *Cancer letters* **256**(2)**,** 137-165.

Raslova, H., Berebbi, M., Rajcani, J., Sarasin, A., Matis, J., and Kudelova, M. (2001). Susceptibility of mouse mammary glands to murine gammaherpesvirus 72 (MHV-72) infection: evidence of MHV-72 transmission via breast milk. *Microb Pathog* **31**(2)**,** 47-58.

Rastelli, J., Homig-Holzel, C., Seagal, J., Muller, W., Hermann, A. C., Rajewsky, K., and Zimber-Strobl, U. (2008). LMP1 signaling can replace CD40 signaling in B cells in vivo and has unique features of inducing class-switch recombination to IgG1. *Blood* **111**(3)**,** 1448-55.

Rickinson, A. (2001). Concluding overview: looking back, looking forward. *Philos Trans R Soc Lond B Biol Sci* **356**(1408)**,** 595-604.

Rickinson, A. B., Callan, M. F., and Annels, N. E. (2000). T-cell memory: lessons from Epstein-Barr virus infection in man. *Philos Trans R Soc Lond B Biol Sci* **355**(1395)**,** 391-400.

Rickinson, A. B., Lee, S. P., and Steven, N. M. (1996). Cytotoxic T lymphocyte responses to Epstein-Barr virus. *Curr Opin Immunol* **8**(4)**,** 492-7.

Rivas, C., Thlick, A. E., Parravicini, C., Moore, P. S., and Chang, Y. (2001). Kaposi's sarcoma-associated herpesvirus LANA2 is a B-cell-specific latent viral protein that inhibits p53. *Journal of virology* **75**(1)**,** 429-438.

Roach, D. R., Briscoe, H., Saunders, B., France, M. P., Riminton, S., and Britton, W. J. (2001). Secreted lymphotoxin-alpha is essential for the control of an intracellular bacterial infection. *J Exp Med* **193**(2)**,** 239-46.

Rodrigues, L., Pires de Miranda, M., Caloca, M. J., Bustelo, X. R., and Simas, J. P. (2006). Activation of Vav by the gammaherpesvirus M2 protein contributes to the establishment of viral latency in B lymphocytes. *J Virol* **80**(12)**,** 6123-35.

Romagnani, P., Maggi, L., Mazzinghi, B., Cosmi, L., Lasagni, L., Liotta, F., Lazzeri, E., Angeli, R., Rotondi, M., Fili, L., Parronchi, P., Serio, M., Maggi, E., Romagnani, S., and Annunziato, F. (2005). CXCR3-mediated opposite effects of CXCL10 and CXCL4 on TH1 or TH2 cytokine production. *J Allergy Clin Immunol* **116**(6)**,** 1372-9.

Rosa, G. T., Gillet, L., Smith, C. M., de Lima, B. D., and Stevenson, P. G. (2007). IgG Fc Receptors Provide an Alternative Infection Route for Murine Gamma-Herpesvirus-68. *PLoS One* **2**(6)**,** e560.

Roughan, J. E., and Thorley-Lawson, D. A. (2009). The intersection of Epstein-Barr virus with the germinal center. *J Virol* **83**(8)**,** 3968-76.

Roughan, J. E., Torgbor, C., and Thorley-Lawson, D. A. (2010). Germinal Center B Cells Latently Infected with Epstein-Barr Virus Proliferate Extensively but Do Not Increase in Number. *Journal of virology* **84**(2)**,** 1158-1168.

Rowe, M., Kelly, G. L., Bell, A. I., and Rickinson, A. B. (2009). Burkitt's lymphoma: the Rosetta Stone

deciphering Epstein-Barr virus biology. *Semin Cancer Biol* **19**(6)**,** 377-88.

Sadagopan, S., Sharma-Walia, N., Veettil, M. V., Bottero, V., Levine, R., Vart, R. J., and Chandran, B. (2009). Kaposi's sarcoma-associated herpesvirus upregulates angiogenin during infection of human dermal microvascular endothelial cells, which induces 45S rRNA synthesis, antiapoptosis, cell proliferation, migration, and angiogenesis. *J Virol* **83**(7)**,** 3342-64.

Sancho, D., Gómez, M., and Sánchez-Madrid, F. (2005). CD69 is an immunoregulatory molecule induced following activation. *Trends in Immunology* **26**(3)**,** 136-140.

Sandoval-Montes, C., and Santos-Argumedo, L. (2005). CD38 is expressed selectively during the activation of a subset of mature T cells with reduced proliferation but improved potential to produce cytokines. *Journal of leukocyte biology* **77**(4)**,** 513-521.

Sarawar, S. R., Cardin, R. D., Brooks, J. W., Mehrpooya, M., Hamilton-Easton, A. M., Mo, X. Y., and Doherty, P. C. (1997). Gamma interferon is not essential for recovery from acute infection with murine gammaherpesvirus 68. *Journal of virology* **71**(5)**,** 3916-3921.

Sarawar, S. R., Cardin, R. D., Brooks, J. W., Mehrpooya, M., Tripp, R. A., and Doherty, P. C. (1996). Cytokine production in the immune response to murine gammaherpesvirus 68. *J Virol* **70**(5)**,** 3264-8.

Sarawar, S. R., Lee, B. J., Anderson, M., Teng, Y. C., Zuberi, R., and Von Gesjen, S. (2002). Chemokine induction and leukocyte trafficking to the lungs during murine gammaherpesvirus 68 (MHV-68) infection. *Virology* **293**(1)**,** 54-62.

Sarid, R., Wiezorek, J. S., Moore, P. S., and Chang, Y. (1999). Characterization and cell cycle regulation of the major Kaposi's sarcoma-associated herpesvirus (human herpesvirus 8) latent genes and their promoter. *J Virol* **73**(2)**,** 1438-46.

Sasmono, R. T., Ehrnsperger, A., Cronau, S. L., Ravasi, T., Kandane, R., Hickey, M. J., Cook, A. D., Himes, S. R., Hamilton, J. A., and Hume, D. A. (2007). Mouse neutrophilic granulocytes express mRNA encoding the macrophage colony-stimulating factor receptor (CSF-1R) as well as many other macrophage-specific transcripts and can transdifferentiate into macrophages in vitro in response to CSF-1. *Journal of leukocyte biology* **82**(1)**,** 111-123.

Sasmono, R. T., Oceandy, D., Pollard, J. W., Tong, W., Pavli, P., Wainwright, B. J., Ostrowski, M. C., Himes, S. R., and Hume, D. A. (2003). A macrophage colony-stimulating factor receptor–green fluorescent protein transgene is expressed throughout the mononuclear phagocyte system of the mouse. *Blood* **101**(3)**,** 1155-1163.

Scheuerer, B., Ernst, M., Durrbaum-Landmann, I., Fleischer, J., Grage-Griebenow, E., Brandt, E., Flad, H. D., and Petersen, F. (2000). The CXC-chemokine platelet factor 4 promotes monocyte survival and induces monocyte differentiation into macrophages. *Blood* **95**(4)**,** 1158-66.

Schuster, V., and Kreth, H. W. (1992). Epstein-Barr virus infection and associated diseases in children. I. Pathogenesis, epidemiology and clinical aspects. *Eur J Pediatr* **151**(10)**,** 718-25.

Schwickert, T. A., Alabyev, B., Manser, T., and Nussenzweig, M. C. (2009). Germinal center reutilization by newly activated B cells. *The Journal of Experimental Medicine* **206**(13)**,** 2907-2914.

Sciacca, F. L., Sturzl, M., Bussolino, F., Sironi, M., Brandstetter, H., Zietz, C., Zhou, D., Matteucci, C., Peri, G., Sozzani, S., and et al. (1994). Expression of adhesion molecules, platelet-activating factor, and chemokines by Kaposi's sarcoma cells. *J Immunol* **153**(10)**,** 4816-25.

Sciammas, R., Shaffer, A., Schatz, J. H., Zhao, H., Staudt, L. M., and Singh, H. (2006). Graded

expression of interferon regulatory factor-4 coordinates isotype switching with plasma cell differentiation. *Immunity* **25**(2)**,** 225-236.

Seet, B. T., and McFadden, G. (2002). Viral chemokine-binding proteins. *Journal of leukocyte biology* **72**(1)**,** 24-34.

Shaffer, A. L., Lin, K.-I., Kuo, T. C., Yu, X., Hurt, E. M., Rosenwald, A., Giltnane, J. M., Yang, L., Zhao, H., Calame, K., and Staudt, L. M. (2002). Blimp-1 Orchestrates Plasma Cell Differentiation by Extinguishing the Mature B Cell Gene Expression Program. *Immunity* **17**(1)**,** 51-62.

Shang, L., Thirunarayanan, N., Viejo-Borbolla, A., Martin, A. P., Bogunovic, M., Marchesi, F., Unkeless, J. C., Ho, Y., Furtado, G. C., Alcami, A., Merad, M., Mayer, L., and Lira, S. A. (2009). Expression of the chemokine binding protein M3 promotes marked changes in the accumulation of specific leukocytes subsets within the intestine. *Gastroenterology* **137**(3)**,** 1006-18, 1018 e1-3.

Shannon-Lowe, C., and Rowe, M. (2011). Epstein-Barr Virus Infection of Polarized Epithelial Cells via the Basolateral Surface by Memory B Cell-Mediated Transfer Infection. *PLoS Pathog* **7**(5)**,** e1001338.

Shannon-Lowe, C. D., Neuhierl, B., Baldwin, G., Rickinson, A. B., and Delecluse, H.-J. (2006). Resting B cells as a transfer vehicle for Epstein–Barr virus infection of epithelial cells. *Proceedings of the National Academy of Sciences* **103**(18)**,** 7065-7070.

Shapiro-Shelef, M., and Calame, K. (2005). Regulation of plasma-cell development. *Nat Rev Immunol* **5**(3)**,** 230-42.

Shapiro-Shelef, M., Lin, K. I., McHeyzer-Williams, L. J., Liao, J., McHeyzer-Williams, M. G., and Calame, K. (2003). Blimp-1 is required for the formation of immunoglobulin secreting plasma cells and pre-plasma memory B cells. *Immunity* **19**(4)**,** 607-20.

Shukla, D., and Spear, P. G. (2001). Herpesviruses and heparan sulfate: an intimate relationship in aid of viral entry. *The Journal of Clinical Investigation* **108**(4)**,** 503-510.

Siegel, A. M., Herskowitz, J. H., and Speck, S. H. (2008). The MHV68 M2 protein drives IL-10 dependent B cell proliferation and differentiation. *PLoS Pathog* **4**(4)**,** e1000039.

Siegel, A. M., Rangaswamy, U. S., Napier, R. J., and Speck, S. H. (2010). Blimp-1-dependent plasma cell differentiation is required for efficient maintenance of murine gammaherpesvirus latency and antiviral antibody responses. *J Virol* **84**(2)**,** 674-85.

Simas, J. P., and Efstathiou, S. (1998). Murine gammaherpesvirus 68: a model for the study of gammaherpesvirus pathogenesis. *Trends Microbiol* **6**(7)**,** 276-82.

Simas, J. P., Swann, D., Bowden, R., and Efstathiou, S. (1999). Analysis of murine gammaherpesvirus-68 transcription during lytic and latent infection. *J Gen Virol* **80 (Pt 1),** 75-82.

Sinclair, A. J., Palmero, I., Peters, G., and Farrell, P. J. (1994). EBNA-2 and EBNA-LP cooperate to cause G0 to G1 transition during immortalization of resting human B lymphocytes by Epstein-Barr virus. *EMBO J* **13**(14)**,** 3321-8.

Smit, M. J., Verzijl, D., Casarosa, P., Navis, M., Timmerman, H., and Leurs, R. (2002). Kaposi's Sarcoma-Associated Herpesvirus-Encoded G Protein-Coupled Receptor ORF74 Constitutively Activates p44/p42 MAPK and Akt via Gi and Phospholipase C-Dependent Signaling Pathways. *Journal of virology* **76**(4)**,** 1744-1752.

Smith, C. M., Gill, M. B., May, J. S., and Stevenson, P. G. (2007). Murine gammaherpesvirus-68 inhibits

antigen presentation by dendritic cells. *PLoS One* **2**(10)**,** e1048.

Smith, P. M., Wolcott, R. M., Chervenak, R., and Jennings, S. R. (1994). Control of acute cutaneous herpes simplex virus infection: T cell-mediated viral clearance is dependent upon interferon-gamma (IFN-gamma). *Virology* **202**(1)**,** 76-88.

Sodeik, B., Ebersold, M. W., and Helenius, A. (1997). Microtubule-mediated Transport of Incoming Herpes Simplex Virus 1 Capsids to the Nucleus. *The Journal of Cell Biology* **136**(5)**,** 1007-1021.

Soulier, J., Grollet, L., Oksenhendler, E., Cacoub, P., Cazals-Hatem, D., Babinet, P., d'Agay, M., Clauvel, J., Raphael, M., Degos, L., and Sigaux, F. (1995). Kaposi's sarcoma-associated herpesvirus-like DNA sequences in multicentric Castleman's disease [see comments]. *Blood* **86**(4)**,** 1276-1280.

Sparks-Thissen, R. L., Braaten, D. C., Hildner, K., Murphy, T. L., Murphy, K. M., and Virgin, H. W. t. (2005). CD4 T cell control of acute and latent murine gammaherpesvirus infection requires IFNgamma. *Virology* **338**(2)**,** 201-8.

Spear, P. (1993). *Seminars in Virology*.

Spear, P. G., and Longnecker, R. (2003). Herpesvirus entry: an update. *J Virol* **77**(19)**,** 10179-85.

Spence, P. J., and Green, E. A. (2008). Foxp3+ regulatory T cells promiscuously accept thymic signals critical for their development. *Proceedings of the National Academy of Sciences* **105**(3)**,** 973-978.

Spender, L. C., and Inman, G. J. (2011). Inhibition of germinal centre apoptotic programmes by epstein-barr virus. *Adv Hematol* **2011,** 829525.

Steed, A., Buch, T., Waisman, A., and Virgin, H. W. t. (2007). Gamma interferon blocks gammaherpesvirus reactivation from latency in a cell type-specific manner. *J Virol* **81**(11)**,** 6134-40.

Steed, A. L., Barton, E. S., Tibbetts, S. A., Popkin, D. L., Lutzke, M. L., Rochford, R., and Virgin, H. W. t. (2006). Gamma interferon blocks gammaherpesvirus reactivation from latency. *J Virol* **80**(1)**,** 192-200.

Steer, B., Adler, B., Jonjic, S., Stewart, J. P., and Adler, H. (2010). A Gammaherpesvirus Complement Regulatory Protein Promotes Initiation of Infection by Activation of Protein Kinase Akt/PKB. *PLoS One* **5**(7)**,** e11672.

Stein, M., Keshav, S., Harris, N., and Gordon, S. (1992). Interleukin 4 potently enhances murine macrophage mannose receptor activity: a marker of alternative immunologic macrophage activation. *J Exp Med* **176**(1)**,** 287-92.

Stevenson, P. G., Belz, G. T., Altman, J. D., and Doherty, P. C. (1998). Virus-specific CD8(+) T cell numbers are maintained during gamma-herpesvirus reactivation in CD4-deficient mice. *Proc Natl Acad Sci U S A* **95**(26)**,** 15565-70.

Stevenson, P. G., Cardin, R. D., Christensen, J. P., and Doherty, P. C. (1999). Immunological control of a murine gammaherpesvirus independent of CD8+ T cells. *J Gen Virol* **80 (Pt 2),** 477-83.

Stevenson, P. G., and Doherty, P. C. (1999). Non-antigen-specific B-cell activation following murine gammaherpesvirus infection is CD4 independent in vitro but CD4 dependent in vivo. *J Virol* **73**(2)**,** 1075-9.

Stevenson, P. G., Efstathiou, S., Doherty, P. C., and Lehner, P. J. (2000). Inhibition of MHC class I-restricted antigen presentation by gamma 2-herpesviruses. *Proc Natl Acad Sci U S A* **97**(15)**,**

8455-60.

Stevenson, P. G., May, J. S., Smith, X. G., Marques, S., Adler, H., Koszinowski, U. H., Simas, J. P., and Efstathiou, S. (2002). K3-mediated evasion of CD8(+) T cells aids amplification of a latent gamma-herpesvirus. *Nat Immunol* **3**(8)**,** 733-40.

Stewart, J. P., Usherwood, E. J., Ross, A., Dyson, H., and Nash, T. (1998). Lung epithelial cells are a major site of murine gammaherpesvirus persistence. *J Exp Med* **187**(12)**,** 1941-51.

Strieter, R. M., Gomperts, B. N., and Keane, M. P. (2007). The role of CXC chemokines in pulmonary fibrosis. *The Journal of Clinical Investigation* **117**(3)**,** 549-556.

Stuckey, J. A., Charles, R. S., and Edwards, B. F. P. (1992). A model of the platelet factor 4 complex with heparin. *Proteins: Structure, Function, and Bioinformatics* **14**(2)**,** 277-287.

Sun, C. C., and Thorley-Lawson, D. A. (2007). Plasma cell-specific transcription factor XBP-1s binds to and transactivates the Epstein-Barr virus BZLF1 promoter. *J Virol* **81**(24)**,** 13566-77.

Sun, R., Lin, S. F., Gradoville, L., Yuan, Y., Zhu, F., and Miller, G. (1998). A viral gene that activates lytic cycle expression of Kaposi's sarcoma-associated herpesvirus. *Proc Natl Acad Sci U S A* **95**(18)**,** 10866-71.

Sunil-Chandra, N., Efstathiou, S., and Nash, A. (1992). Murine gammaherpesvirus 68 establishes a latent infection in mouse B lymphocytes in vivo. *The Journal of general virology* **73,** 3275.

Sunil-Chandra, N. P., Efstathiou, S., Arno, J., and Nash, A. A. (1992). Virological and pathological features of mice infected with murine gamma-herpesvirus 68. *J Gen Virol* **73 (Pt 9),** 2347-56.

Sunil-Chandra, N. P., Efstathiou, S., and Nash, A. A. (1993). Interactions of murine gammaherpesvirus 68 with B and T cell lines. *Virology* **193**(2)**,** 825-33.

Swaminathan, S., Hesselton, R., Sullivan, J., and Kieff, E. (1993). Epstein-Barr virus recombinants with specifically mutated BCRF1 genes. *J Virol* **67**(12)**,** 7406-13.

Tarakanova, V. L., Molleston, J. M., Goodwin, M., and Virgin, H. W. (2010). MHV68 complement regulatory protein facilitates MHV68 replication in primary macrophages in a complement independent manner. *Virology* **396**(2)**,** 323-328.

Tarlinton, D. (2006). B-cell memory: are subsets necessary? *Nat Rev Immunol* **6**(10)**,** 785-790.

Taub, D. D., Turcovski-Corrales, S. M., Key, M. L., Longo, D. L., and Murphy, W. J. (1996). Chemokines and T lymphocyte activation: I. Beta chemokines costimulate human T lymphocyte activation in vitro. *J Immunol* **156**(6)**,** 2095-2103.

Testi, R., Phillips, J. H., and Lanier, L. L. (1989). T cell activation via Leu-23 (CD69). *The Journal of Immunology* **143**(4)**,** 1123.

Thomson, R. C., Petrik, J., Nash, A. A., and Dutia, B. M. (2008). Expansion and activation of NK cell populations in a gammaherpesvirus infection. *Scand J Immunol* **67**(5)**,** 489-95.

Tokoyoda, K., Egawa, T., Sugiyama, T., Choi, B.-I., and Nagasawa, T. (2004). Cellular Niches Controlling B Lymphocyte Behavior within Bone Marrow during Development. *Immunity* **20**(6)**,** 707-718.

Townsley, A. C., Dutia, B. M., and Nash, A. A. (2004). The m4 gene of murine gammaherpesvirus modulates productive and latent infection in vivo. *J Virol* **78**(2)**,** 758-67.

Tripp, R. A., Hamilton-Easton, A. M., Cardin, R. D., Nguyen, P., Behm, F. G., Woodland, D. L., Doherty, P. C., and Blackman, M. A. (1997). Pathogenesis of an Infectious Mononucleosis-like Disease Induced by a Murine γ-Herpesvirus: Role for a Viral Superantigen? *The Journal of Experimental Medicine* **185**(9)**,** 1641-1650.

Upton, C., Mossman, K., and McFadden, G. (1992). Encoding of a homolog of the IFN-gamma receptor by myxoma virus. *Science* **258**(5086)**,** 1369-72.

Usherwood, E. J., Meadows, S. K., Crist, S. G., Bellfy, S. C., and Sentman, C. L. (2005). Control of murine gammaherpesvirus infection is independent of NK cells. *Eur J Immunol* **35**(10)**,** 2956-61.

Usherwood, E. J., Ross, A. J., Allen, D. J., and Nash, A. A. (1996). Murine gammaherpesvirus-induced splenomegaly: a critical role for CD4 T cells. *Journal of general virology* **77**(4)**,** 627-630.

Valmary, S., Richard, P., and Brousset, P. (2005). Frequent detection of Kaposi's sarcoma herpesvirus in germinal centre macrophages from AIDS-related multicentric Castleman's disease. *Aids* **19**(11)**,** 1229-31.

van Berkel, V., Barrett, J., Tiffany, H. L., Fremont, D. H., Murphy, P. M., McFadden, G., Speck, S. H., and Virgin, H. I. (2000). Identification of a gammaherpesvirus selective chemokine binding protein that inhibits chemokine action. *J Virol* **74**(15)**,** 6741-7.

van Berkel, V., Levine, B., Kapadia, S. B., Goldman, J. E., Speck, S. H., and Virgin, H. W. t. (2002). Critical role for a high-affinity chemokine-binding protein in gamma-herpesvirus-induced lethal meningitis. *J Clin Invest* **109**(7)**,** 905-14.

van Berkel, V., Preiter, K., Virgin, H. W. t., and Speck, S. H. (1999). Identification and initial characterization of the murine gammaherpesvirus 68 gene M3, encoding an abundantly secreted protein. *J Virol* **73**(5)**,** 4524-9.

Verzijl, D., Fitzsimons, C. P., van Dijk, M., Stewart, J. P., Timmerman, H., Smit, M. J., and Leurs, R. (2004). Differential Activation of Murine Herpesvirus 68- and Kaposi's Sarcoma-Associated Herpesvirus-Encoded ORF74 G Protein-Coupled Receptors by Human and Murine Chemokines. *Journal of virology* **78**(7)**,** 3343-3351.

Victora, G., and Nussenzweig, M. (2011). Germinal Centers. *Annual review of immunology*.

Viejo-Borbolla, A., Munoz, A., Tabares, E., and Alcami, A. (2010). Glycoprotein G from pseudorabies virus binds to chemokines with high affinity and inhibits their function. *J Gen Virol* **91**(Pt 1)**,** 23-31.

Vigne, S., Palmer, G., Lamacchia, C., Martin, P., Talabot-Ayer, D., Rodriguez, E., Ronchi, F., Sallusto, F., Dinh, H., Sims, J. E., and Gabay, C. (2011). IL-36R ligands are potent regulators of dendritic and T cells. *Blood* **118**(22)**,** 5813-5823.

Virgin, H. W. t., Latreille, P., Wamsley, P., Hallsworth, K., Weck, K. E., Dal Canto, A. J., and Speck, S. H. (1997). Complete sequence and genomic analysis of murine gammaherpesvirus 68. *J Virol* **71**(8)**,** 5894-904.

Wakeling, M. N., Roy, D. J., Nash, A. A., and Stewart, J. P. (2001). Characterization of the murine gammaherpesvirus 68 ORF74 product: a novel oncogenic G protein-coupled receptor. *J Gen Virol* **82**(Pt 5)**,** 1187-97.

Walz, A., Burgener, R., Car, B., Baggiolini, M., Kunkel, S. L., and Strieter, R. M. (1991). Structure and neutrophil-activating properties of a novel inflammatory peptide (ENA-78) with homology to interleukin 8. *The Journal of Experimental Medicine* **174**(6)**,** 1355-1362.

Wang, Q., Tsao, S. W., Ooka, T., Nicholls, J. M., Cheung, H. W., Fu, S., Wong, Y. C., and Wang, X. (2006). Anti-apoptotic role of BARF1 in gastric cancer cells. *Cancer Lett* **238**(1)**,** 90-103.

Wareing, M. D., Shea, A. L., Inglis, C. A., Dias, P. B., and Sarawar, S. R. (2007). CXCR2 is required for neutrophil recruitment to the lung during influenza virus infection, but is not essential for

viral clearance. *Viral Immunol* **20**(3)**,** 369-78.

Washington, A. T., and Aiyar, A. (2012). Herpesviridae - A Look Into This Unique Family of Viruses. *In* "Contributions of the EBNA1 Protein of Epstein-Barr Virus Toward B-Cell Immortalization and Lymphomagenesis" (G. D. M. a. S. Tyring, Ed.).

Webb, L. M., and Alcami, A. (2005). Virally encoded chemokine binding proteins. *Mini Rev Med Chem* **5**(9)**,** 833-48.

Webb, L. M., Smith, V. P., and Alcami, A. (2004). The gammaherpesvirus chemokine binding protein can inhibit the interaction of chemokines with glycosaminoglycans. *FASEB J* **18**(3)**,** 571-3.

Webb, L. M. C., Clark-Lewis, I., and Alcami, A. (2003). The Gammaherpesvirus Chemokine Binding Protein Binds to the N Terminus of CXCL8. *Journal of virology* **77**(15)**,** 8588-8592.

Weber, K. S., Grone, H. J., Rocken, M., Klier, C., Gu, S., Wank, R., Proudfoot, A. E., Nelson, P. J., and Weber, C. (2001). Selective recruitment of Th2-type cells and evasion from a cytotoxic immune response mediated by viral macrophage inhibitory protein-II. *Eur J Immunol* **31**(8)**,** 2458-66.

Weck, K. E., Dal Canto, A. J., Gould, J. D., O'Guin, A. K., Roth, K. A., Saffitz, J. E., Speck, S. H., and Virgin, H. W. (1997). Murine gamma-herpesvirus 68 causes severe large-vessel arteritis in mice lacking interferon-gamma responsiveness: a new model for virus-induced vascular disease. *Nat Med* **3**(12)**,** 1346-53.

Weck, K. E., Kim, S. S., Virgin, H. I., and Speck, S. H. (1999). B cells regulate murine gammaherpesvirus 68 latency. *J Virol* **73**(6)**,** 4651-61.

Weir, J. P. (2001). Regulation of herpes simplex virus gene expression. *Gene* **271**(2)**,** 117-130.

Wen, K. W., and Damania, B. (2010). Kaposi sarcoma-associated herpesvirus (KSHV): molecular biology and oncogenesis. *Cancer Lett* **289**(2)**,** 140-50.

Willer, D. O., and Speck, S. H. (2003). Long-term latent murine Gammaherpesvirus 68 infection is preferentially found within the surface immunoglobulin D-negative subset of splenic B cells in vivo. *J Virol* **77**(15)**,** 8310-21.

Williams, H., and Crawford, D. H. (2006). Epstein-Barr virus: the impact of scientific advances on clinical practice. *Blood* **107**(3)**,** 862-869.

Williams, H., McAulay, K., Macsween, K. F., Gallacher, N. J., Higgins, C. D., Harrison, N., Swerdlow, A. J., and Crawford, D. H. (2005). The immune response to primary EBV infection: a role for natural killer cells. *British Journal of Haematology* **129**(2)**,** 266-274.

Wysocka, J., and Herr, W. (2003). The herpes simplex virus VP16-induced complex: the makings of a regulatory switch. *Trends in Biochemical Sciences* **28**(6)**,** 294-304.

Xia, C. Q., and Kao, K. J. (2003). Effect of CXC chemokine platelet factor 4 on differentiation and function of monocyte‐derived dendritic cells. *International Immunology* **15**(8)**,** 1007-1015.

Yamamoto, R., Nishikori, M., Kitawaki, T., Sakai, T., Hishizawa, M., Tashima, M., Kondo, T., Ohmori, K., Kurata, M., Hayashi, T., and Uchiyama, T. (2008). PD-1-PD-1 ligand interaction contributes to immunosuppressive microenvironment of Hodgkin lymphoma. *Blood* **111**(6)**,** 3220-4.

Ye, B. H., Cattoretti, G., Shen, Q., Zhang, J., Hawe, N., de Waard, R., Leung, C., Nouri-Shirazi, M., Orazi, A., Chaganti, R. S., Rothman, P., Stall, A. M., Pandolfi, P. P., and Dalla-Favera, R. (1997). The BCL-6 proto-oncogene controls germinal-centre formation and Th2-type inflammation. *Nat Genet* **16**(2)**,** 161-70.

Yu, D., Rao, S., Tsai, L. M., Lee, S. K., He, Y., Sutcliffe, E. L., Srivastava, M., Linterman, M., Zheng, L., and

Simpson, N. (2009). The transcriptional repressor Bcl-6 directs T follicular helper cell lineage commitment. *Immunity* **31**(3)**,** 457-468.

Yu, R. Y., Wang, X., Pixley, F. J., Yu, J. J., Dent, A. L., Broxmeyer, H. E., Stanley, E. R., and Ye, B. H. (2005). BCL-6 negatively regulates macrophage proliferation by suppressing autocrine IL-6 production. *Blood* **105**(4)**,** 1777-84.

Yu, Y., Wang, S. E., and Hayward, G. S. (2005). The KSHV Immediate-Early Transcription Factor RTA Encodes Ubiquitin E3 Ligase Activity that Targets IRF7 for Proteosome-Mediated Degradation. *Immunity* **22**(1)**,** 59-70.

Zalani, S., Holley-Guthrie, E., and Kenney, S. (1996). Epstein-Barr viral latency is disrupted by the immediate-early BRLF1 protein through a cell-specific mechanism. *Proc Natl Acad Sci U S A* **93**(17)**,** 9194-9.

Zhang, J. Y., Zhang, Z., Jin, B., Zhang, S. Y., Zhou, C. B., Fu, J. L., and Wang, F. S. (2008). Cutting edge: programmed death-1 up-regulation is involved in the attrition of cytomegalovirus-specific CD8+ T cells in acute self-limited hepatitis B virus infection. *J Immunol* **181**(6)**,** 3741-4.

Zhu, F. X., Cusano, T., and Yuan, Y. (1999). Identification of the immediate-early transcripts of Kaposi's sarcoma-associated herpesvirus. *J Virol* **73**(7)**,** 5556-67.

Zhu, F. X., King, S. M., Smith, E. J., Levy, D. E., and Yuan, Y. (2002). A Kaposi's sarcoma-associated herpesviral protein inhibits virus-mediated induction of type I interferon by blocking IRF-7 phosphorylation and nuclear accumulation. *Proc Natl Acad Sci U S A* **99**(8)**,** 5573-8.

Zhu, J. Y., Strehle, M., Frohn, A., Kremmer, E., Höfig, K. P., Meister, G., and Adler, H. (2010). Identification and analysis of expression of novel microRNAs of murine gammaherpesvirus 68. *Journal of virology* **84**(19)**,** 10266-10275.

Ziegler, S. F., Ramsdell, F., Hjerrild, K. A., Armitage, R. J., Grabstein, K. H., Hennen, K. B., Farrah, T., Fanslow, W. C., Shevach, E. M., and Alderson, M. R. (1993). Molecular characterization of the early activation antigen CD69: a type II membrane glycoprotein related to a family of natural killer cell activation antigens. *Eur J Immunol* **23**(7)**,** 1643-8.

Ziporen, L., Li, Z. Q., Park, K. S., Sabnekar, P., Liu, W. Y., Arepally, G., Shoenfeld, Y., Kieber-Emmons, T., Cines, D. B., and Poncz, M. (1998). Defining an Antigenic Epitope on Platelet Factor 4 Associated With Heparin-Induced Thrombocytopenia. *Blood* **92**(9)**,** 3250-3259.

Zlotnik, A., and Yoshie, O. (2000). Chemokines: a new classification system and their role in immunity. *Immunity* **12**(2)**,** 121-7.

Zlotnik, A., and Yoshie, O. (2012). The chemokine superfamily revisited. *Immunity* **36**(5)**,** 705-16.